

Uncertainty on transmission grids

An Exploratory modeling study on
transmission grids



Written by

KAS KRANENBURG

To be defended on

20TH OF APRIL 2023

Uncertainty on transmission grids

An Exploratory modeling study on transmission grids

Master thesis submitted to Delft University of Technology in partial fulfillment of the requirements for the degree of

MASTER OF SCIENCE

in Engineering Policy and Management

By:

Kas Marten Kranenburg

Student number: 4727754

To be defended in public on April 20th

Thesis committee

Chair and first supervisor Prof. Dr. Ir. L.j. de Vries, TU Delft

Second supervisor Dr. P.W.G. Bots, TU Delft

External supervisor B.Botor, Msc., Encoord GmbH



Contents

| | | |
|----------|--|-----------|
| 1 | Introduction | 8 |
| 2 | Literature review | 10 |
| 2.1 | Electrification in the Netherlands | 10 |
| 2.1.1 | Policy plans for production of electricity | 10 |
| 2.1.2 | Electrification of demand of energy | 10 |
| 2.2 | Economic evaluation of transmission grids | 11 |
| 2.2.1 | Congestion management | 11 |
| 2.2.2 | Transmission Expansion Planning | 11 |
| 2.3 | Production cost models | 12 |
| 2.4 | Deep-uncertainty | 12 |
| 2.5 | Exploratory modelling and analysis | 13 |
| 3 | Methodology | 15 |
| 3.1 | Power network model | 15 |
| 3.1.1 | Input of power network model | 15 |
| 3.1.2 | Output of network model | 17 |
| 3.1.3 | Conceptual model | 17 |
| 3.2 | Congestion seeking algorithm | 18 |
| 3.2.1 | Core mechanics | 18 |
| 3.2.2 | Example of algorithm mechanisms | 18 |
| 3.2.3 | Algorithm output | 20 |
| 3.2.4 | Conceptual model | 21 |
| 3.3 | Exploratory modeling | 22 |
| 3.3.1 | Uncertainty specification | 23 |
| 3.3.2 | Modeling framework | 23 |
| 3.3.3 | Experiment setup | 24 |
| 3.3.4 | Outcome analysis | 26 |
| 3.4 | Power model data | 27 |
| 3.4.1 | Network topology | 28 |
| 3.4.2 | Demand profile construction | 29 |
| 3.4.3 | Conventional generation | 29 |
| 3.4.4 | Renewable generation | 30 |
| 3.5 | Weather years | 31 |
| 3.6 | Verification | 32 |
| 4 | Results | 33 |
| 4.1 | January results and analysis | 33 |
| 4.1.1 | January | 33 |
| 4.1.2 | General results | 34 |
| 4.1.3 | High Vulnerability lines | 35 |
| 4.1.4 | Moderately vulnerable lines | 38 |
| 4.1.5 | Secondary lines | 39 |
| 4.2 | June results and analysis | 40 |
| 4.2.1 | June | 40 |
| 4.2.2 | General results | 40 |
| 4.2.3 | High Vulnerability lines | 41 |
| 4.2.4 | Moderately vulnerable lines | 42 |
| 4.2.5 | Secondary lines | 42 |

| | | |
|----------|---|-----------|
| 5 | Discussion of results | 43 |
| 5.1 | Comparison of June and January experiments | 43 |
| 5.2 | Influence of the uncertainties | 43 |
| 5.2.1 | Influence of weather years | 44 |
| 5.2.2 | General system outcomes | 44 |
| 5.3 | Line vulnerability outcomes | 44 |
| 5.3.1 | Critical importance | 45 |
| 5.3.2 | High importance | 45 |
| 5.3.3 | Planned capacity expansions | 47 |
| 5.4 | Validation of results | 48 |
| 5.5 | Discussion of limitations | 48 |
| 5.5.1 | Congestion methodology | 48 |
| 5.5.2 | Network modeling | 48 |
| 5.5.3 | Data collection and implementation | 49 |
| 5.5.4 | Experimental design | 50 |
| 6 | Conclusion and recommendations | 52 |
| 6.1 | sub-questions | 52 |
| 6.1.1 | Sub question 1 | 52 |
| 6.1.2 | Sub question 2 | 52 |
| 6.1.3 | Critical upgrades | 52 |
| 6.1.4 | Conditional upgrades | 52 |
| 6.1.5 | Sub question 3 | 54 |
| 6.2 | Research question | 54 |
| 6.3 | Further research | 55 |
| 6.3.1 | Development of hydrogen and transmission grid | 55 |
| 6.3.2 | Usage of RDM-framework | 55 |
| 6.3.3 | Capacity expansion | 55 |
| 6.3.4 | Alternative simulation methodology | 56 |
| 7 | Reflection | 57 |
| 7.1 | Research process | 57 |
| 7.2 | Research design | 58 |
| 7.3 | Hiccups and setbacks | 58 |
| 7.4 | Personal reflection | 59 |
| | Bibliography | 60 |
| A | Mathematical model | 64 |
| B | Methodology verification | 65 |
| B.1 | 5- node network topology | 65 |
| B.1.1 | Renewable energy generators | 66 |
| B.1.2 | Fuel generators | 68 |
| B.1.3 | Demand | 68 |
| B.1.4 | Model setup | 68 |
| B.1.5 | Uncertainty specification | 68 |
| B.2 | Evaluation of the performance | 68 |
| B.3 | Results of 5-node experiment | 69 |
| C | 6-node network | 71 |
| C.1 | Line characteristics | 71 |
| C.2 | Generators | 71 |
| C.3 | Verification of model data | 74 |
| C.4 | First model | 74 |

| | | |
|----------|---|------------|
| C.4.1 | Zone characteristics | 74 |
| C.5 | Storage | 75 |
| C.5.1 | Network verification | 75 |
| C.6 | RESA | 76 |
| C.7 | Wind energy | 77 |
| C.8 | Demand | 77 |
| D | Full model | 78 |
| D.1 | Network topology | 78 |
| D.1.1 | Added network upgrades | 79 |
| D.2 | RESA | 79 |
| D.3 | Demand | 79 |
| E | Time reduction by different runs setup. | 83 |
| E.1 | Outcomes | 84 |
| F | Code flowchart development and explanation | 91 |
| F.1 | Modeling tools methodology | 91 |
| F.1.1 | EMA workbench | 91 |
| F.1.2 | SAInt | 91 |
| F.1.3 | Coupling of EMA workbench with SAIInt | 91 |
| G | Weatheryear analysis | 96 |
| H | Congestion management | 104 |
| H.1 | Congestion detection | 104 |
| H.2 | Validation of cost attribution in 6-node network. | 104 |
| H.3 | Cost attribution background | 105 |
| H.3.1 | Influence of line capacities on model costs | 105 |
| I | Results analysis | 109 |
| I.1 | Results january experiment | 109 |
| I.1.1 | Selection of results | 109 |
| I.2 | Prim analysis | 112 |
| I.3 | Prim analysis more vulnerable lines | 112 |
| I.3.1 | Line 4 | 112 |
| I.3.2 | Line 15 | 115 |
| I.3.3 | Line 23 | 116 |
| I.3.4 | Line 24 | 118 |
| I.3.5 | Line 28 | 120 |
| I.3.6 | Line 35 | 121 |
| I.3.7 | Line 38 | 123 |
| I.4 | Results less vulnerable lines | 125 |
| I.4.1 | Line 6 | 126 |
| I.4.2 | Line 13 | 127 |
| I.4.3 | Line 22 | 128 |
| I.4.4 | Line 26 | 129 |
| I.5 | Combined results January | 129 |
| I.5.1 | Line 4 after line 24 | 131 |
| I.5.2 | Line 15 after line 23, and vice versa | 131 |
| I.5.3 | Line 6 after line 15 | 133 |
| I.5.4 | Line 6 after line 23 | 134 |
| I.5.5 | Line 10 after line 28 | 135 |
| I.5.6 | Line 13 after line 24 and line 4 | 136 |
| I.5.7 | Line 26 after line 24 | 138 |

| | | |
|--------|---|-----|
| I.5.8 | Line 31 after line 38 | 139 |
| I.5.9 | Line 37 congestions after line 38 | 139 |
| I.5.10 | Line 40 congestions after line 38 | 139 |
| I.6 | June results | 139 |
| I.6.1 | Selection of results | 139 |
| I.7 | Prim analysis | 142 |
| I.7.1 | Line 15 | 143 |
| I.7.2 | Line 23 | 144 |
| I.7.3 | Line 24 | 145 |
| I.7.4 | Line 31 | 145 |
| I.7.5 | Line 35 | 146 |
| I.8 | Lesser vulnerable lines | 148 |
| I.8.1 | Line 22 | 148 |
| I.8.2 | Line 26 | 149 |
| I.8.3 | Line 28 | 150 |
| I.8.4 | Line 37 | 151 |
| I.9 | Combination of lines for June | 152 |
| I.9.1 | Line 26 after line 24 | 152 |
| I.9.2 | Line 37 after line 31 | 153 |
| I.9.3 | Line 26 after line 15 | 154 |
| I.10 | Comparison with the outcomes of the two experiments | 155 |

Foreword

My aim for this research project was to combine exploratory modeling with power systems. I choose transmission grids because of their criticality in the system. I could not foresee how I would create my algorithm based on the characteristics of these systems. I delved into the complexities and uncertainties of this system and am proud of the results I present in this report. I want to thank those who supported me throughout this process.

First, I would like to express my gratitude to my committee. Without them, this research would not have been possible. I want to thank my chair, Laurens de Vries, whom I contacted with a rough sketch of my research idea. He put me in contact with Encoord and made my unique opportunity with this project possible. Furthermore, the feedback on the writing and the aim of the research was very beneficial. To Pieter Bots, thanks for providing sharp input on my research design and modeling choices. This feedback allowed me to make clearer choices in my writing and research setup. And lastly, my thanks to Benjamin Botor, who invited me to work in Essen, Germany, for three months as part of this research. Working and living in this city alongside an international team of highly-skilled software developers and energy system modelers is something I will never forget. In addition, he was always available for feedback on my work and ready to talk about the research project or anything else. I also want to thank my coworkers at Encoord for welcoming me at Encoord and Essen. You made my stay there pleasant and unforgettable. I want to thank my partner and family for supporting me in choosing to go to Essen and for their support during the hard times of this project. Finally, I want to thank my friends and roommates for their support during this project, especially the people who took the time to visit me in Essen. This meant a lot to me.

Looking back at this graduation project, I'm proud that I have overcome the hurdles during this project and am satisfied with the result.

*K.M. Kranenburg
Delft, April 2023*

Executive summary

Introduction

Following the climate goals of the Dutch government, a tremendous amount of vRES (variable Renewable Energy Sources) will be built. These energy sources will produce large amounts of power, which must travel great distances on the transmission grid. The Dutch TSO, TenneT, is responsible for the transmission grid's design, construction, and maintenance by European and Dutch law. The planning for transmission grids has become more complex since the liberalization of power markets. Because of this complexity, the planned expansions are published every two years. In energy systems, the ever-changing context of the system makes the possible future states of the system uncertain. In this research, we 1. identify the relevant uncertainties for the transmission system, 2. Identify the most vulnerable lines under these uncertainties, and 3. Look at the effect of the delays on the performance of the overall power system. This gives insights into how the transmission system must evolve to maintain the grid's performance.

Literature review

Not only more power from vRES will be generated, but coal plants will also be phased out, and the demand for other energy sources (fuel, gas, etc.) will be electrified. More power flow will lead to congestion on the current grid. The Dutch Transmission System Operator (TSO) uses congestion management to alleviate acute congestion and expansion planning to prevent future congestion. To decide whether grid expansion should be used, Production Cost Models (PCMs) are used. To account for uncertainties in a system, the concept of deep uncertainty can be employed to map the uncertainty of a system. Exploratory modeling uses this concept to understand the consequences of deep uncertainty. Experimental modeling and analysis could thus be used to understand the effects of vRES on the power grid.

Methodology

Direct Current Optimal Power Flow (DCOPF) is used for the formulation of the Production Cost Model (PCM) for the power network modeling. The chosen exploratory modeling framework is a simplified form of the XLRM framework, in which the policies in the model (L) is not altered. The data used as input for the model is selected from a wide range of sources, following the format of the DCOPF formulation. The tool used to build and simulate the DCOPF model is Scenario Analysis Interface for Energy Systems (SAInt) software. The EMA workbench is used to perform exploratory modeling and analysis. Two times 1,000 experiments for a week period have been run with these tools, one set in January and one set in June. To assess which lines in the transmission network might be susceptible to congestion, we analyzed the experiments' outcomes with a congestion-seeking algorithm. The adopted methodology has been verified using a 5-node model.

Results

The results of these experiments are divided into two types of outcomes: the general system outcomes and the line outcomes; the latter has been split up based on the urgency of capacity expansion. The analysis tools by the EMA workbench were used to analyze the results of the experiments, especially the Patient Rule Induction Method (PRIM) algorithm. The experiments showed significant differences in congestion between June and January.

Discussion of results

The most alarming result for the general outcomes was the high unserved demand. The most vulnerable lines connected regions with abundant offshore wind power with a scarcity of renewable power. It was found that a large share of the identified vulnerable lines has also been recognized by the TSOs in their capacity expansion study, evidencing the validity of this research. Some fundamental limitations were identified; Some notable ones are The absence of storage in the model and the implementation of the congestion-seeking algorithm. With storage

in the model, the results would have been partly different. The congestion-seeking algorithm could have been more refined, making the results easier to interpret.

Conclusions and recommendations

Based on the results, we conclude that the transmission grid will be adequate for energy transmission until 2030. Some vulnerabilities in the network have been spotted. Especially the lines connecting the wind farms with the East of the Netherlands are prone to congestion. The lines connecting Eindhoven to the Borssele wind farm, for instance. Furthermore, the 220 kV network with a lower capacity could become congested due to the power generated at the Eemshaven wind farms. Finally, lines in the West of the Netherlands will be prone to significant amounts of power generated at the wind farms in this region. Apart from this, we conclude that the transmission system will be subjected to more change due to developments in the energy system in the coming years. The TSO will need to follow these changes closely and respond adequately to ensure the performance of the transmission grid will not suffer from these changes. For future research, transmission systems with storage of renewable power must be examined. Furthermore, Robust Decision-making can be used to pinpoint the best capacity expansions in the network.

1 Introduction

To overcome the challenges of global warming and environmental degradation, the European Union (EU) has presented the goal to become the first climate-neutral continent by 2050 in the European Green Deal (EU 2019). In 2030 the first step of this goal must be completed by the member states by reducing emissions by 55% in comparison to 1990-levels (EU 2020). The task of the European Union member states is to change their energy infrastructure so that the continent as a whole reaches this goal. The Dutch government presented the Dutch contribution as a climate act (Klimaatakkoord 2019) in 2019. In this act, plans for building large amounts of Variable Renewable Energy Sources (vRES) were announced.

The energy transition has tremendous implications for the backbone of the power system, the electricity grid. The Netherlands comes from an energy system that is highly reliant on gas and wishes to electrify these energy flows (Economische Zaken n.d.). This electrification will significantly impact the electricity grid as researched by Blonsky et al. (2019). Power will be generated at different locations compared to before and needs to be transported over longer distances to reach places with power demand. While the Dutch grid, like most others, has two layers responsible for the transmission and the distribution of power, respectively, the thesis at hand focuses on the former.

The Dutch Transmission System Operator (TSO), TenneT, is responsible for the design, construction, maintenance, and operation of the Dutch transmission grid (TenneT 2022d) and, in addition, for facilitating the energy market. These activities are legally bound to the TSO by the Dutch Electricity Law (Dutch Government 1998) with the liberalization of the energy market following the first and second EU Electricity Market directives of 1996 and 2003 (Jamassb and Pollitt 2005). Thus, it is their task to ensure power from vRES can reach consumers.

Transmission planning has become more complex with the liberalization of power markets and the onset of the energy transition: There is no longer central coordination of generation and transmission assets, and generation, in general, has become less centralized. Any producer or consumer can demand a connection to the grid at any location (Dutch Government 1998). The power lines on the grid could become congested more easily. This brings uncertainty to how the expansion plans of the grid should be designed. The expansion plans of the European TSOs are captured in the ten-year network development plans (TYNDP). These are built upon the national development plans of the European TSOs and published by the European Network of Transmission System Operators for Electricity (ENTSO-E). The TYNDP are non-binding and published every two years, most recently in 2022 (ENTSO-E 2022b) along with the plans for the Dutch grid by TenneT. (TenneT 2022b).

For energy systems in transition, the World Energy Council (WEC) uses the World Energy Trilemma index to map the competing demand of an energy transition (Council 2022). According to this index in energy transitions, the three goals of policies are energy security, social equity, and environmental impact mitigation. These goals are shifting while the context of the system is changing. While writing this thesis, the energy crisis caused by the conflict in Ukraine makes current policy mainly focuses on making energy more affordable, shifting the equilibrium. This illustrates how energy is an essential part of human society, and disruptions in their supply can lead to significant problems. This ever-changing context makes the future and, with that, the transmission planning uncertain. This thesis strives to shed light on how the uncertainties in the system context of the transmission grid might affect the grid.

This thesis will focus on the Dutch energy system's transition to a system based on vRES and how its uncertain nature will affect the network of the TSO. We will not focus on Demand side management (DSM) since this is more affiliated with the work of the Distribution System Operator (DSO) (Kuiken and Más 2019). The network of TenneT consists of the main high-

level network and nine subnetworks. The main network spreads over the whole nation. The subnetworks connect the main network with the networks of the DSO's. Only the main network will be considered to limit the scope of the thesis. Since the most recent TYNDP and the plans for the energy transition in the Netherlands have a timespan from 2022 until 2030, these will also be used. The research question will therefore be:

Is the planned 2030 Dutch electricity grid adequate, and if not, which extra investments may help mitigate the consequences of critical uncertainties?

The following subquestions have been selected to support this research question:

1. *What are the most uncertain factors of the Dutch energy transition for the transmission grid?*
2. *What are the most vulnerable lines to congestion due to the (uncertain) Dutch energy transition?*
3. *What is the effect of the Dutch energy transition on the overall power system?*

The first sub-question will focus on the uncertain nature of the effect of the Energy transition on the Dutch transmission grid. The most influential uncertain factors need to be identified.

The second sub-question is where we will evaluate the lines in the network. We will evaluate which input values influence the network performance most and where future congestion could arise.

The third sub-question will clarify how the context of the Dutch transmission system, the power system, will evolve with the energy transition.

These three sub-questions will give us insights into the development of the Dutch energy transition and how the transmission grid will be affected by it.

2 Literature review

As stated in the previous Chapter, the energy transition causes significant uncertainties in the Dutch transmission grid. This Chapter dives into the relevant literature to answer the research question.

First, we review the relevant policy plans by the Government for the energy transition. The Dutch government has two major plans for renewable power on the network. The offshore wind farm plans and the local plans for each energy region. In addition, the coal plants will be phased out of the system by 2030. In the meanwhile, the power demand until 2030 will likely increase.

Second, we look at the TSO's options regarding congestion. Two options arise from this literature review, congestion management, and transmission expansion planning. The former is used to alleviate congestion and the latter to prevent congestion. Both are costly.

Third, we will look at how the transmission grid is generally simulated. A distinction is made between Linear Programming and Mixed Integer Programming problems. Moreover, multiple model formulations are reviewed.

Fourth, the concept of deep uncertainty is reviewed in the context of the Dutch transmission grid. It is important to identify the uncertainties in the system so we can analyze them and the system accordingly.

Finally, we investigate exploratory modeling and analysis, assessing exploratory modeling and its tools for their effectiveness in examining the dynamics of systems under uncertainty.

2.1 Electrification in the Netherlands

2.1.1 Policy plans for production of electricity

The Dutch government published its climate act in 2019. In this act 30 Regions were appointed; these were called Regionale Energie strategieën regions (abbreviated here as RESA regions, to avoid confusion with the abbreviation RES for Renewable Energy Sources). These regions have the shared task of collectively generating 35 TWh of renewable energy in 2030 (RES n.d.). To make sure that this goal is met, every region has submitted its bid. In these bids, the regions indicate how much wind and solar energy they plan to produce in 2030. The planning process will take an iterative approach; each region will refine its plans regularly. At the moment of writing (2022-2023), each region has published its first bid. The plans are thus not definitive. parallel to the regional plans, the Dutch government presented plans for building offshore wind farms (Rijksoverheid n.d.). In these plans, a total capacity of 21 GW of wind energy will be built by 2030. These plans can together be seen as the start of the electrification of the energy system. Concerning conventional generators, the Dutch government plans to phase coal plants out by 2030 (Rijksoverheid 2021).

2.1.2 Electrification of demand of energy

According to the Klimaat-en Energieverkenning (KEV) 2022 PBL et al. (2022), it is expected that the electricity demand will account for around 20 % of the total energy demand in 2030. This report gives a yearly outlook on the energy system. Whether this percentage will change is highly dependent on how much of the energy demand will electrify in the coming years. Households are very dependent on gas in the Netherlands due to gas connections, and the traffic and industrial sectors mainly operate on conventional fuels. When these take measures to electrify their energy consumption, the share of electric demand could increase, partly due to the lower cost of vRES.

2.2 Economic evaluation of transmission grids

The electrification of the energy sector will lead to more power flows on the transmission grid. This could lead to congestion on the power grid. Congestion can lead to interference with the market solution. Next to the grid operator, the TSO also functions as the market operator. In this role, it strives to fulfill the goals of optimal social welfare, which are to minimize the total costs and the system emissions and maximize the grid's reliability. Since an investment in the grid can be quite costly, it must be properly evaluated whether it is the best way to achieve optimal social welfare for the energy system. The TSO has other tools at its disposal to alleviate the congestion. These are coined under the term "congestion management" (Pillay, Prabhakar Karthikeyan, and Kothari 2015). However, these methods interfere with the cost-optimal solution of the market, meaning that extra costs in the system will occur. Thus, the TSO will reach a point in which it is more appealing to expand the capacity in the transmission grid than to repeat congestion management to alleviate the congested line. The procedure to expand the transmission grid is called Transmission Expansion Planning (TEP). Congestion management is thus used when congestions occur, and network capacity expansion is to prevent network congestions from occurring.

2.2.1 Congestion management

In Chapter 7 of the book "Regulation of the Power sector" (Pérez-Arriaga 2013), it is stated that nodal pricing is used in most power markets as the preferred method of congestion management. In nodal pricing, a security-constrained Economic Dispatch (ED) method (Tsegaye, Shewarega, and Bekele 2018) is used to derive a Locational Marginal Price (LMP) for each of the nodes in the model. When congestion arises after the security-constrained ED, the congestion in the network is handled by the market operator by discharging the costliest generator at the node/zone which is generating a surplus, and by activating the least costly available generator at the demanding node or zone. Assuming that the solution of the ED is the most cost-efficient for the system, any tempering with it will lead to extra costs. This means that the costs of the total power system rise since the generator that is activated is more expensive than the generator that is discharged. It also means that a difference in the LMPs arises. The cost of demanding one more unit of energy is different at the two nodes since two different generators with a cost difference between them would serve the demand increase. The LMP, sometimes referred to as the shadow price of the demand of the nodes (Pillay, Prabhakar Karthikeyan, and Kothari 2015) is thus an important factor to consider while reviewing congestions. To evaluate the performance of the transmission grid in an economical manner, Production Cost Models (PCMs) are often used (Kahn 1995) & (Batlle and Barquin 2005). These can thus be used to measure the costs of congestion management.

2.2.2 Transmission Expansion Planning

Transmission Expansion Planning (TEP) tries to resolve the best way to expand or reinforce an existing electricity transmission network, one of the central tasks of a TSO (Dios, Soto, and Conejo 2007). The authors state that in a competitive market, the TSO should expand the network while minimizing the network transmission cost (investment and operation) and pursuing maximum social welfare under static and dynamic technical constraints. The modeling of the TEP problem of TSOs has become more difficult with the entrance of more vRES since the generation of these power sources is less predictable. Furthermore, it is unclear how the energy transition will be completed: How much will electricity demand increase? How much of the energy demand will be covered by green hydrogen? Governmental and investor plans give some guidance in this respect, however, they are still uncertain. This leads to large uncertainties for the development of the Transmission network and problems with the TEP for the Netherlands. In order to cope with the uncertainties, they must first be identified. The concept 'deep uncertainty' and its connection to the Dutch energy transition will be explored in Section 2.4. As TEP is computationally very expensive, performing one while taking all uncertainties into

account would make for an immense computational runtime.

2.3 Production cost models

The PCM aims to simulate the energy system for a short period in the future while minimizing production costs. To do this, it takes the variable cost for each generator and assumes they are all bidding at their marginal costs. The PCMs for power systems are usually formulated as Linear Programming- (LP) or Mixed Integer Programming (MIP) problems (Capasso et al. 2016). The difference between them is the Unit Commitment (UC) aspect. LP formulations don't have it, MIP formulations do. In the UC formulation, conventional generators cannot stop generating power completely from one timestep to another (Baldick 1995). Constraints ensure that the generation needs to be slowly ramped up and down. For the problem formulation, this means that the decision taken at one timestep will influence other timesteps and that the problem has a dynamic character. Another difference is the type of power flow formulation used in the simulation. Frank et al. (2012) reviewed the existing problem formulations and their characteristics. Their results can be found in Figure 1. The three main formulations are Economic Dispatch (ED), Direct Current Optimal Power Flow (DCOPF), and Alternating Current Optimal Power Flow (ACOPF). In ED, the optimal power flows are calculated by not taking the transmission grid constraints into account. This method only takes the constraints imposed by the generators. (Frank et al. 2012). The result is the optimal solution for the power market. This method is useful in solving power markets, not for simulating power flows on transmission grids since it does not consider any transmission capacities. We will not review this formulation further. DCOPF is more complex and considers the lines' capacities in the grid as well. These are also used as constraints for the LP/MIP formulation. ACOPF is the most complex formulation and also considers the volt-angles and magnitudes. Due to the complexity, it is not practical to run a lot of timesteps with these models.

| General problem type | Problem name | Includes voltage angle constraints? | Includes bus voltage magnitude constraints? | Includes transmission constraints? | Includes losses? | Assumptions | Includes generator costs? | Includes contingency constraints? |
|----------------------|---|-------------------------------------|---|------------------------------------|------------------|---|---------------------------|-----------------------------------|
| OPF | ACOPF, or Full ACOPF | Yes | Yes | Yes | Yes | | Yes | No |
| OPF | DCOPF | No | No; all voltage magnitudes fixed | Yes | Maybe | Voltage magnitudes are constant | Yes | No |
| OPF | Decoupled OPF | Yes | Yes | Yes | Yes | Power-voltage angle are independent of voltage magnitude-reactive power | Yes | No |
| OPF | Security-Constrained Economic Dispatch (SCED) | Yes | No | Yes | Yes | Voltage magnitudes are constant | Yes | Yes |
| Power flow | Power Flow, or Load Flow | No, but can be added | Yes | No, but can be added | Yes | | No | No |
| Economic dispatch | Economic Dispatch | No | No | No | Depends | No transmission constraints | Yes | No |
| OPF | Security Constrained OPF (SCOPF) | Yes | Depends | Yes | Yes | Depends | Yes | Yes |

Figure 1: Different OPF variants as described by (Frank et al. 2012).

2.4 Deep-uncertainty

Deep uncertainty is one or a combination of three characteristics that analysts and decision-makers do not know or can not agree upon (Lempert 2003).

1. The appropriate models to describe interactions between the system's variables.
2. The probability distributions representing the uncertainty of key parameters in the models.

3. How to value the desirability of the outcome variables.

Walker, Lempert, and Jan H Kwakkel (2012) used this definition to mark five different levels of uncertainty among the factors of the system. These levels are ascending in the level of uncertainty across four different aspects, as illustrated in Figure 2.

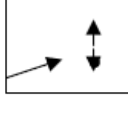
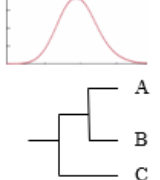

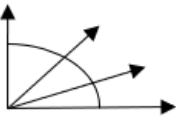
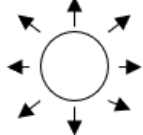
| | | Level 1 | Level 2 | Level 3 | Level 4 | Level 5 | | |
|---------------------------|----------------------------|---|---|---|--|---|------------------------|--|
| Complete Certainty | Context | A clear enough future (with sensitivity)  | Alternate futures (with probabilities)  | Alternate futures (with ranking)  | A multiplicity of plausible futures (unranked)  | Unknown future  | Total ignorance | |
| | System model | A single system model | A single system model with a probabilistic parameterization | Several system models, one of which is most likely | Several system models, with different structures | Unknown system model; know we don't know | | |
| | System outcomes | Point estimates with sensitivity | Several sets of point estimates with confidence intervals, with a probability attached to each set | Several sets of point estimates, ranked according to their perceived likelihood | A known range of outcomes | Unknown outcomes; know we don't know | | |
| | Weights on outcomes | A single estimate of the weights | Several sets of weights, with a probability attached to each set | Several sets of weights, ranked according to their perceived likelihood | A known range of weights | Unknown weights; know we don't know | | |

Figure 2: The levels of uncertainty as described by (Walker, Lempert, and Jan H Kwakkel 2012).

Aided by this figure, researchers can evaluate what elements in a system are uncertain and to what degree. The case study of Hamarat, Jan H. Kwakkel, and Pruyt (2013) identifies the deeply uncertain character of energy transitions.

2.5 Exploratory modelling and analysis

Exploratory modeling and deep uncertainty

According to Jan H Kwakkel (2017), exploratory modeling can be used to understand the consequences of deep uncertainty. For this reason, Jan H Kwakkel (2017) developed the exploratory modeling and analysis workbench (EMA workbench), a Python library, to facilitate the application of related methods. This library can be used to support decision-making under deep uncertainty. By coupling an existing model to the EMA workbench and employing one of the approaches, insightful information about the uncertainties within the model can be explored, and helpful policy insights can be formed.

XLRM framework

One of the key concepts behind the EMA workbench is the XLRM framework as introduced by (Lempert 2003). This framework can be found in Figure 45. The X stands for the external factors; these are the uncertain factors that can't be influenced. The L stands for policy levels. The R stands for the Relationships in the System; this would be the representation of the system in a PCM. The M is the relevant Performance Metric described in Section 2.2.2.

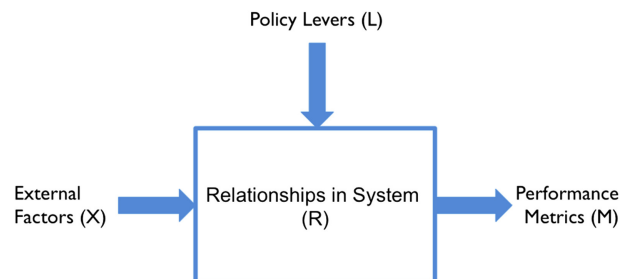


Figure 3: The XLRM framework as introduced by (Lempert 2003).

The EMA workbench uses these concepts to construct experiments. These experiments give us insight into the relationships between the relevant uncertainties, policies, and outcomes.

3 Methodology

This Chapter explains the research methodology, which aims to identify vulnerabilities in the transmission network in 2030. The methodology contains of 5 steps.

To identify the vulnerabilities in the transmission network, we will create a simulation PCM based on the DCOPF formulation that mimics the Dutch power system in 2030. This simulation model calculates the power flows on the lines of the model per hour for the selected representative period. The DCOPF simulation is chosen for its capability of correctly simulating powerflows. It will output the used capacity of the lines, and general power system outcomes, to minimize the total system costs. We will use the governmental plans for renewable generation, planned capacity expansion upgrades, predicted demand, the current transmission grid, and the current transmission expansion plans as inputs.

Since the DCOPF formulation is limited in its functionality, a congestion-seeking algorithm created for this research by the researcher will analyze the simulation output of each experiment for actively constraining congestions. A second simulation for the same experiment is triggered when a congestion is encountered. In this second simulation, the capacity of the congested line is set to infinite capacity. The cost difference (€) between the two simulations will be used to measure the severity of the congestion caused in the line. A third simulation will be triggered if another line becomes congested due to the affected network characteristics in the second simulation. The same process is repeated for this experiment until three lines are set to infinite capacity or no extra congestion is detected. With this design, we can analyze not only the primary vulnerable lines but secondary lines as well. These secondary lines get congested when the primary lines have been congested.

To understand the influence of the uncertainty of the energy transition, we will use exploratory modeling and analysis. In particular, we will classify the development of demand for power and the construction of renewable generation plants as uncertain parameters and vary them in each of our experimental runs. The experimental setup has been split into two sets to keep the computational time manageable. One set will simulate a week in January and another a week in June.

Finally, we will discuss how we assemble the necessary data for this research design.

3.1 Power network model

As explained, the network studied in this research is composed of transmission lines between nodes. It has been attempted to identify the most vulnerable transmission lines in the network. Since testing extreme futuristic scenarios on a real-life power system is impossible, a Dutch transmission grid simulation model was used. We will build this simulation using the DCOPF formulation. This formulation is chosen because it takes the network constraints into account, as opposed to ED, but does not use too complex and detailed calculations to calculate the power flows on the network. The DCOPF formulation consists of a minimizing cost objective function while considering the constraints opposed by the lines, generators, and demand. The model will thus optimize the power flows so that the costs of the system are as low as possible and the power demand is met. When the demand is not met, a high penalty price is imposed. This ensures that the model will try to serve all power demands, for it wants to minimize the total costs. The mathematical formulation used for the simulation model in this research is described in Appendix A.

3.1.1 Input of power network model

The important network input variables in this formulation are listed here:

- Network topology and characteristics

- Renewable generation capacity
- Conventional generation capacity
- Renewable generation profiles
- Demand profiles
- Power storage
- Simulation time

A more exact explanation regarding the input variables is given in Section 3.4. We will introduce these input variables with a short description.

Network topology and characteristics

The network topology and its characteristics are static input variables and are based on the current network topology of the Dutch transmission grid, expanded with the current Dutch expansion plans of the TYNDP. Together they represent the physical grid for the year 2030 for the purpose for this purpose of this research.

Renewable and conventional generation capacity

The capacity (MW) of renewable and conventional generators will be static values in the model; The capacity of the conventional generators will be based on the Dutch plans for conventional generators until 2030. The capacity of the renewable generators will be based on the two policy plans imposed by the government; the offshore wind plans and the RESA plans.

Demand and renewable generation profiles

The demand and renewable generation profiles differ per timestep in the model. renewable generation profiles refer to the patterns of electricity generation from vRES. Since renewable energy sources depend on natural resources like sun, wind, or water, their generation profiles will vary depending on the weather and the time of day or year. Demand profiles will also differ depending on these factors. When it's cold, more power will be necessary for heating.

The renewable generation profiles are based on the value given for the capacity of each renewable generator. The power demand will be allocated to each node following a methodology based on the energy demand.

Power storage

Renewable power storage will not be added to the model; while writing this thesis, the government's policy plans regarding renewable energy storage were not yet concrete. The KEV (PBL et al. 2022) does not mention storage plans. There are explorative studies for the storage of hydrogen in salt caverns (Serge van Gessel et al. 2021), and the Dutch government has started a national program for Hydrogen in the Netherlands (Programma 2023). In addition, recently, the news was published that the TSO has open requests for 27 GW of battery connections to the grid from the private sector(Sultiens 2023). When experimenting with the transmission grid, these plans were not concrete yet. For this reason, they are not embedded in the model.

Simulation time

The base model will have input values for each hour of 2030; since a year has 8760 timesteps we will simulate the base model for 8760 hourly timesteps.

3.1.2 Output of network model

In this research, we will measure the vulnerability of the lines by the congestion management costs it causes. The higher the congestion management costs, the higher the vulnerability of the line under consideration. The standard DCOPF formulation cannot extract these congestion management costs. For this reason, we will add a congestion-seeking algorithm to the model, which will be introduced in Section 3.2. This congestion-seeking algorithm needs the following output from the DCOPF simulation:

- The power flow on each line, for each timestep.
- The shadow prices on each node, for each timestep
- The total amount of system costs.

In addition to the vulnerability of the lines, we want to have insight into the energy system's performance. This is important for interpreting the results since the transmission grid can be seen as a subsystem of the Dutch energy system. The performance of the power system can be measured in multiple ways. For this purpose, we will extract the following extra output from the DCOPF simulation:

- Total emissions for the whole simulation (ton CO₂)
- Curtailment of renewable energy (MWh)
- The unserved demand (MWh)

These three and the system's total costs will give an overview of the system's performance following the Energy trilemma index of the WEC. The policymakers will try to minimize each of these metrics. The costs indicate the affordability of the system. The emissions indicate how sustainable the system will be. The unserved demand indicates how reliable the system will be. The curtailment of renewable energy will indicate how balanced the system will be. The shadow prices on the nodes will help determine whether congestion management has been used while a line was congested.

3.1.3 Conceptual model

A simple conceptual model representing the DCOPF simulation model of the 2030 transmission grid can be found in Figure 4. The conceptual model represents the simulation model used for this research. The simulation model was built using the power system simulation tool SAInt (Pambour et al. 2017), licensed by Encoord Inc.

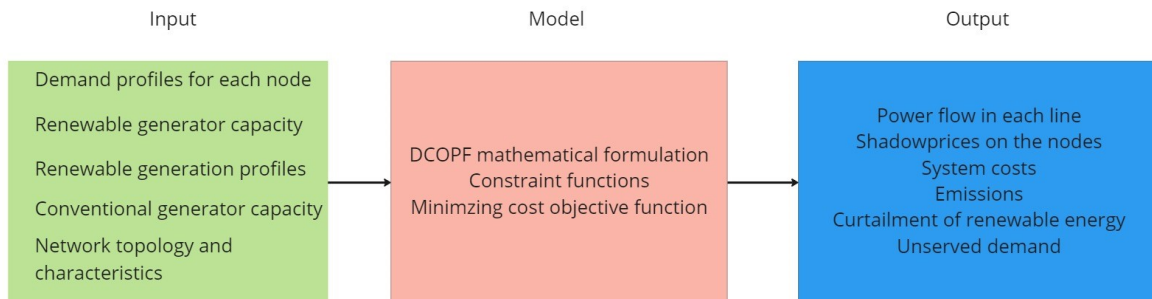


Figure 4: Conceptual model DCOPF.

3.2 Congestion seeking algorithm

The congestion-seeking algorithm is an extension of the DCOPF simulation model. The algorithm aims to analyze the vulnerability of the lines. The inputs that the algorithm uses are the shadow prices of the nodes and the power flows on the lines, both for each timestep, as well as the total costs. The algorithm's output is the congested lines and the severity of congestion in €. The congestion-seeking algorithm not only identifies vulnerable lines that would create bottlenecks but also finds the lines that would become the new bottlenecks in the system when the primarily identified bottlenecks would receive capacity upgrades. We, therefore, categorize the lines into primary lines and secondary lines. Primary lines are vulnerable to congestion before any capacity upgrade, and secondary lines are vulnerable to congestion when a primary line has received a capacity upgrade. We will explain the core mechanics of the algorithm in the following subsection.

3.2.1 Core mechanics

The congestion-seeking algorithm analyses the output of the DCOPF simulations and determines whether the shadow prices of any of the nodes differ from one another. A difference in shadow prices on the nodes indicates that the DCOPF uses congestion management to alleviate congestion on one of the lines. This follows the congestion management theory as discussed in Section 2.2.1. The algorithm then triggers a second simulation within the experiment, where the line that caused the congestion is set to have infinite capacity. The first line of which the capacity is set to infinity is called Line A.

The severity of the congestion is measured by the cost difference between the first and second simulations, which is attributed to line A. If a new line, referred to as Line B, becomes actively congested in the second simulation, a third simulation is triggered where lines A and B are set to have an infinite capacity. The cost difference between the third and second simulations is then attributed to the congestion of line B. This process is repeated until three line capacities have been set to infinity or no new congested lines are identified.

To ensure completeness of the results, the process is repeated for every originally congested line, as well as any lines that become congested in a newly triggered simulation. The originally congested lines are stored in a list, 'InfiniteLinesA', so that no unnecessary extra simulations are triggered to calculate the costs of this line.

In this research, we have set the line depth of the algorithm, thus at three lines. When three lines are set to infinite capacity in a simulation, extra simulations are no longer triggered. A higher line depth could potentially lead to a much higher runtime of an experiment. However, this highly depends on the number of congested lines in the experiment, that triggers the extra simulations. The depth of the algorithm is chosen to be 3 lines as a tradeoff between runtimes and analysis thoroughness.

A more detailed explanation of the congestion-seeking algorithm can be found in Appendix F. A validation and in-depth explanation of the working of the triggering of extra simulations can be found in Appendix H.3; the next Section provides an example of how the algorithm works.

3.2.2 Example of algorithm mechanisms

An example of which simulations are run and how they are triggered is given in Figure 5. This example demonstrates the iterative process of the congestion-seeking algorithm. In the original simulation, Sim(Base), Line 1 was congested at a certain timestep, and Line 2 was congested at a later timestep. Both Lines 1 and 2 are placed in the list 'InfiniteLinesA'. 2 new simulations are triggered, one in which Line 1 is set to infinite capacity, Sim(1), and one in which Line 2 is set to

infinite capacity, Sim(2). In Sim(1), Lines 3 and 4 become congested at separate timesteps and are stored in the list InfiniteLinesB for Line 1. The algorithm then runs another simulation in which Lines 1 and 3 are set to infinite capacity, Sim(1,3). In Sim(1,3), Line 5 became congested. This leads to a third simulation in which Lines 1, 3, and 5 are set to infinite capacity, Sim(1,3,5). Sim(2) returned that Lines 5 and 6 were congested at separate timesteps. This triggered the simulations, Sim(2,5) and Sim(2,6). In Sim(2,5), congestion was detected for Lines 3 and 1. A new simulation for Lines 2,5 and 3 is started, Sim(2,5,3). No new simulation with Line 1 is started after Sim(2,5) since it is earlier identified as a primary Line. Sim(2,6) had no congested Lines.

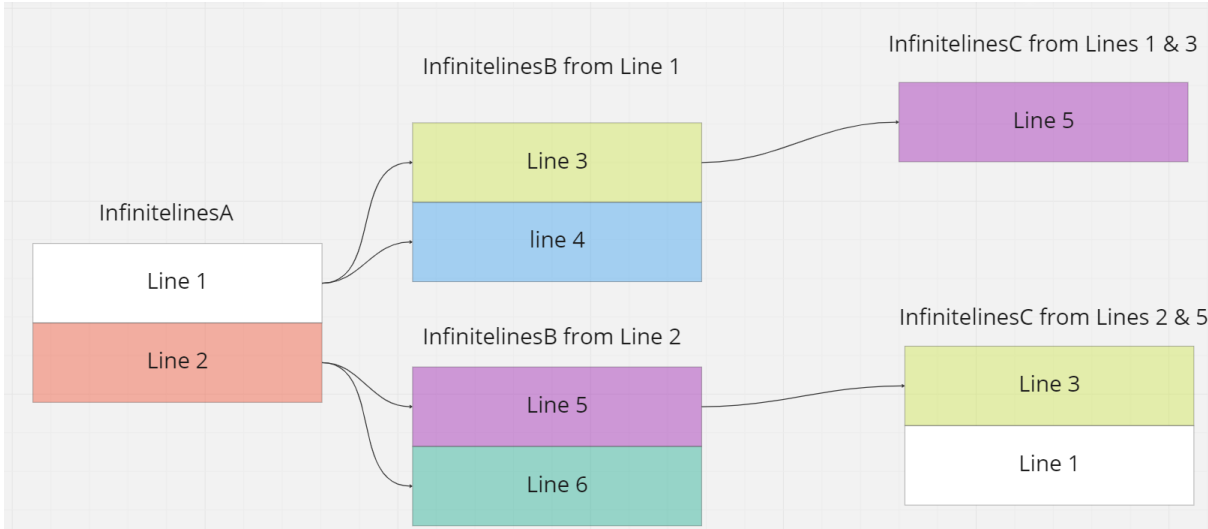


Figure 5: Simulation flowchart

In this experiment, nine different simulations are performed, with different combinations of lines set to infinite capacity. In Table 1, the simulations following this flowchart can be viewed.

| Simulation number | Simulation name | Line A | Line B | Line C |
|-------------------|-----------------|--------|--------|--------|
| 1 | Sim(Base) | x | x | x |
| 2 | Sim(1) | 1 | x | x |
| 3 | Sim(1,3) | 1 | 3 | x |
| 4 | Sim(1,3,5) | 1 | 3 | 5 |
| 5 | Sim(1,4) | 1 | 4 | x |
| 6 | Sim(2) | 2 | x | x |
| 7 | Sim(2,5) | 2 | 5 | x |
| 8 | Sim(2,5,3) | 2 | 5 | 3 |
| 9 | Sim(2,6) | 2 | 6 | x |

Table 1: Simulations leading out of the example run.

How the severity of the congestion is measured for each line is shown in Table 2. The notation of the total costs of a simulation is Sim(Line A, Line B, Line C). The original simulation is denoted as Sim(Base). When multiple possibilities exist for measuring the severity of one of the lines in the run, the highest amount is chosen. This raises somewhat bias in the results. However, as this study aims to identify the most vulnerable lines, the adopted methodology is considered to be the most appropriate.

| Line | Congestion severity |
|------|--|
| 1 | $\text{Sim}(\text{Base}) - \text{Sim}(1)$ |
| 2 | $\text{Sim}(\text{Base}) - \text{Sim}(2)$ |
| 3 | $\text{Max}((\text{Sim}(1) - \text{Sim}(1,3)), (\text{Sim}(2,5) - \text{Sim}(2,5,3)))$ |
| 4 | $\text{Sim}(1) - \text{Sim}(1,4)$ |
| 5 | $\text{Max}((\text{Sim}(1,3) - \text{Sim}(1,3,5)), (\text{Sim}(2) - \text{Sim}(2,5)))$ |
| 6 | $\text{Sim}(2) - \text{Sim}(2,6)$ |

Table 2: Calculation of congestion severity

For Lines 1, 3 and 5, the severity of the congestion through the congestion-seeking algorithm in this example is visualized in Figure 6.

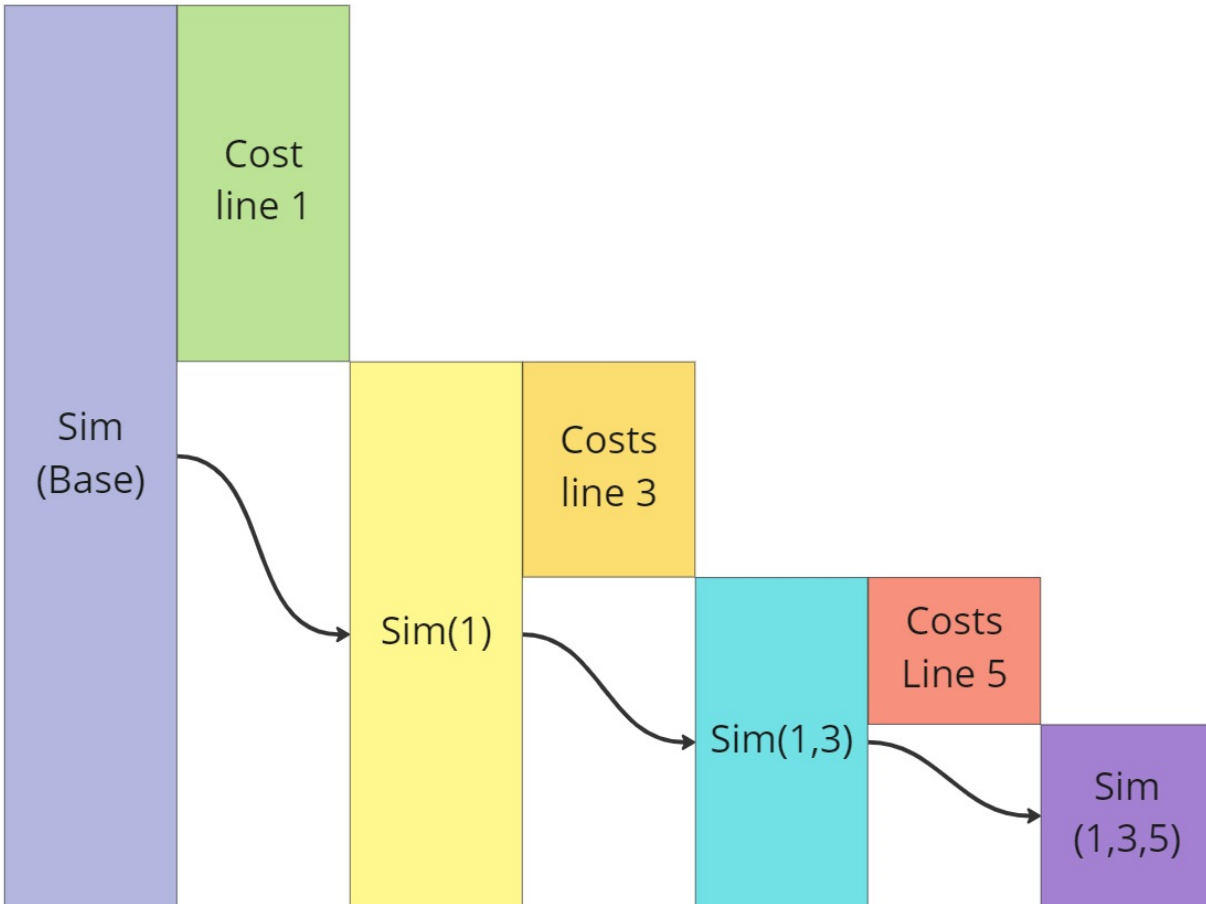


Figure 6: Visual representation of the cost attribution throughout the simulations.

The figure illustrates how the costs are attributed to the congested lines by the algorithm. For example, the costs of $\text{Sim}(\text{Base})$ were €15,000. The costs for $\text{Sim}(1)$ were €10,000. The costs attributed to Line 1 in this experiment are therefore €5,000; since the capacity of line 1 constrains the minimizing objective function by €5,000.

3.2.3 Algorithm output

The output of the algorithm is limited to costs per line. Utilizing the algorithm's depth, we can distinguish between three categories.

- Primary congested lines
- Secondary congested lines

- Non-vulnerable lines.

Primary congested lines

In the original simulation without any upgrade, the congested lines encountered are termed as the primary congested lines. These lines are the first bottlenecks for the network's power flow. Following the algorithm specification, these lines are placed in the list `infiniteLinesA`.

Secondary congested lines

The secondary congested lines become congested after the primary congested lines have been set to infinite capacity by the algorithm. In the original simulation, these lines would not have become congested. However, due to the capacity expansion of the original congestion, these vulnerable lines are revealed. This informs us about the influence of upgrading the primary lines on the network. For instance, the capacity expansion of a primary line could lead to a reallocation of the initial congestion to a secondary line. Lines that would have technically been tertiary lines will also fall in this category.

Non-vulnerable lines

The non-vulnerable lines do not become congested in all conducted simulations. We will not analyze these further.

Amongst these three categories, we will make a subdivision between more vulnerable and less vulnerable lines. How we will distinguish the three line categories will be discussed in Section 3.3.4.

3.2.4 Conceptual model

We can add the congestion-seeking algorithm to the conceptual model of Figure 4. The updated conceptual model is shown in Figure 7. This Figure, shows how the congestion-seeking algorithm is added to the model and what input it needs.

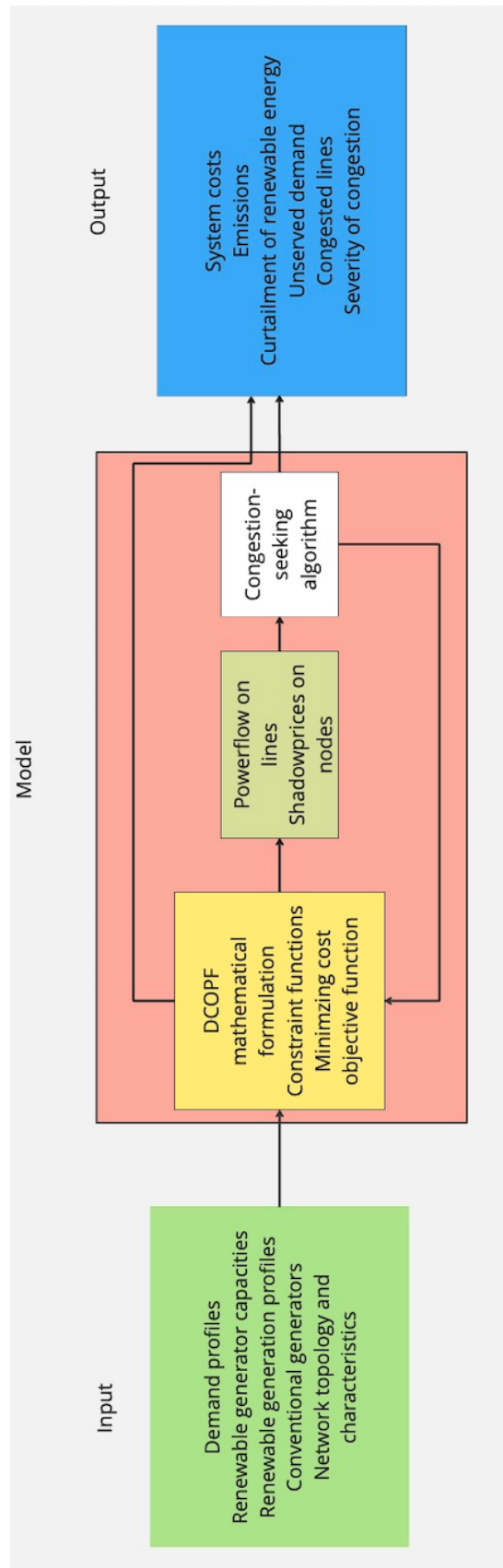


Figure 7: Updated Conceptual model DCOPF with congestion seeking algorithm.

3.3 Exploratory modeling

As discussed in Section 2.5, Exploratory Modelling and Analysis (EMA) is a suite of effective tools for exploring uncertainties in a system. In this research, we aim to find the most impactful uncertainties regarding the vulnerability of the lines. We will first break down the system

into elements to achieve this goal and identify the uncertainties associated with each element. We then introduce our exploratory modeling framework to analyze the identified uncertainties. Finally, we will explain the setup for our experiments using the exploratory modeling framework.

3.3.1 Uncertainty specification

Based on Figure 2 ,the Dutch power system can be decomposed in to the 1) context, 2) system model 3) system outcomes and 4) weight on the outcomes.

The context can be specified as the changing energy system in the Netherlands in 2030. The uncertainty is identified as level 4, the RESA gives an idea about the energy system, yet these plans are not always detailed and prone to future adjustments. The future electricity demand is even harder to predict. Some general data about expected local population growth is available. We can use this population growth to model the global growth of demand. We need the demand growth on a more local level, however.

The system model is the DCOPF formulation describing the 2030 transmission network. The uncertainty in the system model is specified as level 2 or 3 since the TSO could pursue different kinds of expansion on its network. These expansions are not expected to change a great deal for the time scope (2022-2030), as capacity expansions on transmission networks take some time to finish.

The system outcomes are those specified in Sections 3.1.2 and 3.2.3. We classify these as level 4 since it is unclear what ranges of outcomes can be expected.

The weights on the outcomes can be naturally classified as to which outcomes are more important. We classify these as level 3, since we have more interest in the vulnerable primary lines.

We conclude that the most important uncertainties to analyze are in the context of the system. The demand and generation of power for each node in the system are identified as the most uncertain. Since the context of the system is the most uncertain, we find another argument for the analysis of the general system outcomes. Analysis of the context outcomes gives us insights into how the context will change and how this will affect the system in return.

3.3.2 Modeling framework

The XLRM framework is the base for exploratory modelling approaches. As discussed in Section 3.1, the policy plans for the network until 2030 can be considered static. With this choice Implemented in the model, we effectively transform the XLRM framework into an XRM framework leaving out the policy levers (L).

Uncertain factors

We can identify the uncertain factors (X). These are:

- Beverwijk offshore wind farm
- Borssele offshore wind farm
- Eemshaven offshore wind farm
- Geertruidenberg offshore wind farm
- Maasvlakte offshore wind farm
- RESA generators
- Demand for power
- Weather year

Generation and demand uncertainties

The 5 wind farms connected with the nodes and the RESA plans as a whole are chosen to be power generation uncertainties. This means that all profiles for all the generators taken from the RESA plans will be multiplied by the uncertainty parameter in an experiment. The same goes for all demand profiles in the system. The demand for power is taken as the only demand uncertainty. This means that the demand in the whole of the Netherlands will either be high or low in an experiment, and the geographical distribution does not change. The factor

Weather year uncertainties

A weather year is a set of weather data representing a typical year of weather conditions in a given region. In power systems, weather years are often used for experimentation and simulation purposes to evaluate the performance of power systems and the impact of renewable energy sources on the grid.

The weather conditions do not only influence the performance of solar and wind generators. Demand is influenced by the weather as well; when it is very cold, more demand for power will ensue. The demand and vRES generation therefore share a common influencing variable: the weather. For this reason, we group the demand, solar and wind profiles of a year together in a weather year. The weather year variable contains all the demand and renewable generation profiles for the relevant historical years. These profiles are based on historical data. The weather year uncertainty is therefore, not like the other uncertainties. Whereas the other uncertainties determine the factor with which the profile values will be multiplied, the weather year determines which profiles are used. In Section 3.5, it is explained what effect the weather year uncertainty has on the generation and demand.

Relations in the model

The Relationships in the Model (R) is the problem's DCOPF formulation. This is a cost-minimizing objective function bound by constraints. The static input factors that will be 'hard coded' in this model formulation are the current transmission network with the planned capacity expansions and the conventional generators; these will not be viewed as experimental parameters.

Uncertainty and experimental space

In EMA, the ranges of each uncertainty together make up the experimental space. Each uncertainty adds another dimension to this uncertainty space. For this research, we will thus have an uncertainty space of 8 dimensions as listed in Table 3 below. The experiments will be drawn from this uncertainty space and create the experimental space.

Model outcomes

The outcomes (M) of the system are the power flows on the lines, and the following system outcomes:

- Total costs
- Total Emissions
- Unserved Demand
- Curtailment of renewable energy
- Shadow prices on the nodes

3.3.3 Experiment setup

To generate sufficient data to analyze the impact of the uncertainties on the congestion of the lines, we picked 1000 runs to analyze the impact of each uncertainty thoroughly. Since 1000 runs for the whole year is not feasible regarding computational effort, the simulation timesteps

had to be trimmed down. Two weeks were found to give representative results covering annual seasonal variations, see Appendix E for further detail. One set is based on the timesteps between 2030/08/01/00:00 - 15/01/00:00, a week in January. The second set is based on the timesteps between 2030/08/06/00:00 - 2030/15/06/00:00. The same seed will be taken in the production of the experimental space from the uncertainty space. This leads to the same experimental space for both sets. The tool that is used to create this experimental space is the EMA workbench. The values used to create the uncertainty space are given in Table 3. It is important to note that the factor given to the uncertainty multiplies the entire profile for that particular uncertainty. The weather year influences all of the profiles based on values from historical data. For example, in an experiment, a value of 1.5 is drawn for the demand, and the weather year is drawn to be 2017, all of the demand profiles based on the historical data of 2017 will be multiplied by 1.5. For the wind and solar generators, the installed capacity is multiplied by this factor (which is multiplied by the historical time series).

| Uncertainty | Lower bound | Upper bound | Type |
|-------------------------|--------------------|--------------------|-------------|
| BorsseleOffshore | 0,5 | 2 | Continuous |
| MaasvlakteOffshore | 0,5 | 2 | Continuous |
| BeverwijkOffshore | 0,5 | 2 | Continuous |
| EemshavenOffshore | 0,5 | 2 | Continuous |
| GeertruidenbergOffshore | 0,5 | 2 | Continuous |
| RESA | 0,5 | 2 | Continuous |
| Demand | 0,5 | 2 | Continuous |
| Weatheryear | 2015 | 2019 | Discrete |

Table 3: Uncertainties and their ranges

Production uncertainties

Each of the offshore wind farms has been deemed as an individual uncertainty. The uncertainty related to wind farms is threefold:

- The connections to the inland nodes are not definite
- The amount of wind power in each wind farm could differ in the future.
- The type of turbine placed at the offshore wind farms is uncertain.

Also, the nodes' RESA policy plans are also uncertain. These are iterative plans that will be updated regularly. The likelihood that these will be changed in future iterations of the plans is large. All of the plans are taken as one uncertainty since, in this research, it is seen as one policy option by the government. In addition, early experiments, as seen in Appendix E, pointed out that these policy instruments did not have a high influence on the vulnerability of the lines.

Demand uncertainty

How demand for power will develop is uncertain due to uncertainty around the transition from gas to power in the Netherlands. It is also uncertain how the hydrogen industry will develop and what effect this development will have on the power demand in the Netherlands. It is uncertain whether industries currently reliant on gas will switch to power, hydrogen, or another energy form. Therefore, the power demand may rise or fall in the coming years.

XRM framework

The XRM framework can be populated with the identified uncertainties, desired outcomes, and model relationships. The framework can be found in Figure 8.

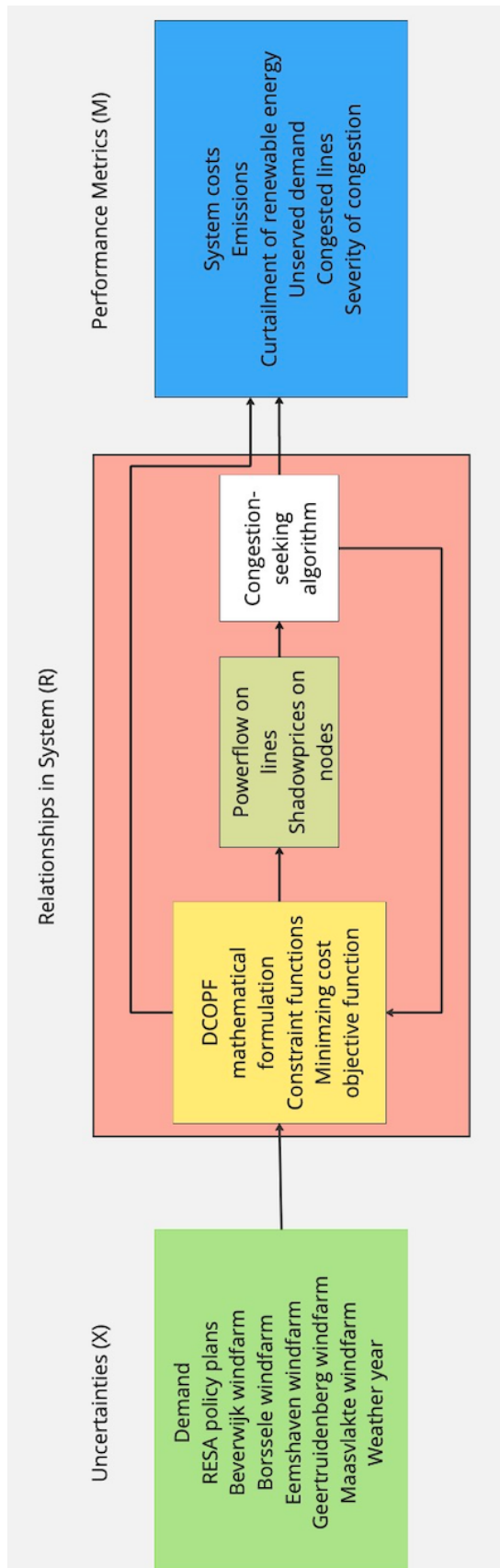


Figure 8: Filled in XRM framework.

3.3.4 Outcome analysis

The experiment's performance metrics must be analyzed to place the network lines in categories. Since the output of the lines is limited to the costs attributed per experimental run, we must find correlations between the analyses of the lines to identify secondary lines. We use scenario

discovery and the location of the lines within the network to find when a line becomes congested. This will give us insights on how the power in the network flows when the line becomes congested. We also analyze the general system outcomes with scenario discovery to see how the uncertainties will influence the power system.

There is a distinction between the general system outcomes, which give an indication of the state of the system, and the outcomes for the lines. We will categorize the lines on 2 characteristics. The first is the vulnerability of the lines. The second is whether the line can be classified as a primary or secondary bottleneck. We are particularly interested in the highly vulnerable lines that are primary bottlenecks. In this research, highly vulnerable lines become congested in more than 20 percent of the experiments. Lines with moderate vulnerability become congested in more than 5 percent of the experiment set, but less than 20 percent. Lines with low vulnerability become congested in less than 5 percent of the experiments. These will not be analyzed. In Table 4, an overview of the importance of each category is shown.

| | Primary congestion | Secondary congestion |
|------------------------|---------------------|----------------------|
| High vulnerability | Critical importance | High importance |
| Moderate vulnerability | Moderate importance | Low importance |

Table 4: Categorization of importance of lines

Scenario discovery

Scenario discovery will be used to determine under which values of the uncertain parameters a line becomes congested. Giving insight into the circumstances under which a line becomes vulnerable will give insight into what the most influential uncertain factors are, and which lines are most vulnerable to congestion. Using the location and the wind farm uncertainties we can get an index how the power will flow when the vulnerable lines becomes congested. The algorithm we will use for scenario discovery is the Patient Rule Induction Method (PRIM) algorithm implemented in the EMA workbench (Jan H Kwakkel 2017) In Table 5, a summary of which experiments will be used for each outcome is shown.

| Outcome | Category | Input set of experiments | Subset |
|------------------|----------|---|--|
| System costs | General | All scenarios | Scenarios with costs |
| Emissions | General | All scenarios | Scenarios with emissions |
| Unserved Demand | General | All scenarios | Scenarios with unserved demand |
| Curtailed Energy | General | All scenarios | Scenarios with 20% of renewable energy curtailed |
| Primary lines | Lines | Scenarios with costs | Scenarios with costs on primary line |
| Secondary lines | Lines | Scenarios with costs on identified primary line | Scenarios with costs on secondary line |

Table 5: Input for outcome analysis

3.4 Power model data

In this Section, the necessary data for the network elements for the DCOPF approach, will be discussed.

3.4.1 Network topology

The first step of the model setup is defining the network topology. This refers to how the generation and demand of the power flows must be aggregated. The network topology can be found in Figure 9. The labels in this picture represent the names of the nodes. An overview of the Full Dutch high-voltage grid as visualized by the TSO can be found in Figure 10. As can be seen, the difference with the actual grid is that there are no interconnections with other countries. This is outside of the research scope. The network model contains 37 nodes, of which five are transformer stations, and 45 lines. The transformer stations connect the 220 kV with the 380 kV network. The data used to create this network can be found in Appendix D.1.

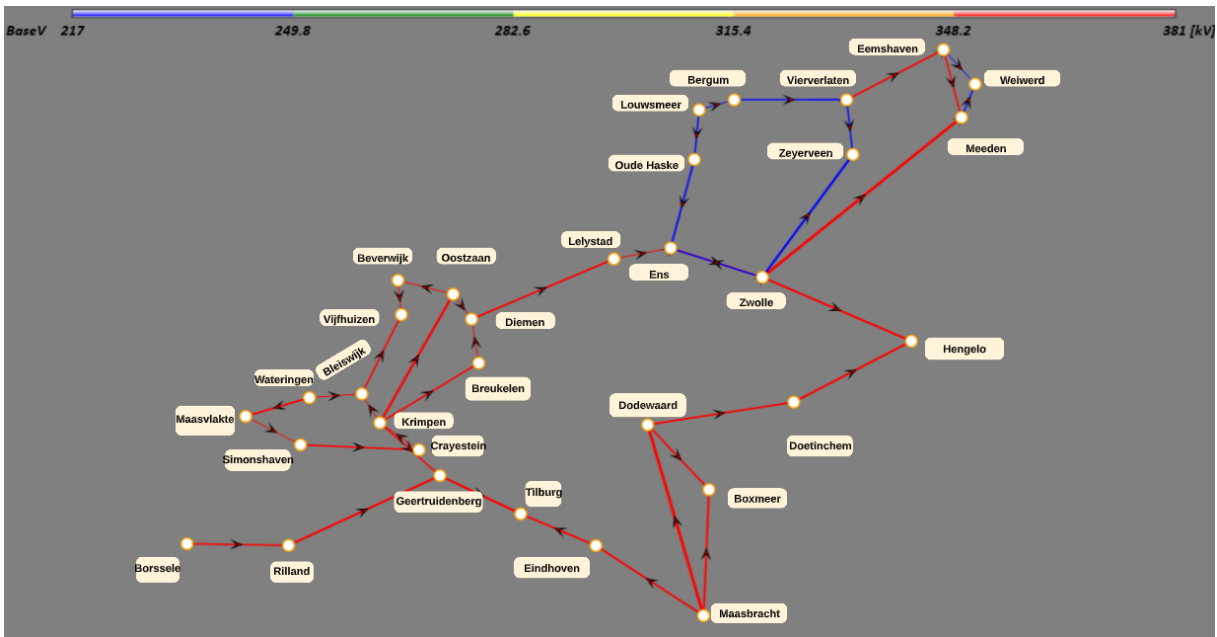


Figure 9: Network topology

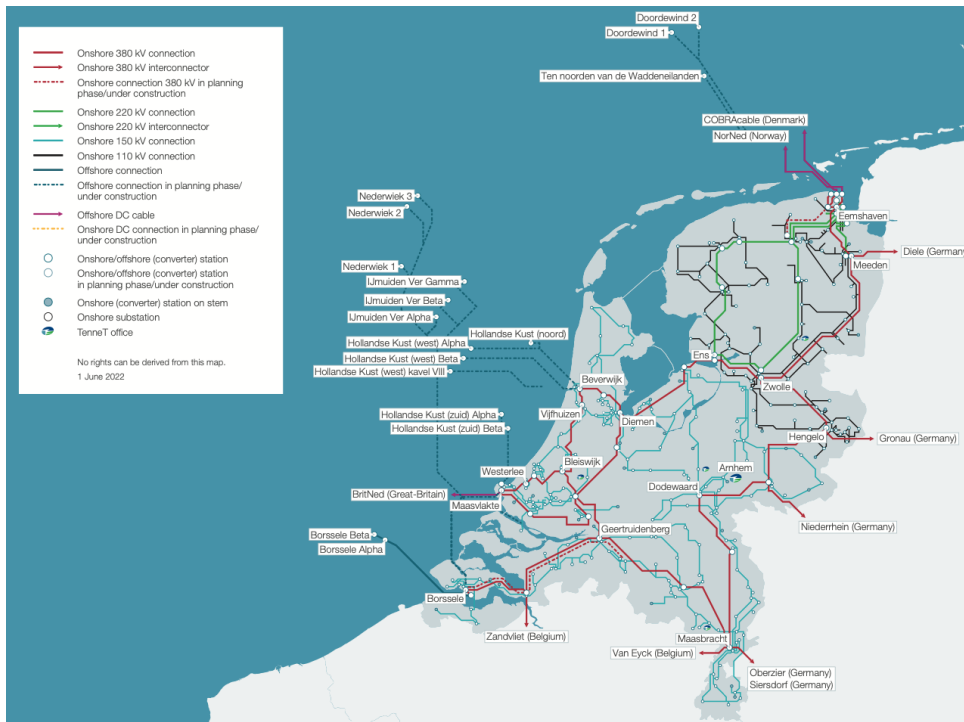


Figure 10: TenneT grid

3.4.2 Demand profile construction

For each of the nodes, a demand profile is set up. These demand profiles are based on the expected development of the demand for power in the Netherlands by (PBL et al. 2022). According to them, the total demand for power is expected to be 130 TWh. The profiles for each year have been gathered from the Transparency Platform of the ENTSO-E (ENTSO-E 2022a) and transformed to the expected hourly power demand. At this point, an hourly profile for each of the historic years has been generated for the total power demand in the Netherlands. This demand must be split and allocated to the 32 regular nodes. To factor this, data from the Regionale Klimaatmonitor is consulted (Klimaatmonitor 2022) and transformed to generate a profile for each of the nodes. This is done for each of the weather years used. A more detailed overview of the allocation of the demand profiles can be found in Appendix D.3.

3.4.3 Conventional generation

The conventional generators stem from the python library Pypsa (Brown, Hörsch, and Schlachterberger 2018) and are matched to the geographical closest node by the python library Powerplantmatching (Gotzens et al. 2019). Since the library of Pypsa is not complete, and at times not entirely accurate, the powerplants have been validated. The corresponding sources for the efficiency and the power can be found in the table below. As it can be seen, conventional generators primarily consist of gas plants and one nuclear plant. Since the Dutch government plans on phasing out the Dutch coal plants by 2030 (Rijksoverheid 2021), these have been let out. For the sake of simplicity, a static price for nuclear and gas fuels is assumed. These prices are 1182 €/kg for nuclear, and 0.33 €/m³ for gas. Dynamic fuel prices have not been added, since the price difference between energy generated from nuclear and gas generators is so high that these must differ a lot to affect the outcomes of the system. Furthermore, the capacity of the nuclear generators in comparison to gas generators is very small. A dynamic price will not bring more insight into the results and will only complicate the system. The gas plants have been divided into high-efficiency, and low-efficiency categories based on their sources, and building year. The low-efficiency generators are thus more expensive for power generation.

| Name | NodeName | Fuel | Capacity | Efficiency category | Source |
|-----------------|-------------|---------|----------|---------------------|----------------------|
| Bergum | Bergum | Gas | 146 | Low | Redactie (2021) |
| Delesto | Delesto | Gas | 530 | High | Delesto (n.d.) |
| Eems | Eemshaven | Gas | 1931 | High | Engie (n.d.[a]) |
| Magnum Centrale | Eemshaven | Gas | 1410 | High | Vattenfall (n.d.[b]) |
| Diemen | Diemen | Gas | 684 | High | Vattenfall (n.d.[a]) |
| Velsen | Beverwijk | Gas | 725 | Low | Vattenfall (n.d.[c]) |
| Merwedekanaal | Diemen | Gas | 328 | High | Eneco (n.d.[b]) |
| Flevo | Lelystad | Gas | 861.1 | High | Engie (n.d.[b]) |
| Sal | Hengelo | Gas | 60 | Low | Monitor (2022) |
| Swentibold | Maasbracht | Gas | 230 | Low | RWE (n.d.[c]) |
| Claus | Maasbracht | Gas | 1304 | High | RWE (n.d.[a]) |
| Rijnmond | Simonshaven | Gas | 820 | High | EEX (n.d.) |
| Moerdijk | Crayestein | Gas | 870 | High | RWE (n.d.[b]) |
| Borssele | Borssele | Nuclear | 485 | Nuclear | EPZ (2021) |
| Roca | Krimpen | Gas | 220 | High | Monitor (2021) |
| Elsta | Borssele | Gas | 455 | Low | Elsta (n.d.) |
| Den Haag | Wateringen | Gas | 107 | Low | Uniper (n.d.[a]) |
| Ucml | Maasvlakte | Gas | 80 | High | Uniper (n.d.[c]) |
| Ld | Bleiswijk | Gas | 85 | High | Uniper (n.d.[b]) |
| Sloecentrale | Borssele | Gas | 870 | High | Sloecentrale (n.d.) |
| Enecogen | Maasvlakte | Gas | 844 | High | Eneco (n.d.[a]) |

Table 6: Generators

3.4.4 Renewable generation

Renewable energy generation is modeled according to the policy plans of the Dutch Government. Currently, there are two policy plans that the government actively pursues. These are the offshore wind plans and the RESA plans. Since these renewable generators do not use conventional fuels, fuel costs are zero. Since we assume the market bidding will be on the marginal costs, no Operational or capital expenses will be attributed to power generation through these power sources. The RESA plans' attribution to the model nodes can be found in Appendix D.3.

RESA plans

The Capacity assigned to the renewable energy generators of the model is based on the plans of the 30 energy regions in the Netherlands. Some areas have been split up since more than one node resides in the region's span. Also, some nodes will have power from multiple areas since they lie at the borders of the areas. The methodology behind this and the exact placement of the capacity on each node can be found in Appendix D.2.

Offshore wind capacity.

Besides the RESA plans, offshore wind farms plans are laid out by the Dutch government Rijksoverheid n.d. An overview of the planned installed capacity of offshore wind is displayed in Figure 18. For these wind turbines, a hub height of 250 meters is maintained in the model, based on the newer generation prototypes developed by companies such as (GE Renewable Energy 2022) and (Vestas n.d.). The higher hub height generally means that this turbine will face higher wind speeds; thus, these turbines will generate more power.

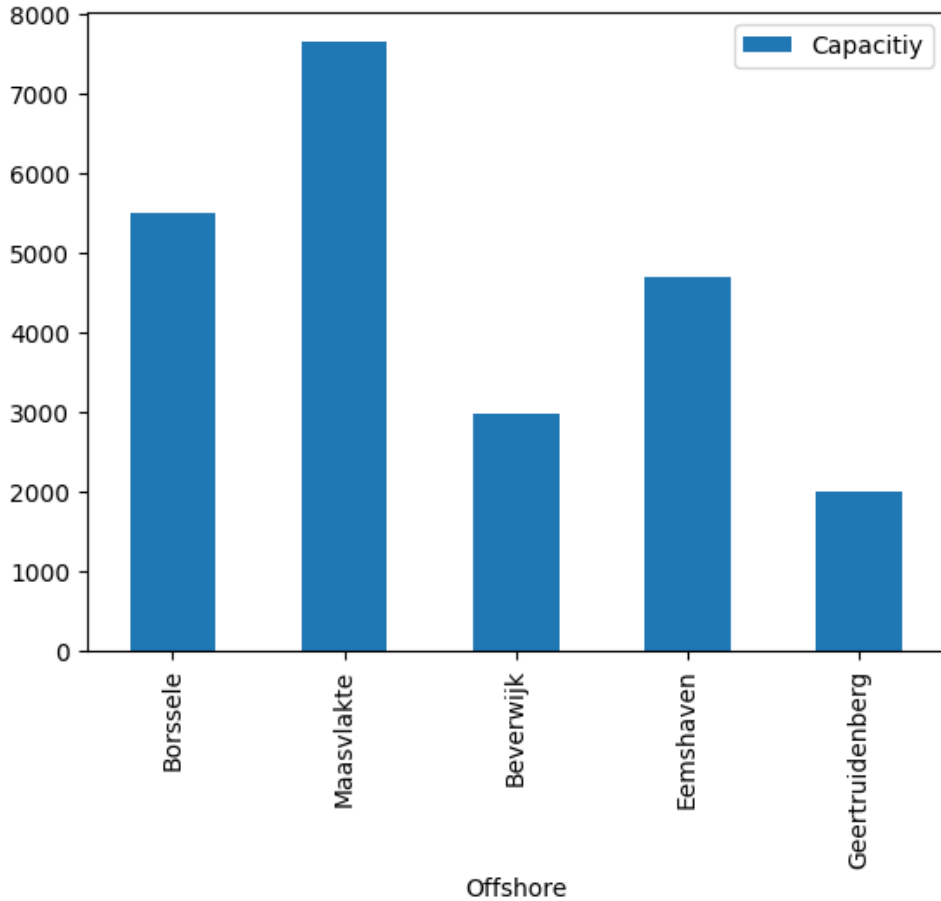


Figure 11: Capacity of offshore windfarms

3.5 Weather years

The historical data from the years 2015 to 2019 are taken to simulate the effect of the weather on the system. In Table 7, the influence of the weather years on the January experiments is shown. In Table 8, the influence of the weatheryears on the June experiments is shown. A '+' indicates that the uncertainty is bigger in the respective weather year. A '-' indicates the opposite. In Appendix G, more information on the influence of the weatheryears can be found.

| | Wind | Demand | Offshore | Solar |
|------|------|--------|----------|-------|
| 2015 | ++ | +/- | ++ | -- |
| 2016 | + | + | + | - |
| 2017 | + | +/- | +/- | - |
| 2018 | - | - | -- | - |
| 2019 | + | +/- | + | -- |

Table 7: January experiments weatheryear classification

| | Wind | Demand | Offshore | Solar |
|------|------|--------|----------|-------|
| 2015 | - | - | +/- | + |
| 2016 | -- | +/- | -- | + |
| 2017 | - | +/- | +/- | + |
| 2018 | - | +/- | - | + |
| 2019 | - | +/- | + | + |

Table 8: June experiments weather year classification

3.6 Verification

The full methodology has been verified by using a simple 5-node model representing the Dutch Transmission system in Appendix B. The congestion-seeking algorithm was slightly altered in the experiment to improve the runtime.

4 Results

In this Section, the results of the weekly experiments in June and January with 1000 runs will be analyzed. As mentioned in Section 3.3.4 we selected different outcome categories. In this Section, we will divide the lines into their categories, and analyze them accordingly. The categories for the lines were:

- primary high vulnerability lines
- Secondary high vulnerability lines
- Primary moderate vulnerability lines
- Secondary moderate vulnerability lines.

4.1 January results and analysis

4.1.1 January

Filtration of runs with costs

As described in Section 3.3.4, the results for the lines have been filtered. Only the runs with any system costs have been selected. For the January runs, 859 of the 1000 runs, had costs in them. Just these 859 have been selected for this analysis.

High vulnerability January lines

Only the lines with more than 200 runs with costs attributed to them are selected as high vulnerability lines. These lines are:

- Line 4 (Borssele - Riland)
- Line 15 (Krimpen - Breukelen)
- Line 23 (Oostzaan - Diemen)
- Line 24 (Riland - Geertruidenberg)
- Line 28 (Zwolle - Hengelo)
- Line 35 (Eemshaven - Weiwerd)
- Line 38 (Bergum - Vierverlaten)

moderate vulnerability January lines

Only the lines that have more than 50 but less than 200 runs with costs attributed to them are selected as moderate vulnerability Lines.

- Line 6 (Breukelen - Diemen)
- Line 13 (Geertruidenberg - Tilburg)
- Line 22 (Maasvlakte - Simonshaven)
- Line 26 (Wateringen - Bleiswijk)
- line 27 (Maasvlakte - Wateringen)
- Line 31 (Louwersmeer - Vierverlaten)
- Line 37 (Vierverlaten - Zeyerveen)

In Figure 12, the high vulnerability lines have been labelled with a pink label. The moderate vulnerability lines have been labelled with a green label.

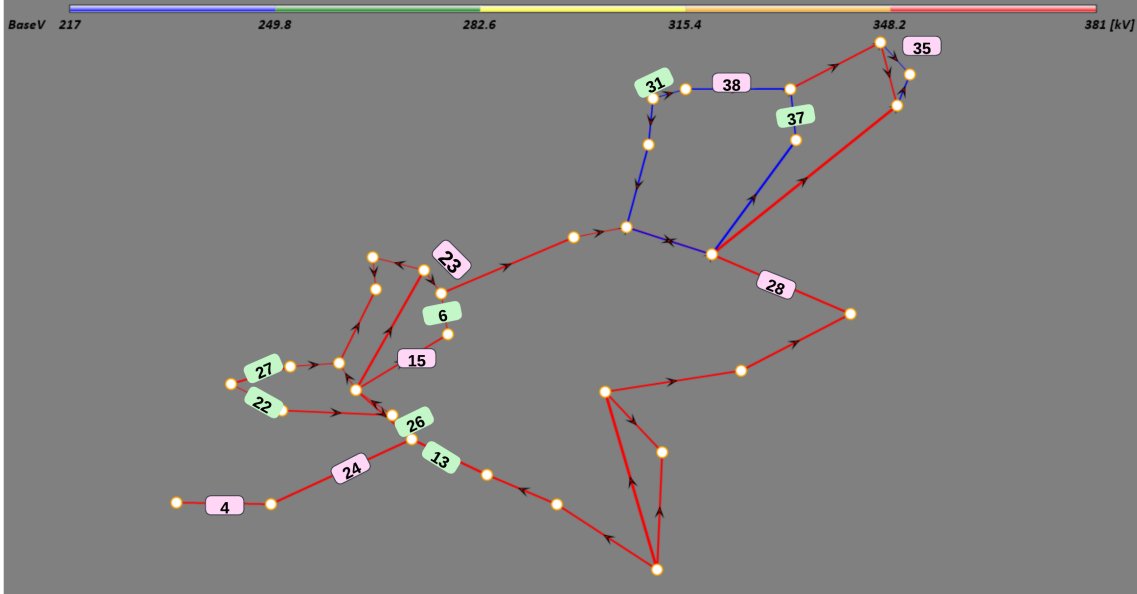


Figure 12: Vulnerability lines in the network following January experiments.

4.1.2 General results

In Table 9, the summary of the PRIM results for the vulnerable lines can be found. Beverwijk and Eemshaven have been left out of the analysis. These had almost no influence on the general outcomes. The PRIM analyses are in Appendix I.

| General Outcomes (runs) | Demand | Borssele | Geertruidenberg | Maasvlakte | RESA | Weather-years |
|-------------------------|---------|----------|-----------------|------------|---------|---------------|
| Costs (859) | 0.9-2.0 | 0.5-1.9 | x | 0.6-2.0 | 0.6-2.0 | 2018 |
| Emissions (859) | 0.6-2.0 | 0.5-1.9 | 0.5-1.9 | 0.6-2.0 | x | 2018 |
| Unserviced demand (595) | 0.9-2.0 | 0.5-1.9 | x | 0.6-2.0 | 0.6-2.0 | 2018 |

Table 9: Thresholds of uncertainties for general system outcomes for January experiments.

For each of the general system outcomes in this table see similar uncertainty thresholds.

System costs

The main uncertainty for the system costs is the demand. The threshold for this uncertainty is 90% of the demand in the base scenario; costs will occur in the system. The prim analysis in the appendix shows that it is still possible for an experiment with a lower demand variable to have costs in them. It is not 100% certain. The other uncertainties do not show strong influences on the cost variable. That costs will still occur in the 2030 system is no surprising finding; It is not the goal of the power system to become completely costless.

System emissions

The same results came from the prim analysis for this variable as for the system costs. This

is because both are a derivative of the fuel consumption in the simulation model. Next to the penalty price of demand, the fuel costs are the only cost factor in the simulation model. The only factor causing emissions is the fuel. The only difference between the two is the threshold for the demand, this is lower for the emissions.

Unserved demand

The unserved demand shares the same results as the system costs. The primary uncertainty is the demand with the same threshold. The other uncertainties do not have a great influence on this outcome.

Curtailed energy

In Figure 13, the percentage of curtailed renewable energy over the runs can be seen. The figure shows that there was a very small amount of runs that had zero percent of curtailed energy. We can learn from this curve shows that in the modeled system, in January, in almost all of the experiments the potential renewable power is not met.

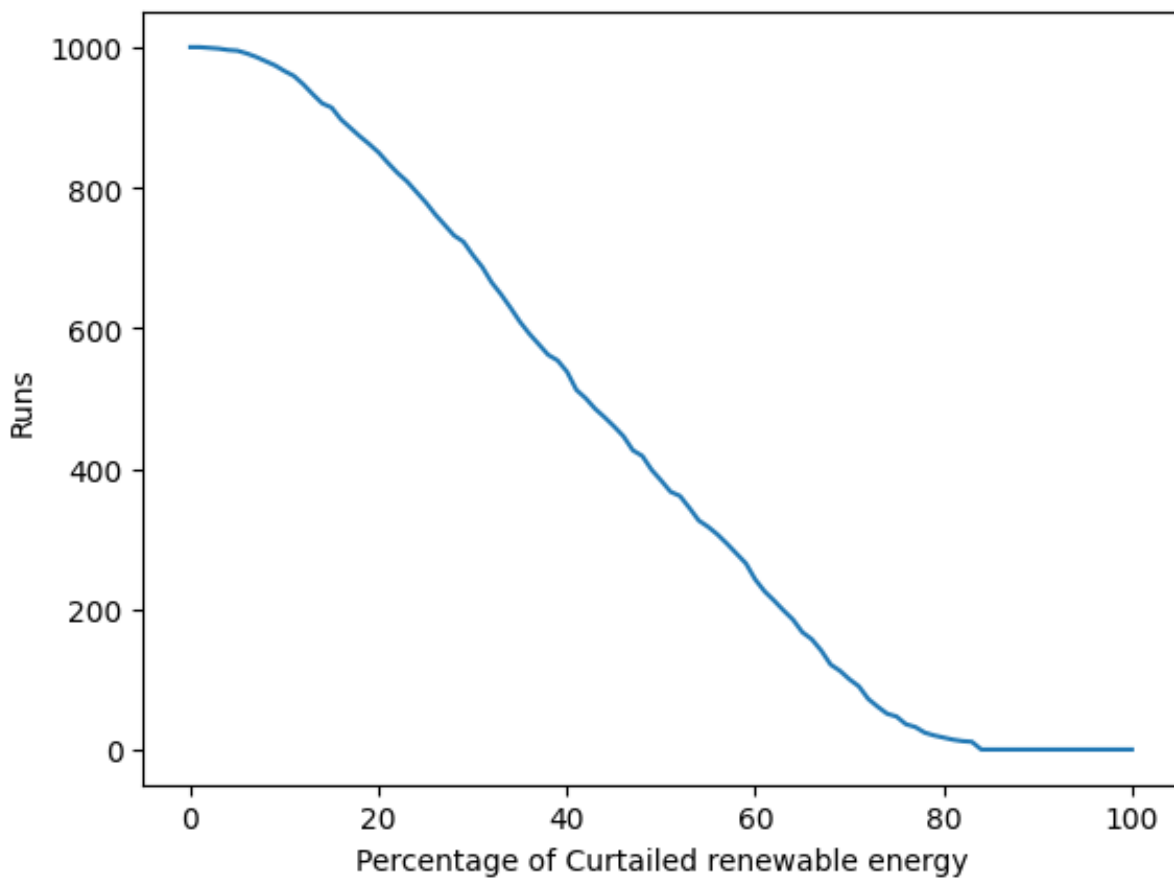


Figure 13: Curtailed energy over the runs

4.1.3 High Vulnerability lines

In Table 10, the summary of the PRIM results for the vulnerable lines can be found. The full PRIM analyses are in Appendix I. An 'x' means that the uncertainty has no significant influence on the congestion of the line.

| Line (runs) | Demand | Borssele | Eemshaven | Geertruidenberg | Maasvlakte | Weather-years |
|-------------|---------|----------|-----------|-----------------|------------|---------------|
| 4 (342) | 1.5-2.0 | 1.0-2.0 | x | 0.5-1.9 | x | 2015-2017 |
| 15 (384) | 1.3-2.0 | x | x | x | 0.8-2.0 | 2016 |
| 23 (462) | 1.2-2.0 | x | x | x | x | x |
| 24 (417) | 0.9-2.0 | 1.0-2.0 | x | 0.5-1.8 | 0.5-1.9 | 2015 |
| 28 (279) | 1.6-2.0 | x | 0.8-2.0 | x | 0.6-1.9 | 2016-2018 |
| 35 (636) | 1.2-2.0 | x | x | x | x | 2016-2019 |
| 38 (690) | 1.0-2.0 | 0.6-2.0 | 1.0-2.0 | x | 0.7-1.9 | 2015, 2018 |

Table 10: Thresholds of uncertainties on highly vulnerable lines by PRIM analysis for January experiments.

The results show that for each of the lines, the Demand for power and the weather year are the most influential uncertainties. The RESA policy plans and the Beverwijk offshore wind farm have little to no influence on the congestion on the lines. These have been left out of the analysis.

Line 4

The primary uncertainty for line 4 is the demand. the threshold for this uncertainty lies on an increase of 50% compared to the base case, which will lead to almost certain congestion on this line. The secondary uncertainty is the capacity on the Borssele windfarm. The threshold of this line lies exactly on the capacity allocated in the base case. The analysis showed that the line will almost certainly become congested when both these thresholds are met.

This occurs especially with the historical data of 2015,2016 and 2017. These years score average or more than average for offshore wind and demand. The uncertainty of Geertruidenberg has a limiting effect on the congestion of this line. When the capacity of offshore wind allocated to this node is more than 90% compared to the base scenario, less congestion will occur in this line.

From the uncertainty parameters and the position of this line, we can conclude that this line becomes congested due to the power generated at the Borssele wind farm. When the power flow from this wind farm becomes too high, the line will become congested. If the capacity from Geertruidenberg is high enough, the line will not become congested since this wind farm is more central in the network. The power from the windfarm in Borssele is not necessary at those points.

Furthermore, we can conclude that this line could be a secondary line while taking the capacity into account. It has a higher capacity than line 24, which is the next line that needs to be used to trasport the power from the Borssele wind farm.

Line 15

The primary uncertainty for line 15 is the demand.The threshold for this uncertainty is met when the demand for power is 30 % higher than the base case. The secondary uncertainty is the capacity of the offshore wind farm of Maasvlakte. The threshold for this uncertainty is met when than 80% of the planned capacity allocated in the base case.

When both the uncertainty thresholds are met, the line has a high chance to become congested.

The most congestion with this combination of uncertain parameters were encountered with the weather year of 2016; this year has a higher share of offshore wind and demand than average. From these uncertainty parameters and the position of the line, we can conclude that this line becomes congested due to transporting power from the Maasvlakte wind farm to the rest of the Netherlands.

Line 23

The primary uncertainty for line 23 is the demand. The threshold for this uncertainty is met when the demand for power is higher than 20 % in comparison to the base case. There are no other uncertainty thresholds for this line.

From the position of the line we would expect that the wind farm of Beverwijk would have influence on its congestion. The factor for this uncertainty is set too low for this to influence the line.

Line 24

The primary uncertainty for line 24 is the wind farm of Borssele. The threshold for this uncertainty is the capacity of the wind farm in the base case. The secondary uncertainty is that of the demand for power. The threshold is 90% in comparison to the demand in the base case. In especially the experiments performed with the historical data of 2015, this line had a lot of congestion. This year had a high output of offshore wind and average wind.

Both the wind farms of Maasvlakte and Geertruidenberg have a limiting effect on the congestion. When both these wind farms have a high capacity, less congestion will occur on this line

From the uncertainty parameters and the position of this line, we can conclude that this line becomes congested due to the power generated at the Borssele wind farm. When the power flow from this wind farm becomes too high, the line will become congested. If the capacity from Geertruidenberg and Maasvlakte is high enough, the line will not become congested since these will produce enough power to serve the demand. The power from the wind farm in Borssele is not necessary at those points.

From the uncertainty parameters, we can conclude that this is a highly vulnerable line; With no extreme input values, the line will still be vulnerable to congestion.

Line 28

The primary uncertainty for line 28 is the demand. The threshold for this is 60% higher than the base case. The secondary uncertainty is the wind farm of Eemshaven. The threshold for this uncertainty is 80% of the base case. When both these thresholds are met, the line is vulnerable to congestion. This especially happens in the profiles based on the historic data from the years 2016 to 2018.

The Maasvlakte wind farm has both a limiting and increasing role in the congestion on this line. Both these roles are not strong. This can be explained by the fact that line 28 and the node of Maasvlakte are far apart from each other in the network.

When this line becomes congested, it is because of the wind power coming from Eemshaven that flows via this line to the East of the Netherlands. Some power coming from the Maasvlakte wind farm also flows via this line to the East of the Netherlands when this line is congested. However, when the power from the Maasvlakte wind farm is too big, the power from this wind farm will flow via the South of the Netherlands to the East. Less power from Eemshaven is necessary, and line 28 will not become congested.

Line 35

The primary uncertainty for line 35 is the demand. The threshold for this uncertainty is met when the demand for power is higher than 20 % in comparison to the base case. There are no other uncertainty thresholds for this line.

We found the relatively big amount of congestion on this line surprising. The demand allocated

to the node of Weiwerd is small, furthermore there is a line that is parallel next to this line. It could be that the DCOPF optimization causes the power flow to go via this line. From the position of the line we would expect that the wind farm of Eemshaven would have an influence on its congestion.

Line 38

For line 38, the two primary uncertainties are the demand and the capacity of the wind farm of Eemshaven. The thresholds for both these uncertainties lie at the input values of the base case. We conclude that this line thus gets congested by power from Eemshaven, being transported to serve demand in the South of the Netherlands.

It is a critically vulnerable line since it could get congested in the base scenario.

4.1.4 Moderately vulnerable lines

| Line (runs) | Demand | Beverwijk | Geertruidenberg | Maasvlakte | RESA | Weather-years |
|-------------|---------|-----------|-----------------|------------|---------|---------------|
| 6 (148) | 1.1-2.0 | x | 0.9-2.0 | 1.1-1.9 | x | 2017 |
| 13 (104) | 1.7-2.0 | 0.8-2.0 | 0.6-2.0 | 1.0-2.0 | 0.7-2.0 | 2015-2017 |
| 22 (102) | 1.1-2.0 | 0.5-1.9 | 0.6-1.7 | 1.5 -2.0 | x | 2016, 2017 |
| 26 (194) | 1.4-2.0 | 0.5-1.9 | x | 1.3-2.0 | x | 2015, 2016 |

Table 11: Thresholds of uncertainties on moderately vulnerable lines for January experiments

The wind farms of Eemshaven and Borssele had no influence on the congestions of these lines. These have not been added to the table.

Line 6

The primary uncertainty for line 6 is the capacity of the Maasvlakte offshore wind capacity. The capacity of the Maasvlakte has both a limiting and decreasing role for the congestion on this line. The lower threshold for this uncertainty lies at 10 % extra capacity in comparison to the base scenario. The upper threshold is at 90% extra in comparison to the base scenario. The secondary uncertainty is the power demand; the threshold lies at 10 & extra in comparison to the base scenario. The capacity of the Geertruidenberg wind farm must be 90 % compared to the base case.

From this line's positioning and uncertainty thresholds, we cannot conclude how the power on this line flows when congestion occurs.

Line 13

The primary uncertainty for line 13 is the demand. The threshold for this uncertainty lies when the demand is 70% higher than in the base scenario. The secondary uncertainty is the capacity of the Maasvlakte wind farm. The threshold for this uncertainty lies at the exact capacity of the wind farm as in the base scenario.

The rest of the uncertainties have little influence on the congestion on this line.

From the position in the network and the uncertainty thresholds, we conclude that this line is used to transport electricity generated at the wind farms in the West of the Netherlands to the South and East of the Netherlands.

Line 22

The primary uncertainty for this line is the capacity of the Maasvlakte offshore wind farm. The threshold for this uncertainty is met when the capacity is more than 50% more than the capacity in the base case. The secondary is the power demand, the threshold for this uncertainty lies at 10% extra in comparison to the base scenario. The wind farm's capacity in Geertruidenberg both supports and limits the congestion of this line. When the capacity is above 70% extra compared to the base case, the line has a lower chance of congestion.

The congestion especially occurs in experiments based on the historical data from 2016 and 2017. These years have a bit higher offshore wind and demand profiles.

From the uncertainty thresholds and the placement of the line in the network, this line is primarily used to transport the energy generated in the offshore wind farm of Maasvlakte to the South of the Netherlands. When a large amount of power is generated at the Geertruidenberg wind farm, this line will be used less. Less power generated at the Maasvlakte is necessary to serve the demand in the South at this point.

Line 26

The primary uncertainty for line 26 is the demand. The threshold for this uncertainty lies at 40% higher than in comparison to the base scenario. The secondary uncertainty is the capacity of the Maasvlakte wind farm. The threshold for this uncertainty is met when this capacity is 30% higher than the capacity in the base scenario. When both these uncertainty thresholds are met, the line is vulnerable to congestion. The capacity of the Beverwijk wind farm has a limiting effect on congestion.

The experiments with profiles based on the historical data from 2015 and 2016 have a higher chance of congestion. The profiles based on these years have higher offshore wind and demand. From these thresholds and the placement of the line in the network we conclude that this line is primarily used to transport power generated at the wind farm of Maasvlakte to the South and East to the Netherlands.

4.1.5 Secondary lines

From the initial PRIM analyses, we tested whether secondary lines could be identified. The following groups were found. More information about the identification process of these lines is in Appendix I.

13, and 24 with primary line 4

These lines lie in the South- West of the Dutch network. As explained in the earlier analyses, these lines transfer the offshore wind from Borssele to the rest of the Netherlands. Line 4 is the biggest bottleneck in this power flow, as seen in Table 10; this line can get congested without any extreme input values. Therefore it can be concluded that line 24 becomes congested after line 4. After both lines 4 and 24 are relieved from their congestion, lines 13 and 26 might become more vulnerable since this is the next line. Both these lines have been analyzed with the results from line 24. Line 13 showed similar results as the original analysis.

Lines 6, 15, and 23

Lines 6, 15, and 23 are part of a small subnetwork in the West of the Netherlands. The lines in this small subnetwork have a lower line capacity than the lines connecting the subnetwork. This makes them susceptible to congestion. It has been tested for both lines 15 and 23 that either would become congested after the other would be congested first. This was inconclusive. Testing which line had more impact on line 6 was also deemed inconclusive since both analyses showed the same values. This could mean that the three lines become congested together at certain times. Due to the low amount of runs in which line 6 is congested, this can not be stated with certainty.

Other inconclusive analyses

We analysed lines 31 and 37, with line 38 as the primary line. These analyses showed inconclusive results. This is surprising since the lines in the network all share the same capacity, and no nodes with a high power demand are situated close to the lines. We suspected a shift in the congestion in scenarios where line 38 was congested.

4.2 June results and analysis

4.2.1 June

4.2.2 General results

| General outcome | Demand | Beverwijk | Borssele | Eemshaven | Geertruidenberg | Maasvlakte | RESA | Weather-years |
|-----------------|---------|-----------|----------|-----------|-----------------|------------|------|------------------------------|
| Unserved demand | 1.2-2.0 | x | x | x | x | x | x | 2016 2017 2018 2019 |

Table 12: Thresholds of uncertainties for general system outcomes for June experiments.

Table 12 shows the for the General results. This table shows that the demand is the most influential factor for the unserved demand. The costs and emissions did not show any significant results. The unserved demand only has a threshold for the demand factor, which lies at 20% extra demand than in the base scenario.

Curtailed energy

In Figure 14, the percentage of curtailed renewable energy over the runs can be seen. The figure shows that there was a very small amount of runs that had zero percent of curtailed energy. We can learn from this curve shows that in the modeled system, in January, in almost all of the experiments, the potential renewable power is not met. The curve is steeper than the curve in January. Meaning that more use of the potential renewable energy is made.

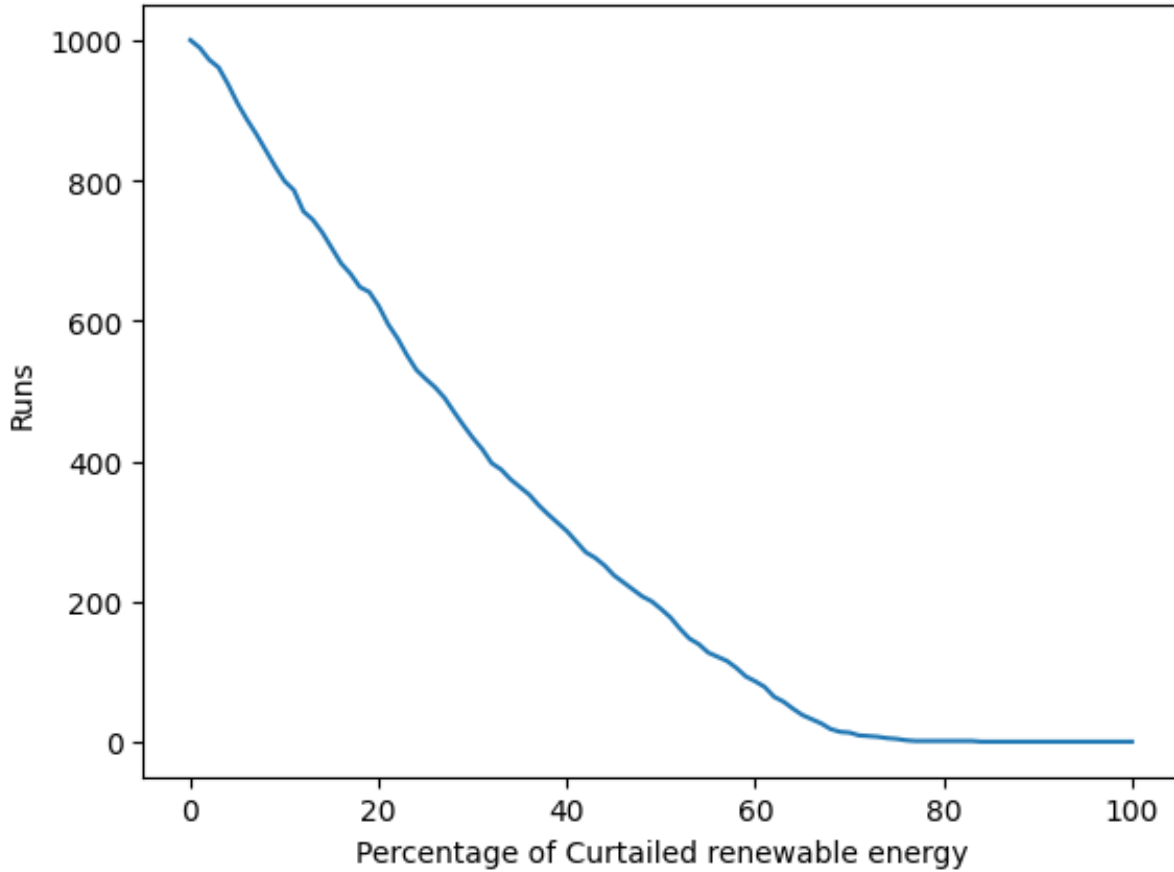


Figure 14: Curtailed energy over the runs in January

4.2.3 High Vulnerability lines

In Table 13, the summary of the PRIM results for the vulnerable lines can be found. The full PRIM analyses are in Appendix I. An 'x' means that the uncertainty has no significant influence on the congestion of the line.

| Line (runs) | Demand | Beverwijk | Borssele | Eemshaven | Maasvlakte | Weather-years |
|-------------|---------|-----------|----------|-----------|------------|------------------|
| 4 (256) | 1.5-2.0 | x | 1.0-1.9 | x | 0.5-1.8 | 2015, 2017, 2018 |
| 15 (277) | 1.4-2.0 | x | 0.6-2.0 | x | 0.9-2.0 | 2015, 2017 |
| 23 (480) | 1.4-2.0 | 0.7-2.0 | x | 0.9-2.0 | x | 2016-2019 |
| 24 (348) | 1.2-2.0 | 0.5-1.8 | 1.3-2.0 | x | 0.5-1.9 | 2016-2018 |
| 31 (206) | 1.4-2.0 | x | 0.5-1.9 | 0.9-2.0 | x | 2019 |
| 35 (689) | 1.1-2.0 | x | x | 0.7-2.0 | x | 2016-2019 |

Table 13: Thresholds of uncertainties on highly vulnerable lines by PRIM analysis for the June experiments.

Geertruidenberg and RESA had minimal influence, so these have been removed from the analysis. We see similar results as with the analysis for the January results. The higher value for demand can be assigned to the lower demand in the June experiments. A higher value is therefore needed for lines to become congested. As we have already explained how these lines can get congested in the results of the January experiments, we will not repeat them here.

4.2.4 Moderately vulnerable lines

| Line (runs) | Demand | Beverwijk | Eemshaven | Geertruidenberg | Maasvlakte | Weather-years |
|-------------|---------|-----------|-----------|-----------------|------------|-----------------|
| 22 (71) | 1.7-2.0 | x | x | 0.7-2.0 | 1.6-2.0 | 2015, 2017-2019 |
| 26 (150) | 1.4-2.0 | x | 0.5-1.8 | x | 1.4-2.0 | 2015, 2018 |
| 28 (118) | 1.8-2.0 | x | 0.7-2.0 | x | x | 2017, 2018 |
| 37 (162) | 1.4-2.0 | 0.5-1.9 | 0.8-2.0 | x | x | 2019 |

Table 14: Thresholds of uncertainties on moderate vulnerability lines by PRIM analysis June experiments

Borssele and RESA have little to no influence; these have been left out of the analysis. We see that the demand uncertainty threshold must be higher than in the January experiments. This is due to the lower demand for power in June compared to January.

Most of the lines have already been discussed in the January experiments, these lines showed similar uncertainty thresholds as well. Only line 37 has not been discussed yet.

Line 37

The primary uncertainty for line 37 is the power demand. The threshold for this uncertainty is when the demand is 40% higher than in comparison to the base scenario. Especially in the experiments with profiles based on the year 2019, this caused congestion. The profiles of this year had a high amount of offshore wind and solar.

In combination with the position of the line, we can conclude that this line becomes congested while transporting power generated at the wind farm of Eemshaven to the South of the network.

4.2.5 Secondary lines

We found no secondary lines in the June experiments that did not already occur in the January experiments.

5 Discussion of results

5.1 Comparison of June and January experiments

the results of the two sets of experiments were largely the same. Roughly the same lines were identified as vulnerable in the two sets. The most important difference between the two sets of experiments is that the risk of congestion for the lines is higher in winter than in summer. Next, there is a slight difference in which lines become congested. This is due to two factors.

Solar generation higher in summer

Firstly, solar generation is higher in Summer due to more sun hours and a higher intensity of solar radiation. Since each node has some solar panels attributed to them, this will probably be used to serve local demand and will not make its way to the transmission network. This leads to a lower necessity of power from conventional generators, leading to less actively constraining congestion.

Demand for power higher in winter

Secondly, the power demand is lower in summer. This is due to the higher temperatures in comparison to the winter season. This means that less power will need to be generated by costly conventional generators and that the amount of actively constraining congestion is lower.

5.2 Influence of the uncertainties

The uncertainties are listed from most influential to least in terms of congestion caused here:

1. Power demand
2. Maasvlakte wind farm
3. Borssele
4. Geertruidenberg
5. Eemshaven
6. Beverwijk
7. RESA policy plans

The most influential uncertainty on the congestion of the lines is the demand. The demand dictates the production of power in this simulation approach. The Maasvlakte is the most influential of the production side uncertainties. This is probably due to the wind farm size in the base scenario. Borssele wind farm is the third most influential due to its size and isolated position in the network. Geertruidenberg is influential despite its low capacity in the base scenario. This is because of its central placement in the network. Eemshaven is slightly influential since it powers a different area than the other wind farms. Because less power is generated by wind power flows in this part of the network, the lines are less congested. Beverwijk is the least influential wind farm because of its low capacity and placement close to the Maasvlakte wind farm. Lastly, the RESA policy plans have the lowest influence on the congestion of the lines. We conclude that this is because of the distribution of the generators in these plans over the network. The power will primarily serve the local demand and have a smaller chance to be transported on the network. Furthermore, the RESA plans primarily exist out of solar generators. In the experiments for January, there was almost no solar generation. This limited the influence of this uncertainty on the congestion of the lines.

5.2.1 Influence of weather years

For the January experiments, for congestion on the high or moderate vulnerability lines were the weatheryears of 2015 and 2016. This means that the historical profiles for demand and renewable for power of these years caused the most congestion. 2015 had a great amount of extra wind power, both offshore and onshore, in comparison to the other years. 2016 had more than average offshore wind, onshore wind and demand for power. As the demand and the offshore wind were the most influential uncertainties, this result is expected.

For the June experiments, for congestion on the high or moderate vulnerability lines was the weatheryear of 2017, although each of the years had some influence on the lines. This is not surprising since each of the years scored similar on the offshore wind generation and the demand.

5.2.2 General system outcomes

The general system outcomes that were analyzed are:

- Costs
- Emissions
- Ratio of curtailed renewable power
- The unserved demand.

Each of these showed significant results for the January experiments, but the costs and emissions did not show significant results for the June experiments. For 2030, it is logical that the power system has costs and emissions. The goal is to be emission less in 2050, not 2030. It is also not surprising that in the modeled runs there will be curtailment of renewable power. The renewable powerflows from the windfarms can become extremely high with the experimental setup. Too much for the network to handle, as was the intention of the experimental setup. With no storage in the model to store this abundant power, this power will be curtailed. What is alarming is that the unserved demand seems to become significant at quite low parameter settings for demand. In the winter experiments, the threshold is as low as 0,9 . This means that with the closing down of the coal plants in the Netherlands, it is probable that there will be unserved demand curtailment in the future power system. This is very costly for the TSO and must be tried to be avoided. Large-scale storage of the curtailed renewable power in batteries or hydrogen will be necessary to serve the demand at these times.

5.3 Line vulnerability outcomes

Out of the results and analyses for the lines, we placed them in the following categories based on their characteristics. The categories are labelled based on the sensitivity to congestion.

- Primary, high vulnerability lines (critical importance)
- Secondary, high vulnerability lines (high importance)
- Primary, moderate vulnerability lines (moderate importance)
- Secondary, moderate vulnerability lines (low importance)

We will discuss which lines we will brand with each label in the following section.

5.3.1 Critical importance

The following lines are primary and highly vulnerable to congestion. :

- Line 24 (Rilland - Geertruidenberg)
- Line 38 (Bergum - Vierverlaten)
- Line 35 (Eemshaven - Weiwerd)
- Line 23 (Oostzaan - Diemen)

Line 24

Line 24, connecting the substations of Rilland and Geertruidenberg, transports the power from the Borssele offshore wind farm to the rest of the Netherlands; its surrounding powerlines have a higher capacity. Therefore, it is a bottleneck. The capacity expansion for this line is already planned but will probably not be ready until 2032. The expansion is from 4080 to 5270 MVA. An increase of 20%, and the same capacity as the surrounding lines.

Line 38

Line 38, connecting the substations of Bergum and Vierverlaten, transports the power from the Eemshaven offshore wind farm to the North-West of the Netherlands. This power comes via line 36, connecting the station of Vierverlaten and Eemshaven. Line 36 has the highest capacity in the model with 10530 MVA. The capacity of line 38 is just 952 MVA. The rest of the lines surrounding this line have a capacity of 1904 MVA. This makes this line a bottleneck.

Line 35

Line 35, connecting the substations of Eemshaven and Vierverlaten, transports the power from the Eemshaven offshore wind farm to the node of Weiwerd and via this node to the South of the Netherlands. This line has a capacity of just 952 MVA. This line does not need a pressing capacity upgrade since it is isolated in the network and does not perform a key role. It is, however, prone to congestion.

Line 23

For line 23, connecting the substations of Oostzaan and Diemen, it is unclear in which direction the power flows when the line becomes congested. This is because none of the production uncertainties influences the congestion on the line in our analysis.

5.3.2 High importance

The following lines will become congested if other lines get capacity expansions and are highly vulnerable are:

- Line 4 (Borssele - Riland)
- Line 13 (Geertruidenberg - Tilburg)

Line 4

Line 4, connecting the substations of Borssele and Riland, connects line 24, with the offshore wind farm of Borssele. These lines are used together to transport offshore wind power from Borssele to the East of the Netherlands. This line will become congested when Line 24 has been upgraded. Since this line will be upgraded after 2030, it's important to closely study the development of electrification in the East of the Netherlands for this line.

Line 13

Line 13, connecting the substations of Geertruidenberg and Tilburg, connects line 24 with the East of the Netherlands. For this line the same applies to line 4: When line 24 is upgraded, and the demand in the East of the Netherlands grows in the following years, this line will become congested.

Moderate importance

The following lines are primary when congested but moderately vulnerable:

- Line 15 (Krimpen - Breukelen)
- Line 22 (Maasvlakte - Simonshaven)
- Line 26 (Wateringen - Bleiswijk)
- Line 28 (Zwolle - Hengelo)
- Line 31 (Louwsmeer - Bergum)
- Line 35 (Eemshaven - Weiwerd)

Line 15

Line 15, connecting the substations of Krimpen and Breukelen, becomes congested when the power demand is 30% than proposed in the basecase. It is however unclear from the analysis whether this power flows in the Southern or Northern direction.

Line 22

Line 22, connecting the substations of Maasvlakte and Simonshaven, becomes congested when the demand for power in the system is very high, and the capacity of the Maasvlakte wind farm is very high as well. It is used to transfer the power of this wind farm to the rest of the network.

Line 26

Line 26, connecting the substations of Wateringen and Bleiswijk, becomes congested when the demand and the offshore windfarm of Maasvlakte are high. Thus, this line is used to serve the demand in the east of the Netherlands. When both of these uncertainties develop faster than anticipated, this line will be congested.

Line 28

Line 28, connecting the substations of Zwolle and Hengelo, becomes congested when the demand in the North-East of the Netherlands electrifies faster than anticipated. Since it is the only line connecting the wind farms with the rest of the Netherlands, this must be closely watched.

Line 31

Line 31, connecting the substations of Louwsmeer and Bergum, is the only line that was congested more frequently in the June experiments. This line becomes congested when the demand in the North-West of the Netherlands is higher than anticipated.

Line 35

Line 35, connecting the substations of Eemshaven and Weiwerd, showed peculiar results. It seems that the only purpose of this line is to transfer wind power to the node of Weiwerd. It could also be used to transfer power to the South. When both the demand for power and the wind farm of Eemshaven have a high value, this line becomes congested.

Low importance

- Line 6 (Breukelen - Diemen)

Line 6

Line 6, connecting the substations of Breukelen and Diemen, lies between lines 15, and 23. These are 2 vulnerable lines. This line becomes congested when the capacity of either line 15 or line 23 are set to infinity.

5.3.3 Planned capacity expansions

In Table 15, an overview the planned network capacity upgrades for 2030 can be found. 4 projects by the TSO can be identified from these plans. In this section, these plans will be evaluated.

| Substation 1 | Substation 2 | 2022 Capacity (MW) | Planned capacity (MW) | Line |
|-----------------|--------------|--------------------|-----------------------|------|
| Vierverlaten | Eemshaven | 1905 | 10530 | 36 |
| Ens | Zwolle | 3290 | 5265 | 12 |
| Diemen | Lelystad | 4280 | 5265 | 8 |
| Eindhoven | Maasbracht | 3720 | 5265 | 21 |
| Eindhoven | Tilburg | New line | 5265 | 39 |
| Geertruidenberg | Tilburg | New line | 5265 | 13 |
| Geertruidenberg | Krimpen | 3720 | 5265 | 16 |
| Borssele | Rilland | 3290 | 5265 | 4 |

Table 15: Planned upgrades for 2030

Vierverlaten - Eemshaven

The first is the start of upgrading the 220 kV-network with the line between Vierverlaten and Eemshaven. This capacity expansion is sensible with the windfarm of Eemshaven in mind. For the year 2030, this expansion has led to a relocation of the congestion to the line between Bergum and Vierverlaten. The next step in the project must be to further upgrade the 220 kV-network.

Ens-Zwolle & Diemen-Lelystad

The second is the joint upgrade of the lines Ens-Zwolle and Diemen-Lelystad. The line Lelystad-Ens is already at a higher capacity. This project is important to ensure the flow of power between the windfarms in the West, and the demand in the East. The next steps in this project must be to further expand the capacity of the lines surrounding Diemen, and the line Zwolle-Hengelo.

Eindhoven-Krimpen

The third project is that of the lines connecting Eindhoven all the way to Krimpen, crossing 4 (future) substations. These lines connect the windfarms in the West with the demand in the East. The substation of Tilburg will be built to ensure this demand. A sensible project with the planned offshore windfarms in mind.

Borssele - Rilland

The fourth project is that of expanding the capacity of the line Borssele-Rilland. This line is important to transfer the wind power from the windfarm of Borssele to the rest of the Netherlands. As already pointed out, this line upgrade reallocates the congestion in Borssele to the line Rilland - Geertruidenberg.

5.4 Validation of results

unfortunately, we could not validate the results of this research with historical data. We can compare the results with other studies concerning transmission expansion in the Netherlands. The TSO mentions in its own capacity expansion plans for 2030 (TenneT 2022b), that the line between Rilland and Geertruidenberg (in this research called Line 24) will be expanded in 2032. In the results, this is the most vulnerable line in the network line. In the same expansion plans the TSO mentions that the lines surrounding connecting Diemen and Krimpen via Breukelen and Oostzaan (lines 6,15, 17, and 23 in the model) are studied for expansion. This is one of the vulnerable groups identified in the results. The line Zwolle - Hengelo (line 28), identified in the study, will also be studied for expansion. In addition, the TSO published a study concerning the security of supply for demand in 2030 (TenneT 2022c). This study concluded that the power system could regularly experience times when demand must be curtailed. This is similar to the results of this study.

5.5 Discussion of limitations

This Section discusses the limitations of this research and the effect these had on the results. The limitations are split up into the following four categories

- Congestion methodology
- Network modeling
- Data
- Experimental design

5.5.1 Congestion methodology

The cost-seeking algorithm was used to find vulnerable lines hidden in normal analysis. The main disadvantage of this algorithm was the extra time this algorithm imposed on an experiment. Many new simulations could be triggered depending on the number of congested lines in the original simulations. The depth of the algorithm was set to three lines in this research, meaning that after 3 lines with a capacity set to infinity, the algorithm would stop triggering extra stimulation. This depth could be altered: A higher depth would lead to more analyzed lines and more simulation time.

Another point concerning the congestion-seeking algorithm is that this research used it to calculate the cost of the congestion it spotted. With the evaluation of the results, we discovered that this did not yield valid results.

Leaving this out of our research outcomes and only focussing on whether a line becomes congested or not gives us the choice of altering the algorithm. First, one less depth of the simulations is required since we no longer need the simulation for the costs. 2. We can implement the information in the outcome gathering that describes if the line is a primary, secondary, or tertiary bottleneck in the simulation and which lines would be its predecessor. This would give insight into how the TSO should plan its capacity expansions.

5.5.2 Network modeling

Storage in model

One of the conclusions of this research is that a system without storage can lead to a high amount of unserved demand and a high amount of curtailed renewable energy. As mentioned in 3.1, both the Dutch government and the private sector have plans to implement power storage. This storage of renewable energy is an option that could solve both problems. The absence of storage

in the model could lead to very different power flows based on the type of storage and the placement of the storage facilities.

Scope of the model

To limit the simulation time, the model scope was only on the high-voltage network of the TSO. In reality, the power network consists of a lot of extra layers. The RESA policy plans, which did not have a share in the congestion since they would serve the local demand, would have a bigger impact on this network layer. The power from the off-shore wind farms could also lead to congestion on this layer. Congestion on this network layer could, in the worst case, lead to curtailment of power generated in the wind farms, both on and offshore. Adding this layer to the model would change the outcomes of this study to some extent.

International connections

The model used in this research did not have any international connections to the transmission grids of other countries. According to data of the ENTSO-E (ENTSO-E 2022a), international connections are used regularly to transport power to and from Belgium and Germany. One of the conclusions of this research is that the Netherlands could have significant unserved demand in 2030. With the power flow from the interconnections to these countries, a portion of this demand could be served. Adding this to the model

Runtime of simulations

The runtime of simulations was a great limitation of this research. One yearly simulation had a runtime of 226 seconds, and one week had a runtime of 16.5 seconds. This has led to running 2 weekly sets of experiments instead of the whole year. Combined with the extra simulations that were called by the congestion-seeking algorithm to determine the severity of the congestion, the runtime for one experiment for the yearly model could take hours. With an experimental design of 1000 runs, the total runtime could take weeks. In this respect, the combination of exploratory and power system modeling is not ideal. Power system models need computational time to minimize the costs of the system by calculating the perfect power flows. The necessity of very high temporal resolution in power system models also drives up the simulation time. Exploratory modeling, especially the prim algorithm used for the analysis, needs many runs to determine how the uncertainties affect the outcomes. Therefore, the research setup had to be compromised between the number of experiments and the simulation time of these experiments to ensure valid results. This might have affected the results, and unique and irregular events that could have occurred in the historical data have been left out of this analysis because of this choice.

5.5.3 Data collection and implementation

The data used in this research primarily relies on open-source data. The TSO and energy companies often secure their power system data for security reasons. Fortunately for research in the field of energy systems, progressively more data has become publicly available in the last couple of years. With the data from the JAO static grid model, the network topology can be accurately recreated. With the data from the ENTSO-E, demand profiles can be created. As described, these demand profiles need to be localized for each node. Having the exact data of the power system would improve the accuracy of power system models. Unfortunately, data of the Dutch power system is not yet publicly accessible for security reasons. On the other hand, data for renewable power generation is easily accessible in the correct format.

Not only the data itself is important. How the data is transformed and used as input in the model is equally important. Since not all data is available, power system modelers must transform the open-source data into what they need. In this step, the validity of the data can worsen. For this research, it can be stated that the validity of the input data is less important. Through our wide range of experiments, A coarse input would suffice (and has sufficed) as well. Since

we are relied on (transformed) data from open sources, a good way to validate our data would be to contact the TSO and let them verify the data. This would give more certainty about the results of the research.

Implementation of Renewable generation

For this research, it was chosen that the turbines of the offshore wind farms would have a height of 250 meters; The onshore wind farms would have a wind turbine of 150 meters. We made this choice since, recent developments in the field offshore wind turbines are shown to perform well on this height. A lower hub height of these offshore wind turbines would result in less power generated at the wind farms due to less windspeed. Especially in the experiments for the week of January, this led to an overflow of power from the off-shore wind farms to the system since the solar farms will not produce much power in winter. This could have created a bias in the model's outcomes to the offshore wind farms and lowered the influence of the RESA policy plans on the outcomes. Conversely, the power generated by the RESA policy plans will probably be used locally on the node where it is produced. The influence of these plans on the transmission grid will be less than that of the offshore wind farms. The attribution of the RESA policy plans could as well be more exact in the model. In this research, the RESA regions have been split up into the nearest nodes. This could have been more refined by considering multiple layers of the Dutch network instead of only using the transmission grid.

Implementation of Demand

For the demand modeling, the choice was made to base the profiles on the data from the TSO and the nodes' share of energy demand on each node. The demand for energy and electricity are not 1:1 related; this could lead to differences in demand data. The share of demand for each node was deemed the same for each weather year. This makes the demand profiles on the nodes in this model all the same; they have a different base factor. In reality, in more industrial regions, the demand profile will be different from more residential regions, leading to different profiles across the nodes. This could lead to different power flows and vulnerable lines; then this research has pointed out.

5.5.4 Experimental design

Choice of uncertainty parameters

Using the same lower- and upper-bound value for each uncertainty was an arbitrary choice. Less significant uncertainties, like the RESA policy plans, could have gotten more extreme values. More influential uncertainties, like the power demand, could have gotten less extreme values. By choosing more balanced uncertainty parameters, we could have better understood the influence of the uncertainties. The RESA uncertainty did not show to have any influence on the congestion of the lines in the current uncertainty thresholds. It would be helpful to see when this uncertainty would become congested. In rebuttal, using different uncertainty ranges would also lead to more valid uncertainties in the PRIM analyses of the lines. This would cause more difficulty in interpreting the results.

Weather years

In retrospect, implementing the weather years as a different uncertainty cluttered the analysis of the results. Implementing the temporal weather year variable would have given us better insight into the severity of the congestion on a line. This is because the capacity expansion in the simulations could repeat itself over the timesteps, resulting in a cost difference over the whole week. Later, we discovered that this did not yield enough valid results. Therefore, congestion alone was chosen as the sole outcome for the lines. While taking only the congestion outcome, we focused more on when the line would become congested. This outcome became difficult to analyze with the weather years and the generation and demand uncertainties. We were effectively trying to measure an event's occurrence over multiple timesteps while subjecting

these timesteps to multiple uncertainties. The correlation between the weather years and other uncertainties made the analysis difficult.

Geographical variety

Using one uncertainty to factor all demand and generation profiles in the model limits the depth of the results. Adding the spatial factor for the RESA policies and demand could have given us more insight into the power flow in the model. On the other hand, it would have given us even more uncertainties. To analyze these extra uncertainties properly, we would need more simulations.

6 Conclusion and recommendations

The research question of this thesis was: *Is the planned 2030 Dutch electricity grid adequate and, if not, which extra investments may help mitigate the consequences of key uncertainties?* The following subquestions have been selected to support this research question:

1. *What are the most uncertain factors of the Dutch energy transition for the transmission grid?*
2. *What are the most vulnerable lines to congestion due to the (uncertain) Dutch energy transition?*
3. *What is the effect of the Dutch energy transition on the overall power system?*

We will first focus on answering each of the sub-questions, then we will answer the main research question. We will continue with recommendations for further research.

6.1 sub-questions

6.1.1 Sub question 1

The first subquestion focused on the effect of the uncertainties of the energy transition on the transmission grid. Out of the results of this research, we found that the most influencing uncertainty is the power demand, followed by the capacity of the offshore wind farms. The RESA policy plans were the least influential for congestion on the transmission grid. From the offshore wind farms, the capacity and the placement of the wind farms determined whether they were influential or not.

6.1.2 Sub question 2

The second subquestion focused on the identification of vulnerable lines. We made a distinction between critical, high, moderate, and low vulnerability lines. After careful reconsideration of these lines we spotted that the critical lines could become congested at almost all future scenarios. No conditions needed to be met. We brand them as critical upgrades. For the other lines, conditions need to be met, especially in the regional demand for power. Therefore we rebrand them to conditional upgrades.

6.1.3 Critical upgrades

Based on the results of this research, an insight into the vulnerability lines on the Dutch transmission network can be made. Out of the research, the most critical lines can be found in 16. The first line, from Rilland to Geertruidenberg is primarily used to transfer power from the Borssele wind farm to the East of the Netherlands. This line is planned to be expanded in 2032. The second line, from Bergum to Vierverlaten, is primarily used to transfer power from the Eemshaven wind farm to the rest of the Netherlands.

| Substation 1 | Substation 2 | Current Capacity (MW) | Line |
|--------------|-----------------|-----------------------|------|
| Rilland | Geertruidenberg | 4080 (5265 in 2032) | 24 |
| Bergum | Vierverlaten | 952 | 38 |

Table 16: Critical lines that need upgrades.

6.1.4 Conditional upgrades

Next to these critical capacity expansions, there are less pressing line vulnerabilities. For these lines to become critical, a certain threshold must be met for one or two of the parameters in the system. The (local) demand for power plays a big role in the vulnerability of these lines since

this is the leading factor in how power will flow on the network. The network can be split up into three zones; The North-East, the South-East, and the West. This can be seen in Figure 15.

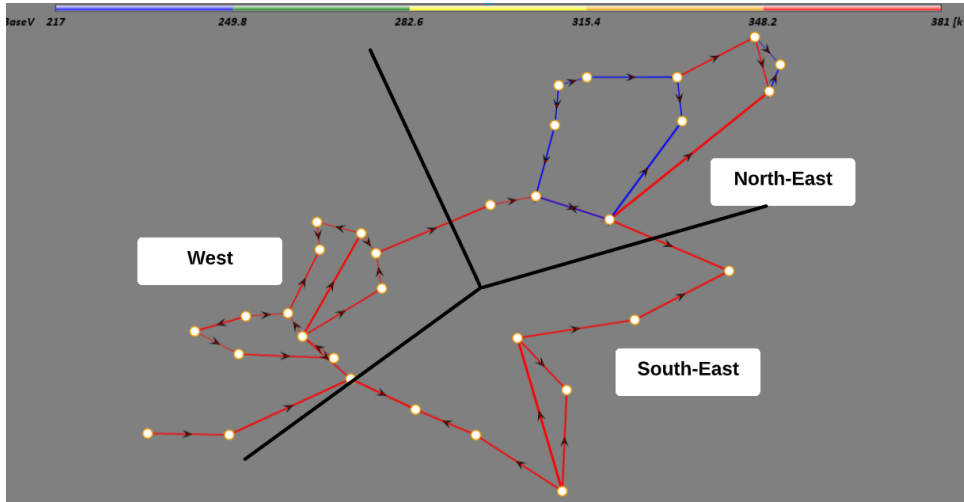


Figure 15: Network with demand regions

Demand growth in the West

The necessary upgrades for when the demand for power in the West becomes higher than anticipated can be found in Table 17. The lines in this table are part of a subnetwork in the West of the Netherlands. This subnetwork has a lower capacity than the surrounding subnetworks. This makes the subnetwork a possible bottleneck for bigger power flows due to wind farms on the network. It is not quite clear in what direction the power will flow on these lines when it becomes congested, this is due to the four windfarms close to these lines.

| Substation 1 | Substation 2 | Current Capacity (MW) | Demand region | Line |
|--------------|--------------|-----------------------|---------------|------|
| Krimpen | Breukelen | 1645 | West | 15 |
| Oostzaan | Diemen | 2040 | West | 23 |
| Breukelen | Diemen | 1974 | West | 6 |

Table 17: Necessary upgrades for demand growth in the West

Demand growth in the North-East

The necessary upgrades for when the demand for power in the North-East rises, becomes higher than anticipated can be found in Table 18. The lines in this table are part of the 220 kV-network. This leads to the lines having a lower capacity. The three lines become congested when there is a high amount of power from the offshore wind-farm of Eemshaven. This power is transported to the South through these lines. The line between Bergum and Vierverlaten is included in this table once more, since an extra capacity expansion is likely to be necessary when demand becomes unexpectedly high in the North-East of the Netherlands.

| Substation 1 | Substation 2 | Current Capacity (MW) | Demand region | Line |
|--------------|--------------|-----------------------|---------------|------|
| Bergum | Vierverlaten | 952 | North-East | 38 |
| Eemshaven | Weiwerd | 952 | North-East | 35 |
| Louwsmeer | Bergum | 1905 | North-East | 31 |

Table 18: Necessary upgrades for demand growth in the North-East.

Demand growth in the South-East

The necessary upgrades for when the demand for power in the South-East becomes higher than anticipated can be found in Table 19. The upper two lines in this table are used to transport

power from the Borssele windfarm to the East of the Netherlands. The third is to transport power from all 4 of the windfarms in the West to the East. Even when the planned upgrade is completed for the line between Rilland and Geertruidenberg, congestion could occur on this line. In addition, only expanding one of the two upper lines could lead to a relocation of future congestion instead of the prevention of future congestion. This is because these two lines essentially form one line from the Borssele windfarm to the East of the Netherlands.

The fourth line, between Zwolle and Hengelo is primarily used to transport power from the Eemshaven windfarm to the East of the Netherlands.

| Substation 1 | Substation 2 | Current Capacity (MW) | Demand region | Line |
|-----------------|-----------------|-----------------------|---------------|------|
| Borssele | Rilland | 5265 | East | 4 |
| Rilland | Geertruidenberg | 4080 (5265 in 2032) | East | 24 |
| Geertruidenberg | Tilburg | 5265 | East | 13 |
| Zwolle | Hengelo | 4080 | East | 28 |

Table 19: Necessary upgrades for demand growth in the East

6.1.5 Sub question 3

The third subquestion examined possible future states of the Dutch energy system. We analyzed this to understand how the transmission grid would be affected by its transition. The four extra factors that were examined were:

- System costs
- System emissions
- Renewable curtailment
- Unserved demand for power

Out of the expected 2030 energy system results, the following can be concluded: For renewable power, costs and emissions will exist, a high share of the generated renewable power must be curtailed, and a great amount of demand will not be served. These four outcomes are all non-beneficiary for the 3 policy goals of the energy system. Storage facilities will need to be built to counter these outcomes. If these cannot be built fast enough, the government might need to reconsider its decision to shut down all coal plants to ensure the demand will be served.

6.2 Research question

By addressing the sub-questions, a comprehensive understanding of the topic is obtained, contributing to answering the main research question. We can conclude that the Dutch transmission grid in 2030 will be adequate for most of the uncertain factors included in this research. The (geographical) development of the power demand will be the most pressing factor for the transmission grid. This research also pointed out that the power system as a whole will experience change in the coming years. Among other developments, storage will be necessary to serve the power demand. The implications of these developments on the transmission grid are unclear. We don't know yet what policy measures will be taken to complete the energy transition and whether they will be taken on institutional or physical layers of the system. Furthermore, we cannot tell how fast these changes will be implemented in the system. The TSO's task is to closely watch the developments in the power system to keep the performance of the transmission grid in order.

6.3 Further research

6.3.1 Development of hydrogen and transmission grid

A problem for the Dutch TSO is that, at the moment, the influence of the upcoming hydrogen network on the transmission grid is unclear. An exploratory study for the hydrogen and transmission grid co-development could be performed. Certain simulation tools, like SAInt, support the coupling of both gas and power networks in simulation models. These simulation models could be coupled with exploratory modeling tools to analyze the co-development of these future systems. The insights of these studies can be used to inform decision-makers on integrating these systems. This can help construct the necessary facilities for network integration in the seemingly best places and reinforce both networks where needed.

6.3.2 Usage of RDM-framework

An iterative RDM approach could be used to model the future of the Dutch transmission system until 2050. This research could test the feasibility of an emission-less power system.

Implementation of policy options from this study in 2030 model

The first iteration of this RDM approach would be to perform experiments in which multiple policy options are added. Following the conclusions of this research, the following policy options could be added:

- Capacity expansion of the lines connecting Diemen - Krimpen
- Capacity expansion of the lines connecting Borssele - Geertruidenberg
- Capacity expansion of the line Zwolle - Hengelo
- Capacity expansion of the 220 kV-network

These policy options will act as the L in the XLRM framework. The XRM of this model would roughly be the same as the one in this study. The cost-seeking algorithm in the model would not be necessary. The hydrogen plans for 2030 could be added in as well. For the outcomes, only the general system outcomes would be analyzed. It will be determined which policy options are most beneficiary for the system.

Further implementation

Based on the most influential policy options from the previous RDM, a model could be created portraying the Dutch transmission grid in 2040. The offshore wind plans and the hydrogen plans for 2040 could be implemented in this model. The power demand must be assumed for this time period. The same congestion-seeking approach used in this research could be used to identify the vulnerable lines for this year. These vulnerable lines could create a new set of policy options. These policy options could then be used as input in a new RDM iteration, in which the most impactful policy options are implemented in a 2050 model. This methodology created a long-term outlook for transmission grids, and possible vulnerabilities could be noticed early on.

6.3.3 Capacity expansion

The cost-seeking algorithm aims to find the most congested lines so that the expansion of the capacity of these lines can be considered. The next step is to find the most appropriate capacity expansion. The TSO has a limited choice in the selection of cable type. Furthermore, the TSO can choose the number of cables it puts in parallel to form the line. With this knowledge, policies can be formed for the capacity expansion of the network using an RDM framework.

6.3.4 Alternative simulation methodology

Experiments without storage

In this research, the DCOPF formulation of the model made that every timestep could be seen on its own model formulation. The mathematical problem for a timestep is not influenced by its former timesteps in the form of renewable energy storage or start-up costs. Effectively, we are running 168 separate simulations if we are running one week. This raises the question of what can be classified as an experiment in light of exploratory modeling. We could also take only one timestep and run this timestep a lot of times while altering the demand and generation of renewable energy. We can then analyze when a line becomes congested and perform an analysis of how probable it is that these values will occur in the coming years. To save extra time with the construction of simulation models for SAint, we can paste the input values after one another and run them in one simulation model. We can then chop up the output of this single simulation model and treat the timesteps as a different experiment in our analysis. The steps in the methodology would be :

1. Create experiments from credible uncertainty ranges.
2. Perform all experiments consecutively in one simulation model.
3. Chop up the output values of the simulation model.
4. The congestion-seeking algorithm finds the experiments in which a line becomes congested and runs all of these timesteps in one simulation for each line.
5. Perform prim analysis to determine which input values line will become vulnerable.
6. Determine how credible it is that these input values will occur using historical data.

Experiments with storage

For simulation models with storage, another approach is required. The storage in the model causes interdependency between timesteps. Future research could point out how these models should be implemented in this methodology.

7 Reflection

In this Chapter we will reflect on the following:

- Research process
- Research design
- Hiccups and setbacks
- Personal reflection

7.1 Research process

There were four key feedback moments in my research. After these four moments, the focus of the research changed, depending on the feedback.

Initially, the goal for my master's thesis project was to add meaning to the Dutch energy transition. We learned through my Master's courses what changes the energy transition would cause in the institutional and physical layers of the Dutch energy system. Through another master course in policy analysis, We learned about uncertainty in policymaking and how this could be mitigated. In this course, there was a case study about the river network in the Netherlands. Combining the components we learned in these two courses, We wanted to analyze the uncertainty of the energy transition on a Dutch energy network, leading to the first steps of this thesis. It became clear that We needed to use the DC-OPF modeling approach to simulate the transmission grid's flows accurately.

After the kick-off meeting, we were advised to test the methodology on a small network representing the Dutch transmission grid. This resulted in the 5-node network.

In the mid-term, the research focused mostly on presenting the results of the 5-node network. The congestion-seeking algorithm was, at this stage especially focused on finding the most vulnerable line in each experiment. No depth was embedded in the algorithm. This resulted in the sole congestion of one single line. The 5-node network and the congestion-seeking algorithm both needed to be upgraded. Also, the simulation time of the experiments was too long. At this stage, we tried running the experiments yearly. All of this needed to change if we wanted to create some meaningful results.

To do this, we created a 6-node network model and altered the depth of the first model. The simulation time was still yearly in this model. we put the results of this model in my report. After handing in my report for the 1st green light meeting, we did continue to work on a complete network model.

For the 1st green light meeting, we wanted to present the results of the 6-node network. The structure of this meeting was not as we had planned. We initially thought we could present the results of our created model. The progress was based solely on the report we handed in 2 weeks before the meeting. Since conclusions and results were absent in this report, it was not sufficient to be graded with a green light. A 2nd green light meeting was planned. We needed to focus more on the structure and argumentation in the report than on the model.

With this feedback, we embedded the results of my latest model in the report and started to support these with a newly written methodology.

After the 2nd Greenlight, the report was accepted as sufficient. We still needed to work on the structure of the report, however. Apart from other points, especially the explanations in the methodology, the structuring of the results and conclusions needed work. We continued working on these points.

7.2 Research design

This research has pointed out that combining exploratory modeling with power network modeling can be useful in identifying both network vulnerabilities and general system KPIs. Due to the long simulation times of the power network modeling tools, it can be argued whether it is the most practical method. Part of this comes from the huge amount of data necessary to input various variables. For the exploration of network expansion, it can be useful. It might even be necessary since the permit application for network expansion must be submitted a couple of years beforehand. Another point is how in power system modeling, the weather years and capacity of the solar generators both influence the flow of power.

Furthermore, we would like to quote Jan H Kwakkel (2017) on one of the ideas that the EMA workbench is built upon:

*'By combining the XLRM framework and the idea of running a model as a **simple function**, it is possible to use the workbench to explore uncertainty about relationships within the model.'*

It is safe to state that the model that we built and used as our input is far from a simple function. This was primarily noticed since the EMA workbench does not fully support the extraction of time series from a simulation. Moreover, much information is lost when focussing on static outcomes in dynamic simulation models. One of the major hiccups in this project was transforming the relatively complex simulation model into a simple function so that we could perform exploratory modeling with the model. This demands a sharp and clear distinction of what the modeler wants to analyze in combining complex models and exploratory modeling.

This brings us to the usage of the tools for this research. Both SAInt and the ema workbench are helpful and excellent tools in their field. SAInt gives the user complete control over the model. Every single parameter in the model can be tinkered with to perfection. In addition, every aspect of the model can be analyzed at each timestep. Therefore, it is a tool with which the experienced system modeler can precisely simulate and explore what the modeler wants. The ema workbench is as well a tool that lets the user take complete control over what the user wants. The analysis techniques on the experiment runs can be changed until the algorithm takes the exact data that the modeler wants. Combining these tools creates many variables that can be changed and tinkered with and large amounts of data that need to be used as input. The two tools are naturally not optimized to work with each other either. This made that quite a lot of time went into understanding which variables were most important and which were irrelevant for modeling the 2030 transmission grid. In addition, the EMA workbench is not optimized for complex software models like SAInt, as the quote from Jan H Kwakkel (2017) indicates. Furthermore, SAInt's interface could be improved to allow better simulation of inputs and more efficient runs of EMA simulations.

7.3 Hiccups and setbacks

We can identify multiple hiccups and setbacks in reflecting on the research process and design.

Modeling process

One of the major setbacks in this research happened in the modeling process. As mentioned in the research, the simulation time initially took a long time. This was because of a memory leak. The Python function called the simulation model a lot of times in sequence. Not all the memory filled by the simulation model or the Python function was removed accordingly. This could lead to runtimes of hours for one experiment. Since the EMA workbench cannot store the results of the experiments until each experiment is done, we had to alter the main function. It took quite some time to 1. Identify the memory leak, and 2. Come up with a suitable solution.

This was not the only setback due to the tooling; another was the great number of variables and methods that could be altered in the research. The full model of the Netherlands had 5334

parameters that could all be altered. This even excluded the input data; it took quite some time to find the right calibration of these parameters. In addition, letting the EMA workbench alter the right input values in this simulation model was not easy.

Lack of meaning in results

The final setback was that the first results had almost zero added meaning. The results for the 5-node network were too simple. This meant that we needed a full refinement of the methodology, which took a lot of extra time. We stayed in the modeling phase too long because we had to re-evaluate the modeling design. In addition, I had to create a congestion-seeking algorithm. In its creation, went a lot of time.

7.4 Personal reflection

This research project, which led me to Essen, Germany, and back, was exciting, educational, and tiring at times. As mentioned, the project had some hiccups. Because of these hiccups, the progress of the project halted. I spent much time perfecting the simulation model and the code used to call the ema workbench and the simulation. Because of this, not enough time was left for the report. I got entangled mainly in the model and code to create meaningful results. Because of this entanglement, I thought writing the report should be a second priority. I was shaken out of this priority a bit too late when I found out that writing a report for the master thesis turned out harder for me than I expected. I found it difficult to express my methodology clearly to the reader. Many of the methodological and coding choices I made in my head and all my analyses were difficult to express in the report. I struggled, especially with the structure of my report. I lost a lot of time prioritizing the results instead of the report. So much so that I failed my first green light meeting; it is safe to say that my time management could have been better.

Going into this project, I believed modeling alone could shed more light on the energy transition and its uncertainties. Especially with exploratory modeling and analysis, it felt as if this was a tool that could, when implemented correctly, predict the future. One of the main things I learned was that not one modeling approach could fix the transmission grid in the energy transition. This stemmed from the idea that everything could be (theoretically) modeled. Now that this project is done, I see that, in practicality, the physical transmission grid depends on many variables. For some of these variables, we do not know their effect. We cannot simulate how the power will flow on the transmission grid when the power market model changes. This institutional change is impossible to model since the fundamental assumptions we use in our current modeling approaches could be completely useless. What we can do, and what I tried to do in this research, is use the existing modeling approaches we have and simulate possible future scenarios. We can use the results of these scenarios and think about what effect the changes in the context of the future will have on the system. Ultimately, simulation models for complex systems are tools, not future predictors.

Bibliography

- Baldick, R. (1995). “The generalized unit commitment problem”. In: *IEEE Transactions on Power Systems* 10.1, pp. 465–475. DOI: 10.1109/59.373972.
- Battle, C. and J. Barquin (Feb. 2005). “A Strategic Production Costing Model for Electricity Market Price Analysis”. In: *IEEE Transactions on Power Systems* 20.1, pp. 67–74. DOI: 10.1109/tpwrs.2004.831266.
- Blonsky, Michael et al. (Nov. 2019). “Potential Impacts of Transportation and Building Electrification on the Grid: A Review of Electrification Projections and Their Effects on Grid Infrastructure, Operation, and Planning”. In: *Current Sustainable/Renewable Energy Reports* 6.4, pp. 169–176. DOI: 10.1007/s40518-019-00140-5.
- Brown, T, J Hörsch, and D Schlachtberger (2018). “PyPSA: Python for Power System Analysis”. In: *Journal of Open Research Software* 6.1. DOI: 10.5334/jors.188.
- Capasso, A. et al. (Nov. 2016). “A LP and MILP methodology to support the planning of transmission power systems”. In: *Electric Power Systems Research* 140, pp. 699–707. ISSN: 0378-7796. DOI: 10.1016/J.EPSR.2016.04.024.
- CBS (2022). *Bevolking op 1 januari en gemiddeld; geslacht, leeftijd en regio*. URL: <https://opendata.cbs.nl/#/CBS/nl/dataset/03759ned/table>.
- Council, World Energy (2022). *Trilemma index 2022*. Tech. rep. World Energy Council. URL: <https://www.worldenergy.org/transition-toolkit/world-energy-trilemma-index>.
- Delesto, Nobian (n.d.). *Nobian Delesto*. URL: <https://www.chemieparkdelfzijl.nl/bedrijven/599094-akzonobel-delesto>.
- Dios, Rafael De, Fernando Soto, and Antonio J Conejo (Sept. 2007). “Planning to expand?” In: *IEEE Power and Energy Magazine* 5.5, pp. 64–70. DOI: 10.1109/mpe.2007.904764.
- Dutch Government (1998). *Elektriciteitswet*. URL: <https://wetten.overheid.nl/BWBR0009755/2022-08-01#Hoofdstuk2>.
- Economische Zaken, Ministerie van (n.d.). *Energierapport: Transitie naar duurzaam*. URL: <https://open.overheid.nl/repository/ronl-archief-c0b58a92-fdcc-4dda-9cfb-e6bf5f82704d/1/pdf/energierapport-transitie-naar-duurzaam.pdf>.
- EEX (n.d.). *Rijnmond Centrale*. URL: <https://web.archive.org/web/20181229023454/https://www.eex-transparency.com/power/>.
- Elsta (n.d.). *Elsta Cogeneration Power plant Hoek Terneuzen — AES*. URL: <https://www.elstacogen.nl/>.
- Eneco (n.d.[a]). *Enecogen*. URL: <https://www.eneco.nl/over-ons/wat-we-doen/duurzame-bronnen/enecogen/>.
- (n.d.[b]). *Warmtebuffer in Utrecht Merwedekanaalzone*. URL: <https://www.eneco.nl/over-ons/wat-we-doen/duurzame-bronnen/warmtebuffers/utrecht-merwedekanaalzone/>.
- Engie (n.d.[a]). *Eemscentrale*. URL: <https://www.engie.nl/over-ons/moderne-centrales/Eemscentrale>.
- (n.d.[b]). *Maxima-centrale*. URL: <https://www.engie.nl/over-ons/moderne-centrales/Maxima-centrale>.
- ENTSO-E (2022a). *Transparency Platform*. URL: <https://transparency.entsoe.eu/>.
- (2022b). *TYNDP*. URL: <https://tyndp.entsoe.eu/>.
- EPZ (Jan. 2021). *Kerncentrale*. URL: <https://www.epz.nl/themas/kerncentrale/>.
- EU (Oct. 2019). *A European Green Deal*. URL: https://ec.europa.eu/info/strategy/priorities-2019-2024/european-green-deal_en.
- (2020). *2030 Climate Target Plan*. URL: https://climate.ec.europa.eu/eu-action/european-green-deal/2030-climate-target-plan_en.
- Frank, Stephen et al. (Apr. 2012). “Optimal power flow: a bibliographic survey I”. In: *Energy Systems 2012 3:3* 3.3, pp. 221–258. ISSN: 1868-3975. DOI: 10.1007/S12667-012-0056-Y.
- GE Renewable Energy (2022). *Haliade-X offshore wind turbine*. URL: <https://www.ge.com/renewableenergy/wind-energy/offshore-wind/haliade-x-offshore-turbine>.

- Gotzens, Fabian et al. (Jan. 2019). “Performing energy modelling exercises in a transparent way - The issue of data quality in power plant databases”. In: *Energy Strategy Reviews* 23, pp. 1–12. DOI: 10.1016/j.esr.2018.11.004.
- Haas, Sabine et al. (Mar. 2021). “wind-python/windpowerlib: Silent Improvements”. In: DOI: 10.5281/ZENODO.4591809.
- Hamarat, Caner, Jan H. Kwakkel, and Erik Pruyt (Mar. 2013). “Adaptive Robust Design under deep uncertainty”. In: *Technological Forecasting and Social Change* 80.3, pp. 408–418. DOI: 10.1016/j.techfore.2012.10.004.
- Hau, Erich (2008). “Wind power systems. Fundamentals, technology, applications, economic aspects. 4. compl. new rev. ed.; Windkraftanlagen. Grundlagen, Technik, Einsatz, Wirtschaftlichkeit”. In: *Windkraftanlagen*. DOI: 10.1007/978-3-540-72151-2.
- Jamasb, Tooraj and Michael Pollitt (Sept. 2005). “Electricity Market Reform in the European Union: Review of Progress toward Liberalization & Integration”. In: *The Energy Journal* 26.01. DOI: 10.5547/issn0195-6574-ej-vol26-nosi-2.
- JAO (Sept. 2022). *Static Grid Model*.
- Kahn, Edward (June 1995). “Regulation by Simulation: The Role of Production Cost Models in Electricity Planning and Pricing”. In: *Operations Research* 43.3, pp. 388–398. DOI: 10.1287/opre.43.3.388.
- Klimaataakkoord, Voortgangoverleg (2019). *Klimaataakkoord*. Tech. rep.
- Klimaatmonitor, Regionale (2022). *Regionale Klimaatmonitor*. website. URL: <https://klimaatmonitor.databank.nl/dashboard/dashboard/energieverbruik>.
- Kuiken, Dirk and Heyd F Más (June 2019). “Integrating demand side management into EU electricity distribution system operation: A Dutch example”. In: *Energy Policy* 129, pp. 153–160. DOI: 10.1016/j.enpol.2019.01.066.
- Kwakkel, Jan H (Oct. 2017). “The Exploratory Modeling Workbench: An open source toolkit for exploratory modeling, scenario discovery, and (multi-objective) robust decision making”. In: *Environmental Modelling & Software* 96, pp. 239–250. DOI: 10.1016/j.envsoft.2017.06.054.
- Lempert, Robert J (2003). “Shaping the next one hundred years: new methods for quantitative, long-term policy analysis”. In.
- Monitor, Global Energy (Jan. 2021). *Rotterdam Capelle (RoCa) power station*. URL: [https://www.gem.wiki/Rotterdam_Capelle_\(RoCa\)_power_station](https://www.gem.wiki/Rotterdam_Capelle_(RoCa)_power_station).
- (Jan. 2022). *Akzo Salinco power station*. URL: https://www.gem.wiki/Akzo_Salinco_power_station.
- Pambour, Kwabena Addo et al. (2017). “SAInt – A novel quasi-dynamic model for assessing security of supply in coupled gas and electricity transmission networks”. In: *Applied Energy* 203, pp. 829–857. ISSN: 0306-2619. DOI: <https://doi.org/10.1016/j.apenergy.2017.05.142>. URL: <https://www.sciencedirect.com/science/article/pii/S0306261917307018>.
- PBL et al. (Nov. 2022). *Klimaat- en Energieverkenning 2022*. Tech. rep. Den Haag: Planbureau voor de Leefomgeving: PBL, TNO, CBS en RIVM. URL: <https://www.pbl.nl/publicaties/klimaat-en-energieverkenning-2022>.
- Pérez-Arriaga, Ignacio J., ed. (2013). *Regulation of the Power Sector*. Springer London. DOI: 10.1007/978-1-4471-5034-3.
- Pfenninger, Stefan and Iain Staffell (Nov. 2016). “Long-term patterns of European PV output using 30 years of validated hourly reanalysis and satellite data”. In: *Energy* 114, pp. 1251–1265. DOI: 10.1016/j.energy.2016.08.060.
- Pillay, Anusha, S. Prabhakar Karthikeyan, and D.P. Kothari (Sept. 2015). “Congestion management in power systems – A review”. In: *International Journal of Electrical Power & Energy Systems* 70, pp. 83–90. ISSN: 0142-0615. DOI: 10.1016/j.ijepes.2015.01.022. URL: <https://linkinghub.elsevier.com/retrieve/pii/S0142061515000411>.
- Programma, Nationaal Waterstof (2023). *Nationaal Waterstof Programma*. Website. URL: <https://www.nationaalwaterstofprogramma.nl/home/default.aspx>.

- Quaschnig, Volker (n.d.). “Regenerative Energiesysteme”. In: (). URL: www.hanser-fachbuch.de/newsletter.
- Redactie, L C (Jan. 2021). *Voorlopig geen sloop voor actieve Centrale Burgum*. URL: <https://lc.nl/friesland/tytsjerksteradiel/Voorlopig-geen-sloop-voor-actieve-Centrale-Burgum-26381866.html>.
- RES, Nationaal Programma (n.d.). *Regionale Energie Strategie*. URL: <https://www.regionale-energiestrategie.nl/default.aspx>.
- Rijksoverheid (Dec. 2021). *Kabinet legt uitstoot kolencentrales fors aan banden*. URL: <https://www.rijksoverheid.nl/actueel/nieuws/2021/12/22/kabinet-legt-uitstoot-kolencentrales-fors-aan-banden>.
- (n.d.). *Wind op zee*. URL: <https://windopzee.nl/>.
- RWE (n.d.[a]). *Clauscentrale C*. URL: <https://benelux.rwe.com/locaties/gasgestookte-centrale-claus-c>.
- (n.d.[b]). *Moerdijkcentrale*. URL: <https://benelux.rwe.com/locaties/warmtekrachtcentrale-moerdijk>.
- (n.d.[c]). *Swentiboldcentrale*. URL: <https://benelux.rwe.com/locaties/warmtekrachtcentrale-swentibold>.
- Serge van Gessel et al. (2021). *Ondergrondse Energieopslag in Nederland 2030-2050 (I): Technische evaluatie van vraag en aanbod*. Tech. rep. URL: <https://www.rijksoverheid.nl/documenten/rapporten/2021/10/12/ondergrondse-energieopslag-in-nederland-2030---2050>.
- Sharp, RE (May 2015). “Spatiotemporal disaggregation of GB scenarios depicting increased wind capacity and electrified heat demand in dwellings”. In: *In: Proceedings of the 38th IAEE International Conference. International Association for Energy Economics (IAEE): Antalya, Turkey. (2015)*. URL: <https://www.iaee.org/en/publications/proceedingssearch.aspx?conference=Energy%20Security,%20Technology%20and%20Sustainability%20Challenges%20Across%20the%20Globe>.
- Sloecentrale (n.d.). *Sloecentrale*. URL: <https://www.sloecentrale.nl/nl/>.
- Staffell, Iain and Stefan Pfenninger (Nov. 2016). “Using bias-corrected reanalysis to simulate current and future wind power output”. In: *Energy* 114, pp. 1224–1239. DOI: 10.1016/j.energy.2016.08.068.
- Sultiens, Els (Feb. 2023). *TenneT: 28 gigawatt aan aansluitverzoeken voor batterijen in behandeling*. URL: <https://solarmagazine.nl/nieuws-zonne-energie/i29038/tennet-28-gigawatt-aan-aansluitverzoeken-voor-batterijen-in-behandeling>.
- TenneT (Sept. 2022a). *Grid Capacity map*. URL: <https://www.tennet.eu/grid-capacity-map>.
- (2022b). *Investeringsplannen*. URL: <https://www.tennet.eu/nl/over-tennet/publicaties/investeringsplannen>.
- (Dec. 2022c). *Monitoring Leveringszekerheid 2022 (2025-2030)*. URL: <https://www.tennet.eu/nl/over-tennet/publicaties/rapport-monitoring-leveringszekerheid>.
- (2022d). *Our tasks*. URL: <https://www.tennet.eu/about-tennet/our-tasks>.
- Tsegaye, Shewit, Fekadu Shewarega, and Getachew Bekele (July 2018). “A Review on Security Constrained Economic Dispatch of Integrated Renewable Energy Systems”. In: *EAI Endorsed Transactions on Energy Web*, p. 166363. DOI: 10.4108/eai.25-9-2020.166363.
- Uniper (n.d.[a]). *Den Haag*. URL: <https://www.uniper.energy/nl/nederland/energiecentrales-in-nederland/den-haag>.
- (n.d.[b]). *Leiden*. URL: <https://www.uniper.energy/nl/nederland/energiecentrales-in-nederland/leiden-city-plant-nl>.
- (n.d.[c]). *Presentatie Uniper*. URL: https://denhaag.raadsinformatie.nl/document/4384502/1/Presentatie_Uniper.
- Vattenfall (n.d.[a]). *Power plants: Diemen CCGT and CHP Plant - Vattenfall*. URL: <https://powerplants.vattenfall.com/diemen/>.
- (n.d.[b]). *Power plants: Magnum - Vattenfall*. URL: <https://powerplants.vattenfall.com/magnum/>.

- Vattenfall (n.d.[c]). *Power plants: Velsen - Vattenfall*. URL: <https://powerplants.vattenfall.com/velsen/>.
- Vestas (n.d.). *V236-15.0MW*. URL: <https://www.vestas.com/en/products/offshore/V236-15MW/V236-15MW>.
- Walker, Warren E, Robert J Lempert, and Jan H Kwakkel (2012). “Deep Uncertainty”. In: *Delft University of Technology*.
- Wiki (n.d.). *Elektriciteitscentrales NL*. URL: https://nl.wikipedia.org/wiki/Lijst_van_elektriciteitscentrales_in_Nederland.

A Mathematical model

The formulation behind the simulation model comprises a small number of formulas. The objective function is central to this formulation. This is a minimizing optimization function.

Equation 1 is the minimizing cost function. Each timestep function will minimize the costs in the system. This system comprises 3 parts: generation, demand, and the number of timesteps. The generation is the cost of the power generation on each generator, with the cost of the generator. The demand is the amount not served against the penalty price of unserved demand per MWh. This is calculated for each timestep.

This objective function is subject to constraining functions. This means that these functions must be met at all times.

Equation 2 ensures that the power generated in the simulation minus the unserved demand for power equals the demand for each timestep.

Equation 3 Ensures that the power generated at each generator is higher than zero and lower than their maximal capacity.

Equation 4 Ensures that the amount of power is not higher than its maximal capacity. The minus sign is added since the power can flow in 2 ways.

Equation 5 ensures the power flows are somewhat correct according to power network physics.

Equation 6 states that each of the radiants on the nodes is free, except for the slack node. The slack node is the reference node.

Equation 7 states that the slack node is arbitrarily set to 0.

Equation 8 states that the unserved demand must be lower than the total demand for the timestep.

$$\text{Min } \sum_t \left(\sum_g P_{g,t} \cdot C_g^{op} + \sum_d P_{d,t}^{notserved} \cdot P_d^{PNS} \right) \cdot \Delta t \quad (1)$$

$$\text{s.t. } \sum_{g|g.no=n} P_{g,t} + \sum_{l|l.to=n} P_{l,t} - \sum_{l|l.from=n} P_{l,t} + \sum_{d|d.no=n} P_{dt}^{notserved} = \sum_{d|d.no=n} D_{dt} \quad \forall n, t \quad (2)$$

$$0 \leq P_{g,t} \leq K_g \quad \forall g, t \quad (3)$$

$$-K_l \leq P_{l,t} \leq K_l \quad \forall l, t \quad (4)$$

$$P_{l,t} = \frac{1}{X_l} (\theta_{l.from,t} - \theta_{l.to,t}) \cdot S_{base} \quad \forall l, t \quad (5)$$

$$\theta_{n,t} \text{ free} \quad \forall n \neq \text{slack}, t \quad (6)$$

$$\theta_{\text{slack},t} = 0 \quad \forall t \quad (7)$$

$$0 \leq P_{d,t}^{notserved} \leq D_{d,t} \quad \forall d, t \quad (8)$$

B Methodology verification

This Section will verify the methodology using a simple 5-node network model representing the Dutch transmission grid. The congestion-seeking algorithm is slightly altered to improve the runtime.

B.1 5- node network topology

The transmission network is cut into 5 zones. These 5 zones are called: **ZuidZee**, **NoordHollandFlevo**, **Groningen**, **Friesland** & **OostNederland**. A more detailed explanation concerning the geographics of these 5 zones is described in C.4.1. For the sake of simplicity in the model, it is assumed that within these 5 zones, no capacity constraints in the lines exist. In this assumption, the power generators can be aggregated. The network topology of this model can be seen in 16.



Figure 16: Current network topology

The lines that connect the different nodes with their capacities reflected are taken from the JAO grid model JAO 2022. In this data, the plans of the TSO for 2030 have been added. The

verification for the data in this model can be found in C.5.1. Table 20 contains an overview of all lines.

| Name | FromName | ToName | Real connection | Capacity (MW) |
|------|-------------------|-------------------|-------------------------|---------------|
| A | ZuidZee | NoordHollandFlevo | Krimpen-Breukelen | 1646.875 |
| B1 | NoordHollandFlevo | ZuidZee | Vijfhuizen-Bleiswijk | 1976.250 |
| B2 | NoordHollandFlevo | ZuidZee | Vijfhuizen-Bleiswijk | 1976.250 |
| C1 | ZuidZee | OostNederland | Geertruidenberg-Tilburg | 2635.000 |
| C2 | ZuidZee | OostNederland | Geertruidenberg-Tilburg | 2635.000 |
| D1 | Friesland | NoordHollandFlevo | Ens-Lelystad | 2635.000 |
| D2 | Friesland | NoordHollandFlevo | Ens-Lelystad | 2635.000 |
| E1 | Groningen | Friesland | Eemshaven-Vierverlaten | 2635.000 |
| E2 | Groningen | Friesland | Eemshaven-Vierverlaten | 2635.000 |
| E3 | Groningen | Friesland | Eemshaven-Vierverlaten | 2635.000 |
| E4 | Groningen | Friesland | Eemshaven-Vierverlaten | 2635.000 |
| F1 | OostNederland | Groningen | Zwolle-Meeden | 2635.000 |
| F2 | OostNederland | Groningen | Zwolle-Meeden | 2635.000 |
| G1 | OostNederland | Friesland | Ens-Zwolle | 2635.000 |
| G2 | OostNederland | Friesland | Ens-Zwolle | 2635.000 |
| H | ZuidZee | NoordHollandFlevo | Krimpen-Oostzaan | 1646.875 |

Table 20: Lines and their capacities in the first Iteration of the model.

B.1.1 Renewable energy generators

The ambition of the amount of renewable generation can be split up between the bids each RESA region has made and the ambitious plans for the offshore wind farms.

RESA plans

The installed capacity of the renewable energy generators has been attributed according to the plans of the 30 regions in the Netherlands, plus the off-shore wind plans of the government. The methodology behind this can be found in D.2. In Figure 17 an overview of the installed capacity per renewable energy source is displayed.

Off-shore wind

Next to this, wind farms will be built off-shore following the government's plans (Rijksoverheid n.d.). An overview of these plans and to which region the farms have been allocated can be found in the following table. A more in-depth description of the data can be found in C.7. An overview of the installed capacity of offshore wind is displayed in 18

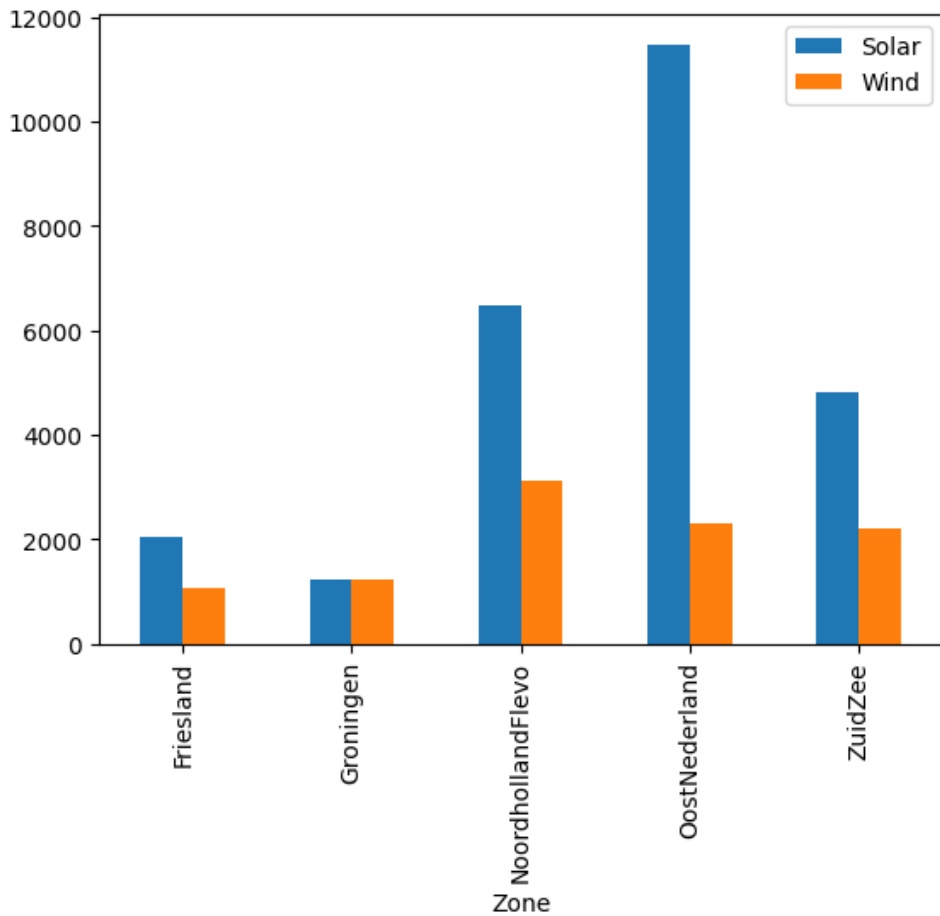


Figure 17: Capacity with the implementation of RESA plans per zone.

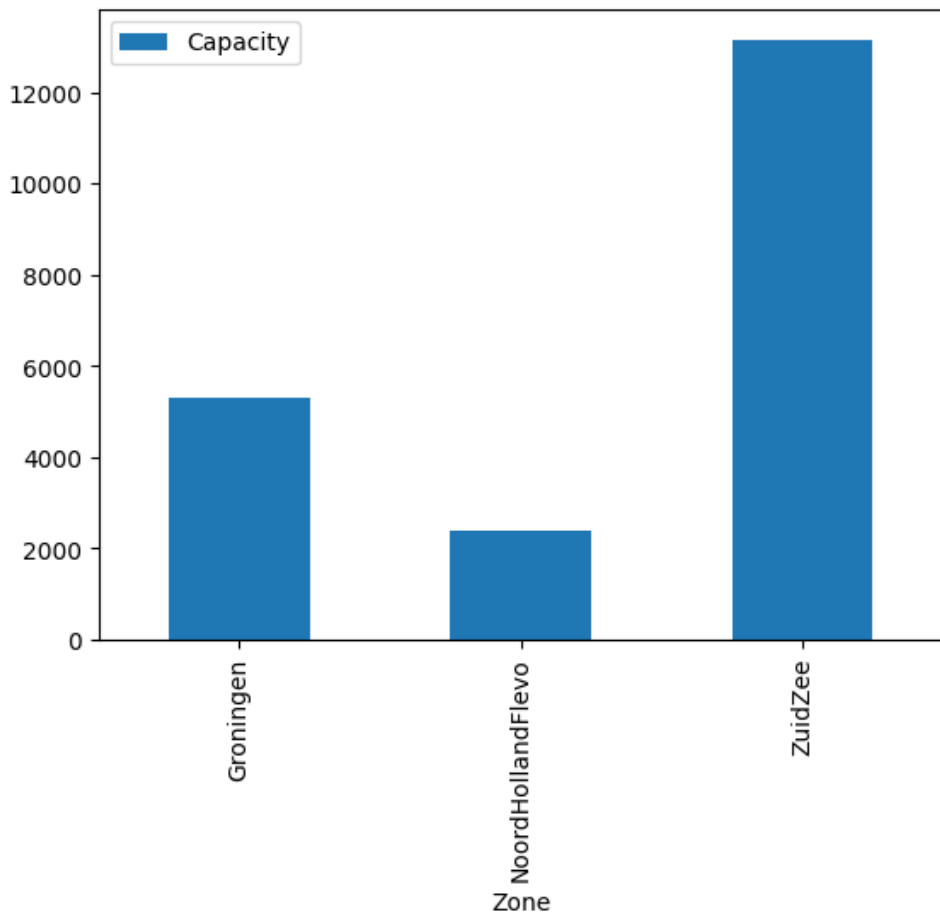


Figure 18: Capacity with implementation of off-shore windfarms.

B.1.2 Fuel generators

The generators have been gathered from pypsa with verification from the Wikipedia page (Wiki n.d.), and the corresponding websites. An overview of the generators, their fuel, capacity, and efficiency will later be added in C.3 It is assumed that the active coal plants will be decommissioned by 2030 following the decision of the Dutch government (Rijksoverheid 2021). For simplicity reasons, biomass generators have been let out of the model. In this phase, one nuclear plant is added, and the rest of the conventional generators use gas as fuel.

B.1.3 Demand

The projection of the demand for electricity is calculated by scaling the yearly demand of the weather year to the demand of 2030. This is done in 2015, 2016, 2017, and 2018. Each node is given a share of the demand, based on its energy demand. In Table 21.

| Zone | Demandrate |
|-------------------|------------|
| NoordHollandFlevo | 0.211 |
| ZuidZee | 0.352 |
| Friesland | 0.045 |
| Groningen | 0.051 |
| OostNederland | 0.353 |

Table 21: Share of the demand per region

B.1.4 Model setup

The corresponding model will be run as a whole year, from the first of January 2030 at 00:00, to the first of January 2031 at 00:00. It will be solved with Gurobi as an LP problem.

B.1.5 Uncertainty specification

Each demand, offshore wind, wind and solar parameters will be used as an uncertain factor. The range of the uncertainty factors for each of them is 0.75-1.5.

B.2 Evaluation of the performance

To evaluate the vulnerabilities in the network, congestions need to be detected. Via SAInt this can be done in 2 ways. The power loads of each of the lines can be called via the interface. It can be stated that congestion occurs when one of these lines is 100. When it is sufficient to count a network's congestion amount, this would be a great way to calculate this. Another way is to look at the model's shadow prices at the nodes. As the literature in Section 2.2.1 describes, these will be different at the nodes when congestion interferes with the economic equilibrium of demand and supply. Within SAInt congestions are handled in the same manner, a congestion causes the model to halt cheaper production at a certain node to start more expensive production at another node. This causes the shadow prices of the nodes to change from another.

The proposed methodology to evaluate the severity of congestion has the following steps:

1. Detection of a congestion
2. Run the model with all capacity constraints alleviated for the congested timestep.
3. Attribute the cost difference of the congested timestep of the 2 runs to the congested line.

Since we want to limit the amount of times congestion is unnecessarily detected, and the rest of the methodology is set in motion, the detection of congestion is done using the shadow prices. The concept of cost attribution can be seen in Figure 19. This cost attribution must be seen

as an indicator of the severity of the influence of the line on the costs of the system. In actual world application, it would, of course, be impossible to create a line with infinite capacity.

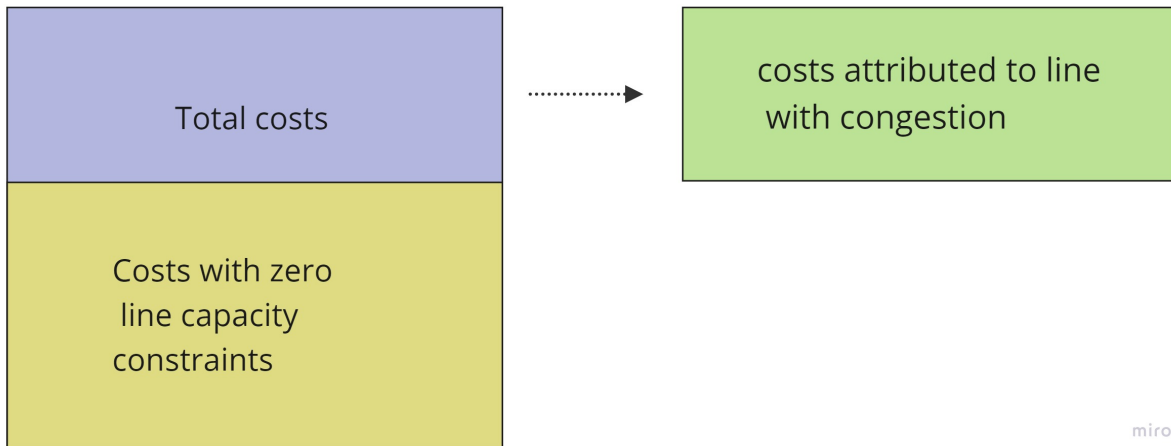


Figure 19: Cost attribution

Each of the lines will naturally have one of these cost attribution outcomes. In addition, the total emissions in the system (in ton Co₂), the Total amount of congestion, and the ratio of Renewable energy divided by the potential renewable energy. The first gives an indication of which uncertainties will affect the number of emissions in the system, the second will indicate which delays affect the number of total congestion, and the third will tell which uncertainty will affect the amount of curtailed renewable energy.

B.3 Results of 5-node experiment

In Figure 20, a global overview of the results can be seen. The visualization technique of Feature scoring has been used. On the y-axis, the uncertainties in the model are shown, on the x-axis, the severity of the congestions on the lines, and some general system outcomes are shown.

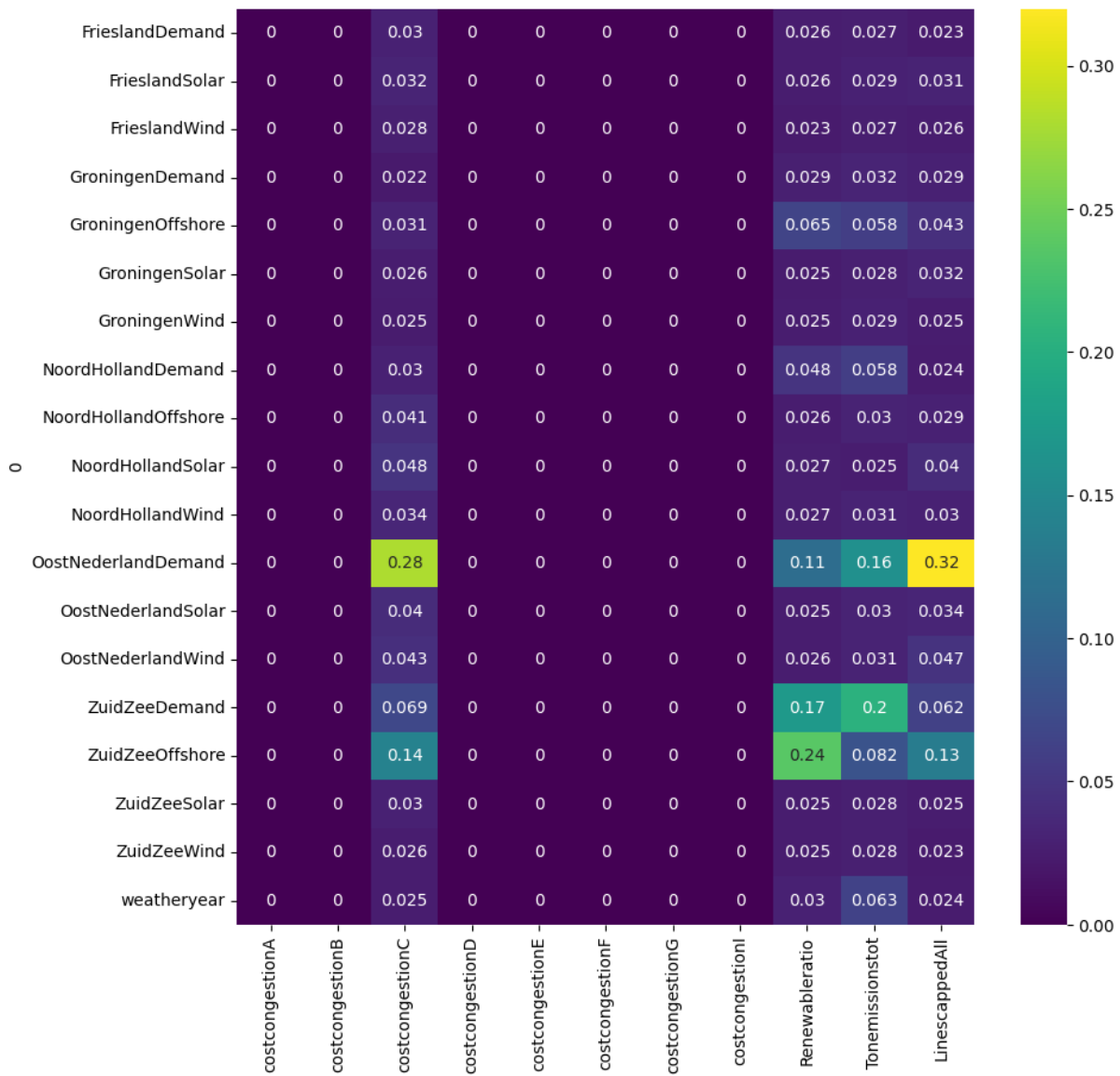


Figure 20: Feature scoring of 250 runs with simple model.

The outcomes of this experiment show that the only line that was congested is line C. The most influential uncertainties to this line are the Demand in OostNederland, and the Offshore wind capacity in ZuidZee. This is the expected outcome; the offshore generation in ZuidZee is by far the most producing renewable generator in the system, and the demand in OostNederland is the biggest.

C 6-node network

In this section, the 6-node network is described, this network was used to explore methodological choices. It's an extension of the 5-node network as described in B.1. The difference between the two is that the node of OostNederland is split up into ZuidOost and Oost. The data and lines are roughly the same in this model. We will therefore not elaborate on this network.

C.1 Line characteristics

C.2 Generators

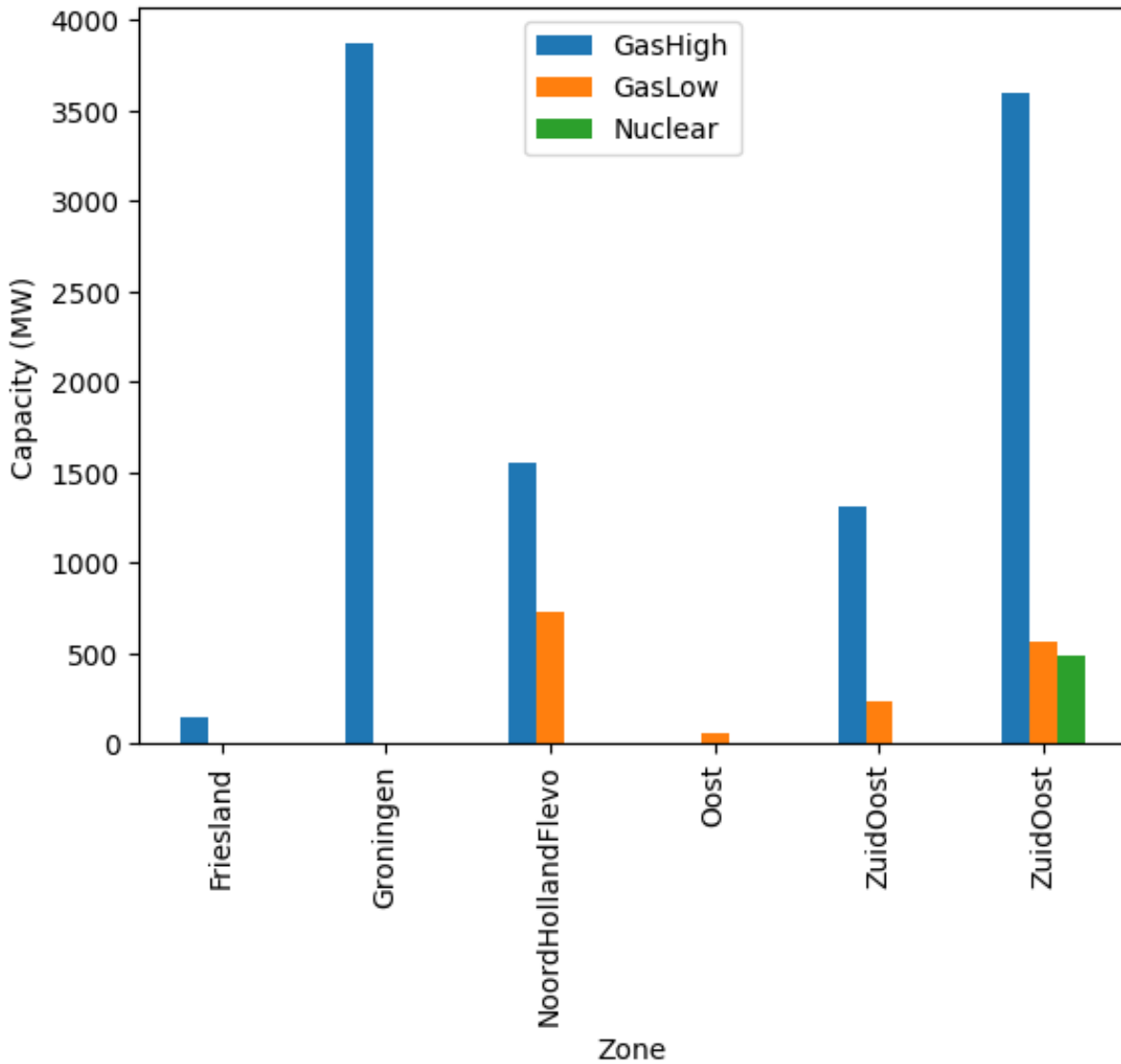


Figure 21: Renewable generators in second network.

| Connection | Name | From Node | To Node | Parallel Lines | Capacity (MW) | Length (KM) |
|-------------------------|------|-------------------|-------------------|----------------|---------------|-------------|
| Krimpen-Breukelen | A | ZuidZee | NoordHollandFlevo | 1 | 1646.875 | 20.010 |
| Vijfhuizen-Bleiswijk | B | NoordHollandFlevo | ZuidZee | 2 | 3952.000 | 14.310 |
| Geertruidenberg-Tilburg | C | ZuidZee | ZuidOost | 2 | 5270.000 | 21.000 |
| Ens-Lelystad | D | Friesland | NoordHollandFlevo | 2 | 5270.000 | 21.000 |
| Eemshaven-Vierverlaten | E | Groningen | Friesland | 4 | 10540.000 | 44.000 |
| Zwolle-Meeden | F | Oost | Groningen | 2 | 5270.000 | 107.850 |
| Ens-Zwolle | G | Oost | Friesland | 2 | 5270.000 | 32.000 |
| Krimpen-Oostzaan | H | ZuidZee | NoordHollandFlevo | 1 | 1646.875 | 72.529 |
| Boxmeer-Dodewaard | I | ZuidOost | Oost | 1 | 1646.875 | 41.700 |
| Maasbracht-Dodewaard | J | ZuidOost | Oost | 1 | 1646.875 | 57.900 |

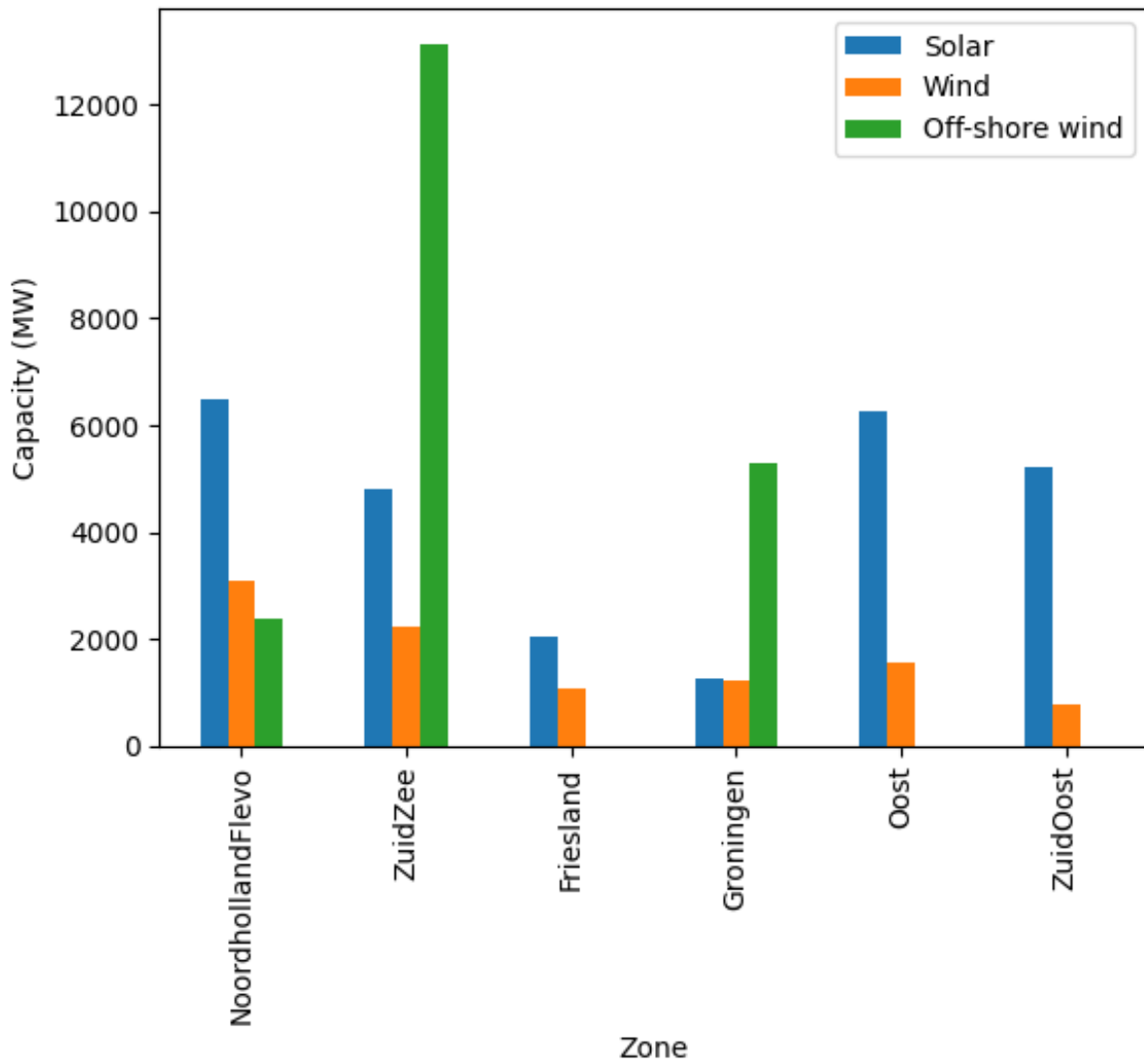


Figure 22: Fuel generators in second network.

Not only were the generators split up in this network, the capacities of the fuel generators were refined as well. In table C.2 the redefined placement of the generators can be found.

| | Name | Zone | Capacity | Efficiency categorie | Source |
|----|------------------------|-------------------|----------|----------------------|--------------------|
| 0 | Bergum | Friesland | 146 | Low | Redactie 2021 |
| 1 | Delesto | Groningen | 530 | High | Delesto n.d. |
| 2 | Eems | Groningen | 1931 | High | Engie n.d.(a) |
| 3 | Magnum_Centrale | Groningen | 1410 | High | Vattenfall n.d.(b) |
| 4 | Diemen | NoordHollandFlevo | 684 | High | Vattenfall n.d.(a) |
| 5 | Velsen | NoordHollandFlevo | 725 | Low | Vattenfall n.d.(c) |
| 6 | Centrale_Merwedekanaal | NoordHollandFlevo | 328 | High | Eneco n.d.(b) |
| 7 | Flevo | NoordHollandFlevo | 861.1 | High | Engie n.d.(b) |
| 8 | Sal | Oost | 60 | Low | Monitor 2022 |
| 9 | Swentibold | ZuidOost | 230 | Low | RWE n.d.(c) |
| 10 | Claus | ZuidOost | 1304 | High | RWE n.d.(a) |
| 11 | Rijnmond | ZuidZee | 820 | High | EEX n.d. |
| 12 | Moerdijk | ZuidZee | 870 | High | RWE n.d.(b) |
| 13 | Borssele | ZuidZee | 485 | Nuclear | EPZ 2021 |
| 14 | Roca | ZuidZee | 220 | High | Monitor 2021 |
| 15 | Elsta | ZuidZee | 455 | Low | Elsta n.d. |
| 16 | Den_Haag | ZuidZee | 107 | Low | Uniper n.d.(a) |
| 17 | Ucml | ZuidZee | 80 | High | Uniper n.d.(c) |
| 18 | Ld | ZuidZee | 85 | High | Uniper n.d.(b) |
| 19 | Sloecentrale | ZuidZee | 870 | High | Sloecentrale n.d. |
| 20 | Enecogen | ZuidZee | 844 | High | Eneco n.d.(a) |

The powerplants are divided in fuel generators with high efficiency, with low efficiency, and the nuclear powerplant in Borssele. The high efficiency powerplants have an efficiency of 58 %, the low efficiency powerplants and the nuclear powerplant have an efficiency of 36 %.

C.3 Verification of model data

C.4 First model

C.4.1 Zone characteristics

The 5 nodes are called: **ZuidZee**, **NoordHollandFlevo**, **Groningen**, **Friesland** & **Oost-Nederland**. **Zuidzee** consists of the provinces Zuid-Holland and Zeeland. This region holds a population of more than 4 million people (CBS 2022), the biggest port in Europe, and holds 2 of the 5 industrial clusters in the Netherlands: The cluster Rotterdam-Moerdijk and the cluster Zeeland-Noord-Brabant (sources). This region is connected to Noord-Holland via 2 stations: Krimpen Moerdijk. It is connected to the region OostNederland via the station of Geertruidenberg. This region will have connections through off-shore wind via connections in the stations of Borssele, Maasvlakte, and Geertruidenberg (Rijksoverheid n.d.).

NoordHollandFlevo consists of the provinces Noord-Holland, Flevoland, and parts of the province Utrecht, this region as well holds over 4 million people (CBS 2022). The industrial cluster 'Noordzeekanaalgebied' is placed in this region (source). it is connected to the region of ZuidZee via the stations of Breukelen, Oostzaan, and Vijfhuizen, and connected to the region of Friesland through the station of Lelystad. The region will have a connection to off-shore wind parks via the station of Beverwijk.(Rijksoverheid n.d.). **Friesland** consists of the province of Friesland and parts of the province Flevoland, this region has around 850,000 inhabitants. This region has no connections to any wind farms or international connections. Within this zone, the 220 kV network of the Netherlands is situated. **Groningen** consists of the province Groningen and parts of the province Drenthe. The region has a population of approximately 900,000 inhabitants. The industrial cluster of 'Noord-Nederland' is situated here. This region has a connection with off-shore wind via the station of Eemshaven. **OostNederland** consists of Noord-Brabant, Gelderland, Limburg, Overijssel, and parts of Drenthe, this region is the largest in landmass, covering about half of the Netherlands. The reason this region is grouped together

is that the lines that run through this region make up a straight line. This makes it easy to demarcate as one region. The region has around 7 million inhabitants, and the industrial cluster of Chemelot is situated inside it.

C.5 Storage

In the KEV 2022, there is no mention of storage facilities for electricity in batteries. There is, however, the mention of large-scale Underground storage of energy by the report of TNO. In the scenarios sketched in this report, the capacity for hydrogen storage must be between 42 and 475 TWh. However, with the partial transformation of the gas network to a hydrogen network, this energy will probably never enter the transmission grid. The reason is that the energy will be produced at the renewable-energy plants, it will be stored in hydrogen at electrolyzers near these plants, and transported to the end-user via the hydrogen network. For this reason, no storage capacity is modeled.

C.5.1 Network verification

One of the important characteristics of the lines is their reactance (X). As seen in the literature section, this is needed to accurately calculate the powerflows on the lines. To verify this reactance, the physical characteristics typical Dutch network lines were examined. According to Hoogspanningsnet, there are Aluminum Magnesium Silicate (AMS) or Aluminum Conductor Steel Reinforced (ACSR) cables. The AMS-cables usually have an intersection of either 460 or 620 mm^2 and referred to as respectively AMS-460 or AMS-620. The AMS-620 lines have a capacity of 1000 Ampere and are typically bundled in cables with 4. The reactance per kilometer of a similar pure aluminum cable is 0.331 on a 60Hz network. In the case of a 50 Hz network like the Netherlands, the reactance of these cables will be $0.331 \times 50 \div 60 = 0.276 \div Km$. The ACSR-cables usually have a width of 437 mm^2 , or 560 and typically have around the same Reactances. While calculating the reactances of the lines, with these numbers, around the same reactances of the lines can be found as in the JAO grid model. Therefore, the Jao grid model is taken as input for the network topology and it's physical characteristics. On this input the planned projects of the TSO are added(TenneT 2022a). the capacities for each of the lines can be found in Table 22.

| Name | FromName | ToName | Real connection | Capacity (MW) |
|------|-------------------|-------------------|-------------------------|---------------|
| A | ZuidZee | NoordHollandFlevo | Krimpen-Breukelen | 1646.875 |
| B1 | NoordHollandFlevo | ZuidZee | Vijfhuizen-Bleiswijk | 1976.250 |
| B2 | NoordHollandFlevo | ZuidZee | Vijfhuizen-Bleiswijk | 1976.250 |
| C1 | ZuidZee | OostNederland | Geertruidenberg-Tilburg | 2635.000 |
| C2 | ZuidZee | OostNederland | Geertruidenberg-Tilburg | 2635.000 |
| D1 | Friesland | NoordHollandFlevo | Ens-Lelystad | 2635.000 |
| D2 | Friesland | NoordHollandFlevo | Ens-Lelystad | 2635.000 |
| E1 | Groningen | Friesland | Eemshaven-Vierverlaten | 2635.000 |
| E2 | Groningen | Friesland | Eemshaven-Vierverlaten | 2635.000 |
| E3 | Groningen | Friesland | Eemshaven-Vierverlaten | 2635.000 |
| E4 | Groningen | Friesland | Eemshaven-Vierverlaten | 2635.000 |
| F1 | OostNederland | Groningen | Zwolle-Meeden | 2635.000 |
| F2 | OostNederland | Groningen | Zwolle-Meeden | 2635.000 |
| G1 | OostNederland | Friesland | Ens-Zwolle | 2635.000 |
| G2 | OostNederland | Friesland | Ens-Zwolle | 2635.000 |
| H | ZuidZee | NoordHollandFlevo | Krimpen-Oostzaan | 1646.875 |

Table 22: Lines and their capacities in the first Iteration of the model.

| RESA | Zone |
|--------------------------|-------------------|
| DrentheFries | Friesland |
| West-OverijsselFriesland | Friesland |
| Friesland | Friesland |
| Groningen | Groningen |
| AmersfoortNoord | NoordHollandFlevo |
| Flevoland | NoordHollandFlevo |
| Holland RijnlandNoord | NoordHollandFlevo |
| Noord-Holland-Noord | NoordHollandFlevo |
| Noord-Holland-Zuid | NoordHollandFlevo |
| Noord-VeluweNoord | NoordHollandFlevo |
| U16 | NoordHollandFlevo |
| DrentheOost | Oost |
| Achterhoek | Oost |
| Arnhem Nijmegen | Oost |
| AmersfoortOost | Oost |
| Foodvalley | Oost |
| Noord-VeluweOost | Oost |
| Fruitedelta Rivierenland | Oost |
| Cleantech regio | Oost |
| Twente | Oost |
| West-OverijsselOost | Oost |
| Hart van Brabant | ZuidOost |
| Metropoolregio Eindhoven | ZuidOost |
| Noord -en Midden Limburg | ZuidOost |
| Noordoost Brabant | ZuidOost |
| Zuid-Limburg | ZuidOost |
| Alblasserwaard | ZuidZee |
| Drechtsteden | ZuidZee |
| Goeree-Overflakkee | ZuidZee |
| Hoeksche Waard | ZuidZee |
| Midden-Holland | ZuidZee |
| Rotterdam den Haag | ZuidZee |
| West-Brabant | ZuidZee |
| Zeeland | ZuidZee |
| Holland RijnlandZuid | Zuidzee |

C.6 RESA

The 30 regions have been attributed to one of the 5 zones. The attribution can be found in the table underneath. Each of these regions has the ambition to fulfill a part of the 35TWh of Energy that is described in the Dutch Climate Act (RES n.d.). Each region has proposed a bid to provide a share. The first bids were proposed in 2021 and can be found in table It can be seen that the bids of the regions are more than the initial 35 TWH. It seems that, in total, the regions overbid the initial Climate Act. In the third and fourth columns, the ambitions of the solar and wind, respectively can be found. In the final 2 columns, the expected capacity that needs to be installed is displayed. This last column is calculated via the indications in the plans of the RESA of Zeeland. In this RESA, it is assumed that an installed capacity of 700 MW of wind will have a yield of 1950 GW every year. For solar, an installed capacity of 500 MW will return in 485GW output of energy every year. In the model, the installed capacity will be submitted to various weather years to generate different output patterns. The installed capacity per RESA can be found in table

| Zone | Solar | Wind |
|-------------------|-----------|-----------|
| NoordhollandFlevo | 6473.3397 | 3102.2267 |
| ZuidZee | 4819.925 | 2215.389 |
| Friesland | 2029.008 | 1077.8975 |
| Groningen | 1237.2 | 1231.37 |
| Oost | 6265.0777 | 1542.5512 |
| ZuidOost | 5216.86 | 768.26 |

| Wind-farm | Zone | Capacity |
|-----------------------------------|-------------------|----------|
| Borssele | ZuidZee | 1502.5 |
| Hollandse Kust Zuid | ZuidZee | 1649 |
| Hollandse Kust Noord | NoordHollandFlevo | 987 |
| Hollandse Kust West | NoordHollandFlevo | 1400 |
| Ten Noorden Van De Waddeneilanden | Groningen | 1300 |
| Ijmuiden Ver Noord | ZuidZee | 4000 |
| Nederwiek | ZuidZee | 6000 |
| Doordewind | Groningen | 4000 |

Table 23: Planned windfarms

This is the installed capacity for the wind and solar generators' energy on the mainland. It is assumed that the windmills have a height of 150 meters and a capacity of 5.6 MW. This type of windturbine is mentioned in multiple RESA. For the solar panels it is assumed that these are regular solar panels, which will for the most part be optimized in their placement, since large most of them will be placed in solar fields, according to the RESA plans.

C.7 Wind energy

For the windfarms it is assumed that the hub height will be 250 meters. This assumption comes from recent advancements in the field of offshore wind energy. The company GE Renewable Energy and Vestas are both developing prototypes for such windturbines (GE Renewable Energy 2022) and (Vestas n.d.) For these wind-farms a regular power curve is taken, and scaled to the maximum capacity of the farm. The normalized version of the graph can be found in figure x. A higher hub height will mean that the windspeed is higher. The windspeed profiles for each weatheryear are taken from the opensource tool Renewables.ninja (Staffell and Pfenninger 2016), (Pfenninger and Staffell 2016). The maximal height for this data is 150 meters. To accurately calculate the windspeed at a height of 250 meters, the Hellmann function of the open source python library, Windpowerlib (Haas et al. 2021) is used. This version of the hellman exponent is based on the work of (Sharp 2015),(Hau 2008) & (Quaschnig n.d.). First the correct coefficient for each coordinate is calculated by comparing the data of the hubheight being 100 meters and the data with a hubheight being 150 meters. The hellmann exponent was for each off-shore wind-farm around 0.09. Then the 150-meter data is used to scale to the data with a hub height of 250 meters. The overview of the off-shore wind plants can be found in Table 23.

C.8 Demand

The yearly demand of the weather years is extracted from the Transparency Platform of ENTSO-E (ENTSO-E 2022a). The yearly demand data is quarterly. The model in SAInt takes an hourly input. The reason for this is to generate results with a fine resolution while not adding unnecessary runtime. to accurately depict the hourly demand the mean of each four timesteps is taken. If the data for a timestep is missing, the data for this timestep is created by taking the mean of the timestep directly before and directly after the missing timestep. The Klimaat-en Energieverkenning (KEV) 2022 (PBL et al. 2022) by Planbureau voor de Leefomgeving (PBL) states that the electricity demand of the Netherlands will rise to 131 TWh in 2030. To account for this increase, the data is upscaled to have the same yearly demand.

D Full model

D.1 Network topology

In Table 24, the lines used as input in the full model and its characteristics can be seen.

| Name | FromName | ToName | XXDEF [pu] = 0 | PMAXDEF [MW] = ° |
|--------|-----------------|-----------------|----------------|------------------|
| Line1 | Oostzaan | Beverwijk | 0.003022708 | 4343.983425 |
| Line2 | Beverwijk | Vijfhuizen | 0.001986181 | 3949.075841 |
| Line3 | Bleiswijk | Vijfhuizen | 0.007077083 | 3949.075841 |
| Line4 | Borssele | Rilland | 0.007072222 | 5265.434455 |
| Line5 | Dodewaard | Boxmeer | 0.00793125 | 1892.265507 |
| Line6 | Breukelen | Diemen | 0.003580069 | 2040.355851 |
| Line7 | Crayestein | Krimpen | 0.002497014 | 5265.434455 |
| Line8 | Diemen | Lelystad | 0.009523611 | 5265.434455 |
| Line9 | Dodewaard | Doetinchem | 0.008591667 | 4080.711703 |
| Line10 | Doetinchem | Hengelo | 0.011138889 | 4080.711703 |
| Line11 | Eemshaven | Meeden | 0.006127153 | 5265.434455 |
| Line12 | Ens | Zwolle | 0.006074583 | 5265.434455 |
| Line13 | Geertruidenberg | Tilburg | 0.0132125 | 5265.434455 |
| Line14 | Krimpen | Bleiswijk | 0.003139514 | 5265.434455 |
| Line15 | Krimpen | Breukelen | 0.00735625 | 1645.448267 |
| Line16 | Krimpen | Geertruidenberg | 0.006467361 | 5265.434455 |
| Line17 | Krimpen | Oostzaan | 0.013825694 | 1645.448267 |
| Line18 | Lelystad | Ens | 0.003974167 | 5265.434455 |
| Line19 | Maasbracht | Boxmeer | 0.0110125 | 1892.265507 |
| Line20 | Maasbracht | Dodewaard | 0.018945139 | 1645.448267 |
| Line21 | Maasbracht | Eindhoven | 0.009271528 | 5265.434455 |
| Line22 | Maasvlakte | Simonshaven | 0.004376319 | 5265.434455 |
| Line23 | Oostzaan | Diemen | 0.002889583 | 1974.537921 |
| Line24 | Rilland | Geertruidenberg | 0.011982639 | 4080.711703 |
| Line25 | Simonshaven | Crayestein | 0.006805208 | 5265.434455 |
| Line26 | Wateringen | Bleiswijk | 0.002537917 | 3251.405776 |
| Line27 | Wateringen | Maasvlakte | 0.009506229 | 5265.434455 |
| Line28 | Zwolle | Hengelo | 0.011476389 | 4080.711703 |
| Line29 | Zwolle | Meeden | 0.0178 | 5265.434455 |
| Line30 | Zwolle220 | Ens220 | 0.005736528 | 1905.255888 |
| Line31 | Louwsmeer | Bergum | 0.001980486 | 1905.255888 |
| Line32 | Louwsmeer | Oudehaske | 0.005200972 | 2095.781477 |
| Line33 | Meeden220 | Weiwerd | 0.005033611 | 1905.255888 |
| Line34 | Oudehaske | Ens220 | 0.007996528 | 2000.518683 |
| Line35 | Eemshaven220 | Weiwerd | 0.004118056 | 952.6279442 |
| Line36 | Vierverlaten | Eemshaven | 0.007945139 | 10530.86891 |
| Line37 | Vierverlaten220 | Zeyerveen | 0.004840278 | 2095.781477 |
| Line38 | Bergum | Vierverlaten220 | 0.0057475 | 952.6279442 |
| Line39 | Eindhoven | Tilburg | 0.01 | 5265.434455 |
| Line40 | Zwolle220 | Zeyerveen | 0.013 | 2095.781477 |
| Line41 | Vierverlaten | Vierverlaten220 | | |
| Line42 | Ens220 | Ens | | |
| Line43 | Zwolle220 | Zwolle | | |
| Line44 | Meeden | Meeden220 | | |
| Line45 | Eemshaven | Eemshaven220 | | |

Table 24: Line characteristics of the full model

D.1.1 Added network upgrades

In table 25 the planned network upgrades until 2030, can be seen. While viewing these plans, two bigger projects and two smaller projects can be spotted. The first bigger project is effectively the line from Lelystad to Zwolle, via Ens. The capacity of this line trajectory will be upgraded to 2 x 2635 MVA. The second big project is the trajectory from Maasbracht to Krimpen. This trajectory will be upgraded to 2 x 2635 MVA. Next to this, the smaller project of Vierverlaten to Eemshaven, and that of Borssele - Riland will be expanded. The project of Tilburg - Riland is planned as well, but will be completed after 2030. This is thus not in the scope of this research.

| Line | Nodes | Planned capacity (MVA) |
|---------|---------------------------|------------------------|
| Line 36 | Vierverlaten - Eemshaven | 4 x 2635 |
| Line 12 | Ens- Zwolle | 2 x 2635 |
| Line 18 | Lelystad - Ens | 2 x 2635 |
| Line 8 | Diemen - Lelystad | 2 x 2635 |
| Line 21 | Eindhoven - Maasbracht | 2 x 2635 |
| Line 39 | Eindhoven - Tilburg | 2 x 2635 |
| Line 13 | Geertruidenberg - Tilburg | 2 x 2635 |
| Line 16 | Geertruidenberg - Krimpen | 2 x 2635 |
| Line 4 | Borssele - Riland | 2 x 2635 |

Table 25: Planned network upgrades until 2030

D.2 RESA

The 30 regions have been attributed to one of the 5 zones. The attribution can be found in the table underneath. Each of these regions has the ambition to fulfill a part of the 35TWh of Energy that is described in the Dutch Climate Act (RES n.d.). Each region has proposed a bid to provide a share. The first bids were proposed in 2021 and can be found in table It can be seen that the bids of the regions are more than the initial 35 TWH. It seems that, in total, the regions overbid the initial Climate Act. In the third and fourth columns, the ambitions of the solar and wind, respectively can be found. In the final 2 columns, the expected capacity that needs to be installed is displayed. This last column is calculated via the indications in the plans of the RESA of Zeeland. In this RESA, it is assumed that an installed capacity of 700 MW of wind will have a yield of 1950 GW every year. For solar, an installed capacity of 500 MW will return in 485GW output of energy every year. In the model, the installed capacity will be submitted to various weather years to generate different output patterns.

D.3 Demand

The yearly demand of the weather years is extracted from the Transparency Platform of ENTSO-E (ENTSO-E 2022a). The yearly demand data is quarterly. The model in SAInt takes an hourly input. The reason for this is to generate results with a fine resolution while not adding unnecessary runtime. to accurately depict the hourly demand the mean of each four timesteps is taken. If the data for a timestep is missing, the data for this timestep is created by taking the mean of the timestep directly before and directly after the missing timestep. The Klimaat-en Energieverkenning (KEV) 2022 (PBL et al. 2022) by Planbureau voor de Leefomgeving (PBL) states that the electricity demand of the Netherlands will rise to 131 TWh in 2030. To account for this increase, the data is upscaled to have the same yearly demand. The share of renewable power and the share of demand of each region can be found in table 26.

For each region, the demand and renewable capacity is split out over the nodes that lie in or near the region. How this has been distributed for the model can be found in Table 27.

| Regio | Solarcapacity (MW) | Windcapacity (MW) | Demand share (%) |
|--------------------------|--------------------|-------------------|------------------|
| Achterhoek | 721.7 | 197.45 | 1.418 |
| Alblasserwaard | 164.96 | 57.44 | 0.447 |
| Amersfoort | 309.3 | 71.8 | 1.119 |
| Arnhem Nijmegen | 1180.495 | 169.807 | 3.395 |
| Cleantech regio | 989.76 | 39.49 | 1.918 |
| Drechtsteden | 298.99 | 28.72 | 1.234 |
| Drenthe | 2078.496 | 403.875 | 2.548 |
| Flevoland | 1237.2 | 1651.4 | 1.984 |
| Foodvalley | 515.5 | 89.75 | 1.476 |
| Friesland | 618.6 | 682.1 | 2.014 |
| Fruitedelta Rivierenland | 515.5 | 251.3 | 3.313 |
| Goeree-Overflakkee | 92.79 | 254.89 | 0.244 |
| Groningen | 1237.2 | 1231.37 | 5.243 |
| Hart van Brabant | 680.46 | 118.47 | 2.033 |
| Hoeksche Waard | 51.55 | 152.934 | 0.391 |
| Holland Rijnland | 670.15 | 143.6 | 1.873 |
| Metropoolregio Eindhoven | 1031 | 359 | 4.010 |
| Midden-Holland | 402.09 | 16.155 | 1.204 |
| Noord -en Midden Limburg | 1031 | 71.8 | 3.502 |
| Noord-Holland-Noord | 1443.4 | 782.62 | 3.535 |
| Noord-Holland-Zuid | 1855.8 | 323.1 | 9.950 |
| Noordoost Brabant | 1309.37 | 157.96 | 0.917 |
| Noord-Veluwe | 316.9294 | 79.9134 | 3.069 |
| Rotterdam den Haag | 1443.4 | 502.6 | 17.928 |
| Twente | 618.6 | 323.1 | 2.965 |
| U16 | 1288.75 | 197.45 | 3.972 |
| West-Brabant | 1031 | 430.8 | 5.404 |
| West-Overijssel | 742.32 | 387.72 | 2.449 |
| Zeeland | 1000.07 | 700.05 | 5.254 |
| Zuid-Limburg | 1165.03 | 61.03 | 5.191 |

Table 26: RESA generation and share of demand

| Regio | Node1 | Node2 | Node 3 | Node 4 |
|--------------------------|-------------|-----------------|------------|--------------|
| Achterhoek | Doetinchem | | | |
| Alblasserwaard | Crayestein | | | |
| Amersfoort | Breukelen | | | |
| Arnhem Nijmegen | Dodewaard | Doetinchem | | |
| Cleantech regio | Lelystad | Doetinchem | Hengelo | |
| Drechtsteden | Crayestein | | | |
| Drenthe | Zeyerveen | Meeden | | |
| Flevoland | Lelystad | Ens | Diemen | |
| Foodvalley | Dodewaard | | | |
| Friesland | Bergum | Louwersmeer | OudeHaske | |
| Fruitedelta Rivierenland | Dodewaard | | | |
| Goeree-Overflakkee | Simonshaven | | | |
| Groningen | Eemshaven | Meeden | Weiwerd | Vierverlaten |
| Hart van Brabant | Tilburg | | | |
| Hoeksche Waard | Crayestein | Simonshaven | | |
| Holland Rijnland | Bleiswijk | Vijfhuizen | | |
| Metropoolregio Eindhoven | Eindhoven | | | |
| Midden-Holland | Krimpen | | | |
| Noord -en Midden Limburg | Maasbracht | | | |
| Noord-Holland-Noord | Diemen | Oostzaan | Beverwijk | |
| Noord-Holland-Zuid | Beverwijk | Diemen | Oostzaan | Vijfhuizen |
| Noordoost Brabant | Boxmeer | | | |
| Noord-Veluwe | Lelystad | | | |
| Rotterdam den Haag | Simonshaven | Bleiswijk | Maasvlakte | Wateringen |
| Twente | Hengelo | | | |
| U16 | Breukelen | | | |
| West-Brabant | Rilland | Geertruidenberg | | |
| West-Overijssel | Zwolle | | | |
| Zeeland | Borssele | Rilland | | |
| Zuid-Limburg | Maasbracht | | | |

Table 27: RESA regions and their corresponding nodes

This leads to a demand for renewable energy attribution to each node. This can be seen in Table 28.

| Node | Solar | Wind | Demandrate |
|----------------|-------------|-------------|-------------|
| Doetinchem | 1641.8675 | 295.5168333 | 0.037547951 |
| Crayestein | 489.725 | 162.627 | 0.018764243 |
| Breukelen | 1598.05 | 269.25 | 0.050916981 |
| Dodewaard | 1621.2475 | 425.9535 | 0.064859611 |
| Lelystad | 1059.2494 | 643.5434 | 0.043692737 |
| Zeyerveen | 1039.248 | 201.9375 | 0.012737551 |
| Bergum | 206.2 | 227.3666667 | 0.00671432 |
| Simonshaven | 479.415 | 457.007 | 0.049216816 |
| Eemshaven | 309.3 | 307.8425 | 0.013107276 |
| Tilburg | 680.46 | 118.47 | 0.020332428 |
| Bleiswijk | 695.925 | 197.45 | 0.054184294 |
| Eindhoven | 1031 | 359 | 0.040096448 |
| Krimpen | 402.09 | 16.155 | 0.012035215 |
| Maasbracht | 2196.03 | 132.83 | 0.086931786 |
| Diemen | 1357.483333 | 892.115 | 0.043272963 |
| Beverwijk | 945.0833333 | 341.6483333 | 0.036660213 |
| Boxmeer | 1309.37 | 157.96 | 0.009167735 |
| Geetruidenberg | 515.5 | 215.4 | 0.027020707 |
| Hengelo | 948.52 | 336.2633333 | 0.036042317 |
| Rilland | 1015.535 | 565.425 | 0.0532921 |
| Zwolle | 742.32 | 387.72 | 0.024494012 |
| Borssele | 500.035 | 350.025 | 0.026271393 |
| Meeden | 1348.548 | 509.78 | 0.025844827 |
| Ens | 412.4 | 550.4666667 | 0.00661275 |
| Louwersmeer | 206.2 | 227.3666667 | 0.00671432 |
| Oudehaske | 206.2 | 227.3666667 | 0.00671432 |
| Weiwerd | 309.3 | 307.8425 | 0.013107276 |
| Vierverlaten | 309.3 | 307.8425 | 0.013107276 |
| Vijfhuizen | 799.025 | 152.575 | 0.03423976 |
| Oostzaan | 945.0833333 | 341.6483333 | 0.045610051 |
| Maasvlakte | 360.85 | 125.65 | 0.044820082 |
| Wateringen | 360.85 | 125.65 | 0.044820082 |

Table 28: Share of demand and renewable capacity on each node

E Time reduction by different runs setup.

In this section, an experiment for time reduction was performed. The experiment has the following setup:

1. A 6-node model representing the Netherlands was used as input, as described in appendix C.
2. For speed reduction, no congestion costs were attributed, the number of congestions per line was counted without activating new simulations.
3. The uncertainty ranges are altered, and more influential uncertainties have a broader range. Noninfluential uncertainties have been left out.
4. The model was run 200 times, as a year, month, and week.

The second point demands more explanation. In this setup, when congestion occurs, the model does not run again with the congestion alleviated. This makes the total runtime faster and fits the exploratory purpose of this experiment.

The following variables have been ruled out as uncertainties.

- The demand in Groningen & Friesland.
- The Solar capacity in Groningen & Friesland.
- The onshore wind capacity in each zone.

The demand variables have been ruled out since the demand in both regions is so low that they will not affect the outcomes of the system. The same reasoning goes for the solar capacity in both regions. The wind in each region is ruled out since these wind generators will produce power simultaneously as the off-shore wind plants. These wind plants are both bigger and have a higher capacity factor. Therefore, they will not have a great influence on the system. An overview of the fixed variables and their values can be seen in 29.

| Former Uncertainties | Fixed value |
|----------------------|-------------|
| NoordHollandWind | 1 |
| ZuidZeeWind | 1 |
| FrieslandWind | 0,8 |
| GroningenWind | 1,2 |
| OostWind | 1 |
| ZuidOostWind | 1 |
| FrieslandDemand | 1,2 |
| GroningenDemand | 0,8 |
| FrieslandSolar | 0,8 |
| GroningenSolar | 1,2 |

Table 29: Fixed factors in the second model.

As can be seen, the values for the renewable generator factors and the demand for the regions of Friesland and Groningen switched. The value for the renewable generators of Friesland is fixed at 0,8, and the demand for Friesland is set at 1,2. The values for Groningen are the opposite. This is because Friesland is a region in which not much energy is produced or consumed. It has no off-shore wind, so its effect on the system is small. The hypothesis is that because of these characteristics, the region functions mostly as a connector for off-shore wind production of Groningen for the demand in Friesland. This will be tested with this experimental setup. For the rest of the uncertainties, the uncertainty ranges for this experiment can be found in table 30.

| Uncertainties | Lower bound | Upperbound | Type |
|----------------------|-------------|------------|------|
| ZuidZeeOffshore | 0.2 | 5 | Real |
| NoordHollandOffshore | 0.2 | 5 | Real |
| GroningenOffshore | 0.2 | 5 | Real |
| NoordHollandDemand | 0.2 | 5 | Real |
| ZuidZeeDemand | 0.2 | 5 | Real |
| OostDemand | 0.2 | 5 | Real |
| ZuidOostDemand | 0.2 | 5 | Real |
| ZuidZeeSolar | 0.2 | 5 | Real |
| OostSolar | 0.2 | 5 | Real |
| ZuidOostSolar | 0.2 | 5 | Real |
| NoordHollandSolar | 0.2 | 5 | Real |

Table 30: Uncertainty ranges for experiment.

E.1 Outcomes

The second network was first run as a whole year 200 times, the congestions in all runs with the same weather years were summed up and counted for each week. The results can be found in 23,24,25,26,27 for the weather years 2015, 2016, 2017, 2018 & 2019 respectively.

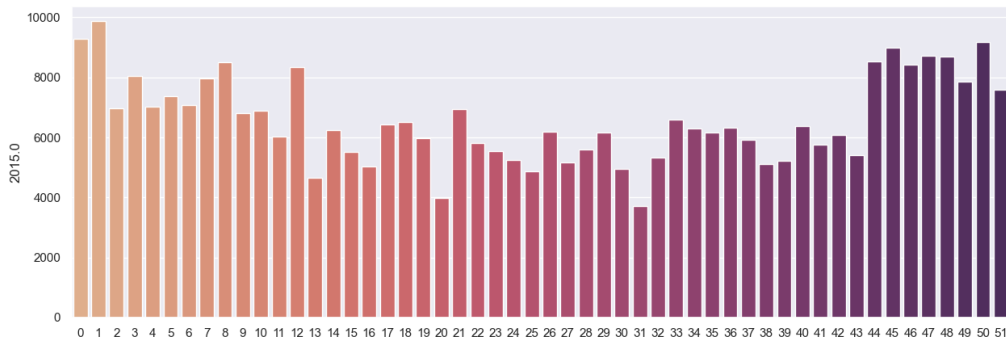


Figure 23: Count of congestions for year 2015

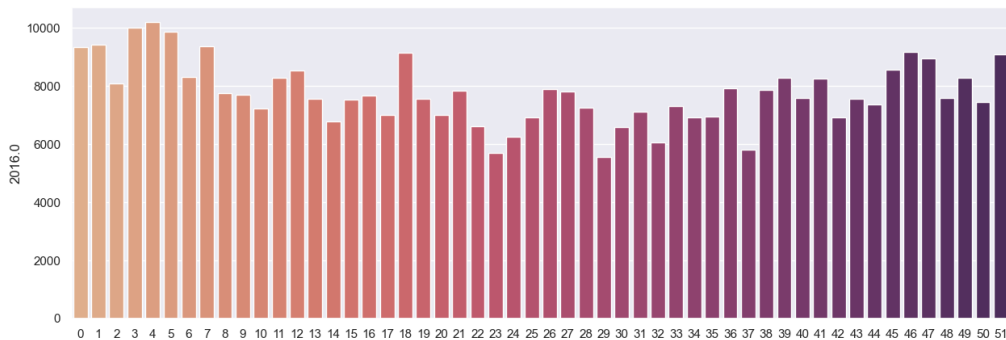


Figure 24: Count of congestions for year 2016

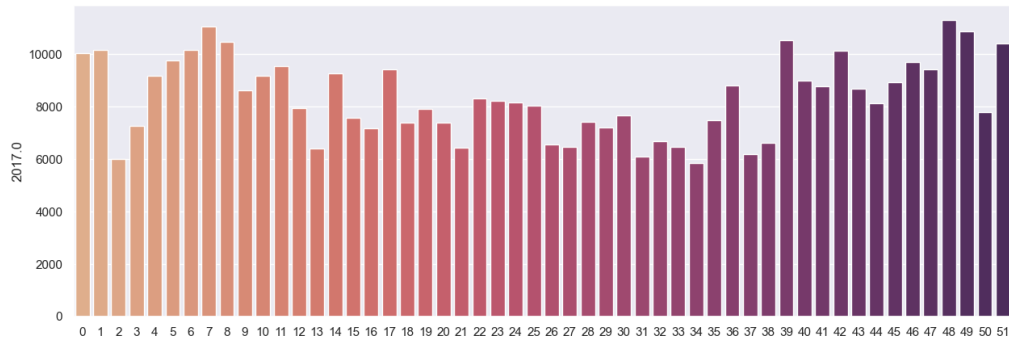


Figure 25: Count of congestions for year 2017

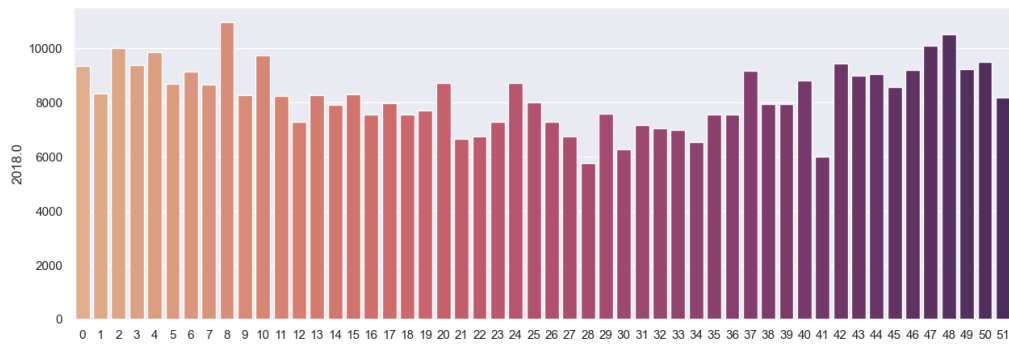


Figure 26: Count of congestions for year 2018

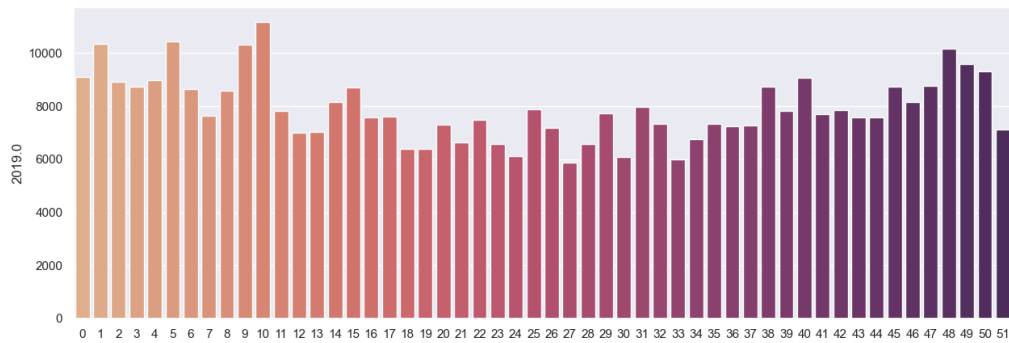


Figure 27: Count of congestions for year 2019

The graphs show a similar pattern throughout the year, in winter the amount of economically affecting congestions will be higher than in summer. For this reason, the model will again be run 200 times for December, the month with the highest amount of congestions, for one week in January (08/01/2030 - 15/01/2030), one week in June (08/06/2030 - 15/06/2030), and one week in December, (08/12/2030 - 15/12/2030). In the figures 28, 29, 30, 31, 32, the feature scores of the yearly, monthly, Weekly in December, weekly in June, and weekly in January can be seen respectively.

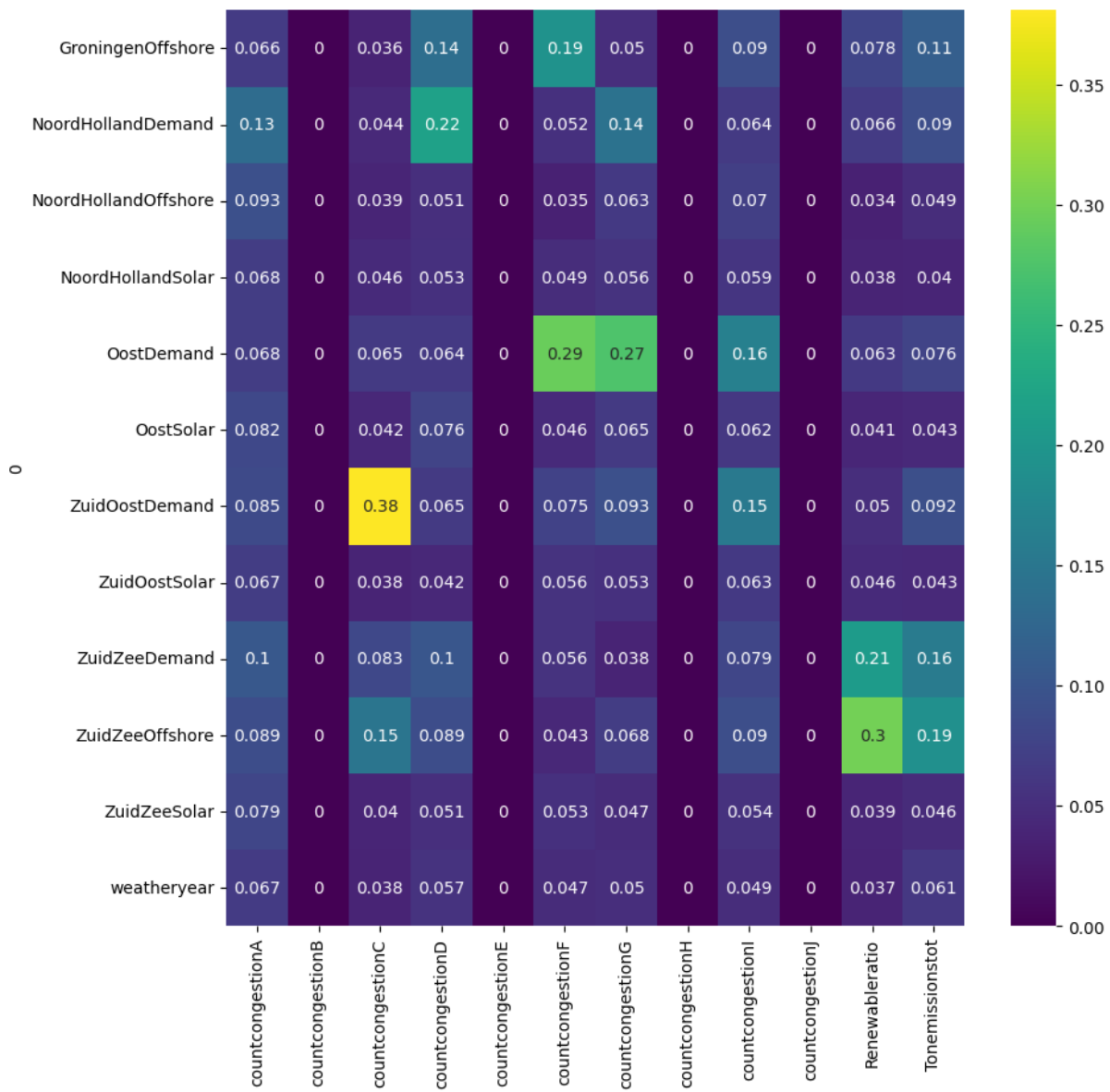


Figure 28: Feature scoring of the yearly experiments

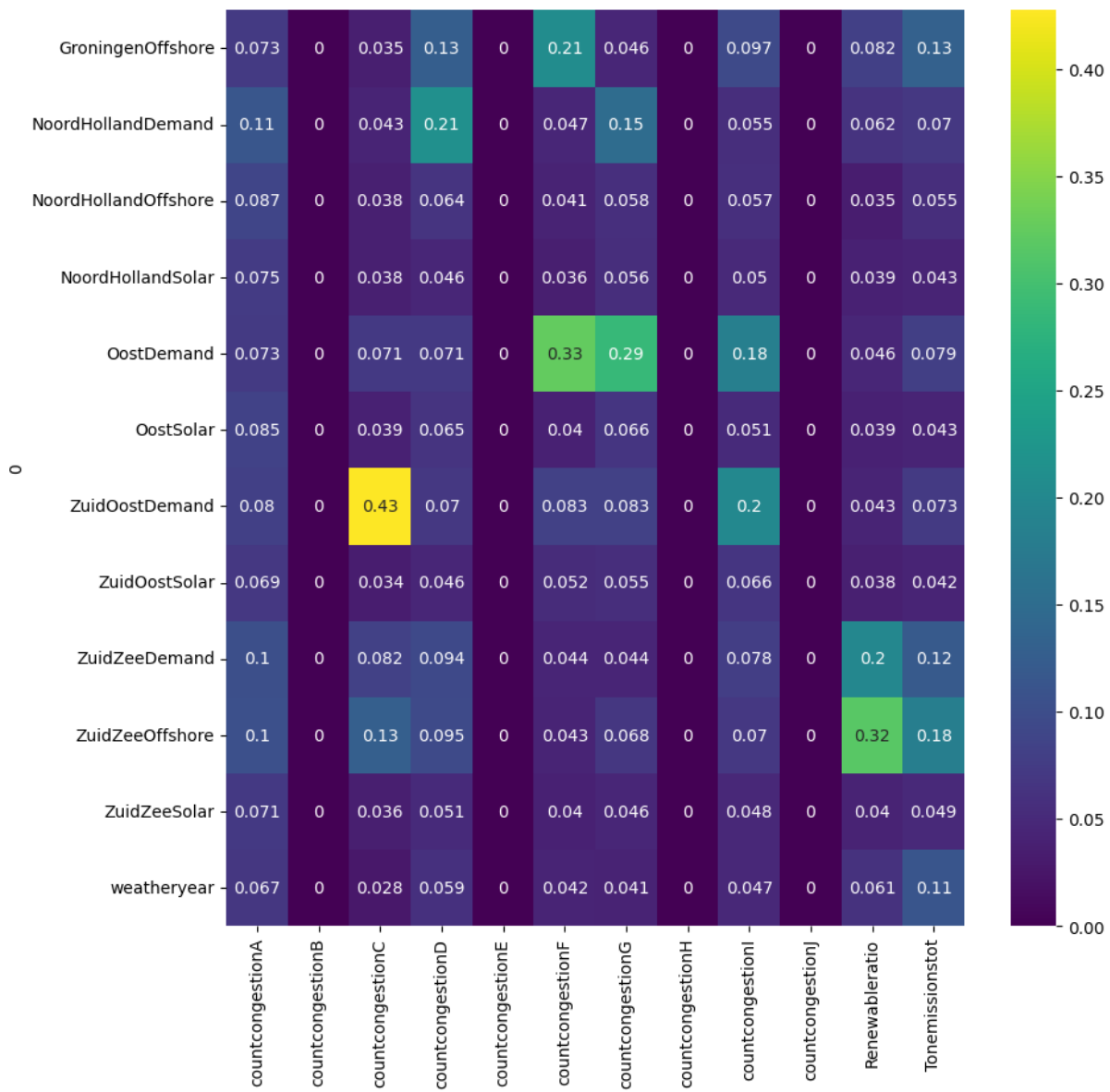


Figure 29: Feature scoring of the December experiments

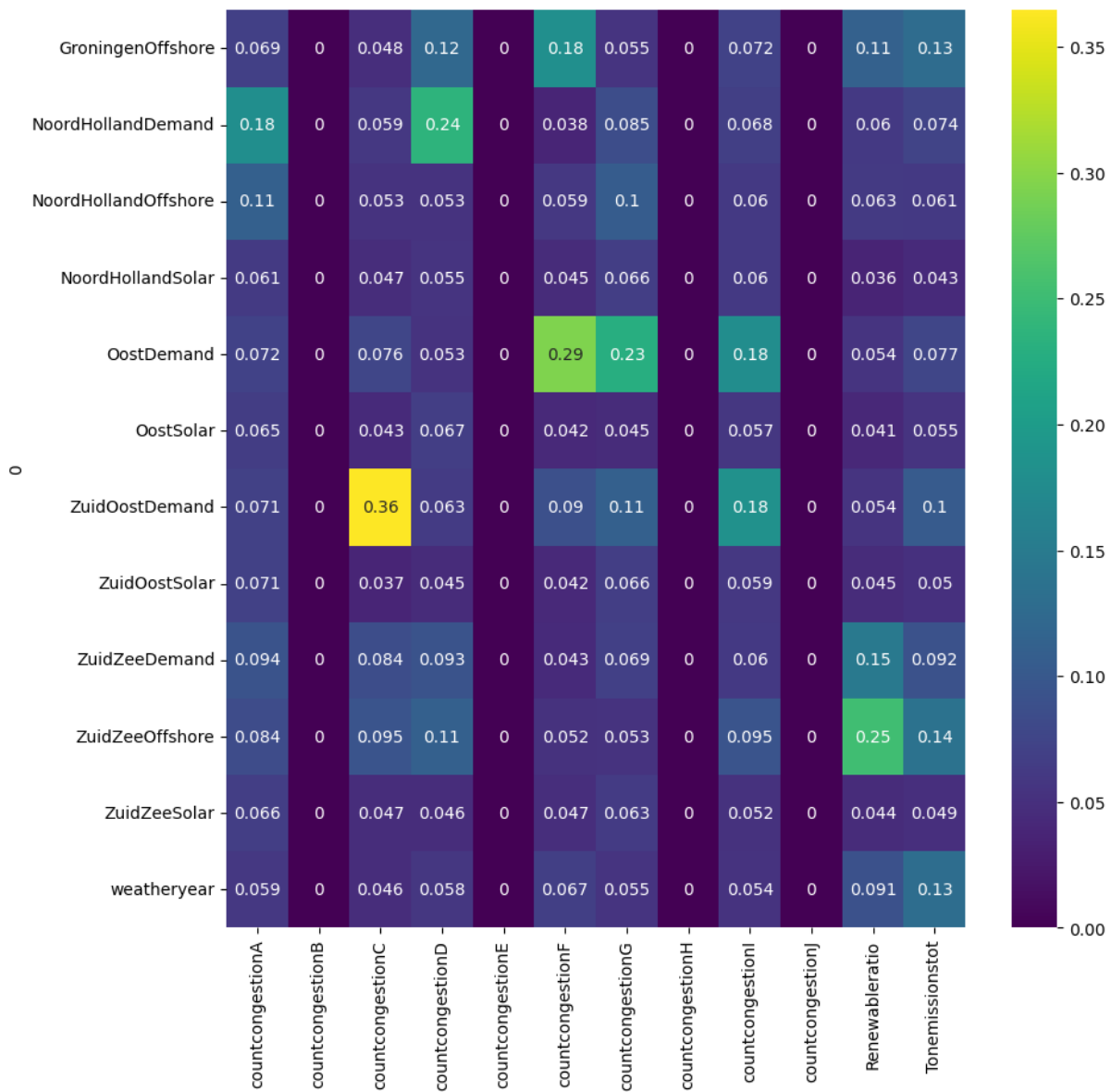


Figure 30: Feature scoring of the weekly December experiments

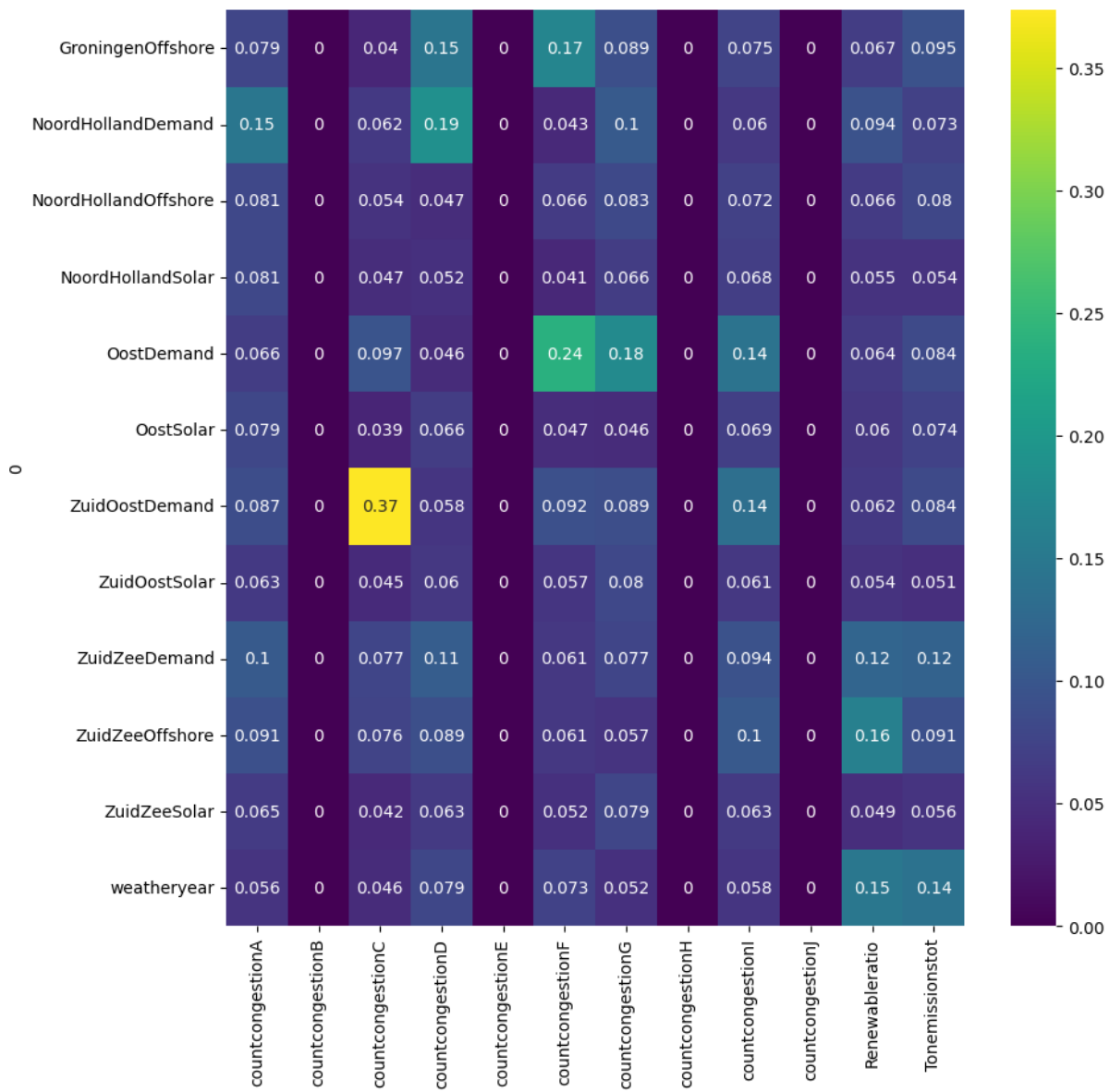


Figure 31: Feature scoring of the weekly June experiments

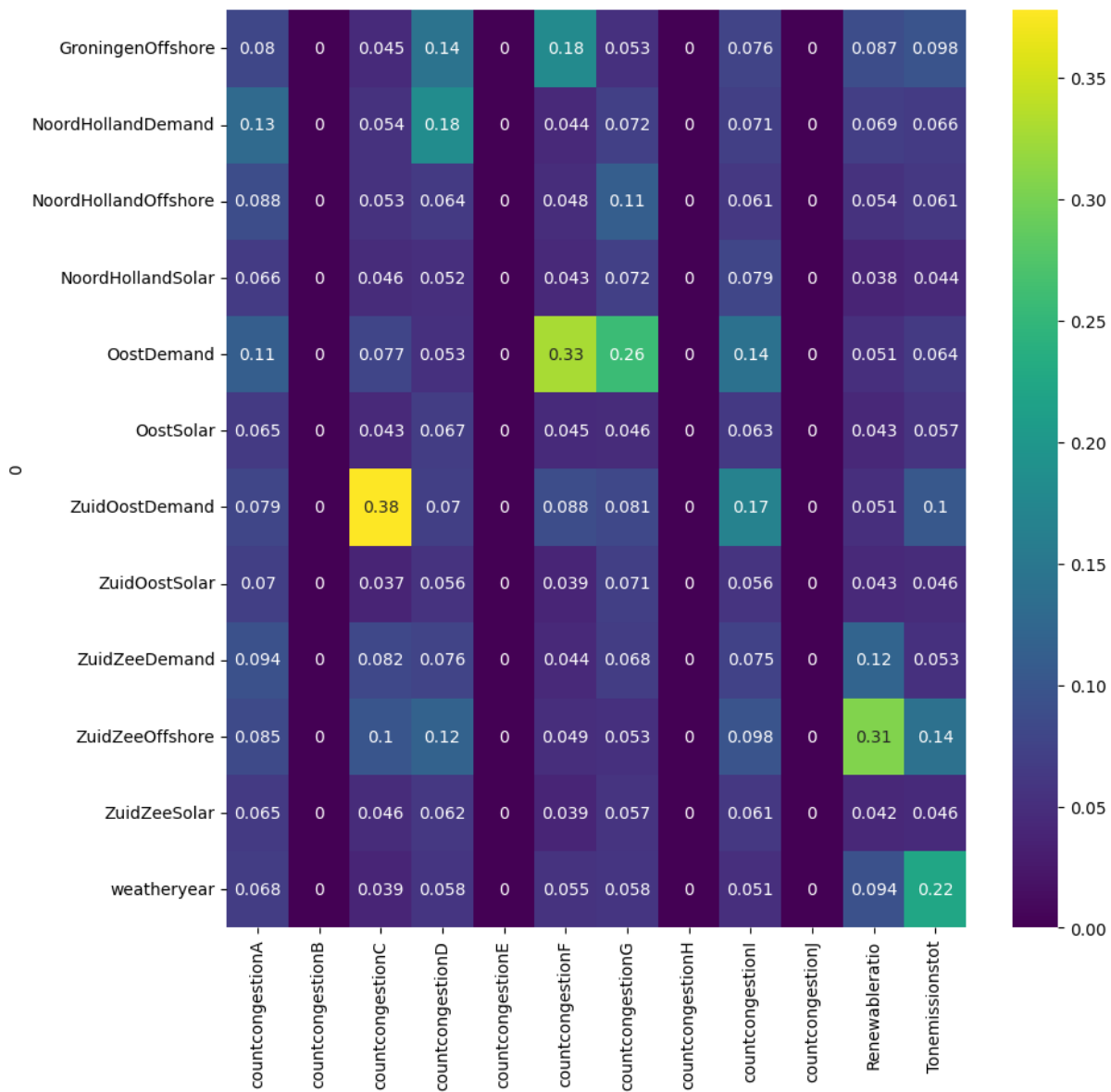


Figure 32: Feature scoring of the weekly January experiments

What stands out of these results is that, between the yearly and monthly run of December the values attributed are just slightly different. The biggest difference is 0.05 for the value of costs attributed to line C, and the uncertainty ZuidOostDemand. Naturally, between the weekly, and monthly run of December no big differences can be found as well. Between the weekly runs of January, and December some bigger differences can be seen. The biggest differences can be seen by comparing the weekly runs in winter with the weekly runs of June. For this reason, to account for as much variance in experiments, but to limit the runtime, the model is run for the weeks in January and June.

F Code flowchart development and explanation

F.1 Modeling tools methodology

In this section, the tools and the implementation of the tools is described. The tools chosen to perform the network simulations is SAInt. To perform the exploratory modeling, the EMA workbench is chosen.

F.1.1 EMA workbench

The EMA-workbench is a python library that can be used for exploratory modeling (Jan H Kwakkel 2017). Its main mechanic is the creation, and running of scenarios by altering pre-specified variables in the given function. To accomplish this, the workbench distinguishes between uncertainties, policies, constants, and outcomes. In this analysis, no policies have been constructed. So these will not be used. The Main features of the workbench that will be used in this research are, multi-processing, and the visualization of results. The multi-processing feature makes it possible to run multiple experiments at once using multiple CPU cores. The visualization of results is supported in multiple ways. The EMA- workbench supports connections with APIs as well.

F.1.2 SAInt

To model the network, the software tool SAInt will be used. SAInt is a tool that can be used to model energy networks. The feature that will be used for the network modeling is the DCUCOPF setup. This setup can be used to model power networks. What is useful about SAInt is that a wide variety of variables can be extracted, and altered. Via the API connection of SAInt, a connection with Python scripts can be made. This gives extra options for the flexibility of the models built into this software.

F.1.3 Coupling of EMA workbench with SAInt

The SAInt software and the EMA workbench are coupled through a python script. The flowchart of this code can be seen in Figure 33. An in-depth description of this flowchart can be found in Appendix F. In the following paragraphs, the core mechanics behind the code of the EMA workbench (in yellow), and the SAInt function (in green) in the flowchart. The 'infinite SAInt' will not be discussed since its functionality is very straightforward. Since in this methodology, a lot of network computations will be done, a distinction is made between the terms 'experiment', 'run', and 'simulation'. With the term 'experiment', a whole EMA workbench cycle is meant. With the term 'run', one scenario as drawn from the EMA workbench is meant. With the term 'simulation' one network simulation performed with SAInt is meant. So, one experiment consists of multiple runs, and one run can consist of multiple simulations, depending on the detection of actively constraining congestions.

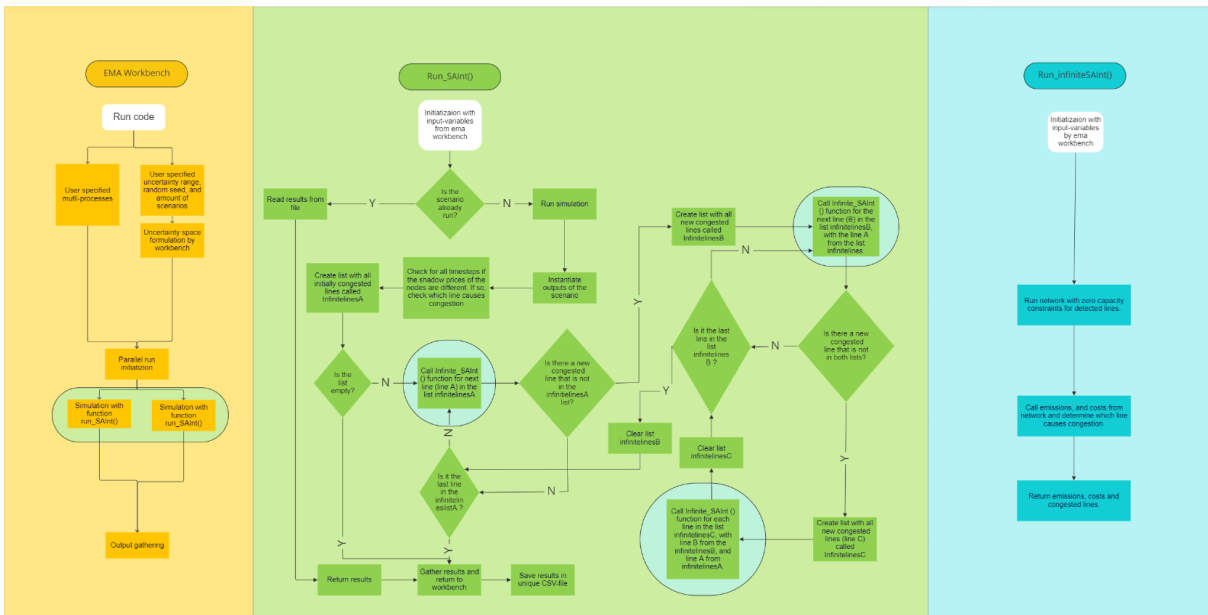


Figure 33: Code flowchart

EMA workbench code

In Figure 34, an overview of the code can be seen. With the code for the EMA workbench, the uncertainty space is drawn from the defined uncertainties and their ranges. The scenarios are then drawn from this uncertainty space, and run in parallel in the SAInt function. The outcomes of the SAInt function are returned to the EMA workbench, which saves the results in a user-specified file. The outcomes that are evaluated are the cost attributed for each of the lines in each run, which are the main outcomes. For extra context, the total system emissions (ton CO₂), the ratio of generated renewable energy to potential renewable energy (-), the total system costs (€), and the total DEMAND not served (MWh), are extracted as outcomes as well.

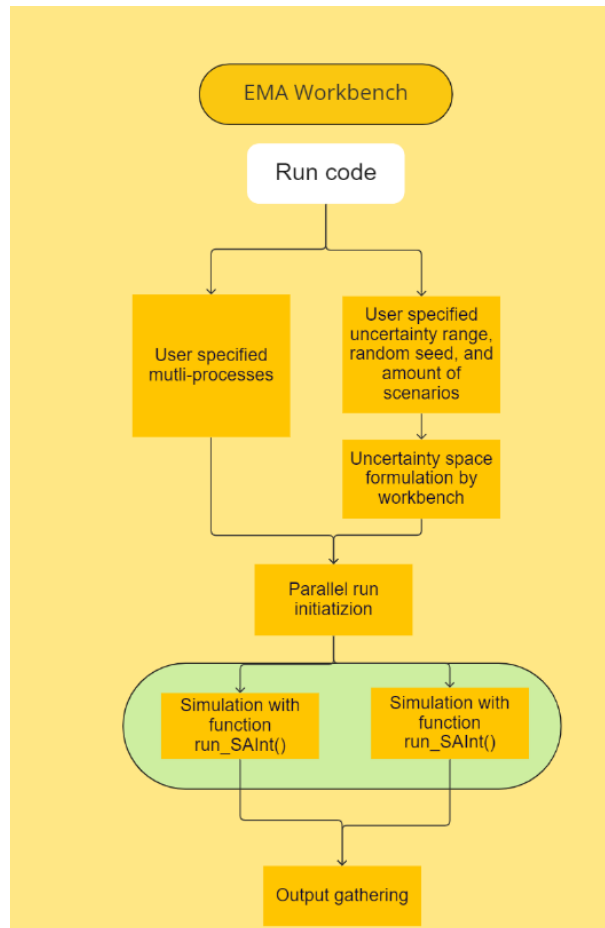


Figure 34: Code flowchart

SAInt function

In Figure 35, the codegraph for the SAIInt-function is shown. This flowchart is explained in great detail in Appendix F.

individually. This function calls an almost exact network copy of the scenario simulation. The difference is that this function sets the capacity of the lines passed to the function to infinity. For each simulation that is called with the lines from the list InfiniteLinesA, it is checked if there are actively constraining lines. If this is the case, and the line is not in the list InfiniteLinesA, this line is added to a new list, called 'InfiniteLinesB'. For each line in 'InfiniteLinesB' combined with the line of A, the function infiniteSAInt is called. If in a simulation, lines are detected that are both not in lists InfiniteLinesA or InfiniteLinesB, the lines are stored in the list InfiniteLinesC. For each line in the list InfitelinesC, the infitelines simulation is called once more, with the corresponding Lines A and B. After the last line C, the list is erased. For the next line in the list InfitelinesB, the process is repeated. If the last line in the list InfitelinesB is simulated, the list is emptied and the same process for the next line in the list InfitelinesA is repeated.

G Weatheryear analysis

This should still be added, in this analysis the profiles for demand and the renewable generation will be analyzed for each weatheryear. Based on this, we can know the characteristics of the weatheryear and better draw conclusions from the results.

| Year | Categorie | max | min | sum | mean |
|------|-----------|--------------|---------|--------------|--------------|
| 2015 | Wind | 9938.000000 | 3140.0 | 1.308246e+06 | 7787.178571 |
| | Demand | 20281.000000 | 8814.0 | 2.395522e+06 | 14259.059524 |
| | Offshore | 22838.000000 | 7649.0 | 3.625852e+06 | 21582.452381 |
| | Solar | 6507.980563 | 0.0 | 6.566186e+04 | 390.844404 |
| 2016 | Wind | 9209.000000 | 1859.0 | 7.136990e+05 | 4248.208333 |
| | Demand | 19947.000000 | 10219.0 | 2.519262e+06 | 14995.607143 |
| | Offshore | 22838.000000 | 10573.0 | 3.307124e+06 | 19685.261905 |
| | Solar | 12626.856343 | 0.0 | 1.168317e+05 | 695.426582 |
| 2017 | Wind | 9548.000000 | 0.0 | 7.481740e+05 | 4453.416667 |
| | Demand | 20098.000000 | 10188.0 | 2.471858e+06 | 14713.440476 |
| | Offshore | 22838.000000 | 57.0 | 2.772987e+06 | 16505.875000 |
| | Solar | 8077.391366 | 0.0 | 9.190868e+04 | 547.075456 |
| 2018 | Wind | 5515.000000 | 21.0 | 3.449400e+05 | 2053.214286 |
| | Demand | 19108.000000 | 10530.0 | 2.378618e+06 | 14158.440476 |
| | Offshore | 22741.000000 | 123.0 | 1.682551e+06 | 10015.184524 |
| | Solar | 7878.119515 | 0.0 | 9.569422e+04 | 569.608433 |
| 2019 | Wind | 9897.000000 | 24.0 | 9.233050e+05 | 5495.863095 |
| | Demand | 19394.000000 | 11109.0 | 2.422073e+06 | 14417.101190 |
| | Offshore | 22838.000000 | 1025.0 | 3.161218e+06 | 18816.773810 |
| | Solar | 6690.948819 | 0.0 | 5.138552e+04 | 305.866174 |

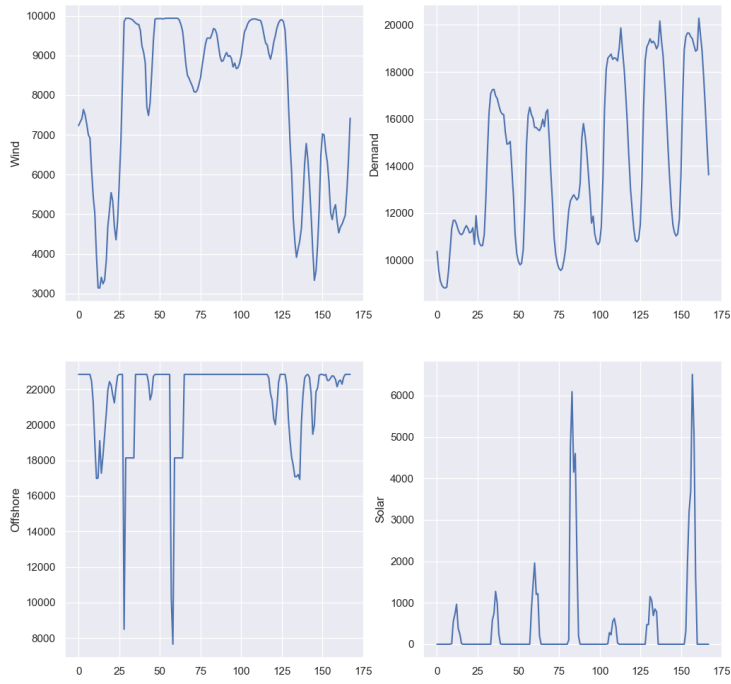


Figure 36: Weatheryear 2015 january plot

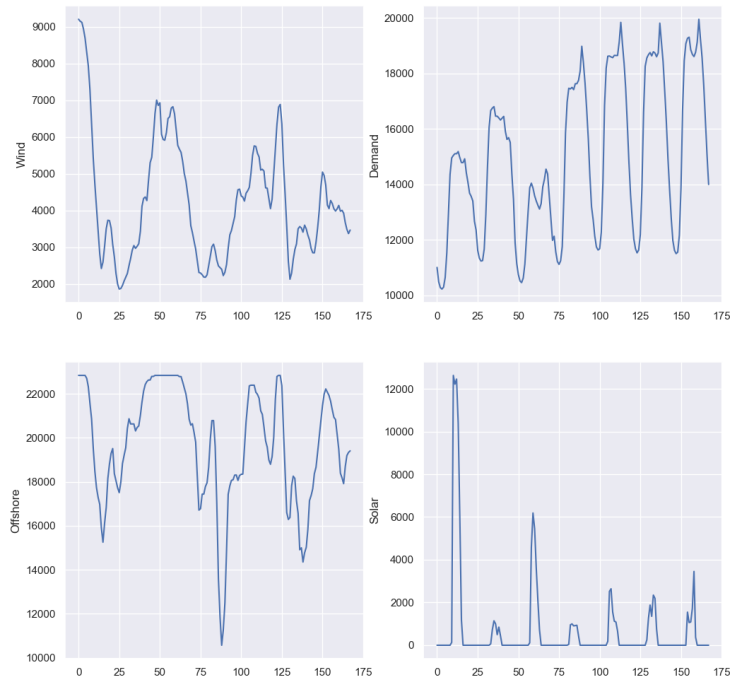


Figure 37: Weatheryear 2016 january plot

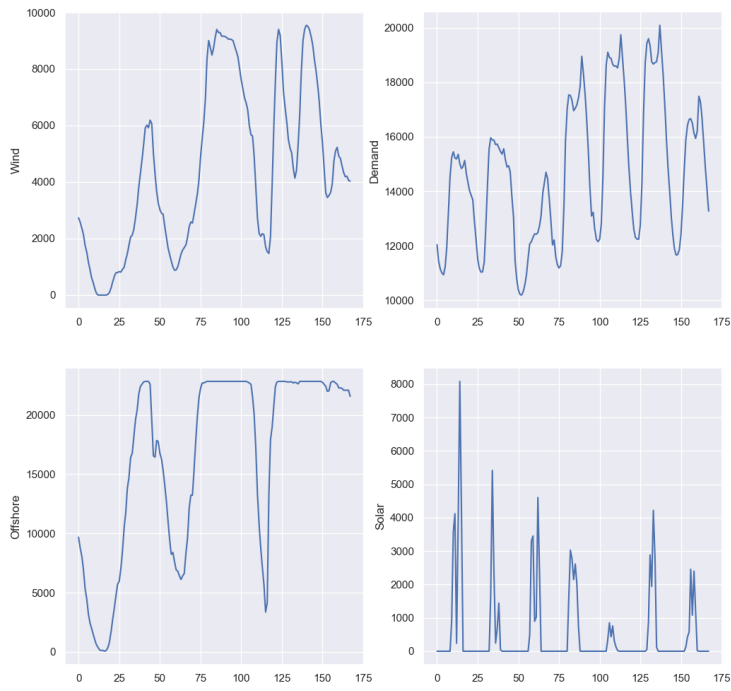


Figure 38: Weatheryear 2017 january plot

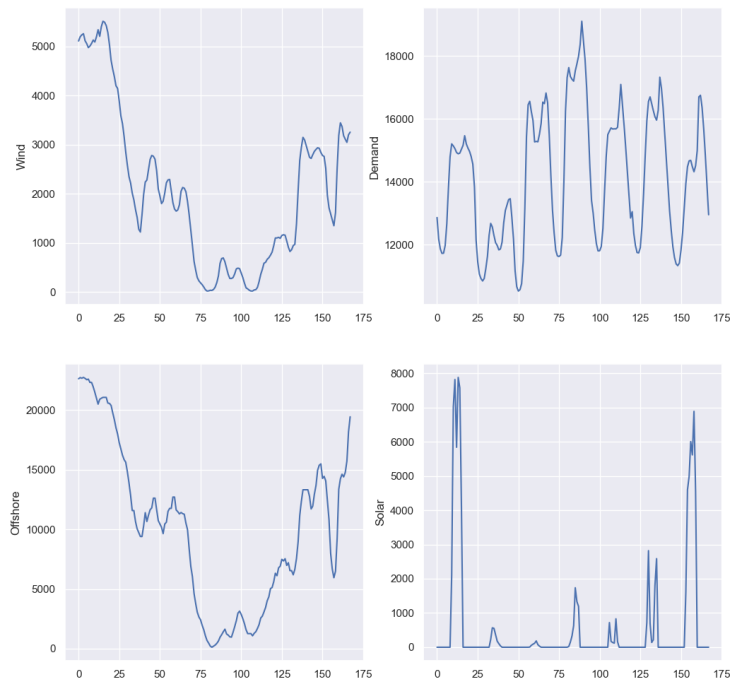


Figure 39: Weatheryear 2018 january plot

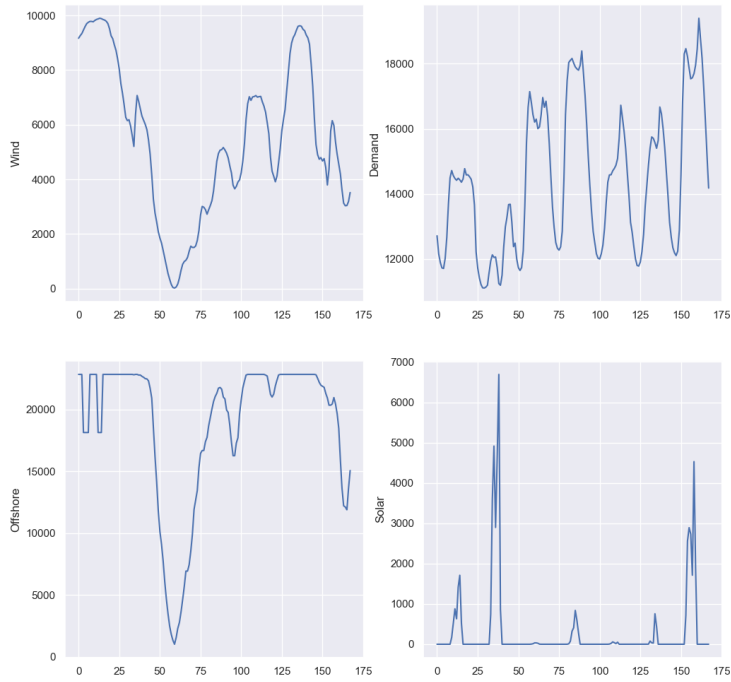


Figure 40: Weatheryear 2019 January plot

| | Wind | Demand | Offshore | Solar |
|------|------|--------|----------|-------|
| 2015 | ++ | +/- | ++ | -- |
| 2016 | + | + | + | - |
| 2017 | + | +/- | +/- | - |
| 2018 | - | - | -- | - |
| 2019 | + | +/- | + | -- |

Table 31: January experiments weatheryear classification

| Year | Categorie | max | min | sum | mean |
|------|-----------|--------------|---------|--------------|--------------|
| 2015 | Wind | 9938.000000 | 3140.0 | 1.308246e+06 | 7787.178571 |
| | Demand | 20281.000000 | 8814.0 | 2.395522e+06 | 14259.059524 |
| | Offshore | 22838.000000 | 7649.0 | 3.625852e+06 | 21582.452381 |
| | Solar | 6507.980563 | 0.0 | 6.566186e+04 | 390.844404 |
| 2016 | Wind | 9209.000000 | 1859.0 | 7.136990e+05 | 4248.208333 |
| | Demand | 19947.000000 | 10219.0 | 2.519262e+06 | 14995.607143 |
| | Offshore | 22838.000000 | 10573.0 | 3.307124e+06 | 19685.261905 |
| | Solar | 12626.856343 | 0.0 | 1.168317e+05 | 695.426582 |
| 2017 | Wind | 9548.000000 | 0.0 | 7.481740e+05 | 4453.416667 |
| | Demand | 20098.000000 | 10188.0 | 2.471858e+06 | 14713.440476 |
| | Offshore | 22838.000000 | 57.0 | 2.772987e+06 | 16505.875000 |
| | Solar | 8077.391366 | 0.0 | 9.190868e+04 | 547.075456 |
| 2018 | Wind | 5515.000000 | 21.0 | 3.449400e+05 | 2053.214286 |
| | Demand | 19108.000000 | 10530.0 | 2.378618e+06 | 14158.440476 |
| | Offshore | 22741.000000 | 123.0 | 1.682551e+06 | 10015.184524 |
| | Solar | 7878.119515 | 0.0 | 9.569422e+04 | 569.608433 |
| 2019 | Wind | 9897.000000 | 24.0 | 9.233050e+05 | 5495.863095 |
| | Demand | 19394.000000 | 11109.0 | 2.422073e+06 | 14417.101190 |
| | Offshore | 22838.000000 | 1025.0 | 3.161218e+06 | 18816.773810 |
| | Solar | 6690.948819 | 0.0 | 5.138552e+04 | 305.866174 |

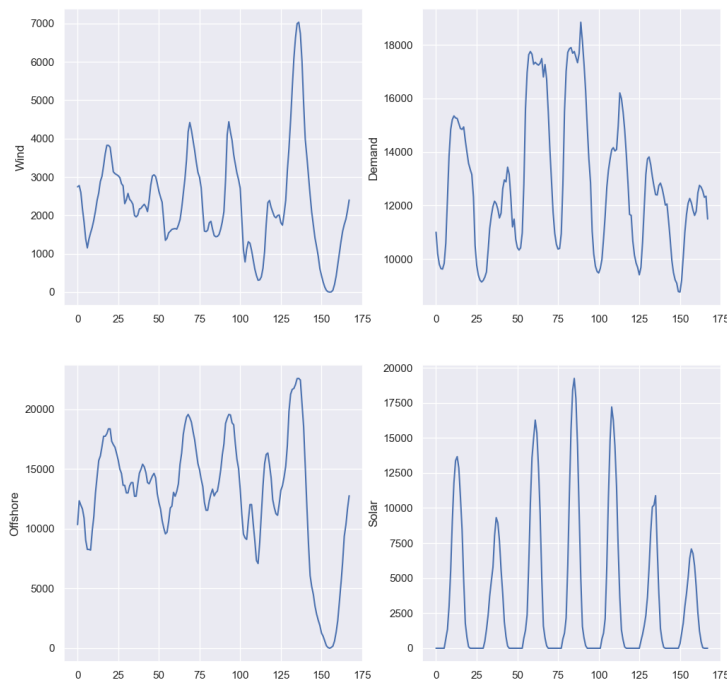


Figure 41: Weatheryear 2015 june plot

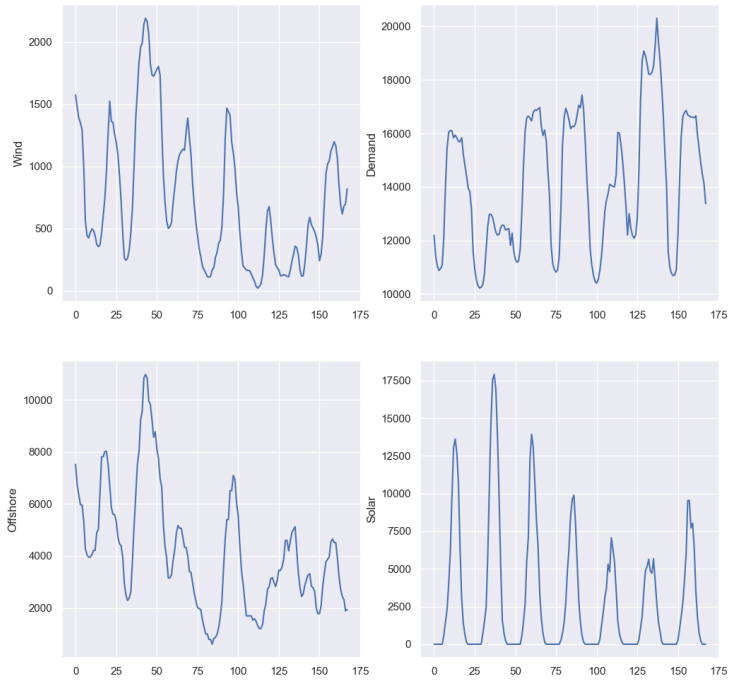


Figure 42: Weatheryear 2016 june plot

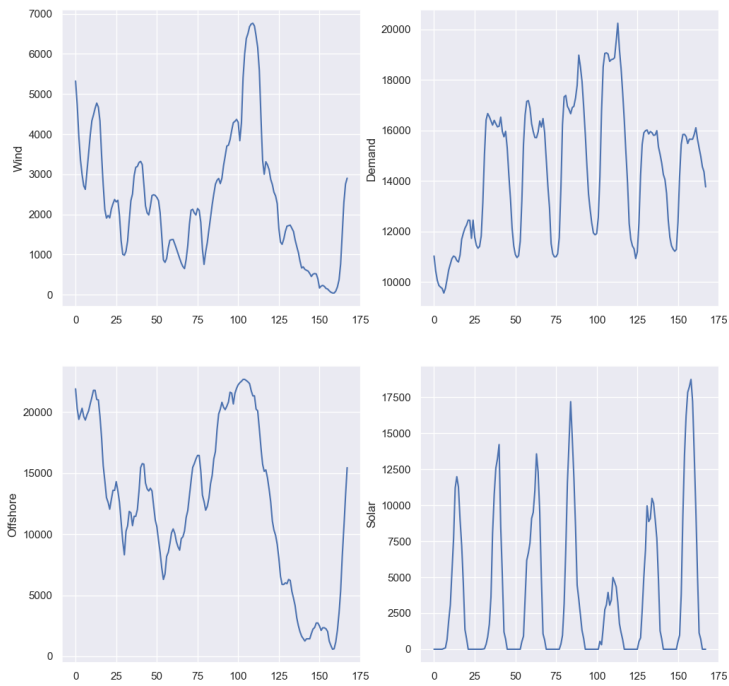


Figure 43: Weatheryear 2017 june plot

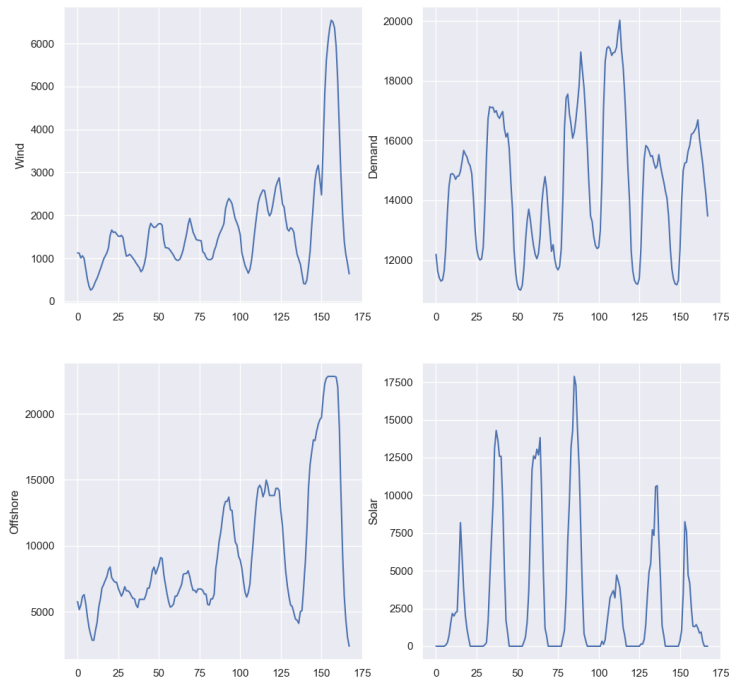


Figure 44: Weatheryear 2018 june plot

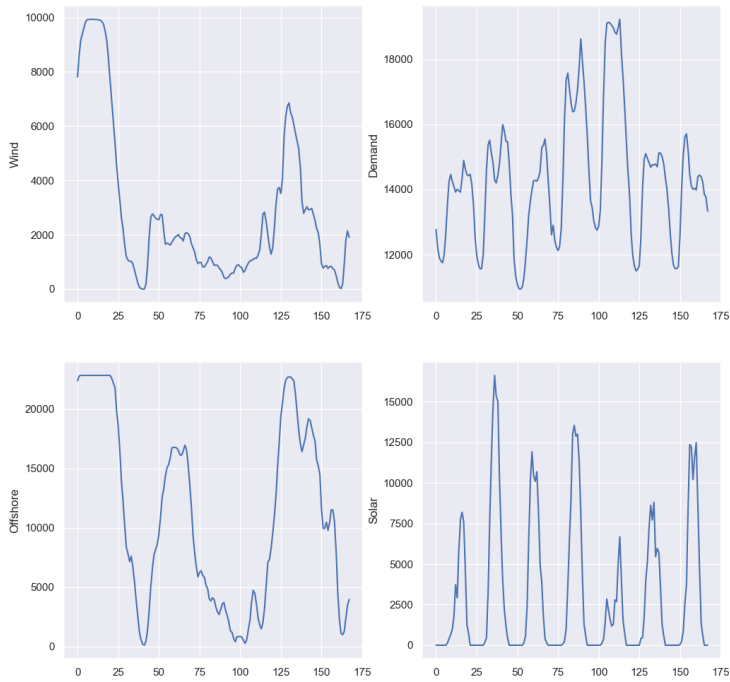


Figure 45: Weatheryear 2019 june plot

| | Wind | Demand | Offshore | Solar |
|------|------|--------|----------|-------|
| 2015 | - | - | +/- | + |
| 2016 | -- | +/- | - | + |
| 2017 | - | +/- | +/- | + |
| 2018 | - | +/- | - | + |
| 2019 | - | +/- | + | + |

Table 32: June experiments weatheryear classification

H Congestion management

H.1 Congestion detection

The key mechanic in the algorithm for detecting congestion is when the LMPs of the nodes in the model are different at a certain timestep. In this validation, we will check whether this is the case using the 5-node model, as introduced in Appendix B.1. The model was run for a full year with the standard model settings to test this. The shadow prices for each node in the model and the loads for each line for all timesteps were extracted from this run. For each timestep the average shadowprice of all the nodes was calculated. This was compared with the shadowprices for each individual node. The difference between all of them was summed up for each timestep. Then it was checked which timesteps had any lines with a load of 100. The timesteps with noticeable shadow price differences also showed an overloaded line. This is shown in table 33. A big shadow price difference appears in timestep nr in this model setup. 4651. The congestion at this timestep thus caused a big difference in the costs at the different nodes in the model. As can be seen, only lines C1 & C2 are overloaded in this model. It's logical that both these lines are overloaded since they are in parallel, and they connect the region with the largest off-shore wind farms with the region with the highest demand. In all of the timesteps where there was a difference in the shadow prices on the nodes, lines C1 & C2 were overloaded. Vice versa, in all of the timesteps when lines C1 & C2 were overloaded, there was a difference in the shadow prices on the nodes. No other lines were overloaded in any of the other timesteps. This indicates that comparing the shadow prices is thus a sufficient indicator of congestion on transmission lines.

| Timestep | Difference in LMP | C1 | C2 |
|----------|-------------------|-------|-------|
| 4651 | 114.764990 | 100.0 | 100.0 |
| 752 | 2.085991 | 100.0 | 100.0 |
| 753 | 2.085991 | 100.0 | 100.0 |
| 233 | 0.008690 | 100.0 | 100.0 |
| 8010 | 0.007982 | 100.0 | 100.0 |
| 8011 | 0.007982 | 100.0 | 100.0 |
| 751 | 0.004648 | 100.0 | 100.0 |
| 4650 | 0.004648 | 100.0 | 100.0 |
| 876 | 0.004441 | 100.0 | 100.0 |
| 4652 | 0.004441 | 100.0 | 100.0 |
| 875 | 0.004234 | 100.0 | 100.0 |
| 7987 | 0.004234 | 100.0 | 100.0 |
| 874 | 0.002354 | 100.0 | 100.0 |
| 7242 | 0.002117 | 100.0 | 100.0 |

Table 33: Shadowprices and Loads of the lines.

H.2 Validation of cost attribution in 6-node network.

In the results, some runs were encountered in which negative outcomes on the lines occurred. Naturally, this is counterintuitive since costs will only be allocated when a line is relieved from congestion. The problem

| Outcomes | Count January | Count June | Sum January | Sum June |
|-----------------|---------------|------------|-------------|----------|
| costcongestionA | 229 | 196 | 8404083 | 5272129 |
| costcongestionB | 229 | 0 | 0 | 0 |
| costcongestionC | 320 | 190 | 12631249 | 5450164 |
| costcongestionD | 48 | 63 | 1197009 | 939275 |
| costcongestionE | 0 | 0 | 0 | 0 |
| costcongestionF | 28 | 2 | 2068708 | 34128 |
| costcongestionG | 0 | 0 | 0 | 0 |
| costcongestionH | 1 | 0 | 709942 | 0 |
| costcongestionI | 159 | 283 | 7560986 | 7505008 |
| costcongestionJ | 6 | 4 | 985138 | 60742 |

H.3 Cost attribution background

Cost minimization focus

As described in appendix A, the objective function will minimize the costs of the system while meeting demand. The model solver will thus focus on the affordability of the system. This is what power markets try to achieve as well. It is important to note that in the real power markets, the co₂-emissions are priced by the co₂-market; the sustainability KPI is in this way, internalized within the power price. When it is impossible to serve power demand in the system, demand must be curtailed. Since this is not a wishful situation, a penalty price is set. As seen in the data, no extra price for the emissions is set since gas is the only fuel that emits co₂, and there is no dynamic fuel price. The penalty price for demand curtailment is quantified to 2000 €/ MWh.

Implications of cost minimization focus

In power markets, this means that when renewable power is available and there is enough demand, the renewable generators will always generate power in the model. In a system without storage of power, when there is not enough demand, renewable power will be curtailed. These systems can be described by the timesteps in the model as well. In appendix H.1 multiple timesteps are shown in which the renewable inflow of the system greatly differs.

H.3.1 Influence of line capacities on model costs

In the timesteps shown in appendix H.1, we could see how some of the lines would be overflowed, especially while there is a lot of renewable power flow in the system. When this happens, the model solver must disable power generators that would overflow the lines and turn on other power generators. The crux lies in that these would not be active in an economically optimal situation, meaning that these could generate more costs. This depends on whether the network congestion actively constraints the solution of the DCOPF. In the rest of this appendix, we will distinguish between two types of congested lines. The actively constraining congestions and the non-actively constraining congestions. Examples for both are given in the following 2 paragraphs.

Non-actively constraining congestions

In Figures, 46, and 47, two successive timesteps in the network from Section 3.4 run are shown. In both timesteps, there is a surplus of renewable energy in the network. The timesteps are 1 hour apart from each other, but the timesteps are solved in a different way. The input variables for the two timesteps differ only slightly since they are so close to one another. In the first timestep, shown in Figure 46 the power is produced in the offshore wind farms connected to the node Maasvlakte. This is represented as the big green dot in the model's left side. The flow of this generated power leads to congestion on line 15; this is the small red-colored line in the upper part of the left side of the network. In the second timestep, shown in Figure 47, a large

portion of the power is produced in the offshore wind farms in Eemshaven. The big purple dot on the upper right side of the network represents this node. The congestion in this situation arises in line 38, the red line in the upper right side of the network. Both timesteps result in a total cost of 0, due to all power coming from renewable generators. The congestion does not actively constrain the objective function of minimization of costs in this case, the costs could not be lower. Thus, the model solver does not seem to 'care' about how the power flows in the model.

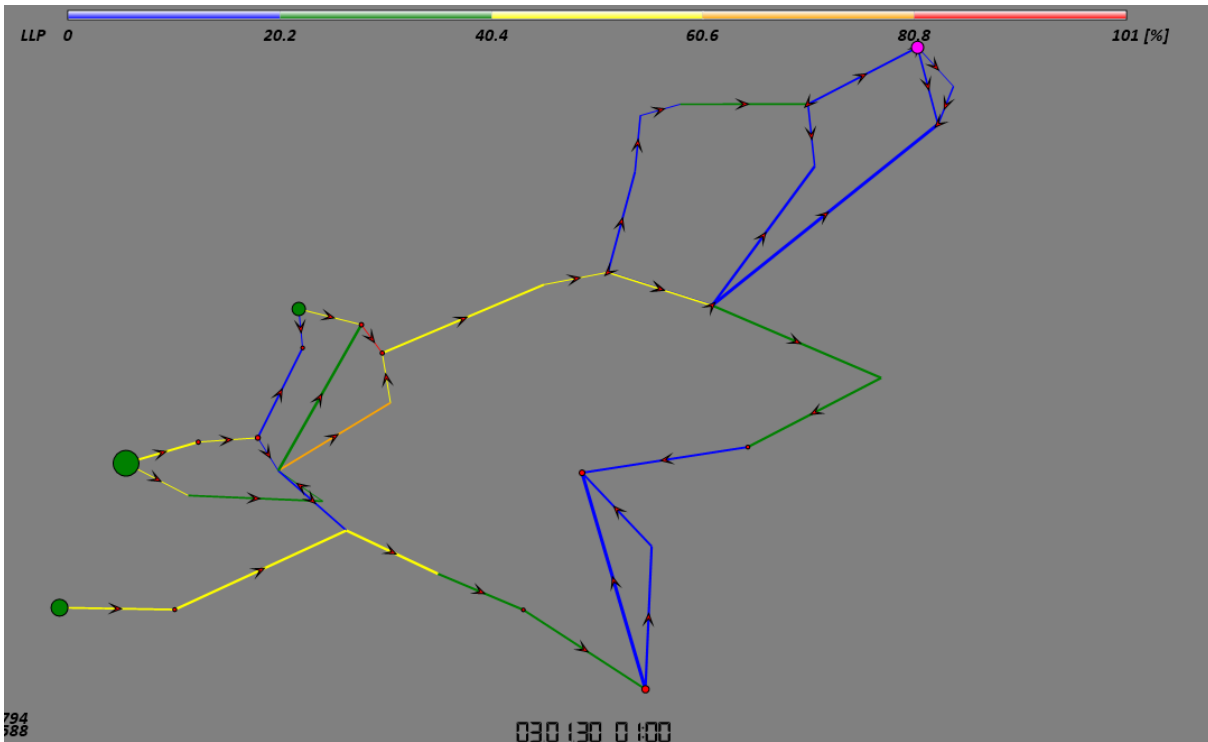


Figure 46: Congestion on line 15.

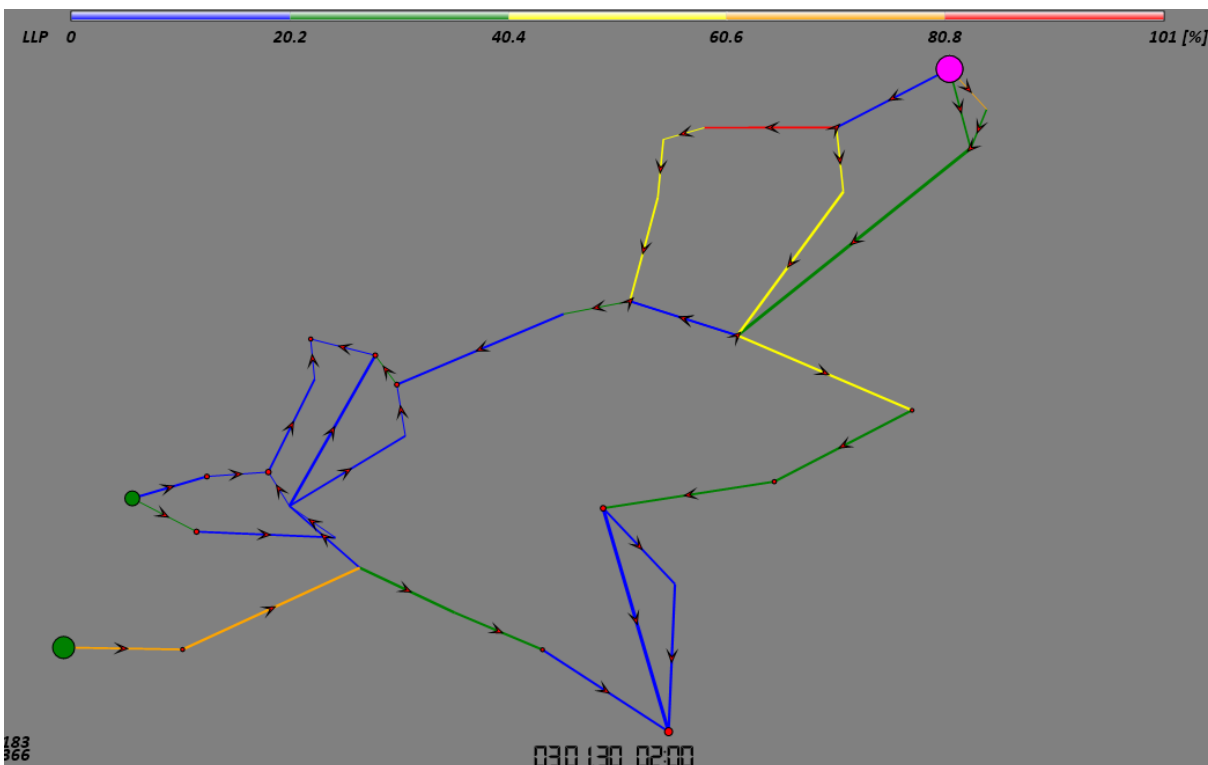


Figure 47: Congestion on line 38.

Actively constraining congestions

At a yearly run of the full Netherlands model, congestion occurs on 23 January at 16:00 in line 38. The state of the network in this timestep can be seen in figure 48. The total network costs at this timestep are 673015 euros.

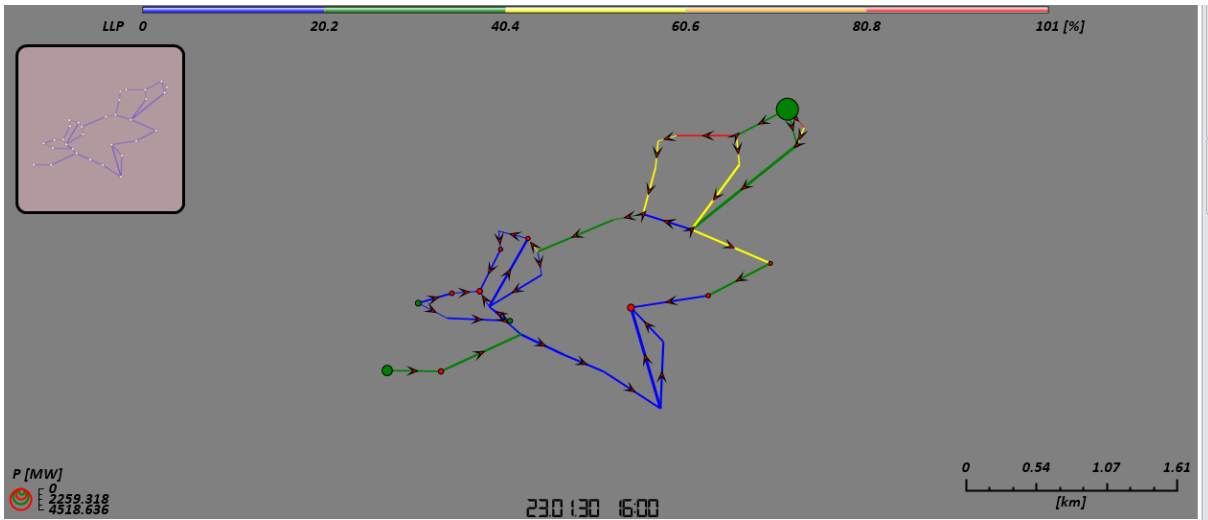


Figure 48: Non active congestion on line 38.

The same model is run again, but this time the capacity of line 38 is set to infinite capacity. The state of this network can be seen in Figure 49. The total network costs at this timestep are 631892. No other line is congested in this network; the objective function is at this point not constrained by any line capacity.

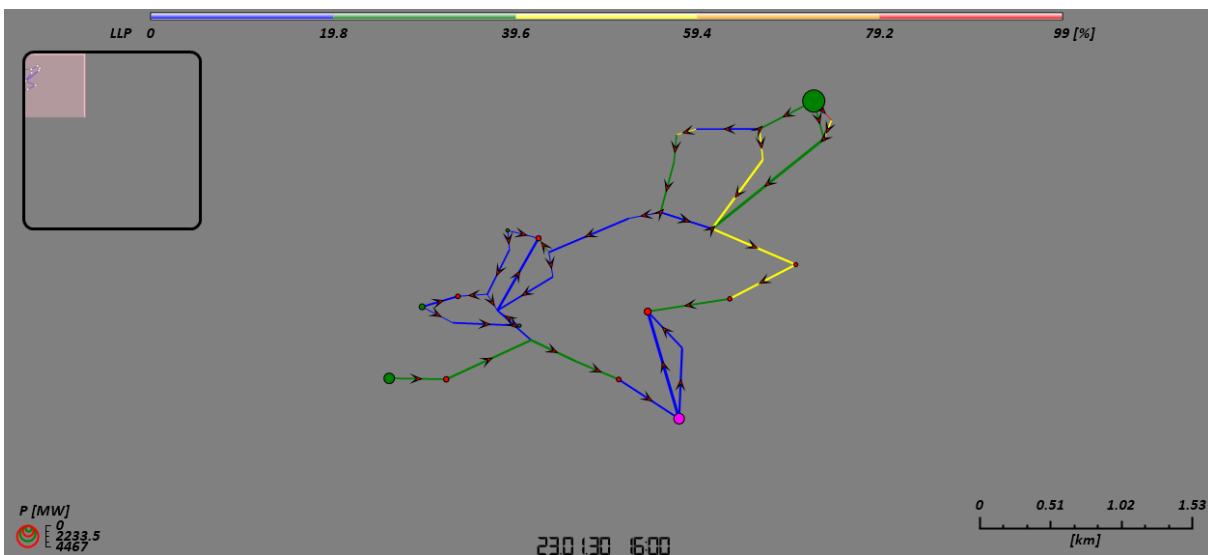


Figure 49: Non active congestion relieved on line 38.

The difference in costs in the two situations is $673,015 - 631,892 = 41,125$. In Figure 48, the congestion is relieved by the solver through congestion management. More expensive generators have been switched on, and less expensive generators have been switched off in comparison to the market equilibrium to meet the demand for power. In figure 49, no congestion management is necessary since the congestion capacity is removed from the network.

This leads to the cost difference between the two situations. The only difference between the two network models is the capacity of line 38. The capacity of line 38 is thus actively altering the outcome of the objective function. The difference in costs can be seen as the costs of the congestion management procedure. This is an example of actively constraining congestion. By calculating the costs that arise through congestion management and attributing these to the line, the vulnerability of the line can be quantified. This will be the base of the vulnerability

analysis. For the rest of this research, this will be referred to as the cost attribution method since costs are attributed to the lines.

Detection of actively constraining congestions

For the vulnerability analysis, it is only interesting to consider the actively constraining congestions. We must therefore find a way to filter the congestion of interest. As described in Section 2.3, the locational Marginal prices, or in other terms, the shadow prices on the nodes of the model, will differ when congestion management has been applied in a power system. To check this, an experiment with a smaller model has been performed; this experiment can be found in H.1. This experiment concluded that a difference in the shadowprices on the nodes is a useful indicator to find congestions that actively constrain the cost minimization function.

Implications and conclusion on vulnerability analysis

As seen in the example in Section H.3.1, the vulnerability of a line will be based on the costs of the congestion management it causes. In this example, the cost of the congestion management procedure was 41,125. This number does not mean a lot without the proper context. Since the system has a lot of components, and each change in a component might lead to different system costs, it is difficult to precisely attribute the change in costs to one of the variables. Therefore, the costs that are attributed must not be seen as absolute costs, they are highly circumstantial to the input variables of the network. Following this, one experiment can not be seen as enough data to analyze network vulnerabilities. As the power flow is highly sensitive to different inputs. This gives an additional reason to perform exploratory modeling. It can, however, be used as a way to quantify the severity of a congestion in the model, since it actively constraints the optimization function.

I Results analysis

As described in the main text, the data analysis techniques as provided by the ema workbench are used to provide meaning to the results.

I.1 Results january experiment

The january experiment was the experiment with the setting as described in the methodology. As described there, the runtime for this experiment is from 08/01/2030 00:00 to 15/01/2030 00:00; a full week in winter. 1000 experiments have been performed for this week.

I.1.1 Selection of results

No cost filtration

The first step in the result analysis is the selection of them. The runs without any costs in them will be filtered out. These runs have by definition zero costs attributed to any of the lines. This means that in the analysis, these runs will only clutter the analysis. There is no added value in leaving these in the further analysis. The PRIM analysis for the runs with any costs can be found in Figure 50. As can be seen, the PRIM algorithm can't scrape away lesser influential factors. Only the demand seems to be a clearly influential factor. After a certain demand input to the model, the costs will rise. This is of course as would be expected.

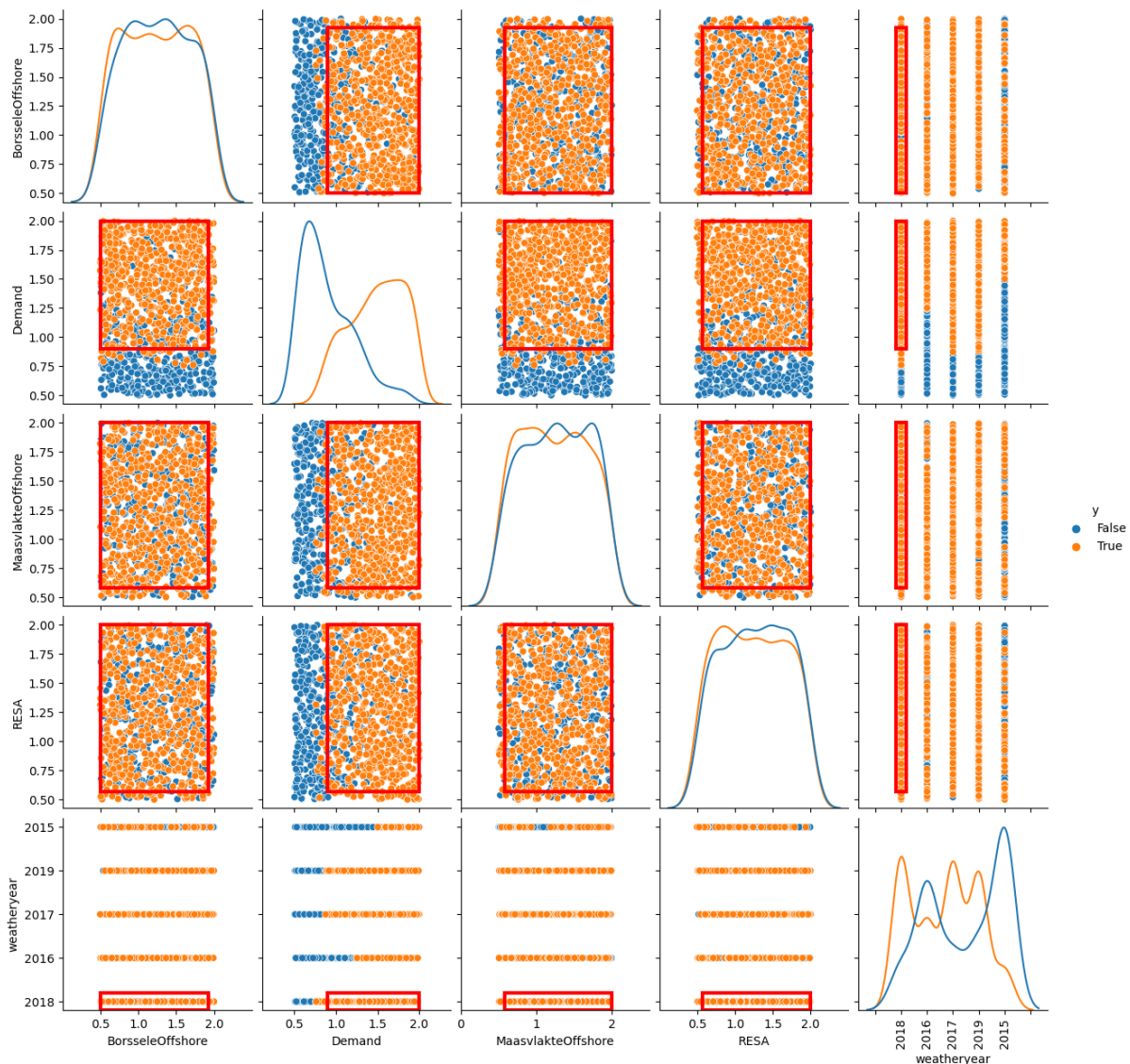


Figure 50: Prim scatterplot of total costs.

For the january experiment 859 runs out of the 1000 runs remained.

Vulnerable lines selection

In Figure 51, the ratio of the total costs over all the runs, as compared to the costs attributed to the lines are viewed. Not all lines are viewed in this picture, only the lines that have a percentage higher than 1% of the total costs over all runs. In Figure 52, for each line the amount of runs that costs are attributed are displayed. Again, not all lines are added in this picture; Minimal 10 cost attributing runs are needed. An argument can be made that a combination of these factors determines whether a line is vulnerable or not. For a line to be vulnerable, a lot of congestion management needs to take place because of the restricting capacity on the line. The costs must therefore be high. As well, the line must be congested in a high number of runs, since these lines will probably become congested fast.

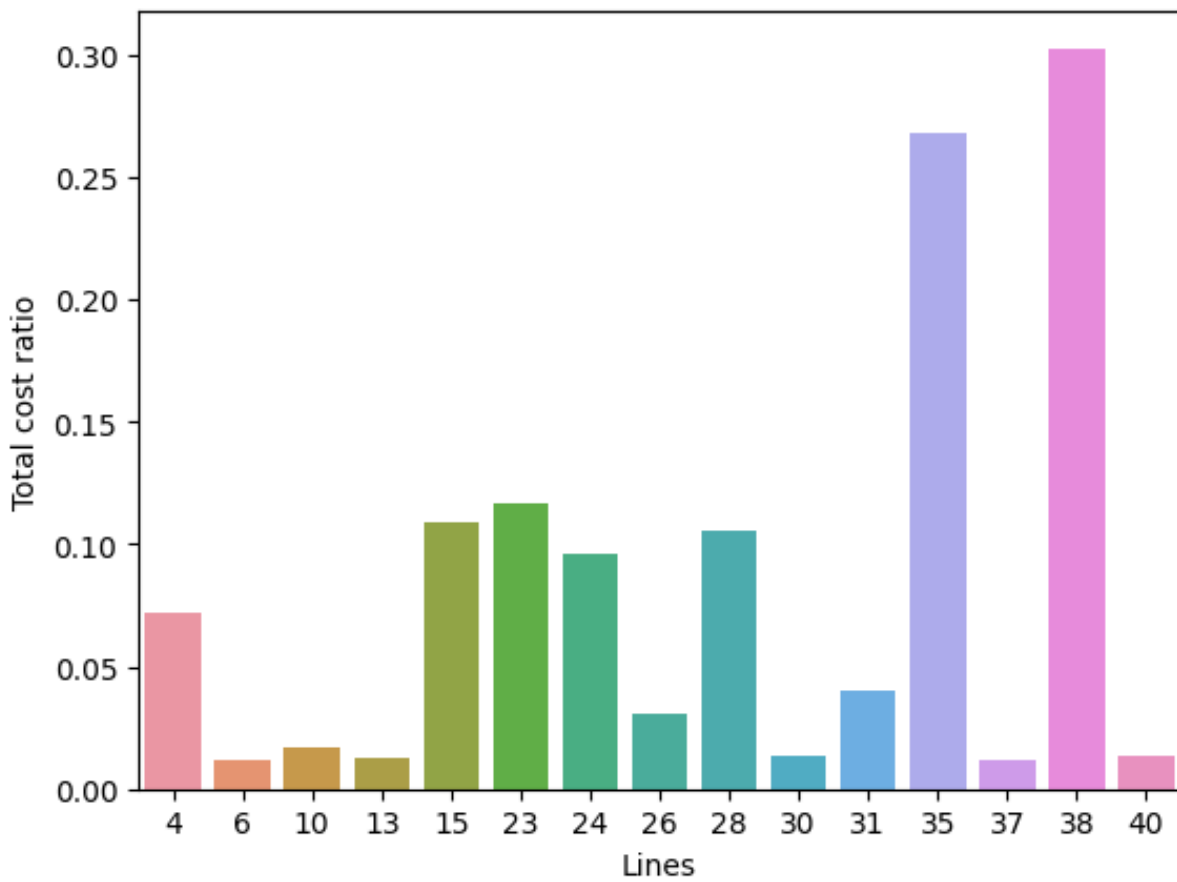


Figure 51: Cost influence of the total costs for january

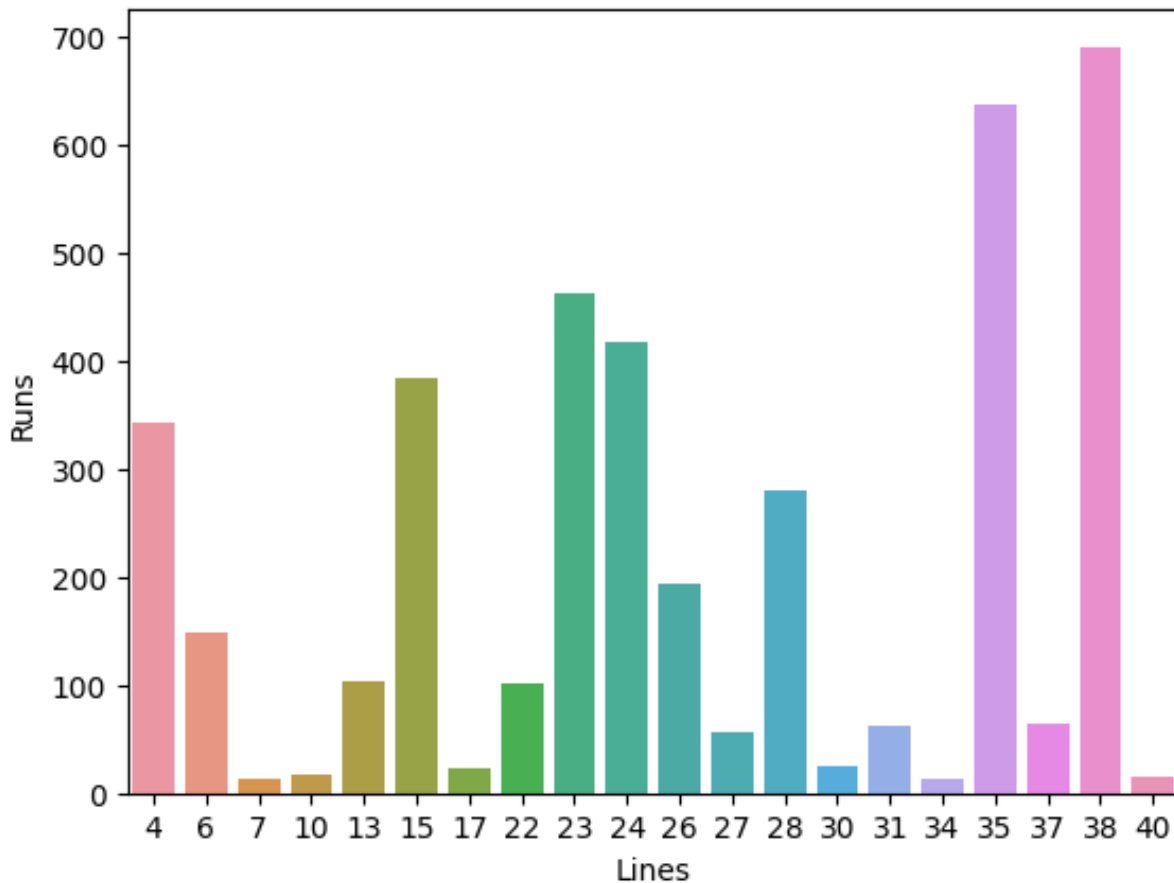


Figure 52: Amount of runs that have cost attributed to a certain line in January experiments.

What comes to mind while looking at these two figures is that the same lines score high in both figures. The following lines are deemed the most vulnerable:

- Line 4 (Borssele - Riland)
- Line 15 (Krimpen - Breukelen)
- Line 23 (Oostzaan - Diemen)
- Line 24 (Riland - Geertruidenberg)
- Line 28 (Zwolle - Hengelo)
- Line 35 (Eemshaven - Weiwerd)
- Line 38 (Bergum - Vierverlaten)

The following lines are deemed less vulnerable; these lines will be subjected to some further analyses.

- Line 6 (Breukelen - Diemen)
- Line 13 (Geertruidenberg - Tilburg)
- Line 22 (Maasvlakte - Simonshaven)
- Line 26 (Wateringen - Bleiswijk)
- Line 27 (Maasvlakte - Wateringen)
- Line 31 (Louwersmeer - Vierverlaten)

- Line 37 (Vierverlaten - Zeyerveen)

For reference, the lines can be seen in Figure 53. In this figure, the most vulnerable lines are noted in red, and the less vulnerable lines are highlighted in blue. The lines will first be analyzed individually with a PRIM analysis where possible. If this is not possible, combinations of lines will be analyzed with a PRIM analysis. Since it is a network the codependency of the lines is very important and should be analyzed further.

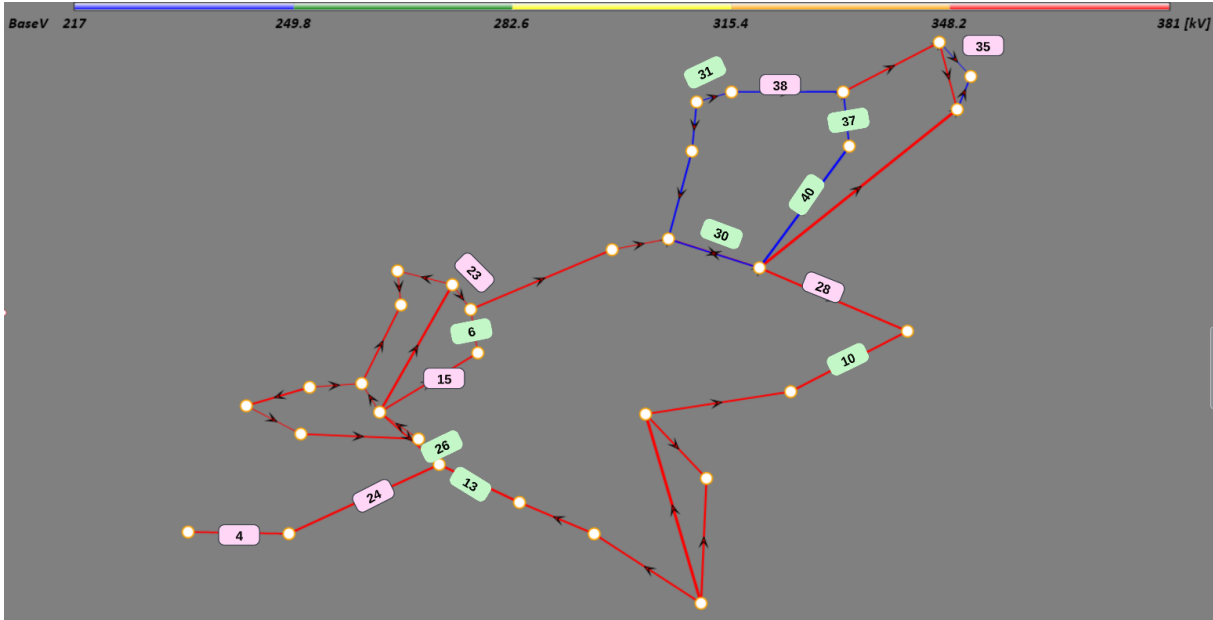


Figure 53: Vulnerable lines in the network.

I.2 Prim analysis

For further analysis for the lines a PRIM analysis will be done.

I.3 Prim analysis more vulnerable lines

A PRIM analysis for each of the vulnerable lines is conducted in 2 different ways: In the first, the decision-rule for the PRIM algorithm is that the costs for the line must be bigger than zero. In the second, the decision-rule for the PRIM algorithm is that the costs for the line must be higher than 1 % of the total costs for that run. Since the total costs per run vary a lot, it ranges from 0 to 2 billion, a percentage of this total costs is deemed more appropriate than a static amount of total costs. Both these decision-rules are tested to find insightful results. For some lines this analysis one or both of the analyses could not be performed, since the amount of runs was too small.

I.3.1 Line 4

In Figure 54, the PRIM analysis for the first decision-rule for line 4 can be found.

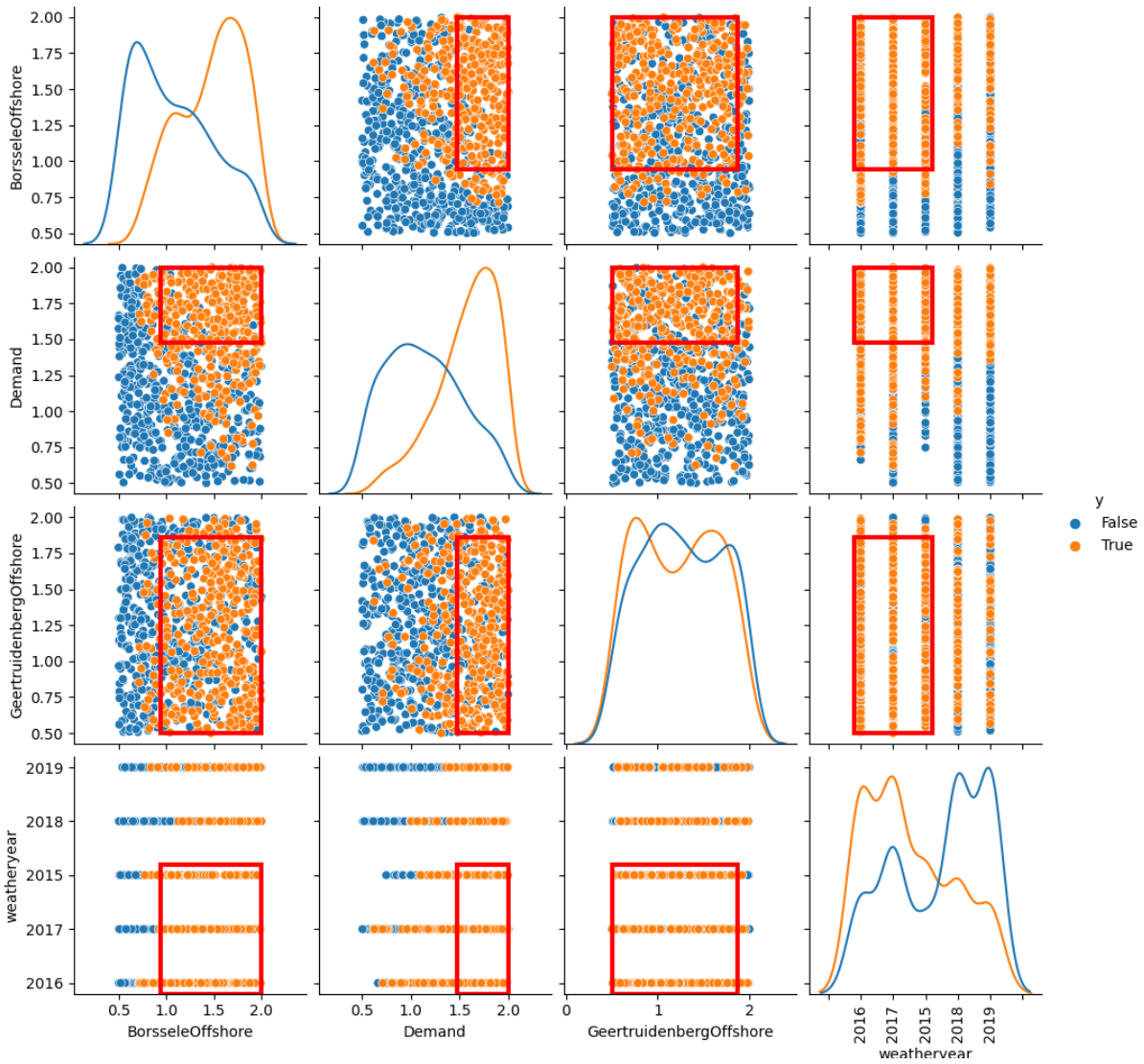


Figure 54: Prim scatterplot of line 4 with decision-rule 1.

In Figure 55, the PRIM analysis with decision-rule 2 can be found. This decision-rule did not generate a nice overview of the results unfortunately.

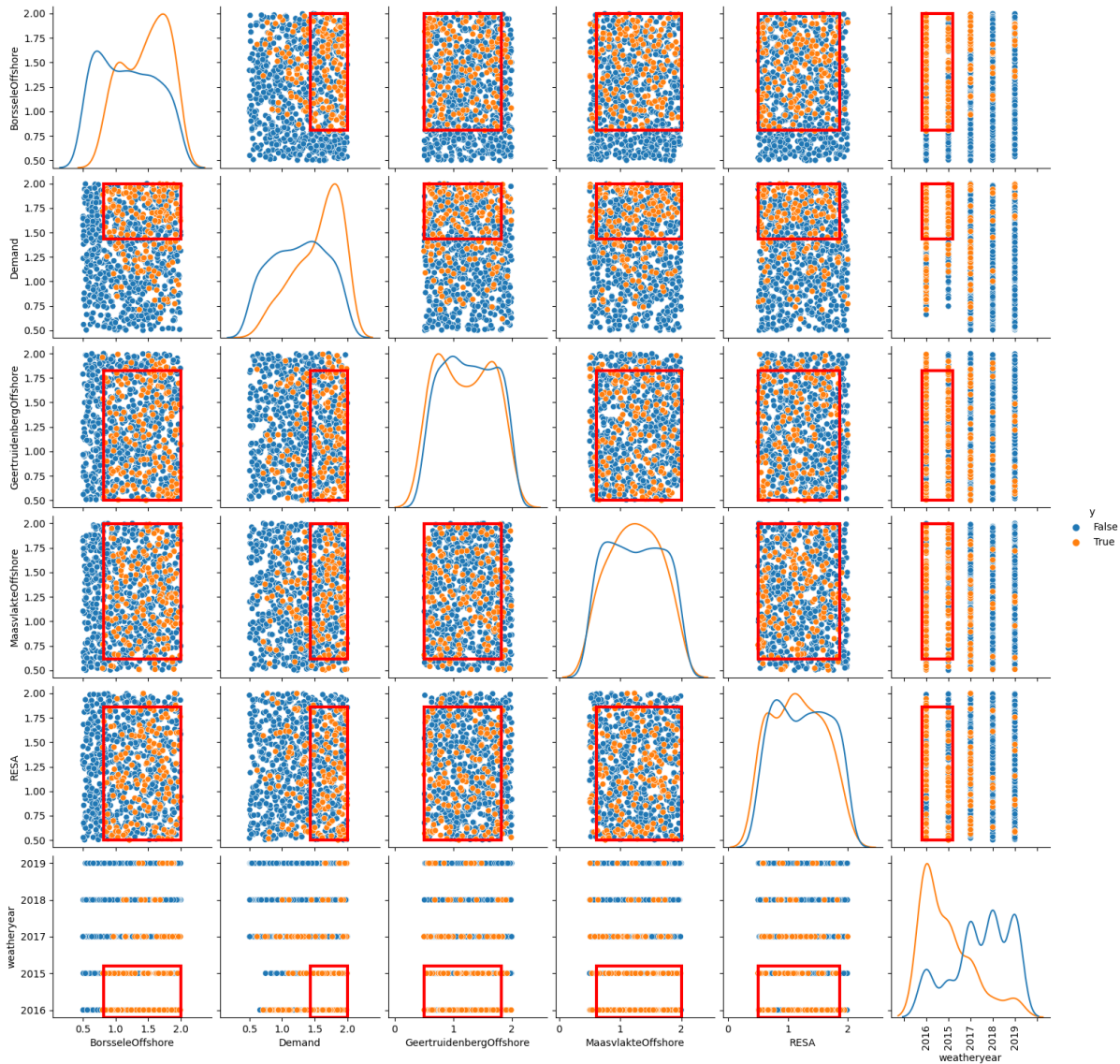


Figure 55: Prim scatterplot of line 4 with decision-rule 2.

What is overarching from these figures, is that the demand must be very high, to actively generate congestion. Furthermore, the two offshore windfarms in the region are important factors for the congestion; especially the windfarm connected to Borssele. The exact role of the windfarm in Geertruidenberg is not really clear, it seems that with almost every value of this uncertainty, congestion is occurring. The box does not reach to the highest points in this uncertainty however. This could point out that if the offshore wind is very high in this windfarm, the wind from Borssele is curtailed. With the curtailment of that energy, the line is no longer necessary.

Taking it's position to other lines into account, it can be concluded that this line is critical for the network. It is the only line that transfers the offshore wind from the Borssele windfarms. In this role, it is heavily dependent on the capacity of line 24 as well. If that line has a lower capacity than line 4, the flow of the wind power of Borssele to the rest of the Netherlands will be constrained to lowest capacity of those two lines. At the moment, the capacity of line 24 is lower than that of line 4. Therefore, line 24 will primarily be congested when line 4 has been congested first, and it's capacity been set to infinity. Line 24 will be analyzed further but only with the runs that have cost attributed to line 4.

I.3.2 Line 15

In Figure 56, the PRIM analysis with the first decision-rule can be found. In Figure 57, the PRIM analysis with the second decision-rule can be found.

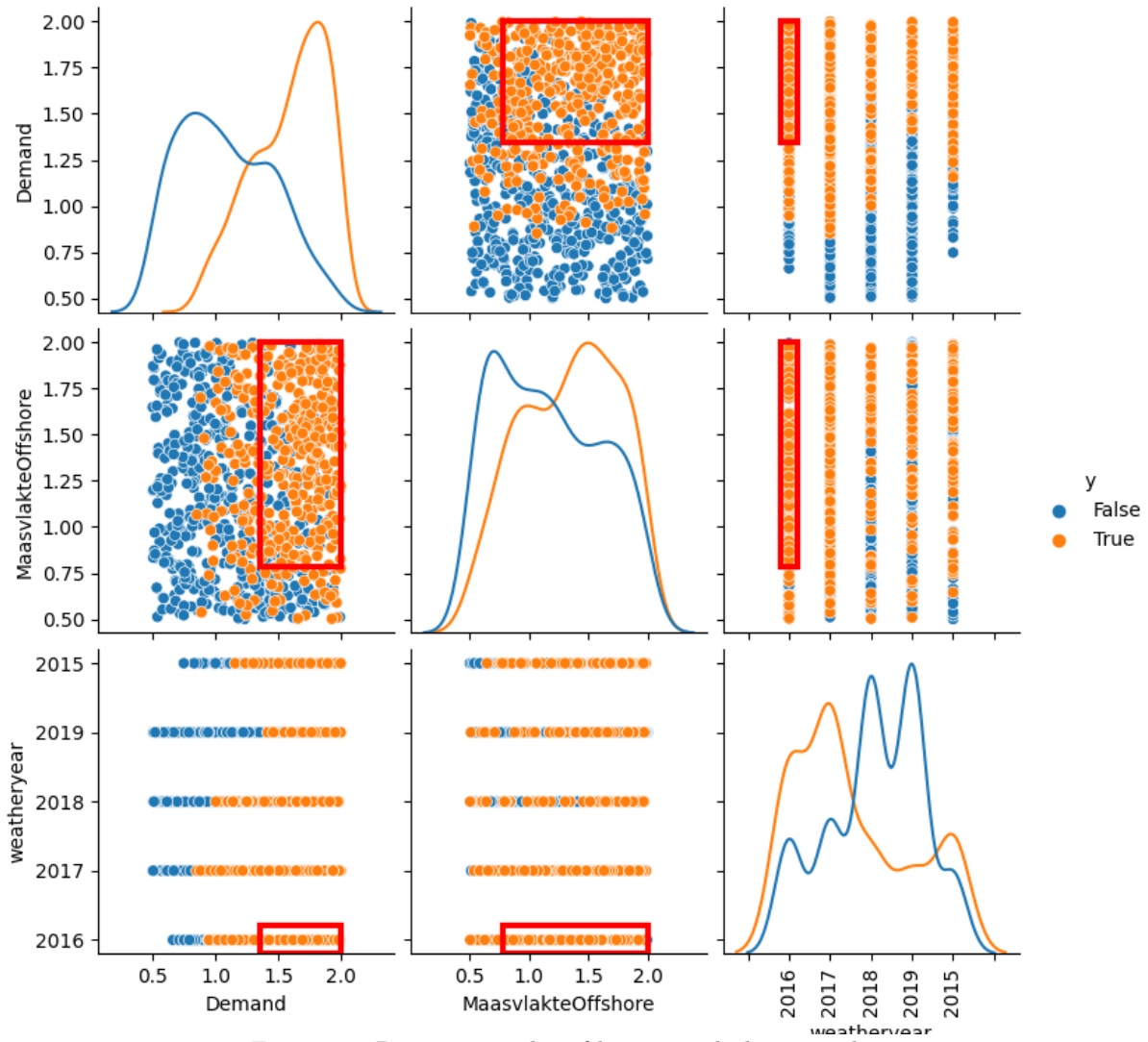


Figure 56: Prim scatterplot of line 15 with decision-rule 1.

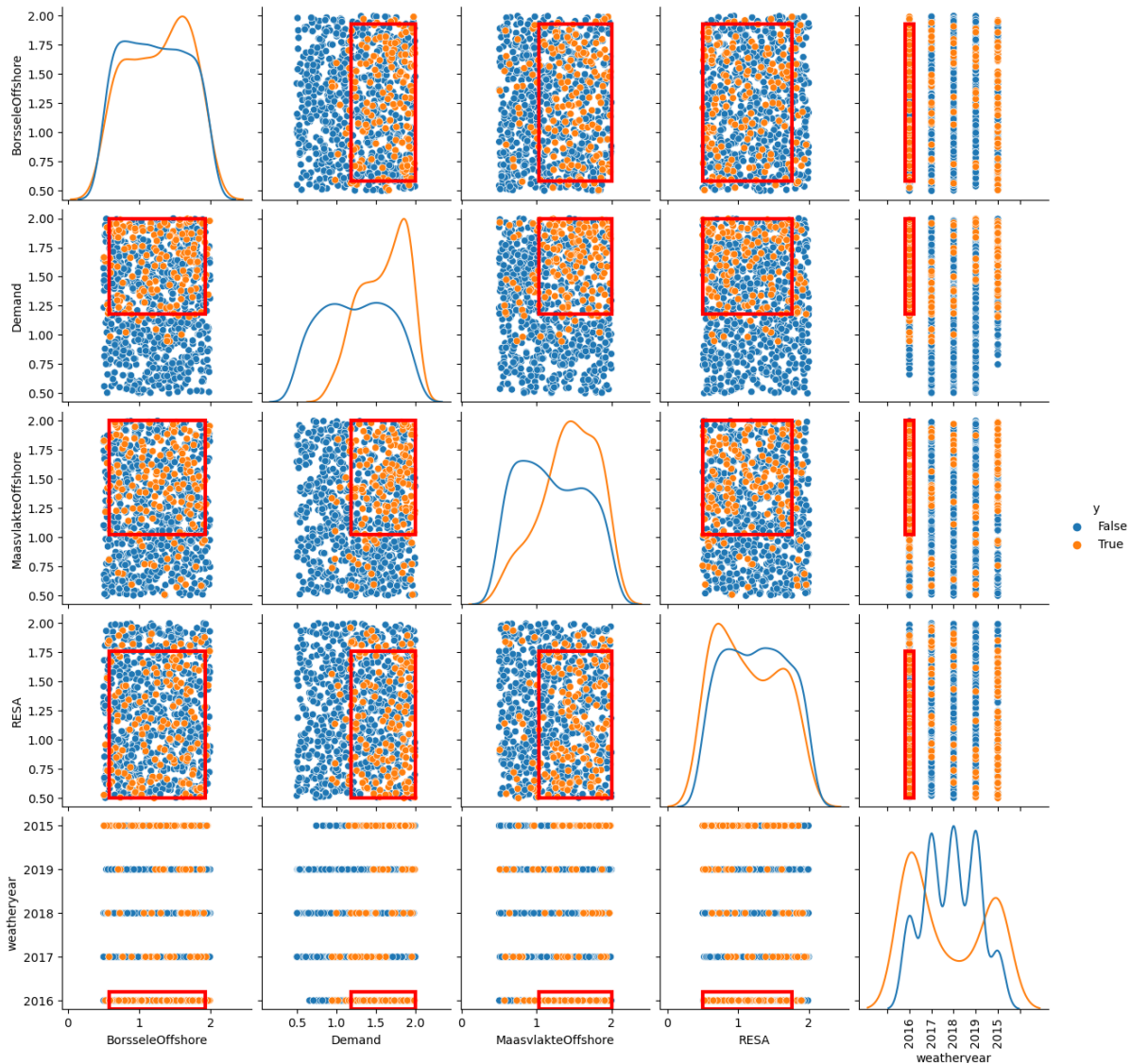


Figure 57: Prim scatterplot of line 15 with decision-rule 2.

While reviewing Figure 56, what comes to mind is that, the demand is the most influential factor. The weatheryear, and the Maasvlakte wind farm are the most influential after this uncertainty. This line is thus most probably used to transfer wind from the Maasvlakte wind farms to the rest of the East of the Netherlands.

The second decision-rule does not give much extra clarity, the runs that are marked as true are scattered around the plot. In addition, more uncertainties are added; this makes it harder to interpret. The two added uncertainties; The RESA-policy plans, and the offshore wind farm of Borssele both have a box that centers below the maximum value. This could mean two things: 1. The higher the uncertainty, the more renewable energy is in the system, and thus the price of energy is lower. The threshold of 1 percent of the system costs is therefore not met. 2. The powerflow is different in the system, and the offshore wind from the Maasvlakte that would normally flow on this line, does not flow. Therefore no congestion is detected.

Looking geographically at the other vulnerable lines, and taking the offshore windfarms into account, it could very well be that there is a connection in dependencies with the lines 15, 6, and 23. These will therefore be analysed together.

I.3.3 Line 23

In Figure 58, the PRIM analysis with the first decision-rule can be found. In Figure 59, the PRIM analysis with the second decision-rule can be found.

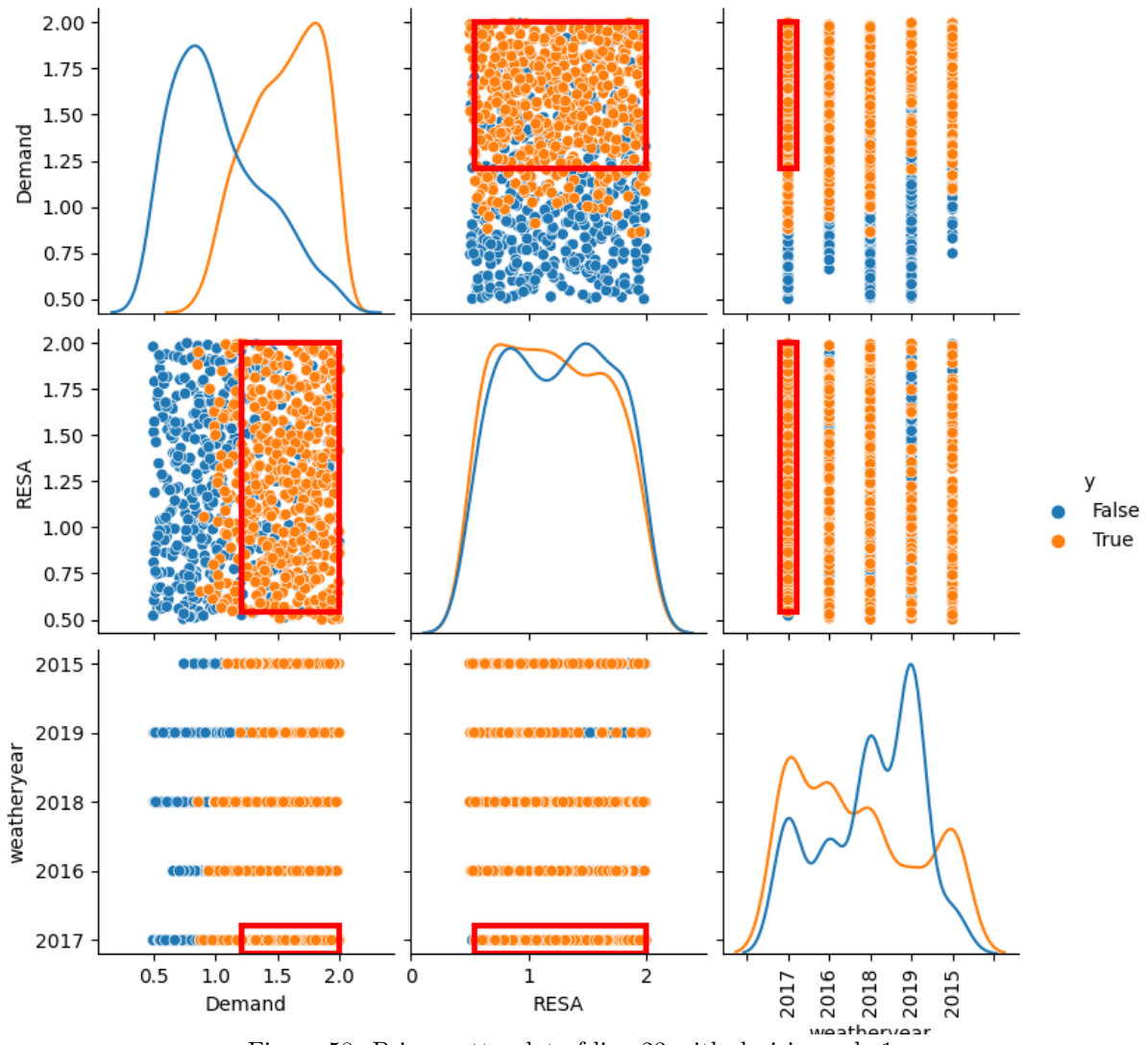


Figure 58: Prim scatterplot of line 23 with decision-rule 1.

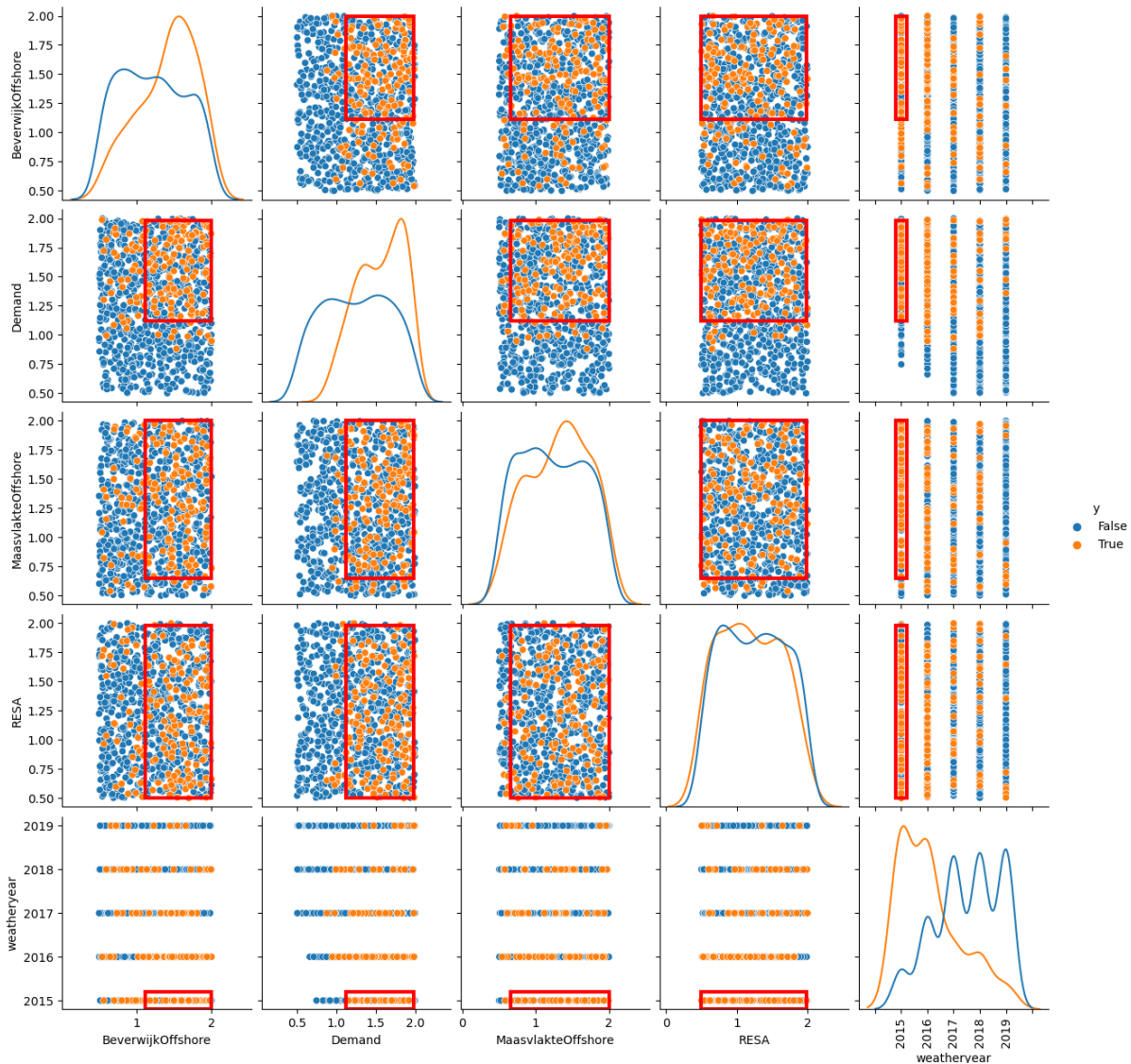


Figure 59: Prim scatterplot of line 23 with decision-rule 2.

In Figure 58, the only clear result that can be found is that the demand for power must be somewhat high. The RESA-policy plans is the second uncertainty. This uncertainty is however, not limited in it's box. The distribution of the positive and negative cases shows no clear difference as well.

In Figure 59, the results become cluttered. The Beverwijk offshore windfarms is the only added uncertainty that shows a very clear difference in the distribution. This is quite logical, since this line can be viewed as the connection between the windfarm in Beverwijk, and the east of the Netherlands.

As already stated, the lines 5, 15 and 23 need to be evaluated together since they are geographically close.

I.3.4 Line 24

In Figure 60, the PRIM analysis with the first decision-rule can be found. In Figure 61, the PRIM analysis with the second decision-rule can be found.

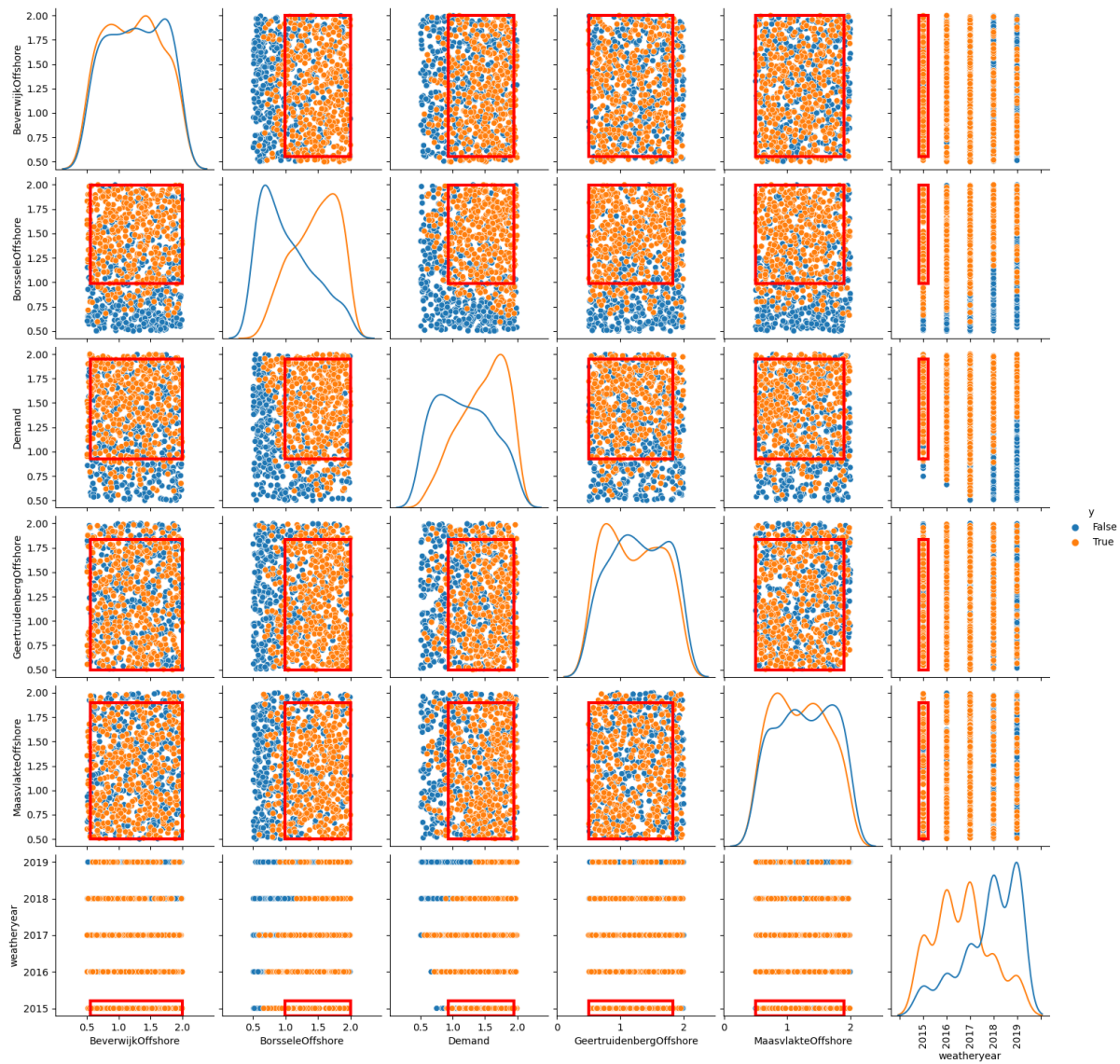


Figure 60: Prim scatterplot of line 24 with the first decision-rule.

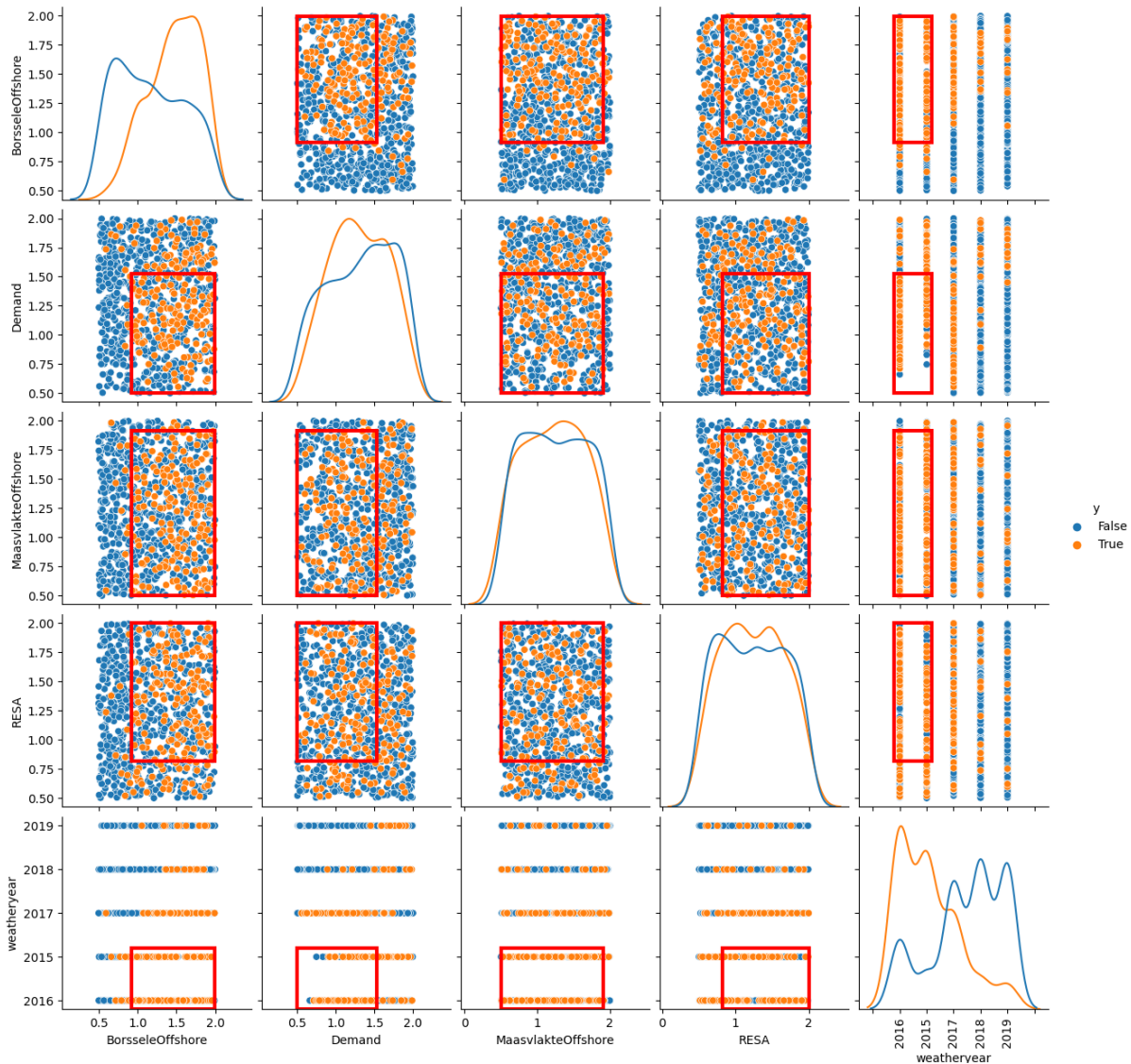


Figure 61: Prim scatterplot of line 24 with the second decision-rule.

What comes to mind in both figures, is that the most influential uncertainty is the offshore windfarm of Borssele. When there is enough windpower output, this line will be congested. In Figure 60, the demand plays a role in the distribution as well. In Figure 61 it no longer plays a role.

I.3.5 Line 28

For line 28, the second decision-rule did not give any results. In Figure 62, the results for the first decision-rule can be found.

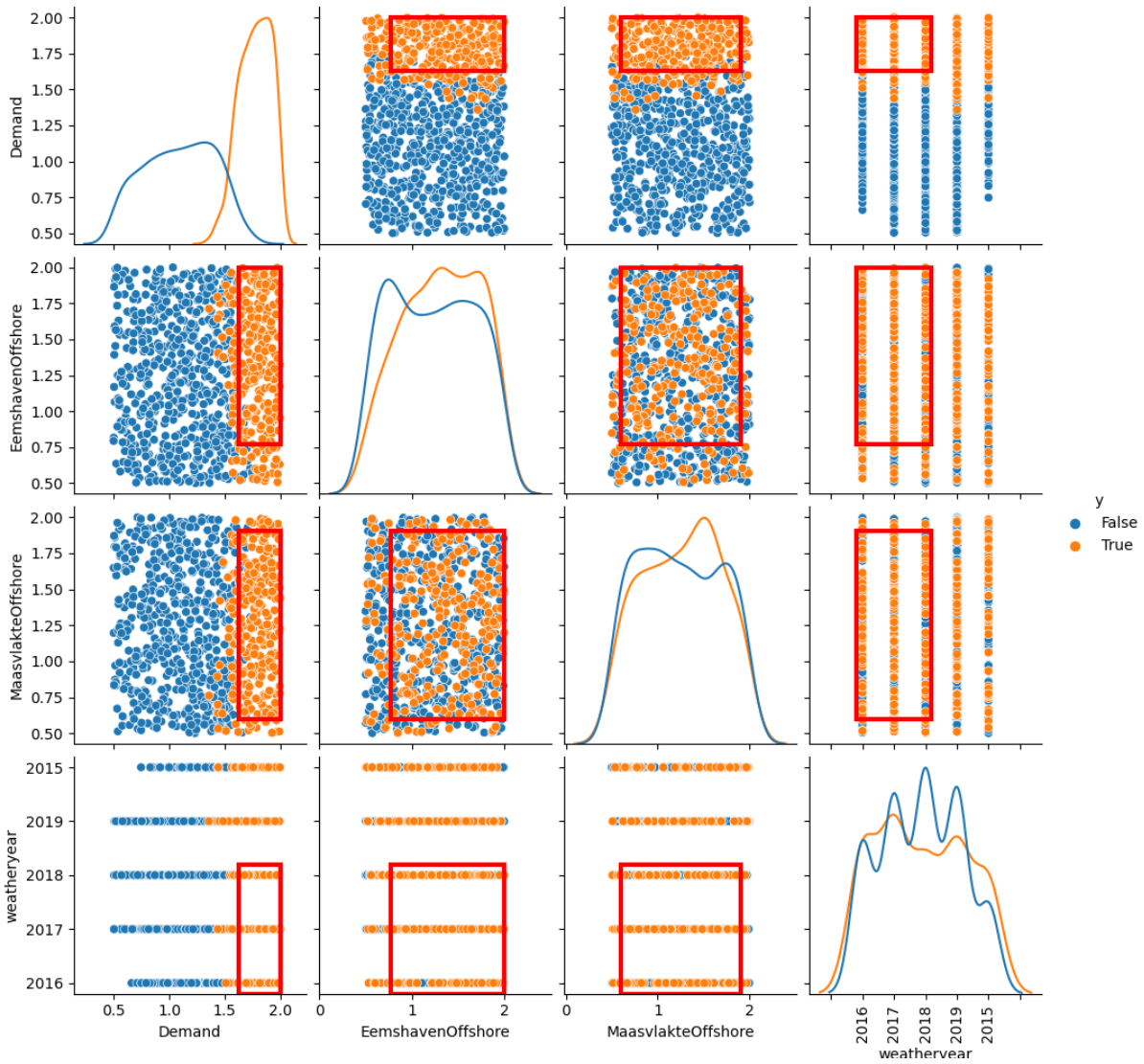


Figure 62: Prim scatterplot of line 28 with the first decision-rule

The results for this line show that the demand for power must be very high for the line to become congested. The other uncertainties do not play a big role in this line.

I.3.6 Line 35

In Figure 88, the PRIM analysis with the first decision-rule can be found. In Figure 64, the PRIM analysis with the second decision-rule can be found.

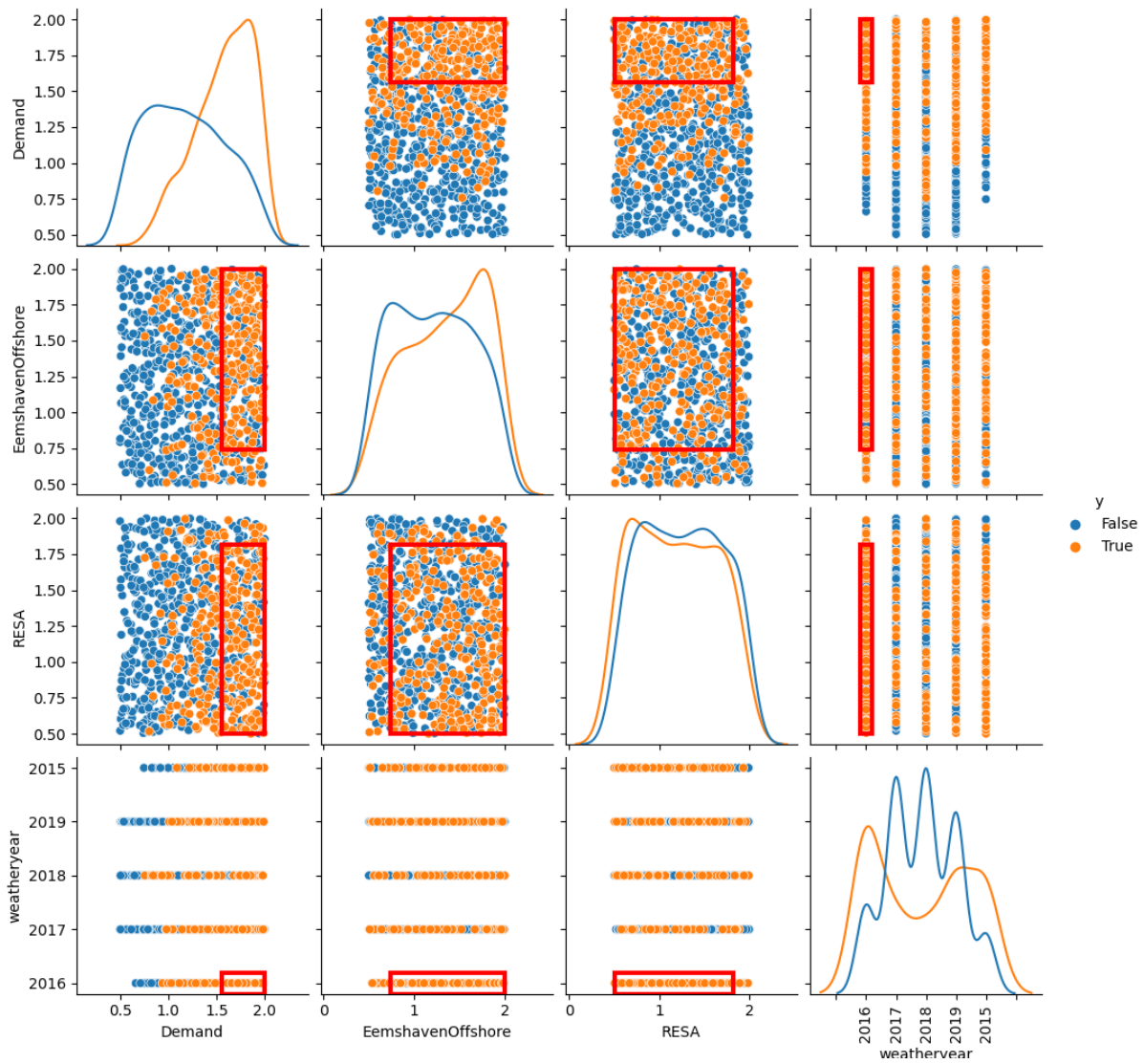


Figure 63: Prim scatterplot of line 35 with the first decision-rule

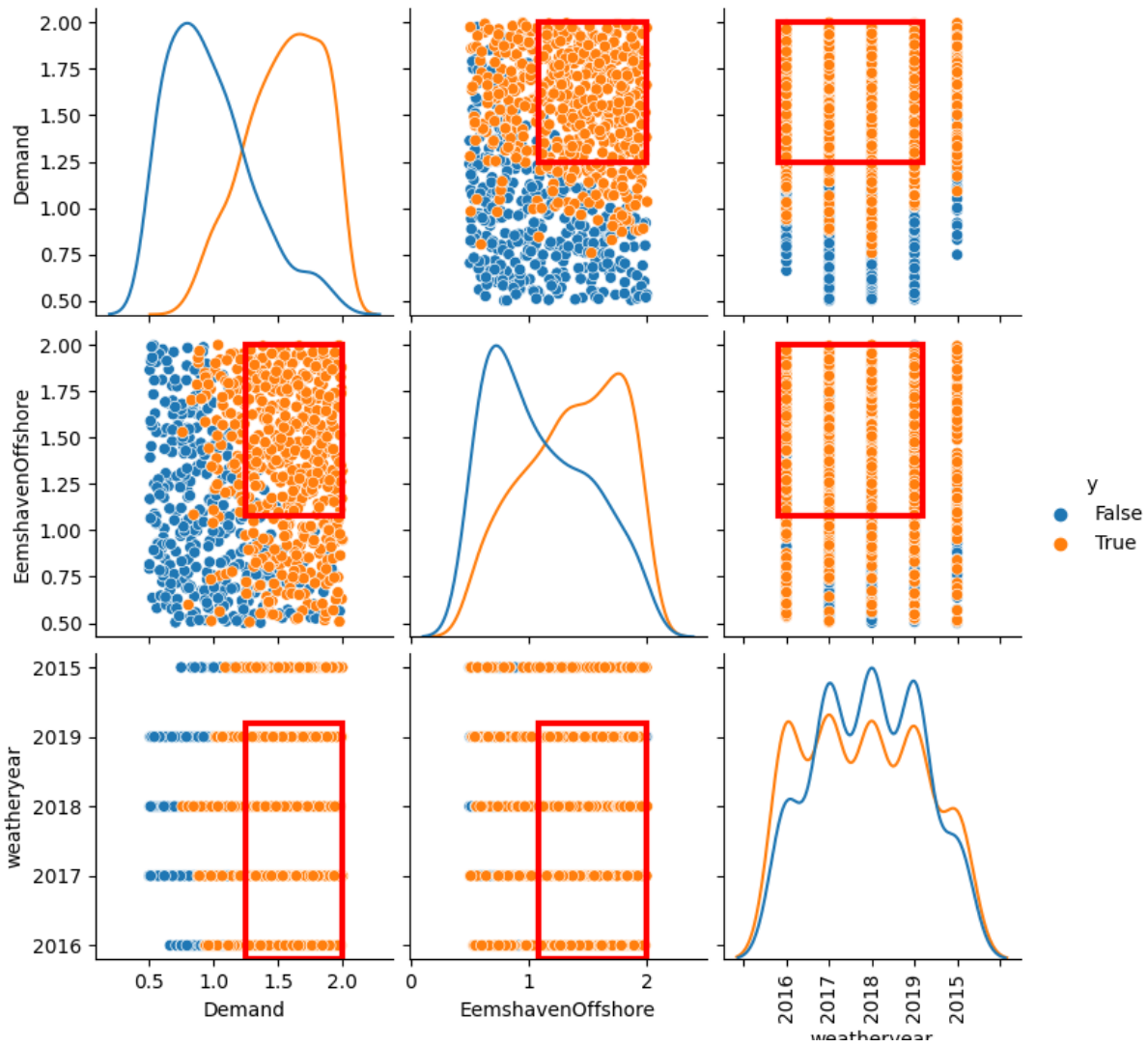


Figure 64: Prim scatterplot of line 35 with the second decision-rule.

Following these figures, The most influential uncertainties for this line are the Demand for power and the offshore windfarm of Eemshaven. Looking, at this line in geographical context, this makes sense. Apart from this, the line is not interesting to look at. Since it is very isolated, and has a very low capacity.

I.3.7 Line 38

In Figure 65, the PRIM analysis with the first decision-rule can be found. In Figure 66, the PRIM analysis with the second decision-rule can be found.

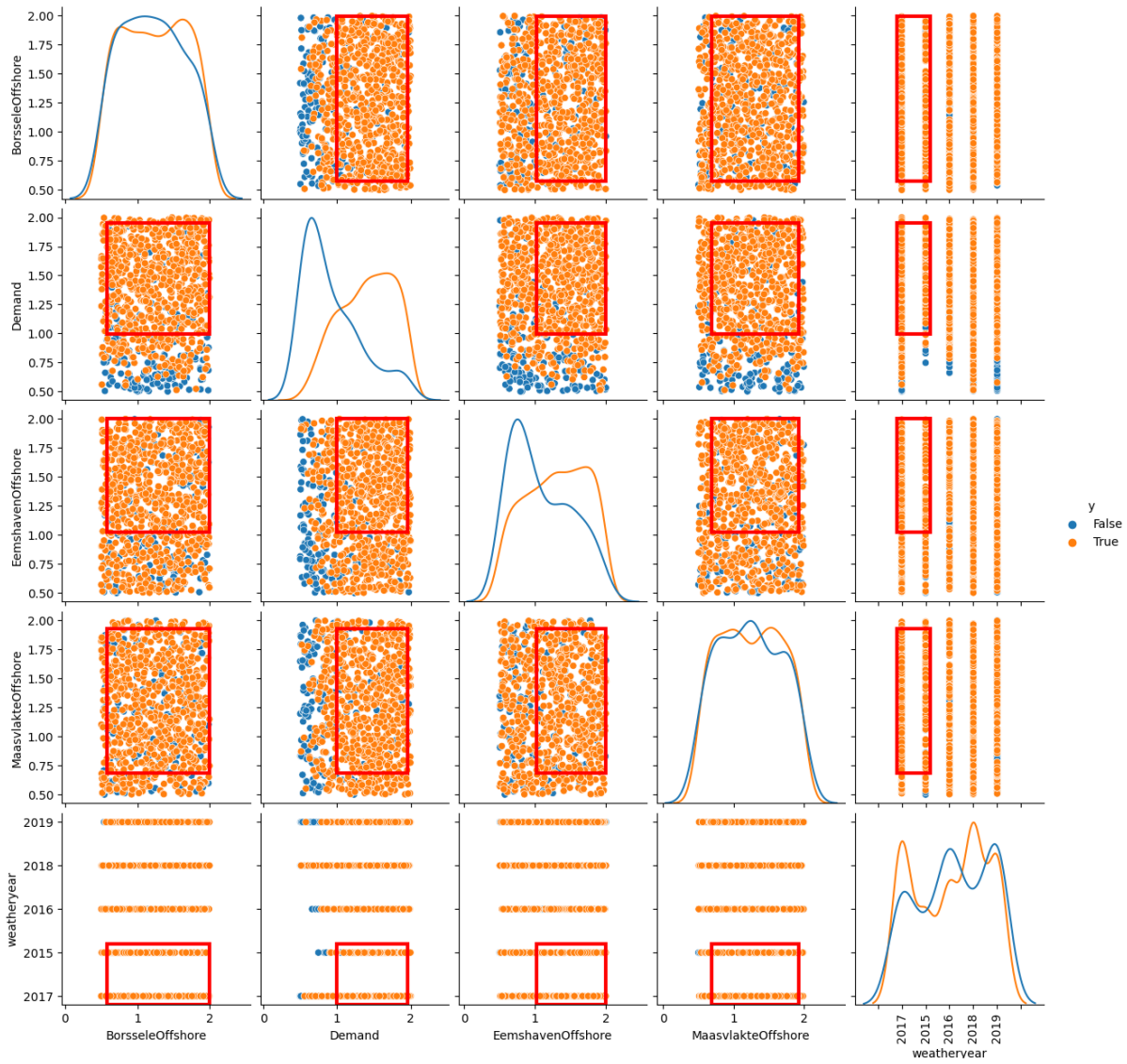


Figure 65: Prim scatterplot of line 38.

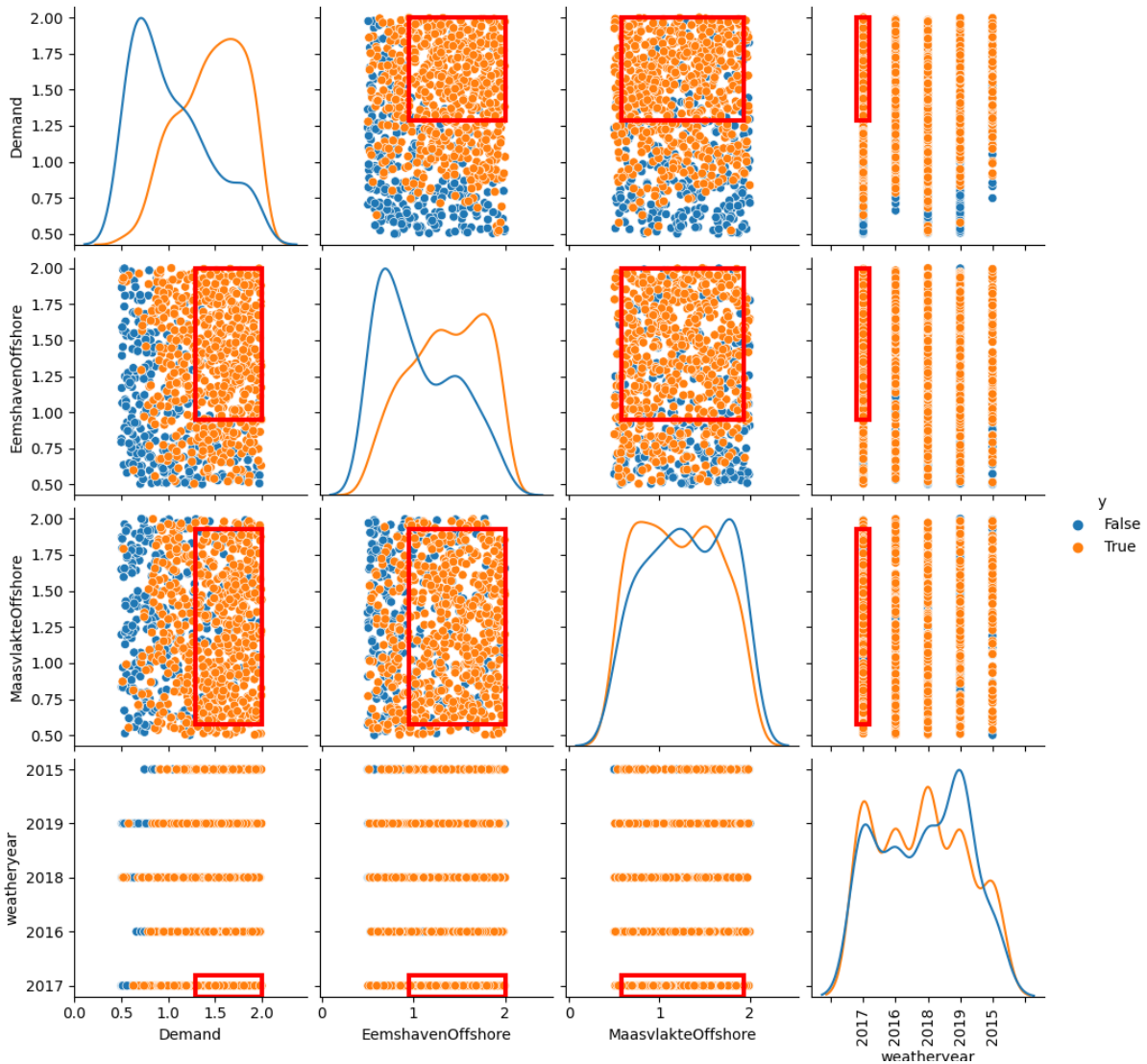


Figure 66: Prim scatterplot of line 38 with the second decision-rule.

This line is primarily vulnerable to the wind from Eemshaven, and the demand factor. Given it's location, it functions as the critical line in transporting the offshore wind from Eemshaven to the south of the Netherlands. That, with the fact that the line has a very low capacity makes it very vulnerable. It is surprising that the other lines surrounding it do not show any problems. Furthermore, the lines surrounding it should be investigated with it.

I.4 Results less vulnerable lines

The lesser vulnerable lines have all been tested for the two decision rules in the PRIM analysis. The second did not give any results. For the lines 10,30,31,37 and 40 no results for the first decision rule could be found as well.

I.4.1 Line 6

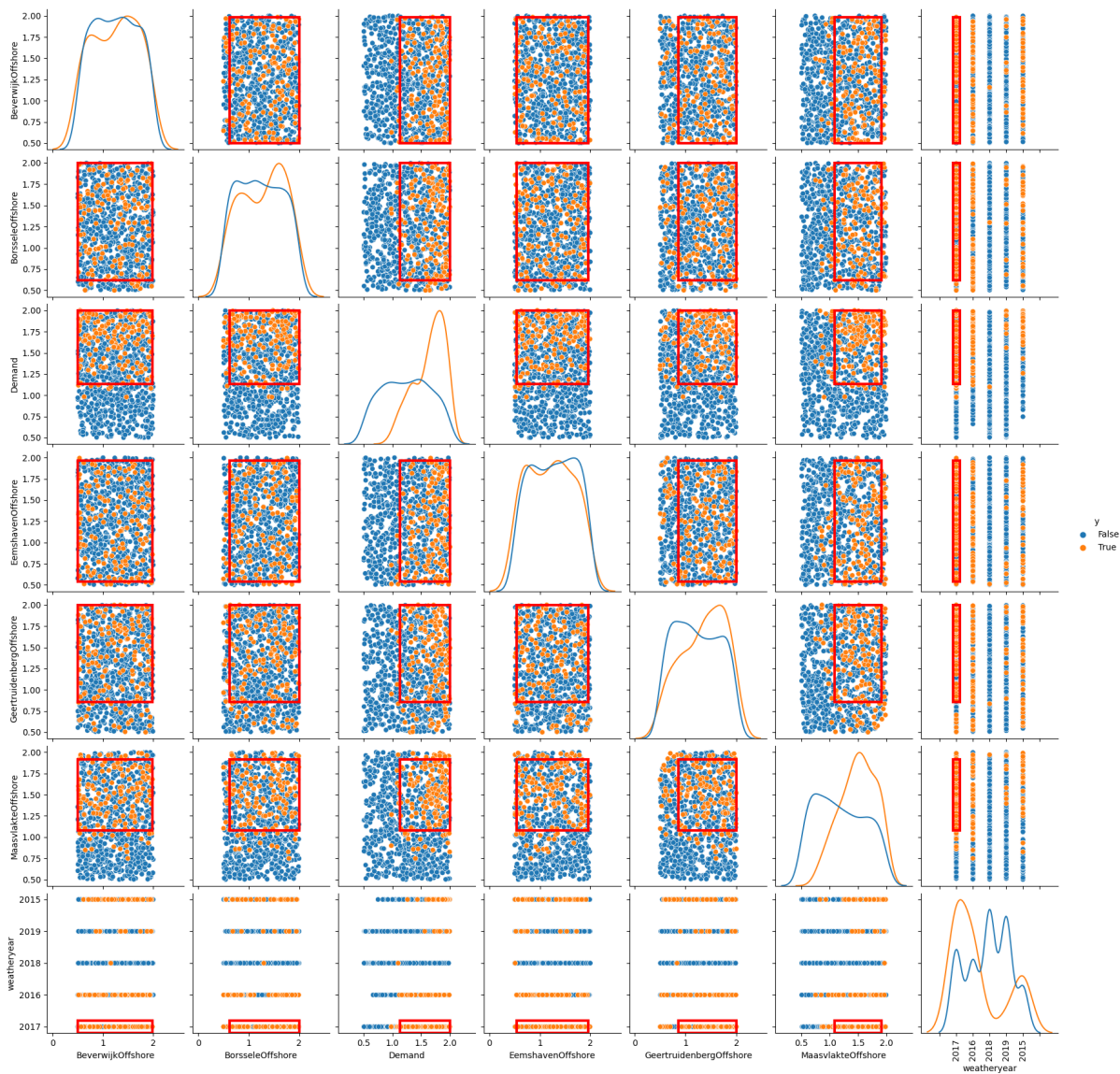


Figure 67: Prim scatterplot of line 6.

In Figure 67, the PRIM scatterplot for line 6 can be found. This is a very cluttered scatterplot. Not much information can be extracted from this plot; apart from the demand needing to be high, and the maasvlakte offshore. Due to how it;s situated it will be analyzed with the lines 15, and 23.

I.4.2 Line 13

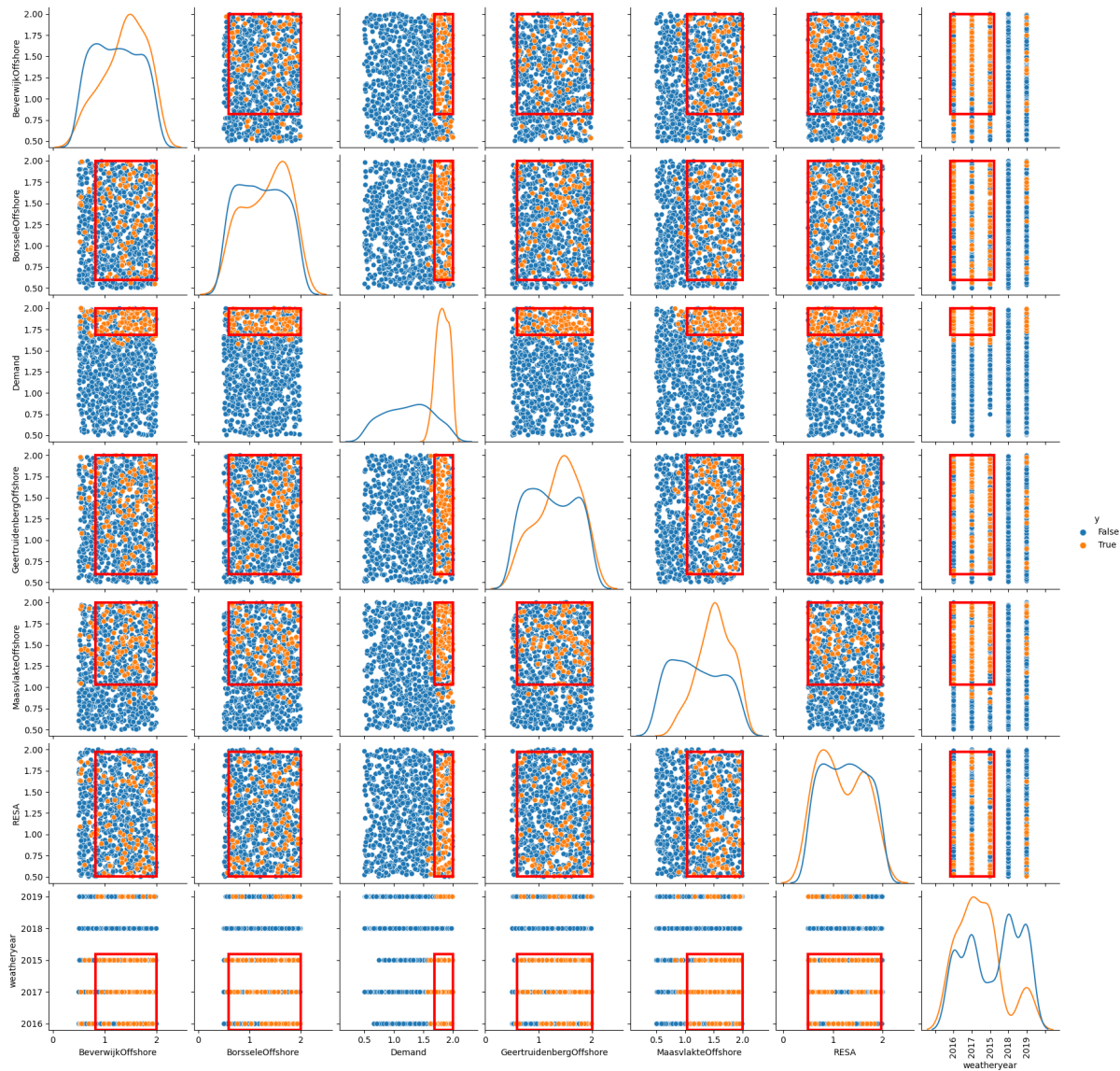


Figure 68: Prim scatterplot of line 13.

In Figure 68, the PRIM scatterplot for line 13 can be found. As can be seen, the demand must be very high for this line to become congested. It is therefore not really vulnerable. Furthermore, the offshore wind from the Maasvlakte is the most restricting uncertainty. The other offshore windfarms have some influence as well. Given the location of this line, this is no surprise.

I.4.3 Line 22

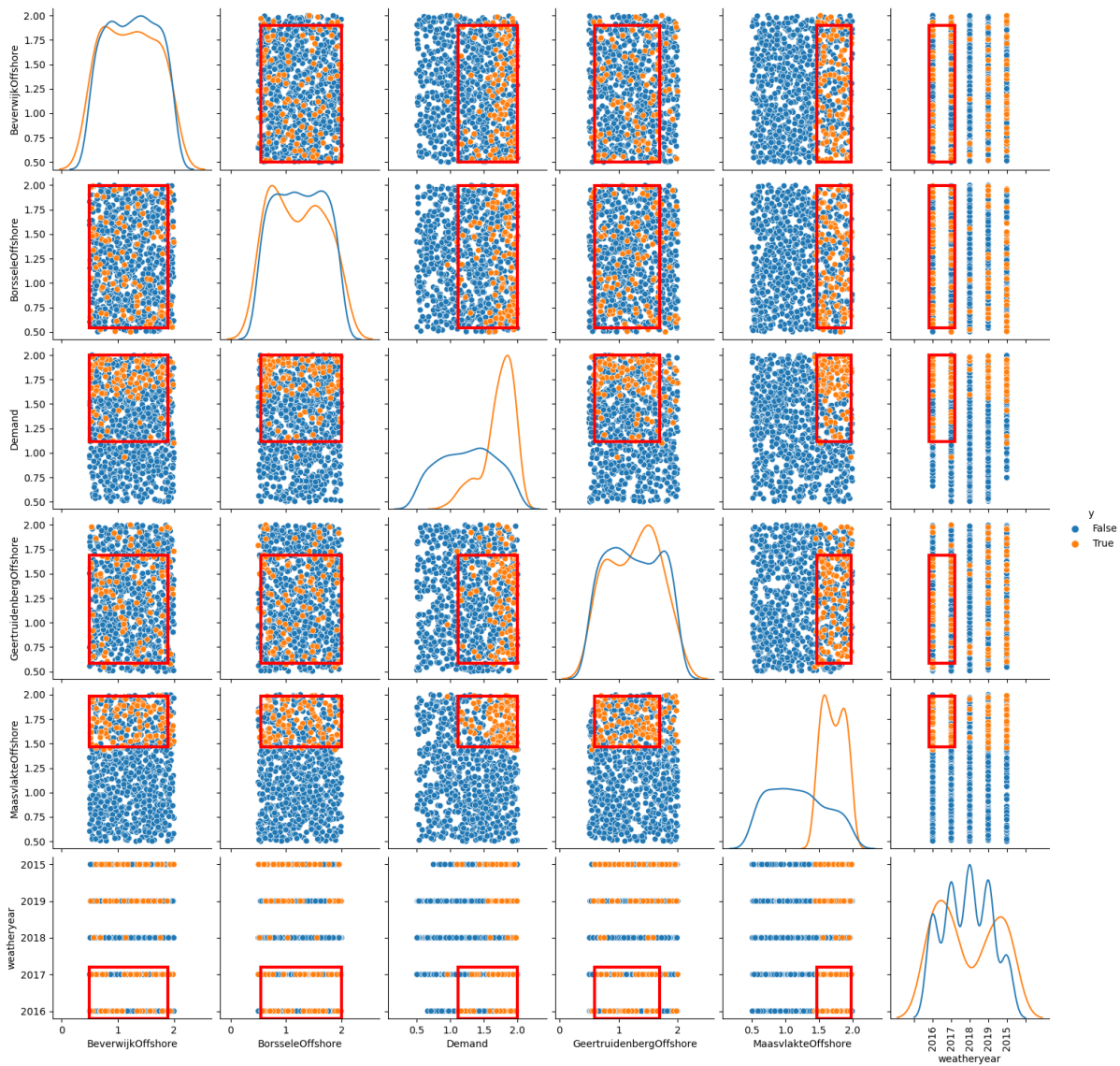


Figure 69: Prim scatterplot of line 22.

In Figure 69, the PRIM scatterplot for line 22 can be found. As can be seen, the capacity of the Maasvlakte wind farm must be really high for this line to become congested. The demand must be 1.1 as well.

I.4.4 Line 26

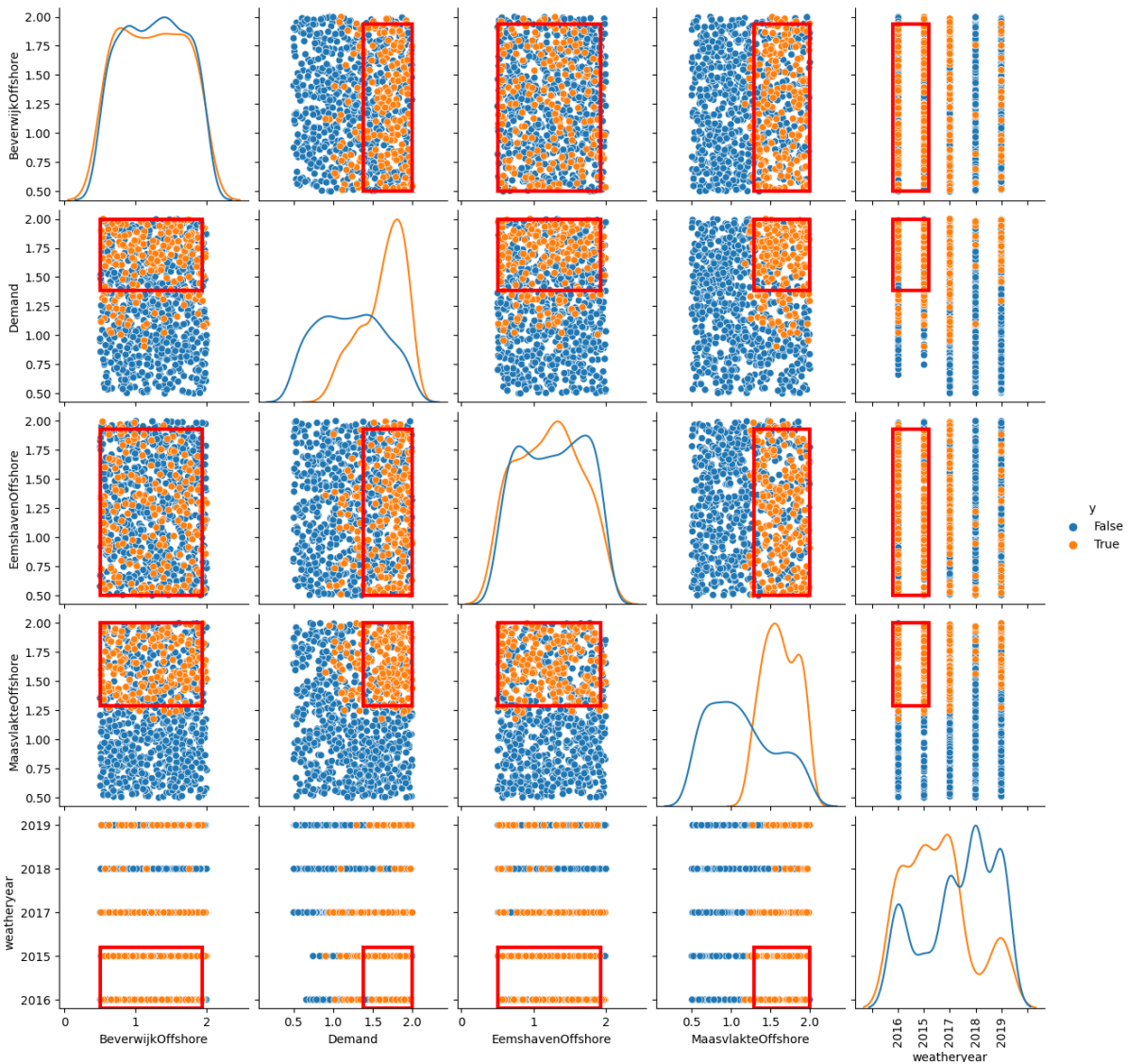


Figure 70: Prim scatterplot of line 26.

In Figure 70, the PRIM scatterplot for line 26 can be found. As can be seen, the demand must be very high for this line to become congested. Furthermore, the offshore wind from the Maasvlakte is the most restricting uncertainty. The other offshore wind farms have some influence as well. Given the location of this line, this is no surprise. It connects the west with the east of the Netherlands. This line will be analyzed as a secondary line to line 24.

I.5 Combined results January

- Line 4 congestions after line 24
- Line 15 congestions after 23
- Line 23 congestions after 15
- Line 6 congestions after line 15
- Line 6 congestions after line 23
- Line 10 congestions after line 28
- Line 13 congestions after line 24

- Line 26 congestions after line 24
- Line 31 congestions after Line 38
- Line 37 congestions after line 38
- Line 40 congestions after line 38

| Vulnerable line after congestion | Demand | Beverwijk | Borssele | Eemshaven | Geertruidenberg | Maasvlakte | RESA | Weather-years |
|----------------------------------|---------|-----------|----------|-----------|-----------------|------------|---------|------------------------------|
| 4 after 24 | 1.5-2.0 | x | 0.8-2.0 | x | x | x | x | 2015 2016 2017 2019 |
| 23 after 15 | 1.3-2.0 | x | x | x | x | 0.5-1.8 | x | 2015 2017 |
| 15 after 23 | | x | x | 0.6-2.0 | x | 0.7-2.0 | x | 2016 |
| 6 after 15 | 1.0-2.0 | x | 0.6-2.0 | 0.6-2.0 | 1.0-2.0 | 1.0-1.9 | x | 2017 |
| 6 after 23 | 1.1-2.0 | x | 0.6-1.8 | 0.6-1.9 | 1.0-2.0 | 1.0-1.9 | 0.5-1.8 | 2017 |
| 10 after 28 | 1.9-2.0 | 0.5-1.8 | 0.5-1.9 | x | x | 0.5-1.9 | x | 2016 2017 2019 |
| 13 after 4 | 1.7-2.0 | 0.9-2.0 | x | x | 0.6-2.0 | 1.1-2.0 | x | 2015 2016 2017 2019 |
| 13 after 24 | 1.7-2.0 | x | 1.0-2.0 | x | 0.6-2.0 | 1.0-1.9 | x | 2015 2016 2017 |
| 26 after 24 | 1.3-2.0 | 0.5-1.9 | x | 0.5-1.9 | x | 1.3-2.0 | x | 2016 |

Table 34: Thresholds of uncertainties on revealed vulnerable lines by PRIM analysis with decision-rule 1 for January experiments.

I.5.1 Line 4 after line 24

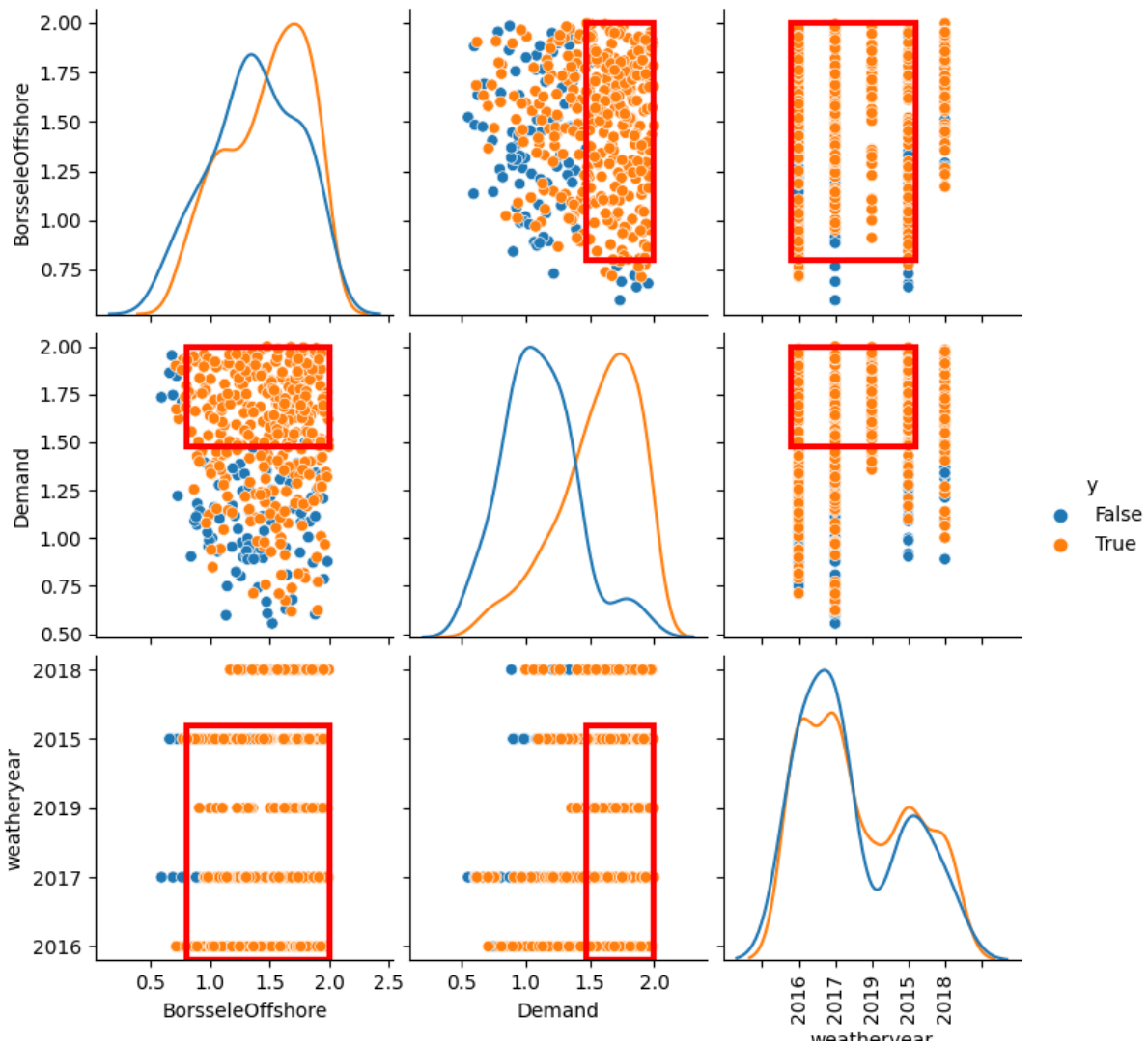


Figure 71: Prim scatterplot of line 4 with filtration of line 24.

In Figure 71, all the runs in which line 24 had no costs attributed to it have been filtered out. Meaning that the runs in which the capacity has been set to infinity of line 24 are left in the analysis. While comparing the PRIM analysis of line 4 in figure 54 with Figure 71, we see that the same cases are yellow in both scatterplots for the Demand-BorsseleOffshore comparison. This shows that line 4 only becomes congested after the capacity of line 24 has risen.

I.5.2 Line 15 after line 23, and vice versa

Both line 15 and line 23 have been analyzed with filtration on the results for both of them. This was done to try to find any correlation between the two. These lines are both part of a subnetwork that has some individual lines.

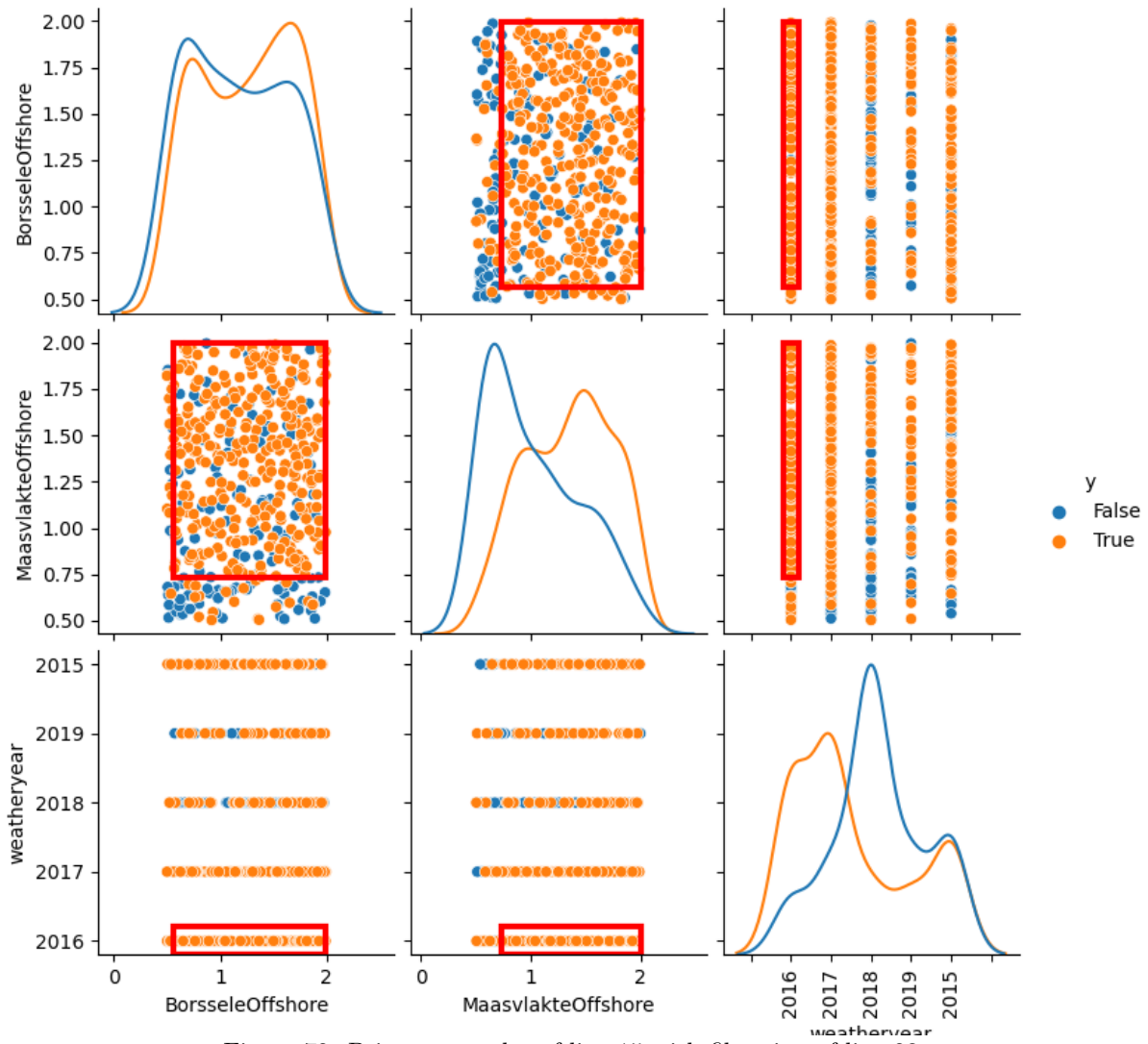


Figure 72: Prim scatterplot of line 15 with filtration of line 23.

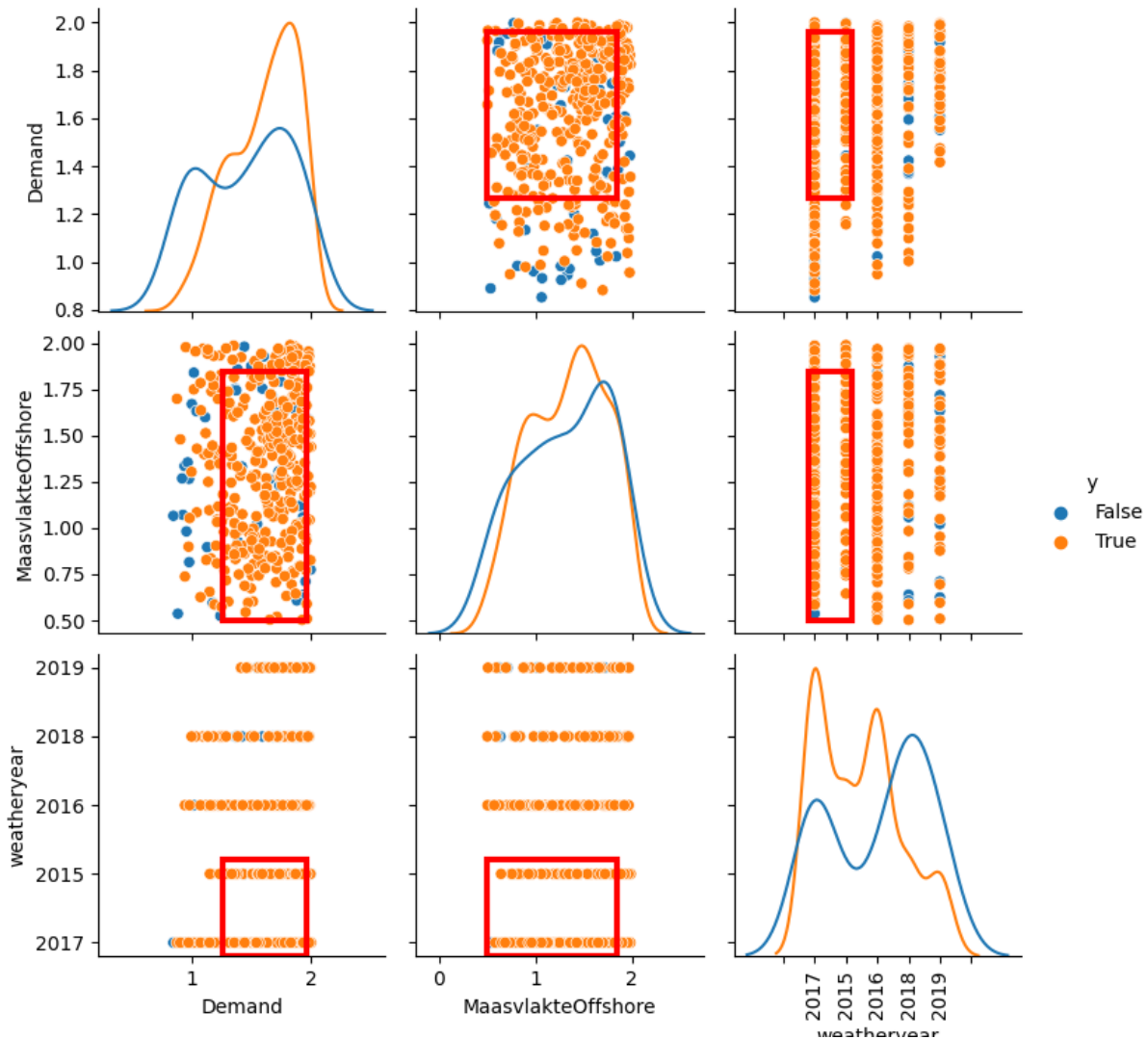


Figure 73: Prim scatterplot of line 23 with filtration of line 15.

Out of Figures 72 and 73, at first glance no clear correlation seems to exist between them. But when the stand-alone PRIM scatterplots in Figures 56, and 58 are taken into account as well it seems that these lines have the same demand threshold for which they get congested. Therefore, it seems that the power will get divided over the subnetwork, and then flow via line 8 to the north of the Netherlands. This line has a higher capacity than lines 15 and 23 combined.

I.5.3 Line 6 after line 15

In Figure 74, the PRIM analysis of line 6 filtered with line 15 is shown. Comparing this figure with Figure 67 gives no extra value.

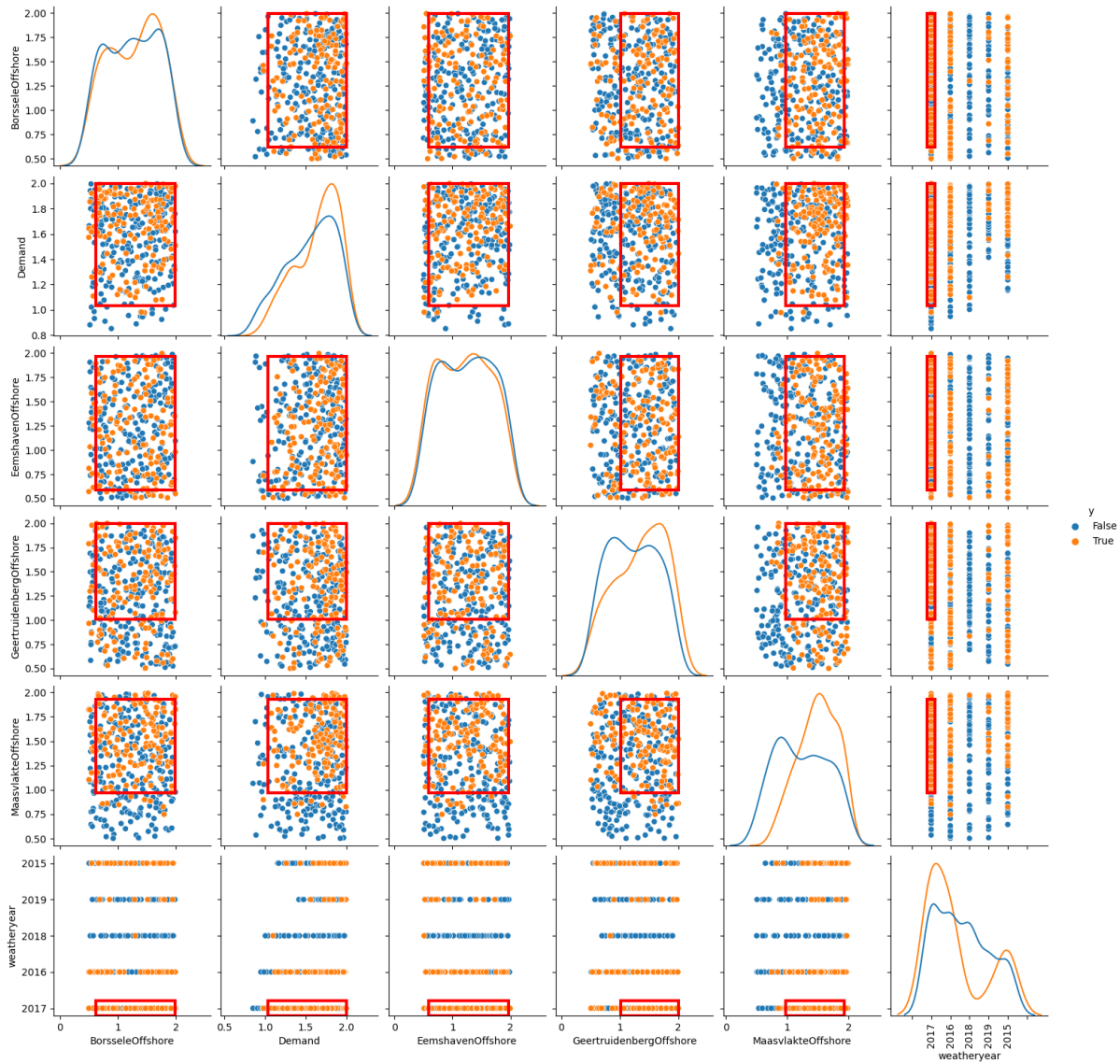


Figure 74: Prim scatterplot of line 6 with filtration of line 15.

I.5.4 Line 6 after line 23

In Figure 75, the PRIM analysis of line 6 filtered with line 23 is shown. Comparing this figure with Figure 67 gives no extra value.

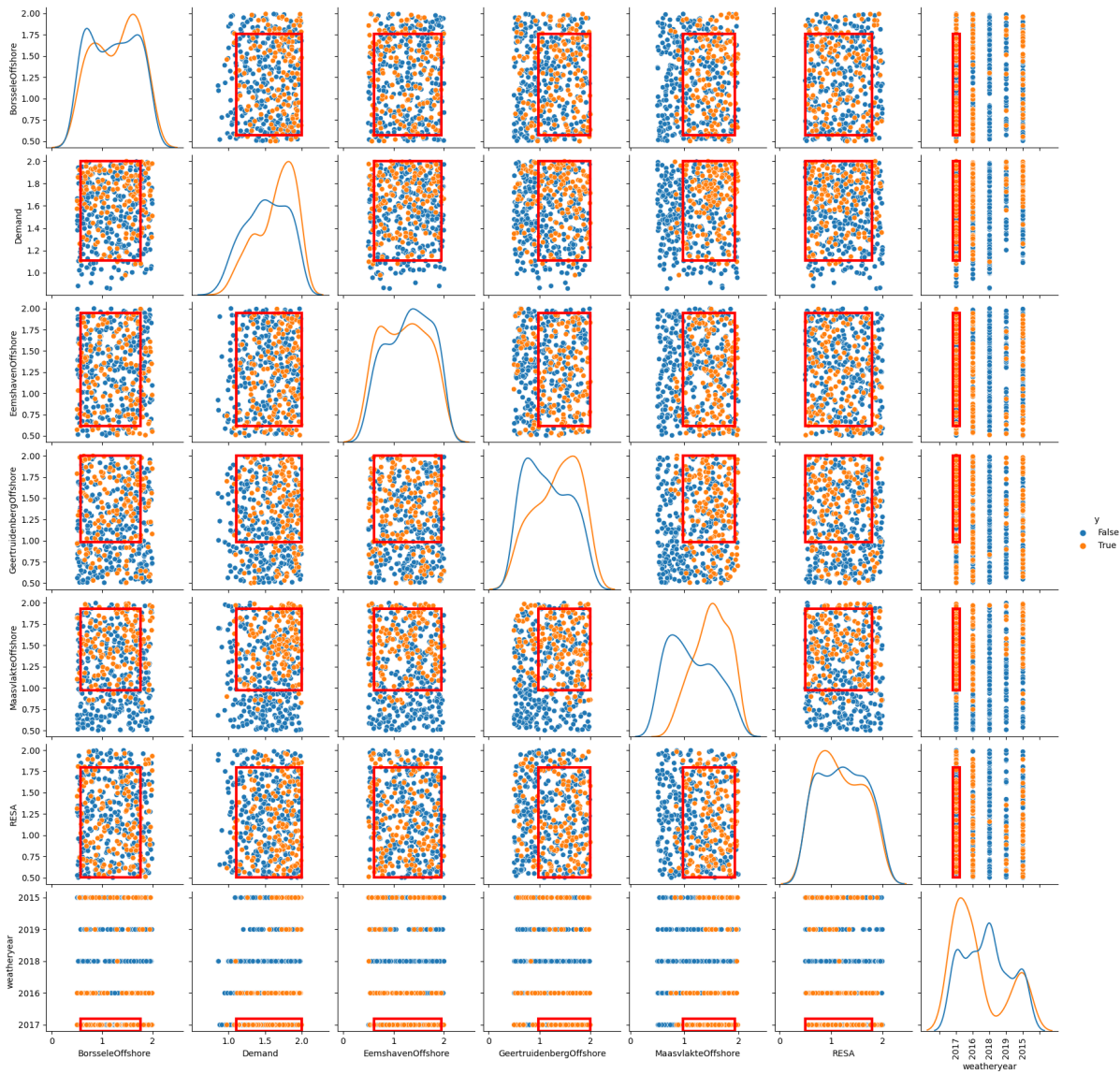


Figure 75: Prim scatterplot of line 6 with filtration of line 23.

I.5.5 Line 10 after line 28

In Figure 76, the results for line 10 have been filtered with the results of line 28. The PRIM analysis of line 10 did not give any results; this has. Key factor in this plot is the demand. Also, the amount of runs with congestions is fairly low. Line 10 is thus not a vulnerable line. Main reason for this is that offshore wind can reach the east of the Netherlands via the south as well.

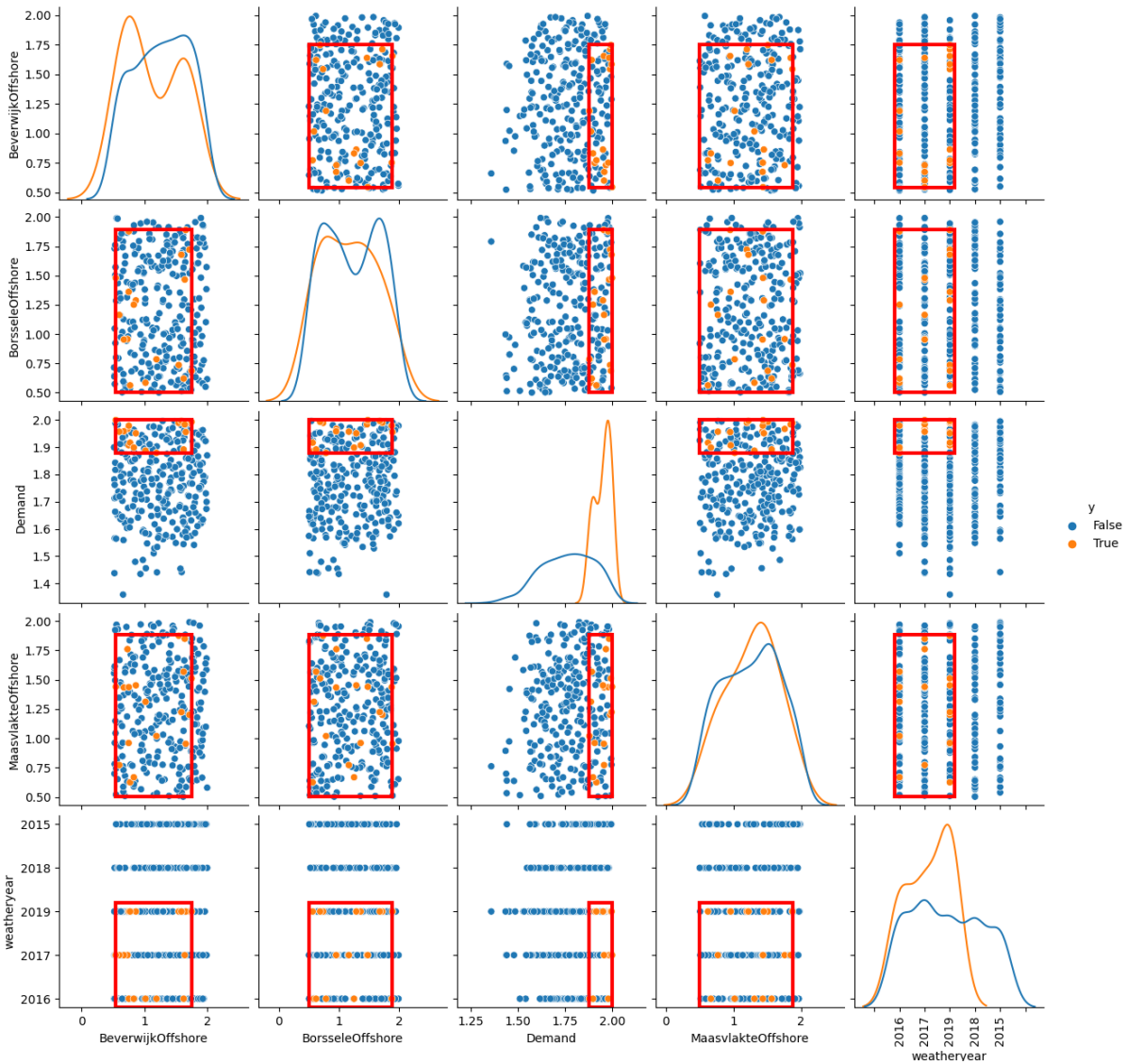


Figure 76: Prim scatterplot of line 10 with filtration of line 28.

I.5.6 Line 13 after line 24 and line 4

In Figure 77 the results of the PRIM analysis with filtration of the cost-having runs can be seen. While comparing this figure with Figure 68, the same runs are deemed positive. This means that line 13 probably only becomes congested after line 24 has been congested; which is quite logical.

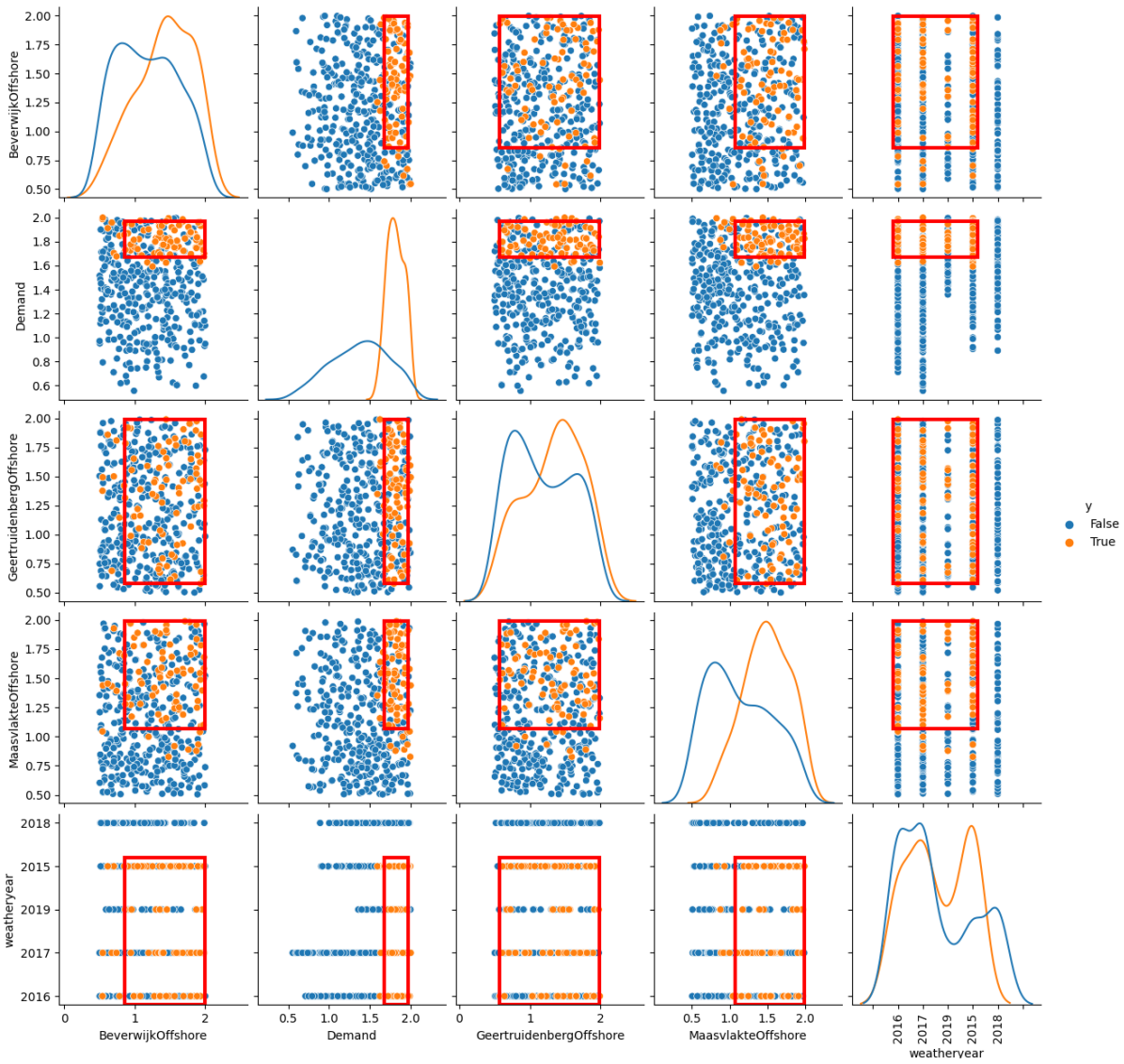


Figure 77: Prim scatterplot of line 13 with filtration of line 24.

An even further analysis concerning line 4 and line 13 has been done as can be seen in Figure 78, this showed comparable results as Figure 77. The difference is that the windfarms of Borssele and Beverwijk have been switched.

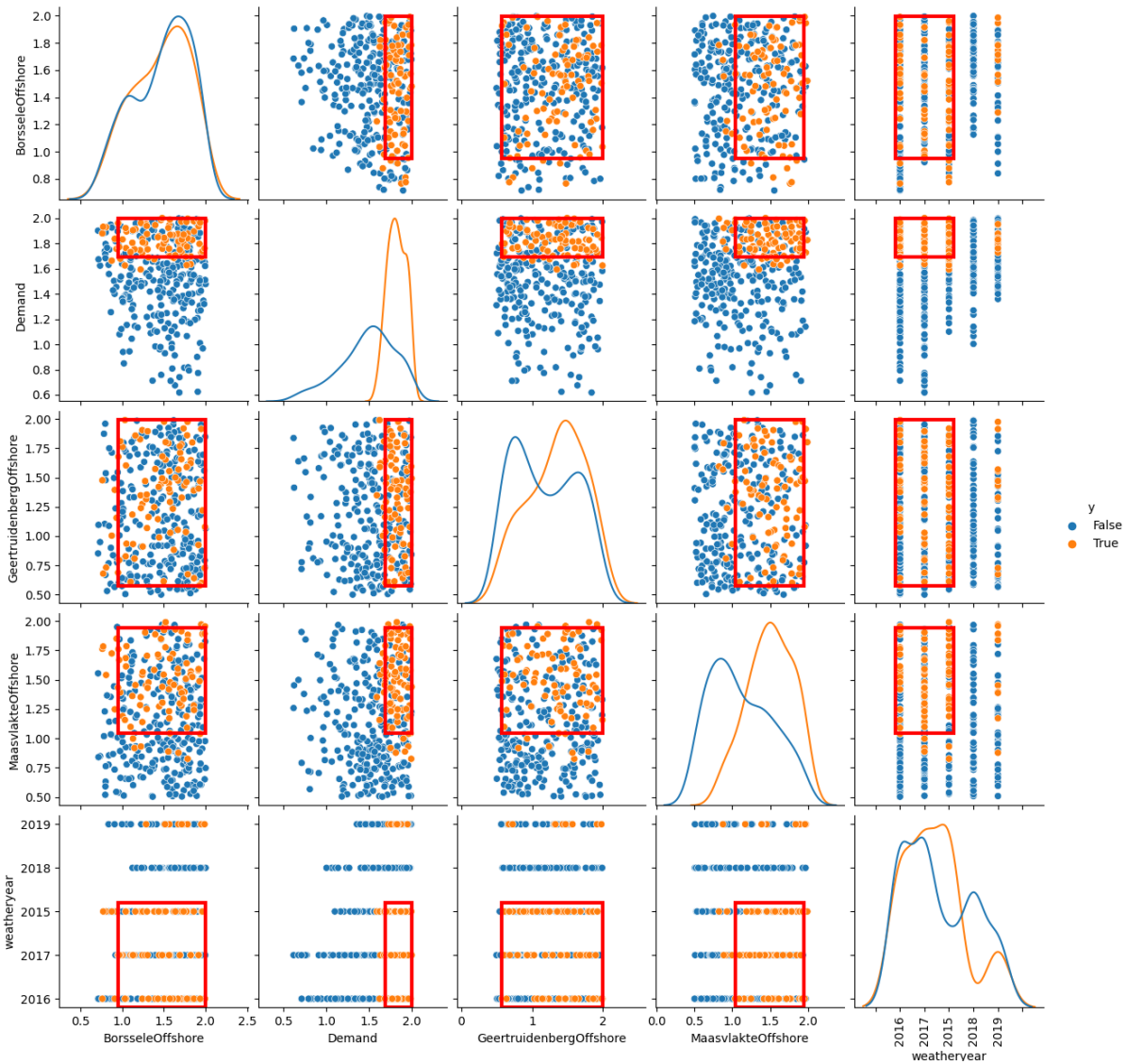


Figure 78: Prim scatterplot of line 13 with filtration of line 4.

I.5.7 Line 26 after line 24

In Figure 79, the results for the selection of runs with results for line 24 and line 26 can be seen. While comparing these results with Figure 70, what stands out is that the positive dots for the two plots seem to be somewhat equal to another. There are some minor differences, but the general idea is that first line 24 becomes congested, and then congestions could be formed on line 26. This is a plausible explanation given how the windfarms, and demand are situated.

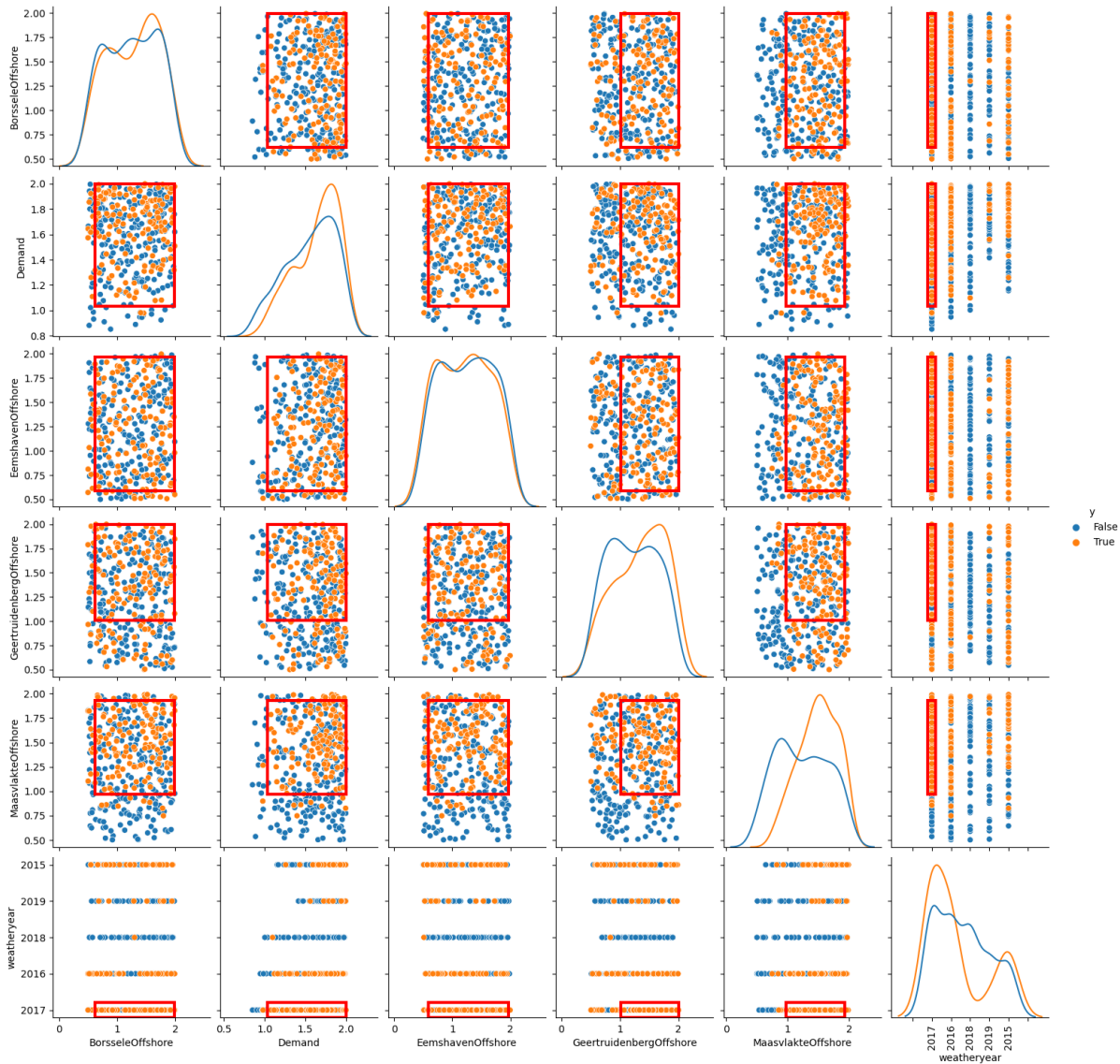


Figure 79: Prim scatterplot of line 26 with filtration of line 24.

I.5.8 Line 31 after line 38

No results

I.5.9 Line 37 congestions after line 38

No results

I.5.10 Line 40 congestions after line 38

No results.

I.6 June results

The january experiment was the experiment with the setting as described in the methodology. As described there, the runtime for this experiment is from 08/06/2030 00:00 to 15/06/2030 00:00; a full week in summer. 1000 experiments have been performed for this week.

I.6.1 Selection of results

No cost filtration

The first step in the result analysis is the selection of them. The runs without any costs in them

will be filtered out. These runs have by definition zero costs attributed to any of the lines. This means that in the analysis, these runs will only clutter the analysis. There is no added value in leaving these in the further analysis. The PRIM analysis for the runs with any costs can be found in Figure 50. As can be seen, the PRIM algorithm can't scrape away lesser influential factors. Only the demand seems to be a clearly influential factor. After a certain demand input to the model, the costs will rise. This is of course as would be expected.

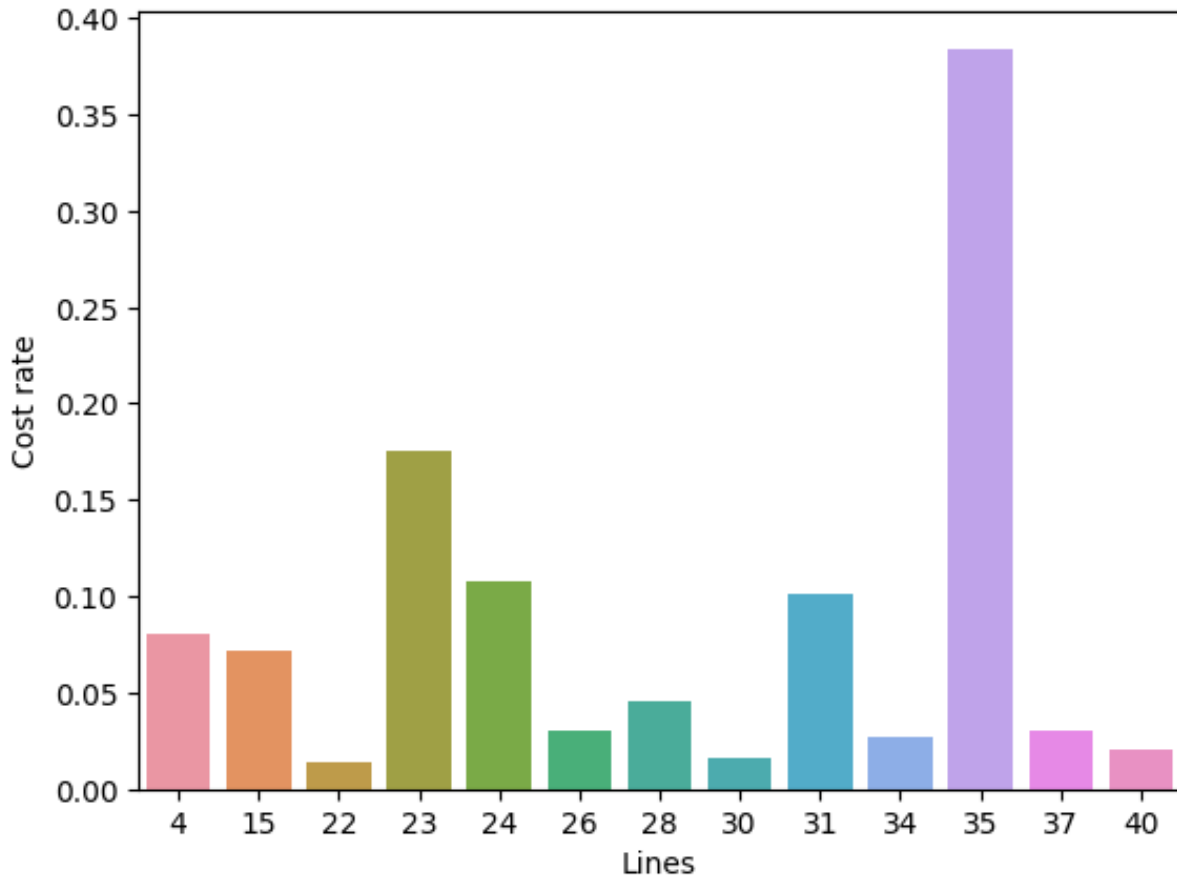


Figure 80: Cost influence of the total costs for June

For the June experiments 999 out of the 1000 runs remained after this filtration.

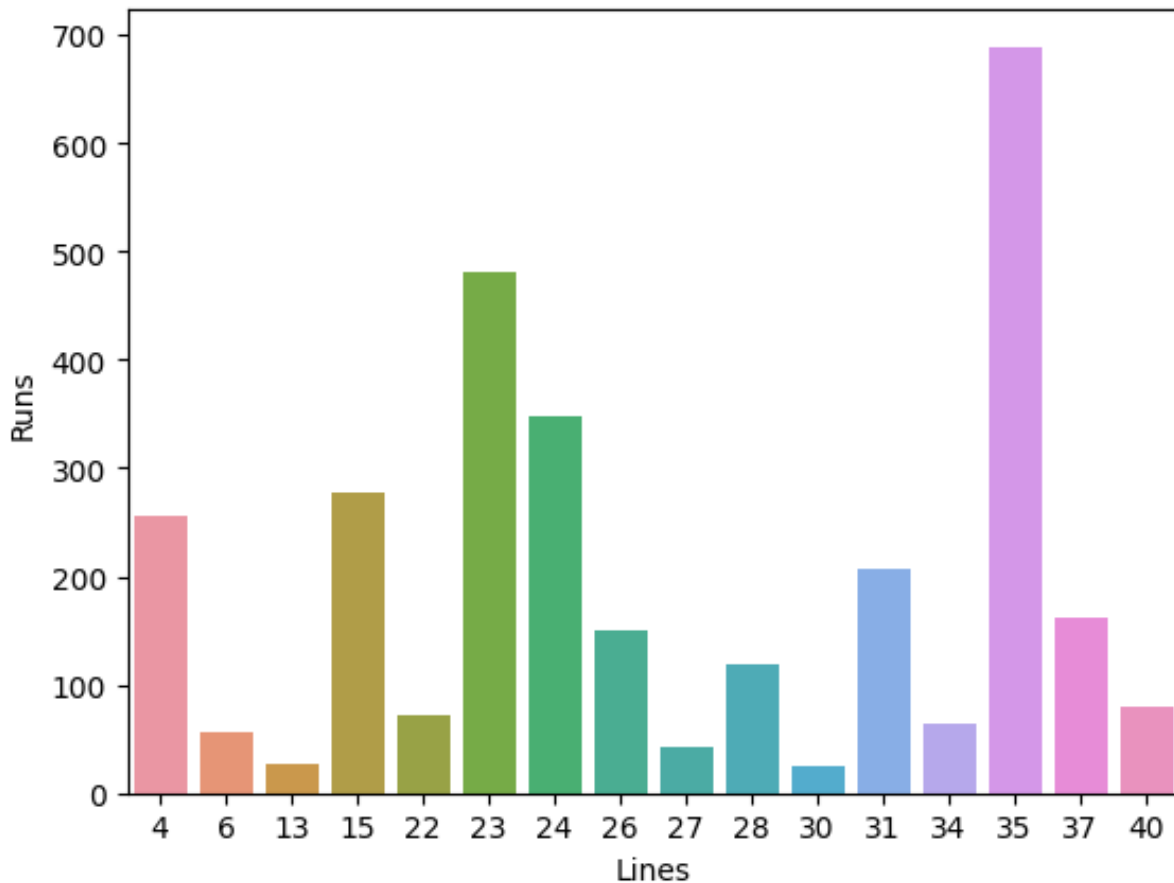


Figure 81: Amount of runs that have cost attributed to a certain line in June experiments.

What comes to mind while looking at these two figures is that some of the same lines score high in both figures. The following lines are deemed the most vulnerable:

- Line 15 (Krimpen - Breukelen)
- Line 23 (Oostzaan - Diemen)
- Line 24 (Riland - Geertruidenberg)
- Line 31 (Louwsmeer - Bergum)
- Line 35 (Eemshaven - Weiwerd)

The following lines have been deemed less vulnerable:

- Line 22 (Maasvlakte - Simonshaven)
- Line 26 (Wateringen - Bleiswijk)
- Line 28 (Zwolle - Hengelo)
- Line 34 (Oude Haske - Ens)
- Line 37 (Vierverlaten - Zeyerveen)

In Figure 82, the more vulnerable lines have been marked in red, the lesser vulnerable lines have been marked in blue.

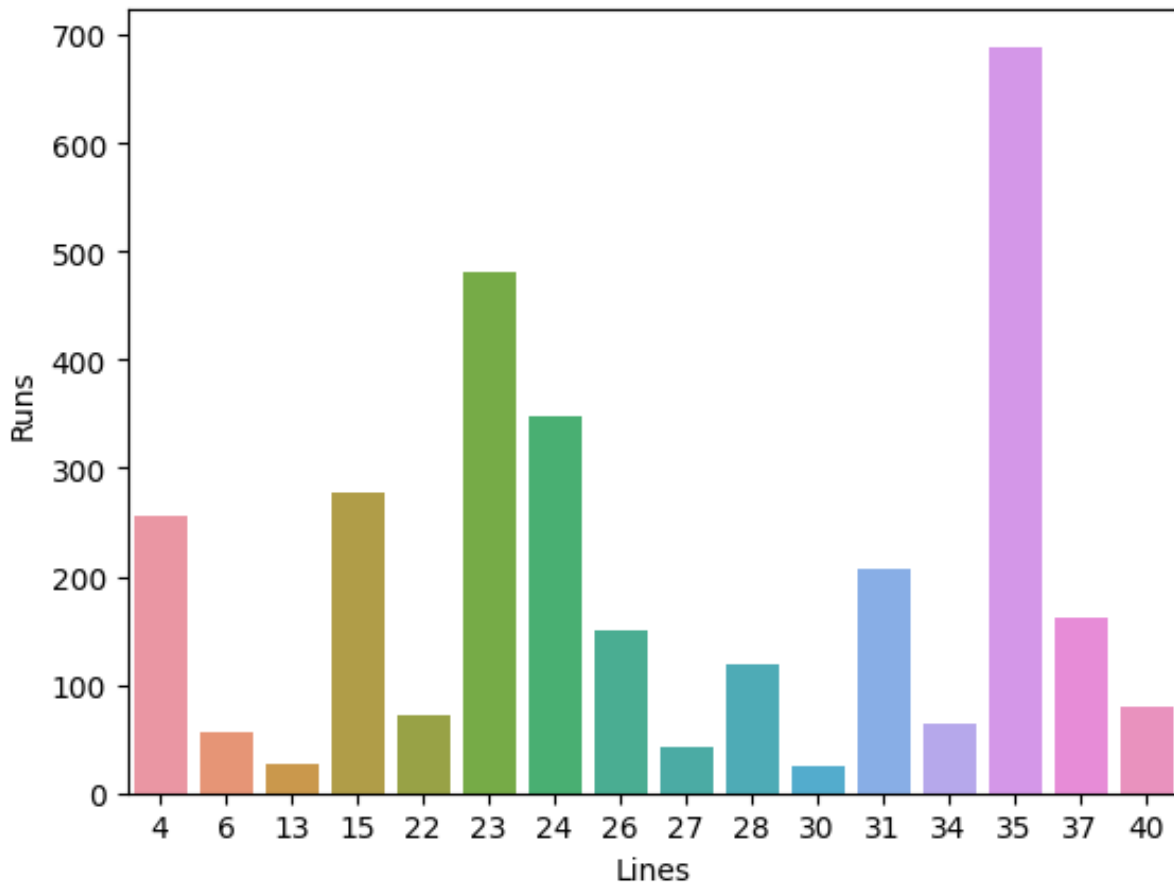


Figure 82: Interesting lines in the june results.

I.7 Prim analysis

Decision rules. Same decision rules Second decision rule did not give any results however.

I.7.1 Line 15

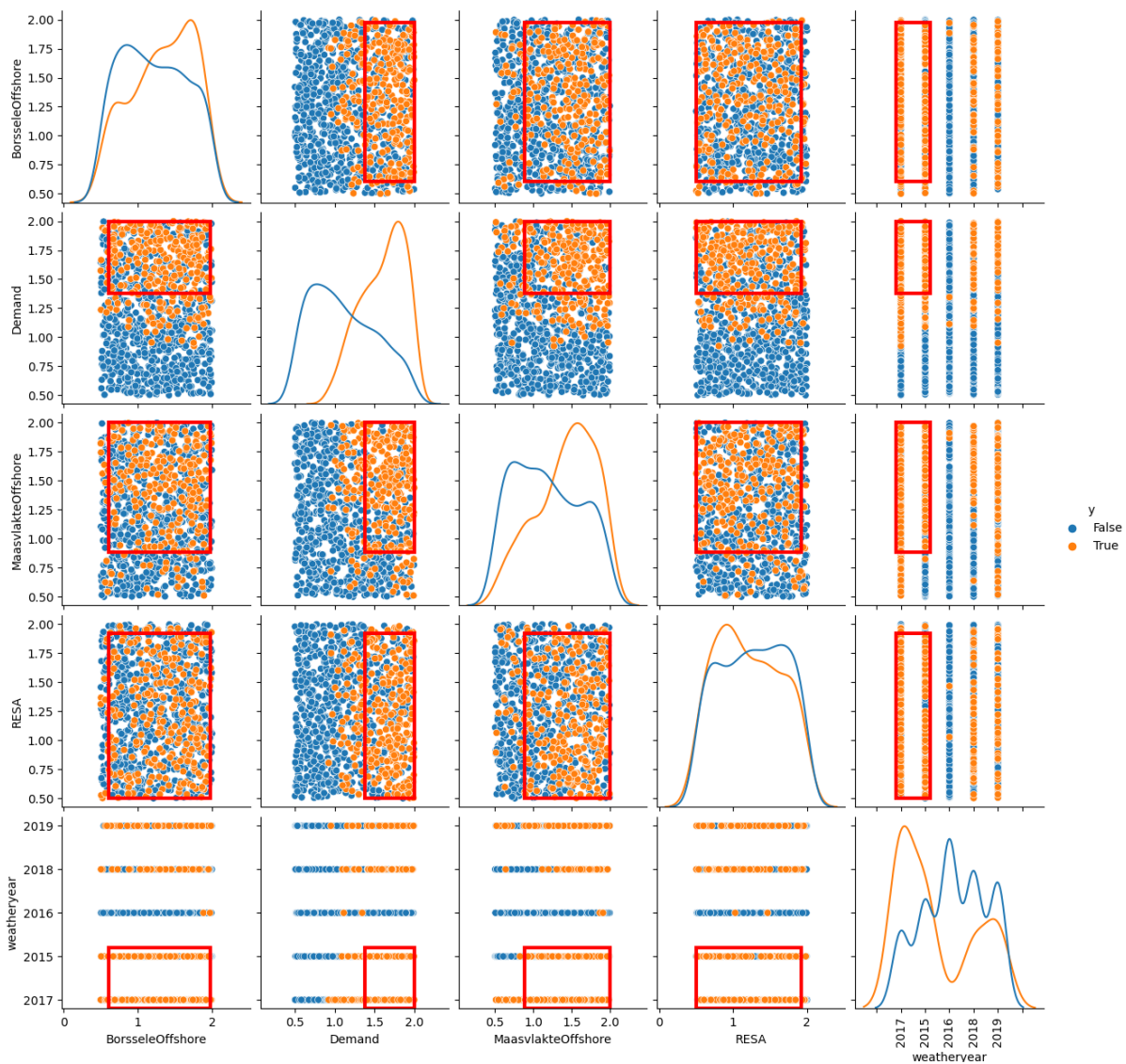


Figure 83: Prim scatterplot of line 15 for June experiments.

In Figure 83, the results for the PRIM analysis of line 15 of June can be found. The demand uncertainty, and the offshore windfarm of Maasvlakte seem to be the most decisive uncertainties for the congestion on this line. This is similar to the results of the January experiments as shown in figure 56. However, in the January experiments, the Beverwijk offshore windfarms, and the RESA policy plans seem to influence the results as well. Not by a lot however. The RESA even seem to have a negative effect on the amount of congestions. This could be appointed to the fact that in summertime the solar panels built due to the RESA policy plans have a higher output.

I.7.2 Line 23

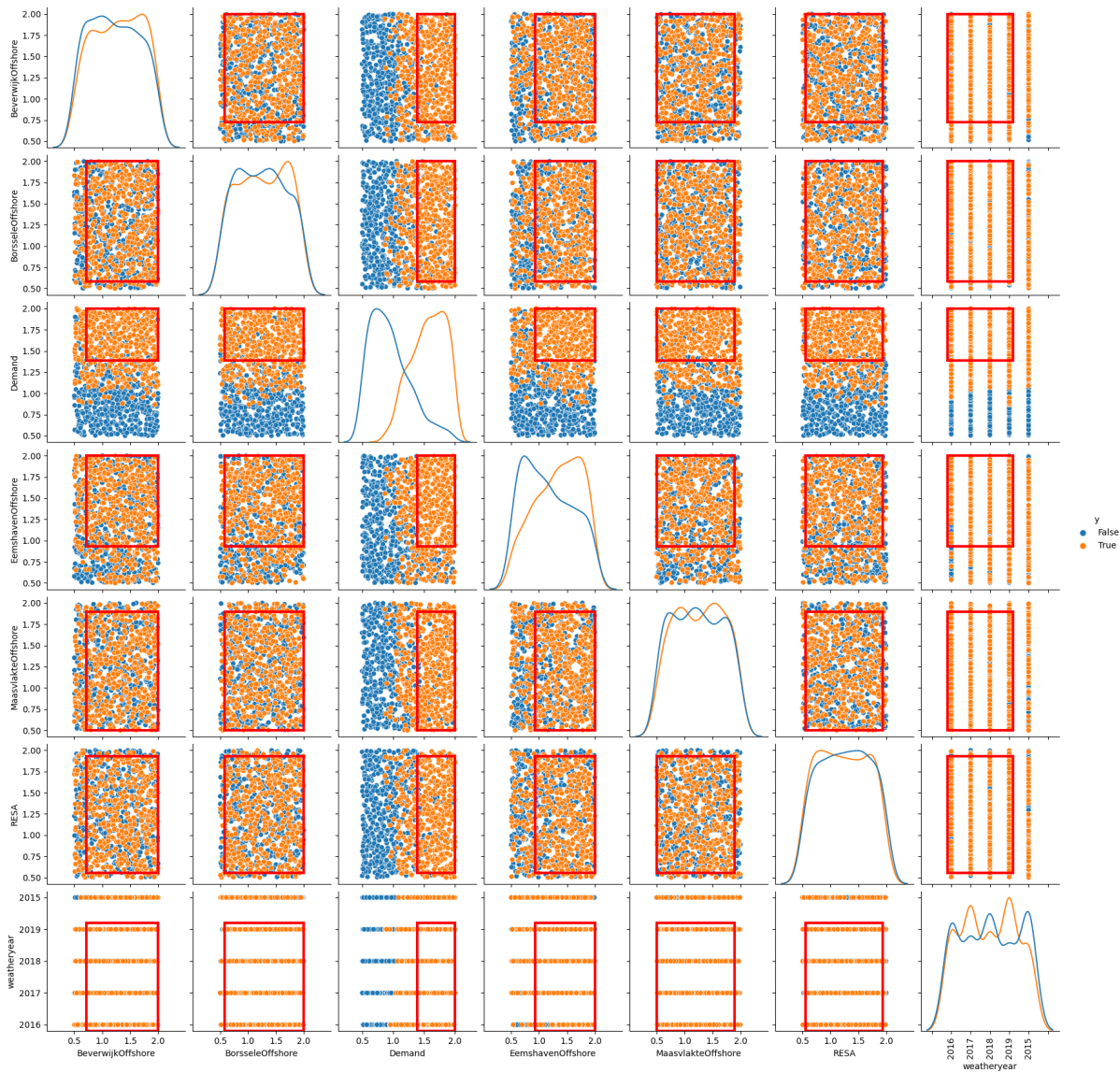


Figure 84: Prim scatterplot of line 23 for June experiments.

In Figure 84, the results for the PRIM analysis of line 23 for the June experiments can be found. What can be seen is that the demand is, again, the most prominent factor in the analysis. The rest of the uncertainties do not have any influence. While comparing these results with the results for January in Figure 58. A lot of extra uncertainties have been added, these extra uncertainties do not give a lot of extra meaning to the results however.

I.7.3 Line 24

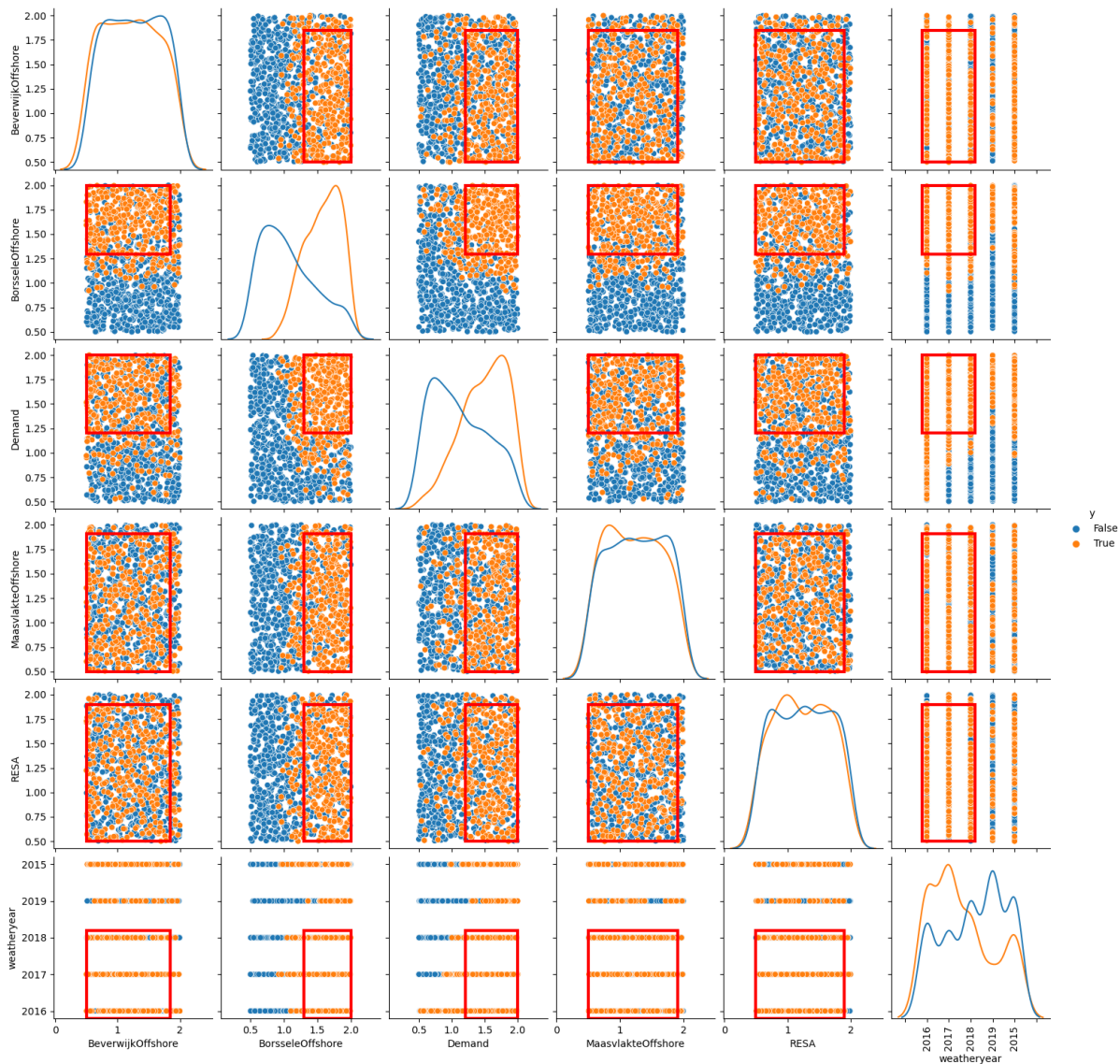


Figure 85: Prim scatterplot of line 24 for the June experiments.

In Figure 85, the results for the PRIM analysis of line 24 for the June experiments can be found. Both the demand and the offshore windfarm in Borssele have the biggest influence on the outcomes. While comparing these results with the results for January in Figure 58, the thresholds for both these uncertainties have become higher. The rest of the uncertainties do not have a clear distinction in the results.

I.7.4 Line 31

In Figure 86, the results for the PRIM analysis of line 31 for the June experiment can be seen. The demand for power, and the Eemshaven wind farm are the most influential for the congestion on this line in these experiments. However, this line can get congested even when the demand and offshore wind are low.

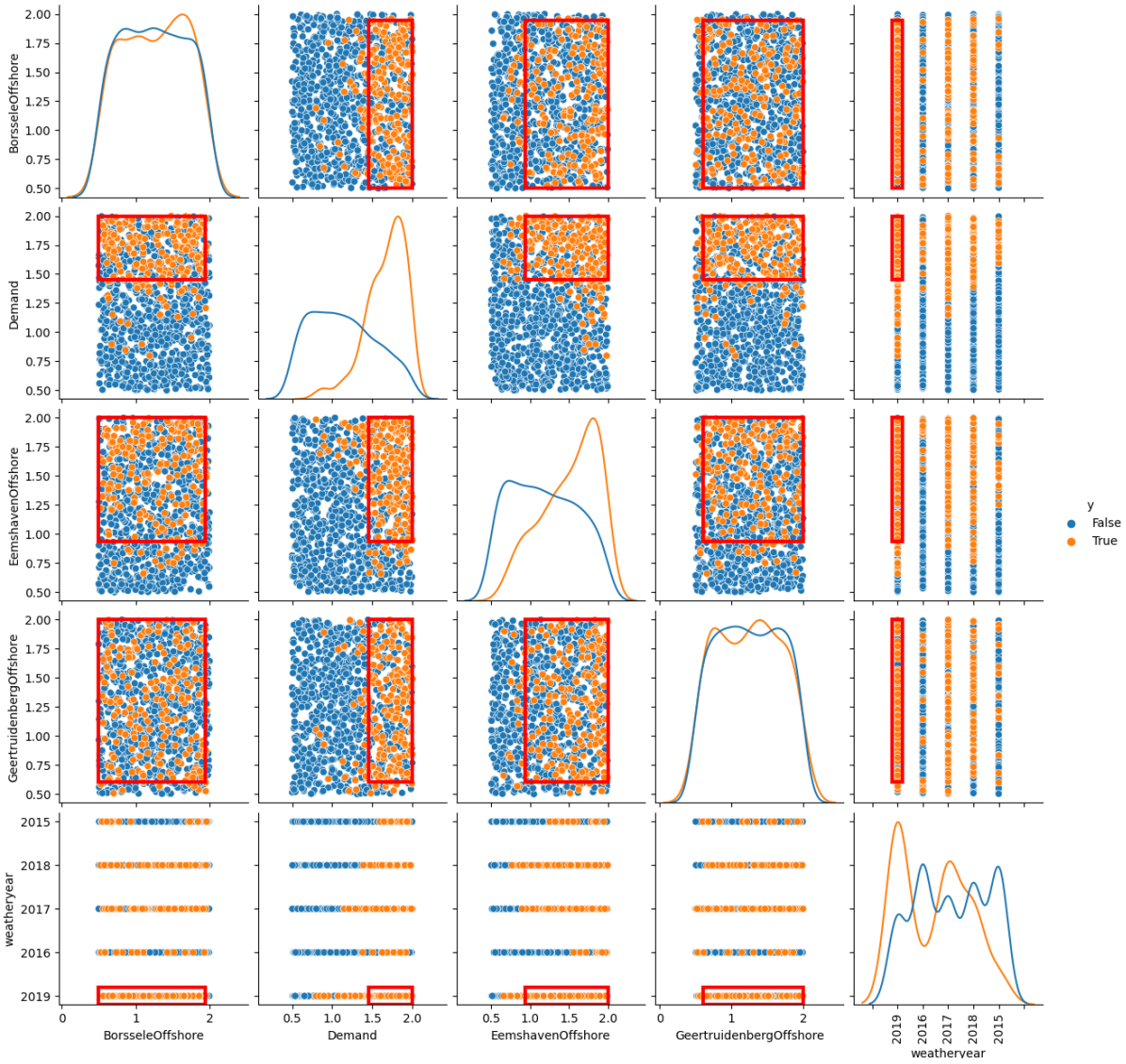


Figure 86: Prim scatterplot of line 31 for the June experiments.

I.7.5 Line 35

In Figure 87, the results for the PRIM analysis of line 31 for the June experiment can be seen. The demand for power, and the Eemshaven wind farm are the most influential for the congestion on this line in these experiments. The rest of the uncertainties do not have a strong influence however.

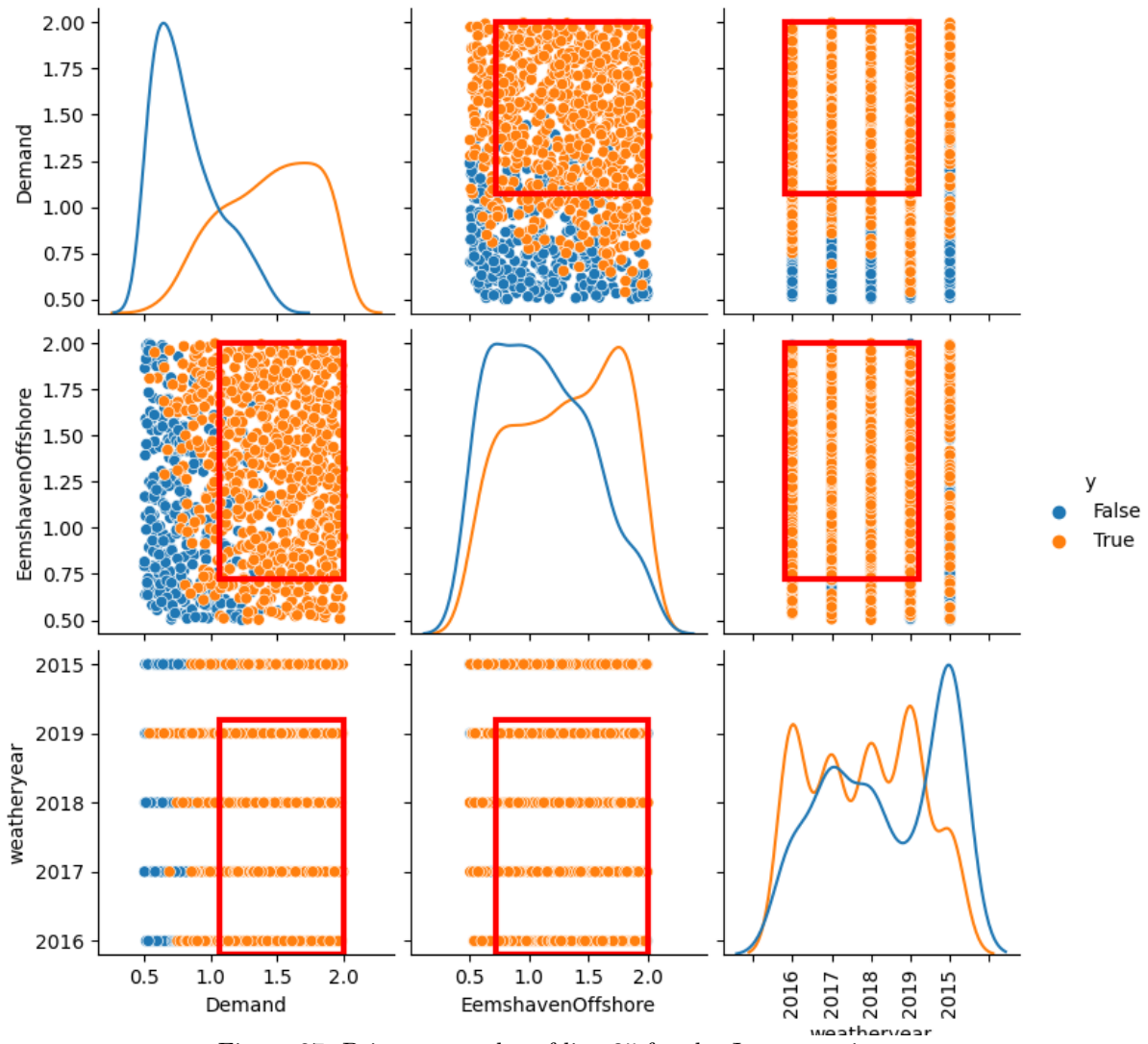


Figure 87: Prim scatterplot of line 35 for the June experiments.

1 percent of total costs does not give a lot of extra value, but should be investigated.

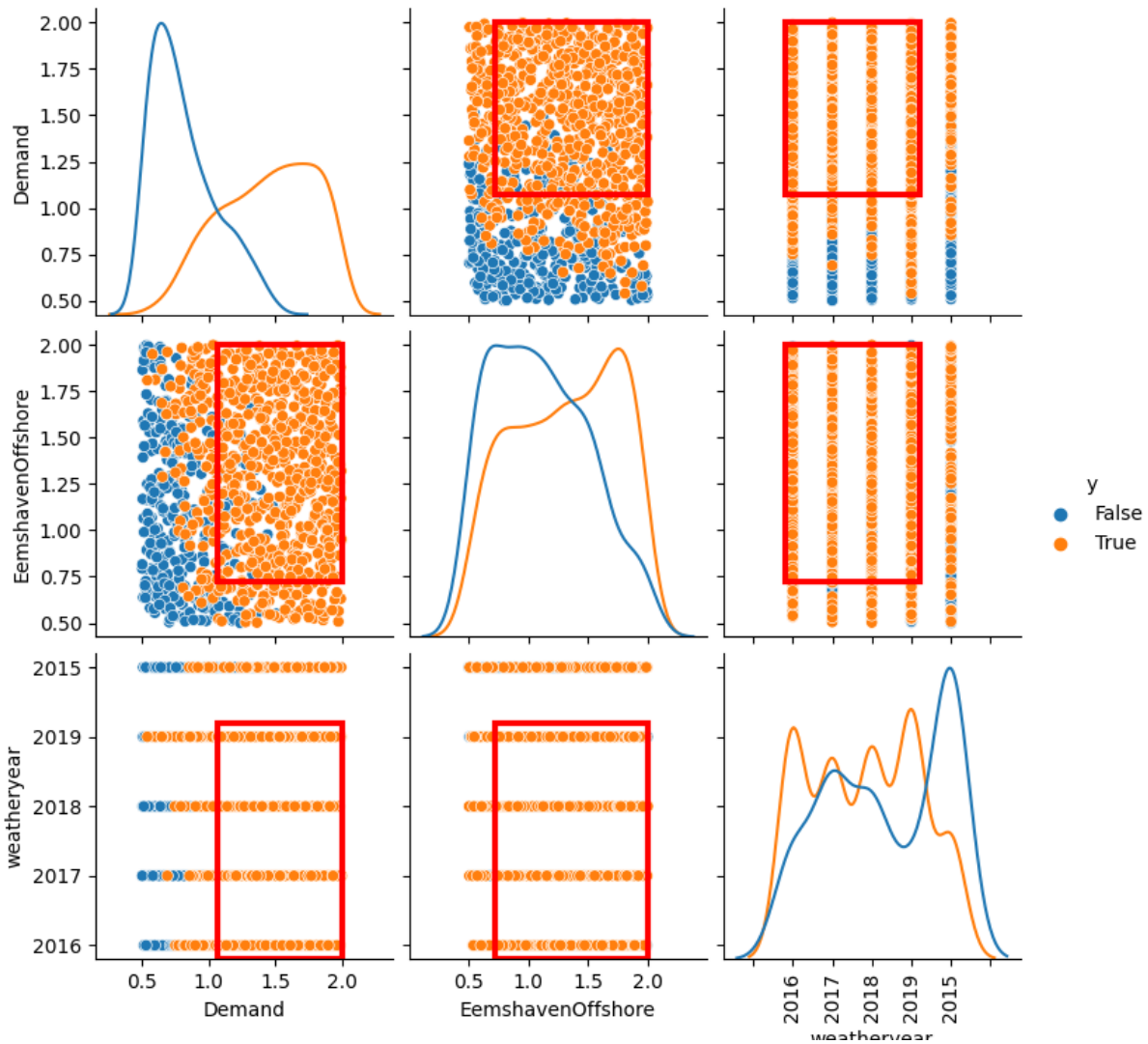


Figure 88: Prim scatterplot of line 35.

I.8 Lesser vulnerable lines

- Line 22 (Maasvlakte - Simonshaven)
- Line 26 (Wateringen - Bleiswijk)
- Line 28 (Zwolle - Hengelo)
- Line 34 (Oude Haske - Ens)
- Line 37 (Vierverlaten - Zeyerveen)

For line 34 no results could be found, for all of them the 2nd rule was not good.

I.8.1 Line 22

In Figure 89, the results for the PRIM analysis of line 31 for the June experiment can be seen. The demand for power, and the Maasvlakte wind farm are the most influential for the congestion on this line in these experiments. Both of these have to be very high for this line to become congested.

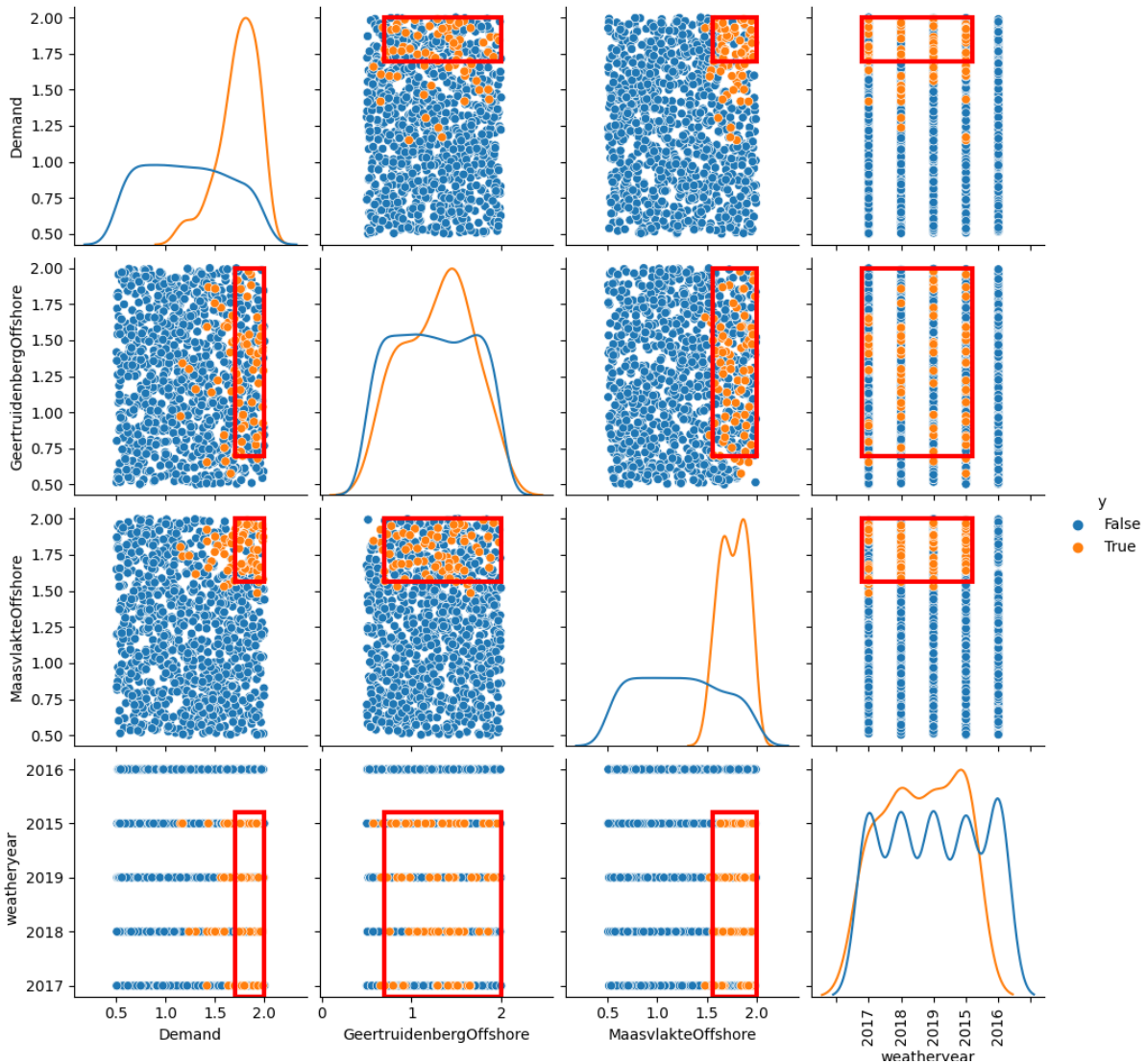


Figure 89: Prim scatterplot of line 22 for June experiments.

I.8.2 Line 26

In Figure 90, the results for the PRIM analysis of line 31 for the June experiment can be seen. The demand for power, and the Maasvlakte wind farm are the most influential for the congestion on this line in these experiments. Both of these have to be fairly high for this line to become congested. These results are quite similar to the results for the January experiments for this line, as shown in Figure 70.

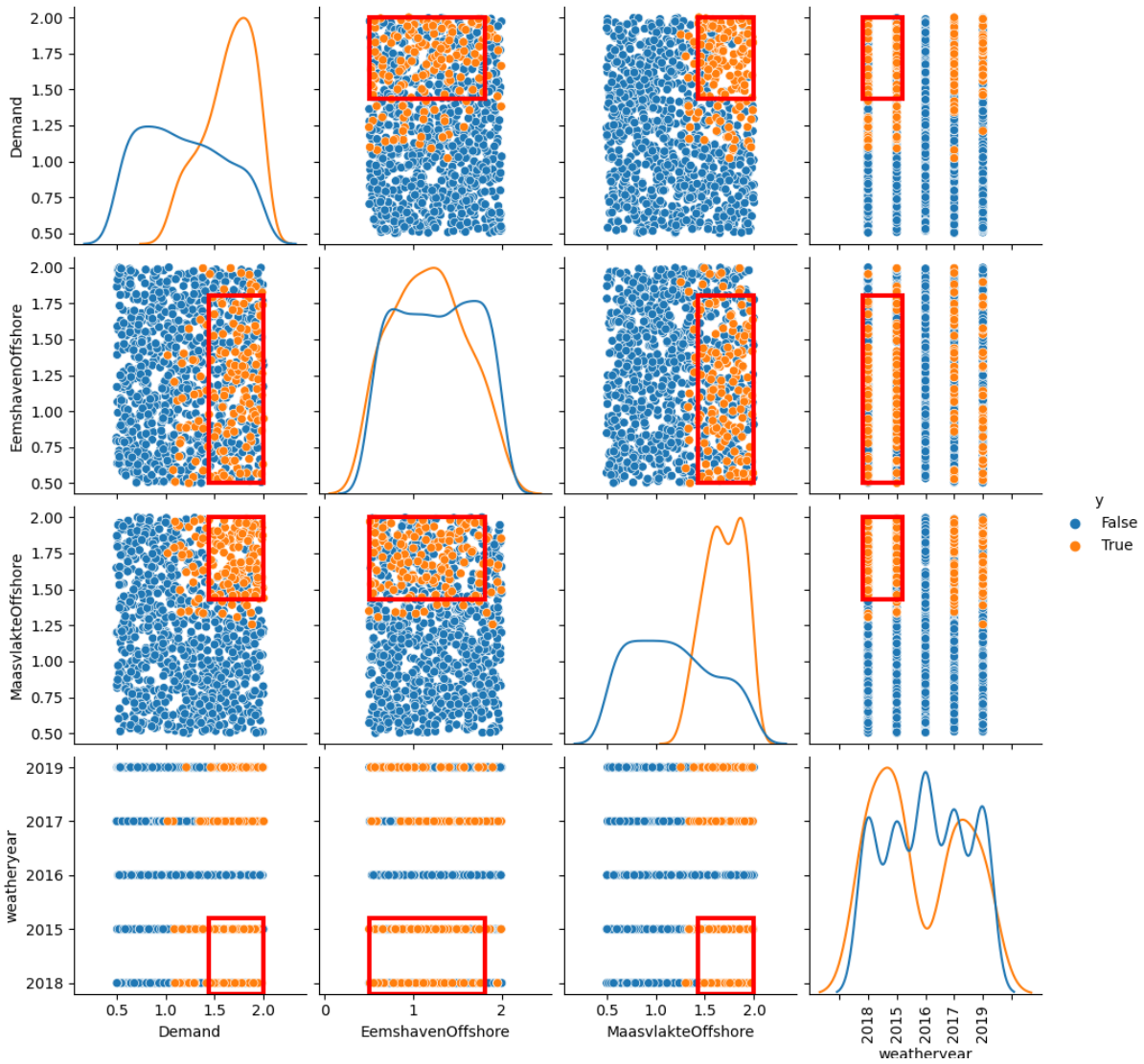


Figure 90: Prim scatterplot of line 26 for June experiments.

I.8.3 Line 28

In Figure 91, the results for the PRIM analysis of line 28 for the June experiment can be seen. The demand for power, the Maasvlakte wind farm, and the Eemshaven windfarms are the most influential to the congestion of this line. The demand must be very high for this line to become congested. With that, these results are very similar to the results for the January experiments for line 26, as shown in Figure 70.

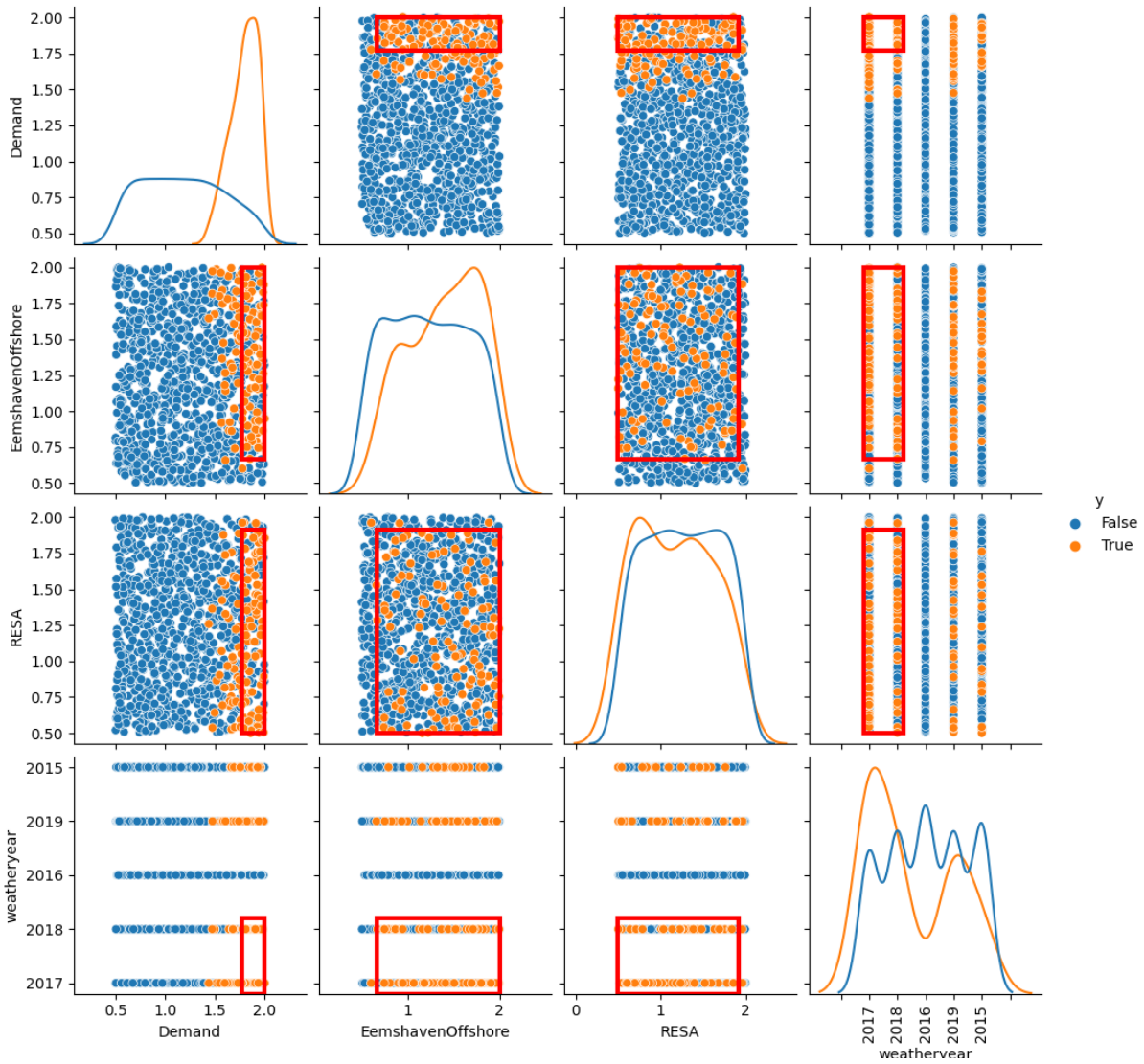


Figure 91: Prim scatterplot of line 28 for the June experiments.

I.8.4 Line 37

In Figure 92, the results for the PRIM analysis of line 28 for the June experiment can be seen. The demand for power, the Maasvlakte wind farm, and the Eemshaven windfarms are the most influential to the congestion of this line. The demand must be very high for this line to become congested.

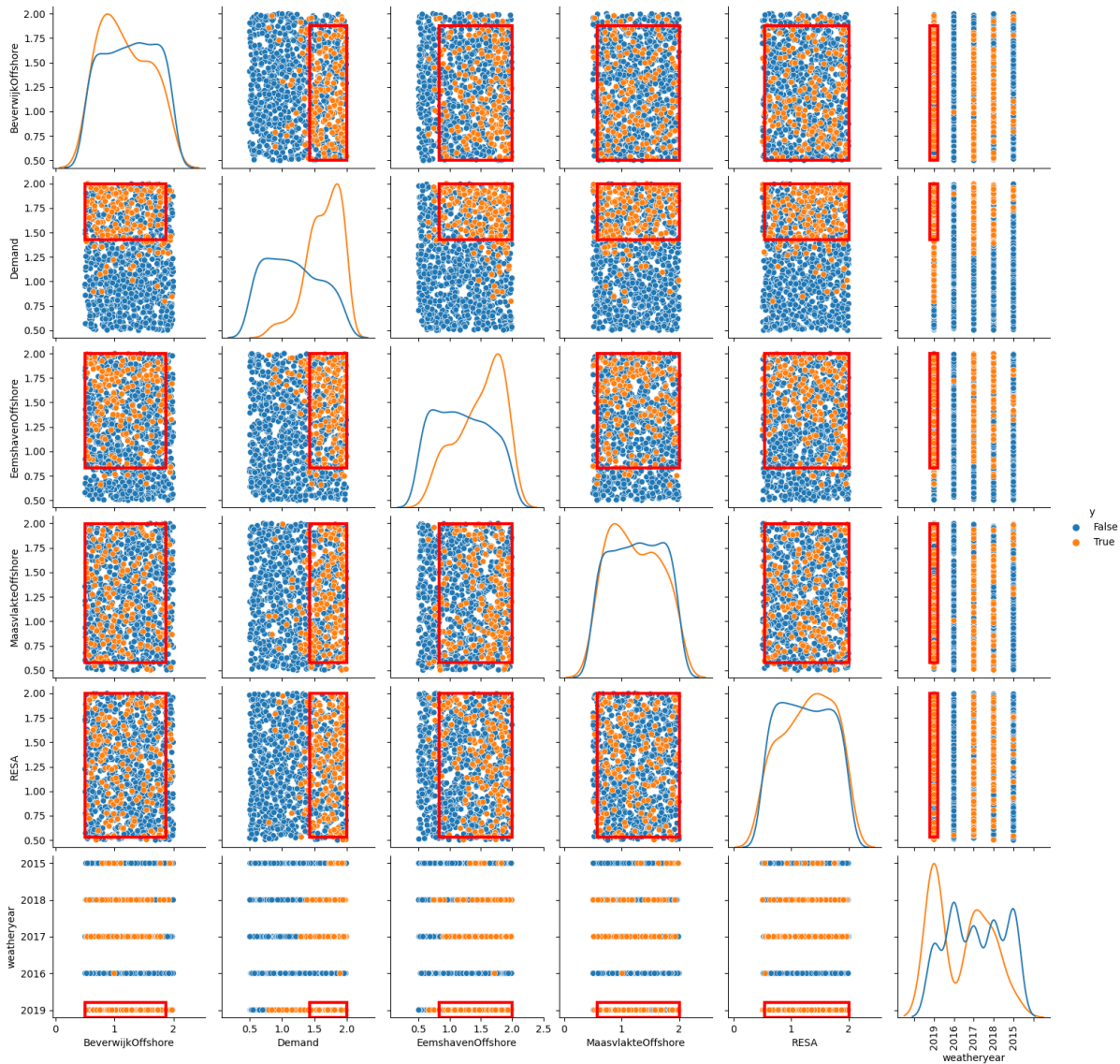


Figure 92: Prim scatterplot of line 37 for the June experiments.

I.9 Combination of lines for June

- Line 26 congestions after line 24
- Line 37 after line 31
- Line 26 after line 15

I.9.1 Line 26 after line 24

In figure 93 the results for the filtration of the results for line 26 for line 24 can be found. This figure does not show a lot of extra information in comparison to the original analysis in Figure 70.

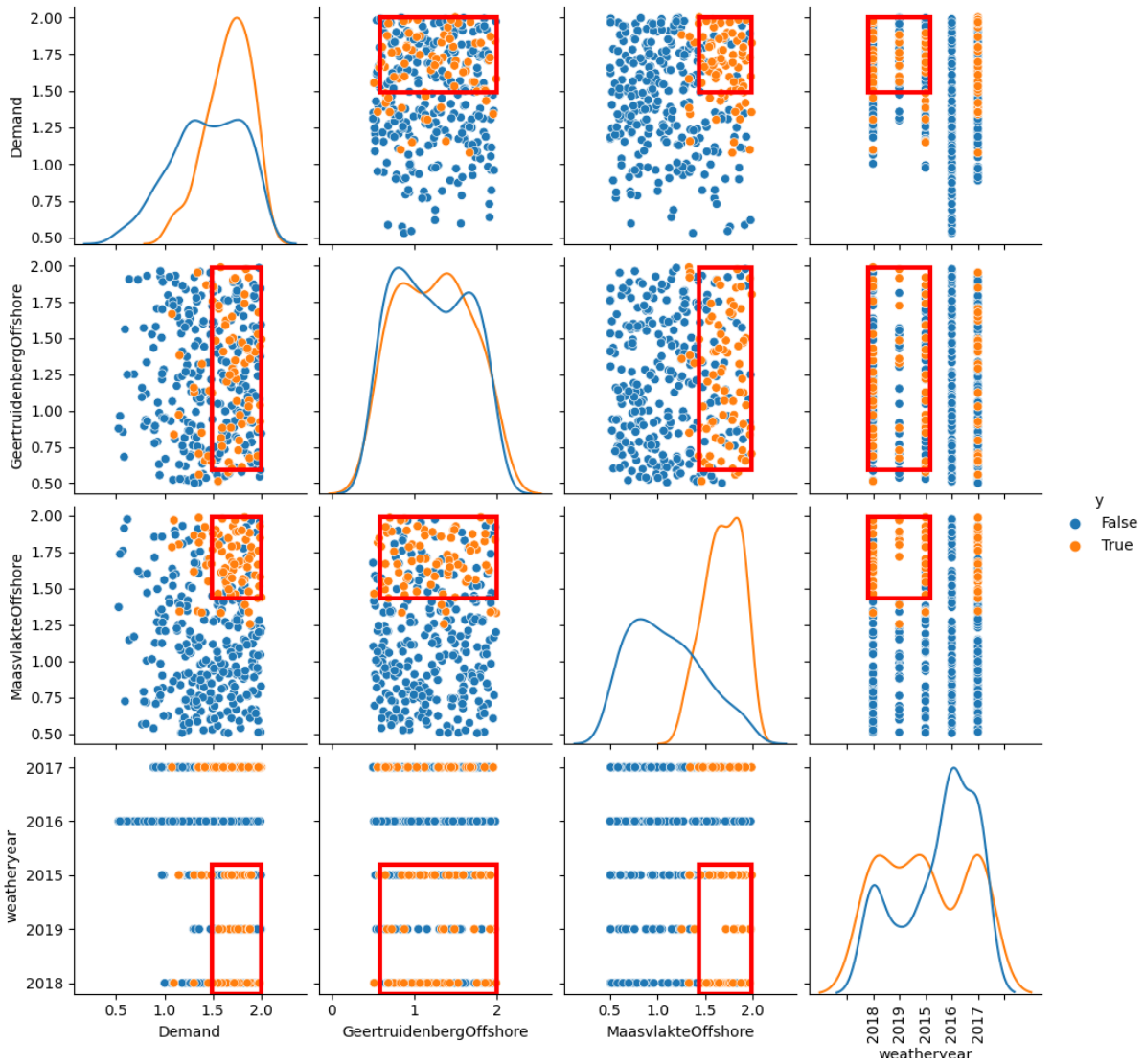


Figure 93: Prim scatterplot of line 26 after line 24 has been filtered out for the June experiments.

I.9.2 Line 37 after line 31

Nothing comes out of this. Apart from that the same dots are orange, in respect to the earlier analysis.

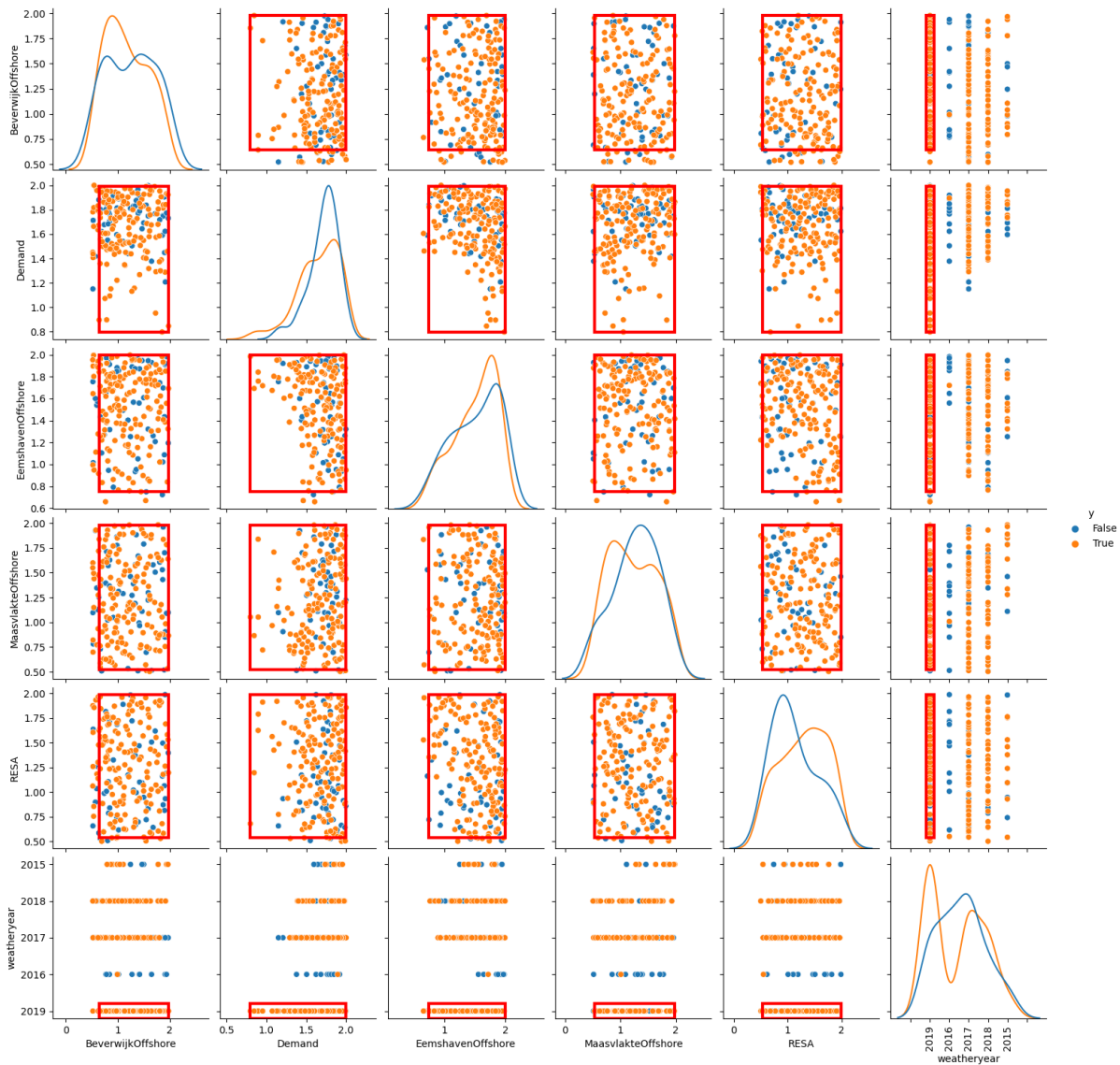


Figure 94: Prim scatterplot of line 37 after line 31 has been filtered out.

I.9.3 Line 26 after line 15

Same boxes as original PRIM of 26. Would mean that line 26 gets congested after line 15.

Nice result; Gives the same idea as line 26 after line 24. Compare this with Line 26 after Line 15 for January.

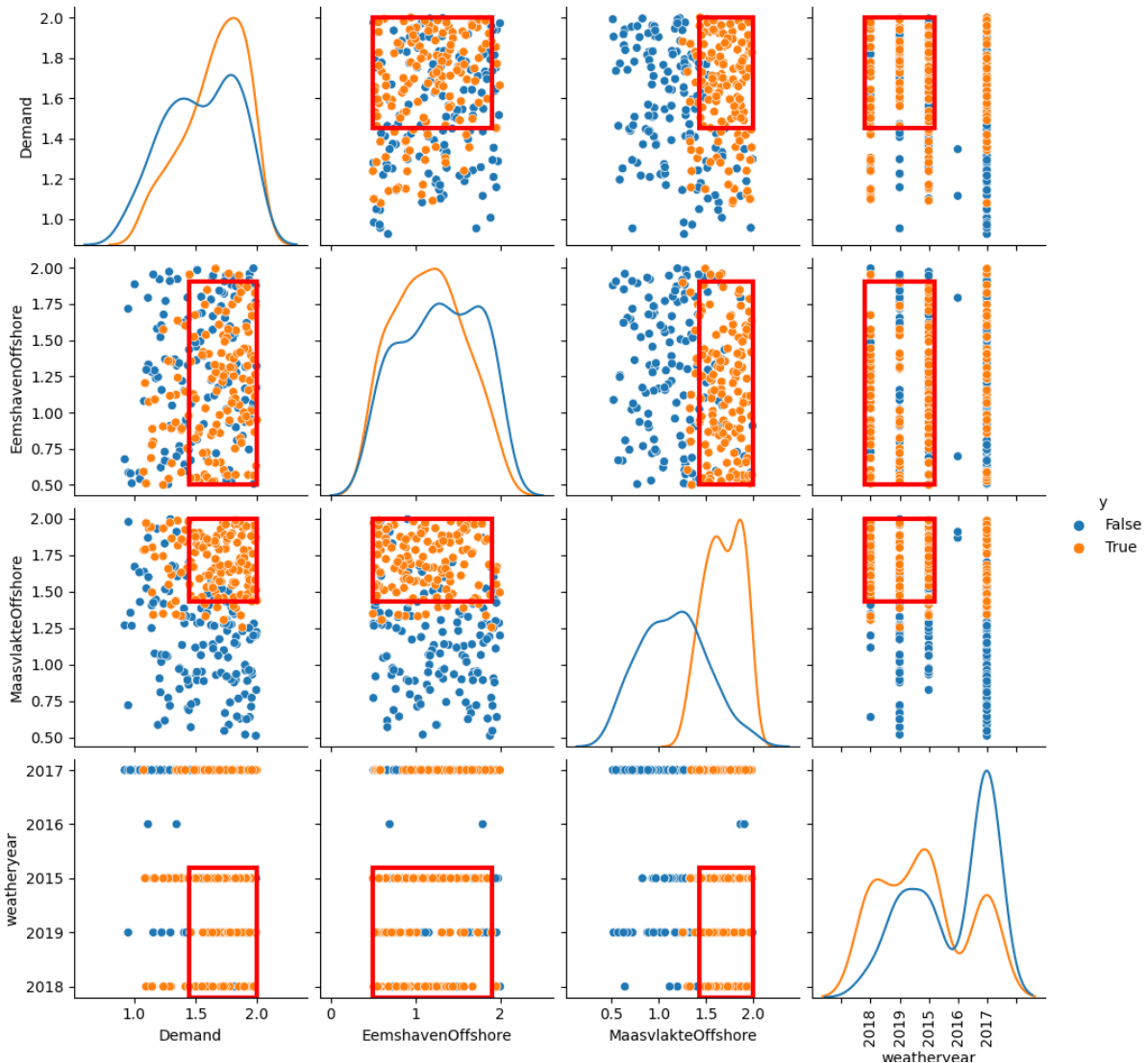


Figure 95: Prim scatterplot of line 26 after line 24 has been filtered out.

I.10 Comparison with the outcomes of the two experiments

Looking back, the lines for January were:

- Line 4 (Borssele - Riland)
- Line 15 (Krimpen - Breukelen)
- Line 23 (Oostzaan - Diemen)
- Line 24 (Riland - Geertruidenberg)
- Line 28 (Zwolle - Hengelo)
- Line 35 (Eemshaven - Weiwerd)
- Line 38 (Bergum - Vierverlaten)

The following lines are deemed less vulnerable; these lines will be subjected to some further analyses.

- Line 6 (Breukelen - Diemen)
- Line 13 (Geertruidenberg - Tilburg)

- Line 26 (Wateringen - Bleiswijk)
- Line 30 (Ens - Zwolle, 220 kV)
- Line 31 (Louwersmeer - Vierverlaten)
- Line 37 (Vierverlaten - Zeyerveen)
- Line 40 (Zwolle - Zeyerveen)

The lines for June were:

- Line 15 (Krimpen - Breukelen)
- Line 23 (Oostzaan - Diemen)
- Line 24 (Riland - Geertruidenberg)
- Line 31 (Louwsmeer - Bergum)
- Line 35 (Eemshaven - Weiwerd)

The following lines have been deemed less vulnerable:

- Line 22 (Maasvlakte - Simonshaven)
- Line 26 (Wateringen - Bleiswijk)
- Line 28 (Zwolle - Hengelo)
- Line 34 (Oude Haske - Ens)
- Line 37 (Vierverlaten - Zeyerveen)

Between the experiment the following lines could be compared:

- Line 15
- Line 23
- Line 24
- Line 26
- Line 28
- Line 35
- Line 37

The June experiments had a far lower amount of vulnerable lines and congestions in general. This can be attributed to two differences in summer and wintertime. The first is the solar output. This is generally higher in summer. The amount of energy that can be transformed from the sun is a lot higher. Since every node has its own local solar supply in the model, the demand can be served locally. Therefore, less network capacity needs to be used to transfer power. The second is the demand for energy. Since in the winter time, the temperature is lower, extra power is needed for heating, lightning, etc. Therefore, the power flows on the network are less high in the summer.